Role of Notch Ligands in Tumour Angiogenesis



Thesis submitted by
Chern Ein Oon
Merton College

For the degree of
Doctor of Philosophy
Department of Medical Oncology
Trinity Term 2011
University of Oxford

Supervisor: Professor Adrian L. Harris

Abstract

The well conserved Notch signalling pathway plays a crucial role in vascular development and physiology. Delta-like 4 (DLL4) and Jagged1 (JAG1) are two key notch ligands implicated in angiogenesis. Both ligands were shown to have opposite effects on vasculature. DLL4-Notch signalling inhibits sprouting resulting in fewer but better perfused blood vessels, promoting tumour growth. In contrast to DLL4, very little is known about JAG1- Notch signalling in tumour angiogenesis and its influence on tumour growth and progression. The overall aim of this work is to study the functional difference between DLL4 and JAG1-Notch signalling. The effects of murine DLL4 and murine JAG1 over-expression on tumour growth and angiogenesis was also investigated in a mouse U87 xenograft model. Firstly, the downstream target genes of DLL4 and JAG1-Notch signalling were established through microarray and QPCR. Angiogenic assays such as sprouting, network formation and migration assays were employed to study the functional effects of these two ligands in endothelial cells. The thesis firstly demonstrates that JAG1 has opposing effects on endothelial cells compared to DLL4 by increasing sprout coverage and network formation. JAG1 is less potent than DLL4 in stimulation of Notch target genes in primary endothelial cell (HUVEC) but both displayed equal potency in HMEC-1, an immortalised endothelial cell line. The growth of U87 cell lines which over-expressed murine DLL4 or murine JAG1 was slower compared to wild-type U87 cell line *in vitro*. JAG1- and DLL4- Notch signaling have different effects on vessel formation, which impacted on the tumour growth *in vivo.* Interestingly, tumours over-expressing mDLL4 had less but larger vessels compared to control, whereas mJAG1 produced more yet functional vessels; both tumours had significantly reduced pericyte coverage. Both U87 mDLL4 and mJAG1 over-expressing tumours showed increased resistance towards anti-VEGF therapy, compared to control tumours. Sensitivity to therapy was restored in combinational treatment with DBZ and bevacizumab. The mechanism behind the differential responsiveness of the Notch receptors to DLL4 or JAG1 ligands could either reflect modulation by fringes, a family of glycosyltransferases that regulate Notch signalling or by a positive feedback loop present for DLL4-Notch signalling only. Fringe was found to be abundantly expressed in endothelial cells and highly vascularised tumours. This work has highlighted some key novel differences between the two Notch Ligands.

Submitted for the degree of D.Phil in Medical Oncology by:
Chern Ein Oon
Merton College, University of Oxford,
Trinity Term 2011

Supervisor: Professor Adrian L. Harris
Department of Medical Oncology,
Weatherall Institute of Molecular Medicine,
John Radcliffe Hospital, Headington, OX3 9DS, UK.

This thesis is dedicated to my beloved mom and dad.

‘No mountain is too high for you,

because you know that the view from the top

is worth the climb’

-Mom and Dad-

Acknowledgements

I would like to express my deepest gratitude to Professor Adrian L. Harris, having been my supervisor for the past 3 and half years, whose brilliant ideas and motivation have spurred me on in the field of oncology and guided me step by step to make this thesis possible. For the conferences you have sponsored me and all the networking opportunities, thank you for helping me in my career development. Thank you also for proofreading my thesis and your invaluable comments and suggestions.

Sincere thanks to Dr. Richard Sainson for his patience, commitment and many hours of sacrifice of online conferencing to help me develop this project despite having left the lab for a new job. You have helped me mature into the scientist I am today. Character development, right working attitude, networking, experimental planning and execution, I have learnt much from you. You will always be a scientist I very much look up to.

To Dr. Ji-Liang Li, who has helped me advance my *in vivo* work, for all scientific contributions, discussions, data interpretation and over-seeing my project, thank you. Many thanks to Dr. Esther Bridges whom I work very closely with for the past one year to optimise the angiogenic assays. It has been a pleasure working with you and co-writing a review paper with you. Thank you for helping me with last minute analysis, proofreading my thesis and helping me with illustrations, you have an artistic side which I very much admire. For those times you have lent me your listening ears and moral support, thank you very much.

To Dr. Helen Sheldon, for the many scientific discussions on experimental techniques and guiding me every step of the way. Those scientific emails bouncing back and forth with latest literature attached and data interpretation have been put to good use in this thesis. Thank you especially for the time you have invested in this proofreading marathon for the past two months and providing useful comments and suggestions. To Dr. Massimo Massiero, for the valuable discussions on scientific papers and sharing your views through your expertise, thank you very much.

I would also like to thank Dr. Adrian Jubb, Dr. Russell Leek, Dr. Helen Turley and Mr. Graham Steers for helping me with sectioning of tumours, immunostaining, scoring of tumour sections, and contributing scientific opinions and expertise to help me develop the this project. Heartfelt gratitude also to Dr. Francesca Buffa for helping me with last minute statistics

analysis and advice despite being snowed under piles of work, I appreciate your effort and commitment. I would like to thank other members of the Harris' lab for making my journey in Oxford a memorable one. Thank you for scientific advice, useful discussions and moral support. I would also like to express my sincere appreciation to Jenny Dollard, Peter Thomas, Penny Berry, Rose and Linda for helping me with administrative work and for the continuous clean supply of autoclaved materials needed for my experiments.

Last but not least, I would like to express my gratitude to my family for your love and moral support through these years abroad, even though sometimes this journey seemed arduous, thank you for believing in me. Special thanks to Dr. Sven Petersen who has offered to share my burden during these months of writing marathon by helping me with thesis formatting and providing moral support. Unfortunately, technology and I do not often see eye to eye. I appreciate all the hours you have put into helping me format my thesis to get this done on time!

My DPhil project would not have been possible without funding from the Ministry of Higher Education Malaysia. I am very grateful for the fellowship received.

Abbreviations

ADAM	A disintegrin and metalloprotease
bFGF	Basic fibroblast growth factor
cDNA	complementary DNA
CCRCC	Clear cell renal cell carcinoma
CD31	Cluster of differentiation 31
CSL	CBF1/RBP-Jκ, drosophilia Su(H), and C.elegans Lag1
CT	Cycle threshold
E	Embryonic Day
DAPI	4',6-diamidino-2-phenylindole
DAB	3,3' Diaminobenzidine
DEPC	Diethylpyrocarbonate
DBZ	Dibenzazepine
DLL-	Delta-like
DNA	Deoxyribonucleic acid
DSL	Delta/ Serrate/ Lag2 domain
dNTP	Deoxyribonucleotide triphosphate
ECGS	Endothelial cell growth supplement
EGF	Epidermal growth factor
EV	Empty vector
FCS	Fetal calf serum
FFPE	Formalin-fixed, paraffin-embedded
GlcNAc	N-acetylglucosamine
g	Grams
HCl	Hydrochloric acid
HES	Hairy and Enhancer of Split
HEY	Hes-related protein families
HIF	Hypoxia inducible factors
IHC	Immunohistochemistry
JAG-	Jagged
kg	Kilograms
L	Litre
LFng	Lunatic fringe
M	Molar
MAPK	Mitogen- activated protein kinase
MFng	Manic fringe
mg/kg	Milligrams/kilogram
ml	Millilitres
mm	Millimetres
mRNA	Messenger RNA (Ribonucleic acid)
mM	Millimolar
ng	Nanograms
nm	Nanometres
NRP-1	Neuropilin1
PBS	Phosphate-buffered saline
PCR	Polymerase chain reaction
RFng	Radical fringe
RNA	Ribonucleic acid
rpm	Revolutions per minute

PDGF	Platelet-derived growth factor
PDGFR	Platelet-derived growth factor receptor
QPCR	Quantitative PCR
SDS	Sodium dodecyl sulphate
shRNA	Short hairpin RNA
siRNA	Small interefering RNA
SMA	Smooth muscle actin
TACE	Tumour necrosis factor-alpha converting enzyme
TGFβ	Transforming growth factor beta
TNFα	Tumour necrosis factor-alpha
vSMC	Vascular smooth muscle cell
VEGF	Vascular endothelial growth factor
VEGFR	Vascular endothelial growth factor receptor
www	World wide web
µg	Micrograms
µl	Microlitres
µm	Micrometres
µM	Micromolar
^{o}C	Degrees celcius
%	Percent

Table of contents

1 Introduction 1

1.1 Formation of new blood vessels 2

1.2 The classical Notch signalling pathway 5

1.3 The regulation of new blood vessels during development 8

1.4 Role of Notch signalling in tumour biology 12

1.4.1 Aberrant expression of Notch ligands and receptors in solid tumours 13

1.5 Mechanisms that effect Notch signalling and their subsequent influence on tumour vasculature 15

1.5.1 Fringe can modulate Notch signalling pathway in cells 16

1.5.2 Tumour associated growth factors produced by tumour, stromal and inflammatory cells can induce Notch ligand expression in endothelial cells. 17

1.5.3 Interaction with neighbouring vascular cells, tumour cells and inflammatory cells 20

1.5.4 Research aims 23

2 Methodology 24

2.1 Materials 24

2.1.1 Chemicals 24

2.1.2 Cell Lines 24

2.1.3 Cell culture reagents 24

2.1.4 Real-time PCR primers and probes 25

2.1.5 Small interfering RNAs 26

2.1.6 Antibodies 27

2.1.7 Molecular weight markers 29

2.1.8 Matrigel basement membrane matrix 29
2.1.9 Lentiviral particles 29
2.1.10 Mouse model 30
2.1.11 Over-expressing cell line 30
2.2 General laboratory methods 30
2.2.1 Isolation of HUVEC 30
2.2.2 Mammalian cell culture 31
2.2.3 RNA extraction and analysis 33
2.2.4 Protein extraction and analysis 36
2.2.5 Websites 38
2.3 Experimental methods 39
2.3.1 RNA interference 39
2.3.2 Lentiviral transduction 39
2.3.3 Coating plates with recombinant DLL4 or JAG1 protein 40
2.3.4 *In vitro* angiogenic assays 41
2.4 Immunostaining 43
2.4.1 Preparation of sections 43
2.4.2 Staining protocols 44
2.5 Mouse models 49
2.6 Statistical methods 50
3 Effect of DLL4 and JAG1 on Notch signalling *in vitro* 51
3.1 Introduction 51
3.2 DLL4 and JAG1 were expressed in HUVEC and HMEC-1 cells 52
3.3 Exogenous ligands can activate Notch signalling in HUVEC and HMEC-1 54
3.4 Characterisation of HMEC-1 mDLL4 and HMEC-1 mJAG1 65

3.4.1 mDLL4 and mJAG1 were up-regulated in HMEC-1 over-expressing cell line 65
3.4.2 mDLL4 and mJAG1 activation of Notch signalling up-regulated downstream and Notch target genes in HMEC-1 67
3.5 Activation of Notch signalling did not affect cell proliferation in HMEC-1 cells 68
3.6 Role of mDLL4 and mJAG1 in angiogenesis 68
3.6.1 Both mDLL4 and mJAG1 increased HMEC-1 cell motility 69
3.6.2 mDLL4 and mJAG1 had different effects on network formation 70
3.6.3 mDLL4 and mJAG1 elicited different effects on sprouting 72
3.7 Role of endogenous DLL4 and JAG1 ligands in angiogenesis 75
3.7.1 Silencing either DLL4 or JAG1 in HMEC-1 reduced cell number *in vitro* .. 78
3.7.2 Silencing either endogenous DLL4 or JAG1 inhibited cell migration 78
3.7.3 Silencing either DLL4 or JAG1 had different effects on HMEC-1 network formation 80
3.8 Silencing endogenous DLL4 or JAG1 had opposite effects on sprouting 81
3.9 Discussion 88
4 Effects of DLL4 and JAG1 over-expression on xenograft tumours 99
4.1 Introduction 99
4.2 Characterisation of U87 cell lines 102
4.2.1 mDLL4 and mJAG1 were successfully transduced into the U87 cell line .. 102
4.3 Both mDLL4 and mJAG1 reduced U87 cell proliferation but did not affect apoptotic cell death in U87 cells *in vitro* 105
4.4 Both mDLL4 and mJAG1 decreased mouse survival by promoting xenograft tumour growth *in vivo* 106

4.5 DBZ eradicated the effects of mDLL4 and mJAG1 on tumour growth 107
4.6 DLL4-Notch signalling mediated tumour resistance to VEGF inhibition 110
4.7 JAG1-Notch signalling also mediated tumour resistance to VEGF inhibition 113
4.8 mDLL4 and mJAG1 produced different vascular phenotypes in U87 xenograft sections with decreased pericyte coverage. 116
4.9 Both mDLL4 and mJAG1 increased vessel perfusion in U87 xenograft tumours 120
4.10 DLL4 was highly expressed in tumour vessels 122
4.11 mDLL4 increased JAG1 expression in vessels and tumour cells and stroma . 124
4.12 Tumour cell proliferation was unaffected by mDLL4 and mJAG1 expression 126
4.13 mDLL4 but not mJAG1 decreased tumour hypoxia 128
4.14 mDLL4 and mJAG1 decreased tumour necrosis which contributed to tumour growth 130
4.15 Preliminary experiment: Blocking DLL4-Notch signalling delayed tumour growth in U87 xenograft tumours 132
4.16 Discussion 133
5 Expression profile of Fringe in endothelial cells and tumour 153
5.1 Introduction 153
5.2 MFng is highly expressed in endothelial cells 156
5.2.1 Notch activation did not affect MFng, LFng and RFng gene expression in HMEC-1 161
5.3 MFng is expressed in angiogenic tumours 162
5.4 Fringe expression pattern in CCRCC tumours 168
5.4.1 Validation of Fringe antibody 169

5.4.2 Fringe was abundantly expressed in CCRCC tumour vasculature.....172

5.5 Discussion.....175

6 Overall Conclusion and Future Perspectives.....180

6.1 Overall conclusion.....180

6.1.1 DLL4- and JAG1- Notch signalling promoted different sprouting phenotypes in *in vitro* and *in vivo*.....180

6.1.2 DLL4- versus JAG1-Notch signalling.....183

6.2 Future perspectives: Targeting the DLL4- and JAG-1 Notch signalling pathway 189

7 Bibliography.....194

Appendix: Publications and Presentations 218

Table of Figures

Figure 1.1: Process of angiogenesis in tumours. 3
Figure 1.2: The Notch signalling pathway, which is mediated by a series of proteolytic events. 7
Figure 1.3: Distribution of predominant ligands and receptors, which play an important role in tumour angiogenesis. 12
Figure 3.1: A) DLL4 and B) JAG1 protein expression in HUVEC and HMEC-1 at low confluency. 54
Figure 3.2**:** Exogenous activation of Notch signalling in HUVEC 55
Figure 3.3: QPCR showing dose curve of A) rhDLL4/BSA and B) rrJAG1/BSA on DLL4 and HEY1 downstream gene expression in HUVEC at 8hr. 57
Figure 3.4**:** Downstream target gene expression profile in A) HUVEC and B) HMEC-1 stimulated with rhDLL4 (1 µg/ml) or rrJAG1 (2.6 µg/ml) over a time course. 60
Figure 3.5: Protein expression profile of DLL4, JAG1 and N1 ICD upon Notch activation 63
Figure 3.6: Protein expression profile of DLL4, JAG1 and N1 ICD upon Notch activation 64
Figure 3.7: Expression of mDLL4 and mJAG1 in HMEC-1 mDLL4 or HMEC-1 mJAG1 over-expressing cells respectively at both the A) transcript level and B) protein level, indicating successful retroviral transduction. 66
Figure 3.8: The up-regulation of downstream and target genes in over-expressing cell lines. 67
Figure 3.9**:** mDLL4 and mJAG1 did not affect HMEC-1 cell number relative to EV cells. 68
Figure 3.10**:** DBZ (200nM) inhibited Notch signalling in HMEC-1 EV and HMEC-1 mDLL4 at 8hr. 69
Figure 3.11**:** mDLL4 and mJAG1 promoted HMEC-1 cell migration. 70
Figure 3.12**:** mDLL4 reduced number of nodes and polygons whereas mJAG1increased number of nodes and polygons on the Matrigel assay after 8hr, relative to EV control. .. 72
Figure 3.13**:** A) Effect of mDLL4 and mJAG1 on sprouting in HMEC-1 spheroids over a time course and B) changes quantified on Day3. 74
Figure 3.14**:** Confirmation of successful knockdown of DLL4 expression on the mRNA level A) by two different siRNA duplexes (20nM) and B) over a time course, as well as reduction of DLL4 protein expression over a time course using Duplex 2, confirmed by C) western blot and D) immunofluorescence, compared to Scrambled (Scr) control. 76
Figure 3.15**:** Confirmation of successful knockdown of JAG1 expression on the mRNA level A) by two different siRNA duplexes (5nM) and B) over a time course, as well as reduction of DLL4 protein expression over a time course using Duplex 2, confirmed by C) western blot and D) immunofluorescence, compared to Scrambled (Scr) control. 77
Figure 3.16**:** Both A) DLL4 and B) JAG1 knockdown reduced HMEC-1 cell number compared to the Scrambled (Scr) and Mock growth curves. 78
Figure 3.17**:** Silencing of either A) DLL4 or B) JAG1 hampered migration of HMEC-1 cells. 79
Figure 3.18**:** Effect of A) DLL4 or B) JAG1 siRNA in HMEC-1 cells on network formation. 81
Figure 3.19**:** Effect of DLL4 suppression on HMEC-1 sprouting. 83
Figure 3.20**:** Effect of JAG1 suppression on HMEC-1 sprouting. 85

Figure 4.1: Expression of mDLL4 and mJAG1 in U87 transduced with mDLL4 and mJAG1 respectively at both A) the transcript and (B-C) protein level confirmed successful retroviral transduction. 103
Figure 4.2: Up-regulation of A) HEY1 and B) HES1 in mDLL4 and mJAG1 expressing U87 cells, indicating activation of Notch signalling on neighbouring cells. 104
Figure 4.3**:** mDLL4 and mJAG1 over-expressed in U87 A) decreased cell number and (B-C) U87 cells were resistant to apoptosis in normoxia (N), 0.1% hypoxia (H) and under serum starvation (-S) for 72hr *in vitro*. 105
Figure 4.4**:** A) Percentage mice survival was compiled on a Kaplan-Meier survival plot. B) Both mDLL4 and mJAG1 promoted U87 xenograft tumour growth. 107
Figure 4.5**:** Tumour growth curves of A) U87 mDLL4 and B) U87 mJAG1 compared to U87 EV, treated with DBZ (8.1 mmol/kg) or PBS (control). 108
Figure 4.6**:** Assesment of A) human HEY1 (hHEY1) and B) murine HEY1 (mHEY1) Notch target genes in xenograft tumours. 110
Figure 4.7**:** A) Overall tumour growth curves of U87 EV and U87 mDLL4 treated with DBZ (8.1 mmol/kg), bevacizumab (mAb) (10mg/kg) or PBS (control), B) linear plot of tumour volume for U87 EV and U87 mDLL4 treated with bevacizumab (mAb) (10mg/kg) or PBS (control) and C) linear plot of U87 EV and U87 mDLL4 treated with DBZ (8.1 mmol/kg) or bevacizumab (mAb) (10mg/kg). 112
Figure 4.8: tumour growth after treatment with DBZ or bevacizumab or both simultanously 115
Figure 4.9**:** A) Immunofluorescence staining for vessels, CD31 (green); pericytes, NG2 (red) and merged images (yellow) to show vascular phenotypes in xenograft models and quantification of B) vessel number C) relative vessel size and D) percentage of pericyte coverage on vessels in U87 xenograft sections. 118
Figure 4.10**:** A) Immunofluorescence staining for vessels using CD31(green) and biotinylated tomato lectin (red) to measure vessel perfusion, merged images show colocalization of tomato lectin on vessels (yellow) and B) quantification of percentage area perfusion per vessel area. 121
Figure 4.11: DLL4 expression in U87 xenograft tumours**.** 123
Figure 4.12: JAG1 expression in xenograft tumours 125
Figure 4.13: A) Histopathology staining for MIB1 in xenograft tumours and B) proliferation index of xenograft tumours. 127
Figure 4.14: A) Histopathology staining for intratumoural hypoxia using Carbonic anhydrase IX (CAIX) on xenograft tumours and B) hypoxia index of xenograft tumours and C) dual staining for CAIX (brown) and vessels (CD34) (grey). 129
Figure 4.15: A) Hematoxylin and eosin (H&E) staining on xenograft tumours and B) necrosis index of xenograft tumours. 131
Figure 4.16**:** Preliminary results: Tumour growth curves of U87 EV and U87 mJAG1 treated with 5mg/kg anti-DLL4 antibody or PBS (control). 133
Figure 4.17: Cartoon demonstrating the effects of mDLL4 over-expression on U87 A) tumour vessels and B) tumour growth. Illustration by Dr. Esther Bridges. 149
Figure 4.18: Cartoon demonstrating the effects of mJAG1 over-expression on U87 A) tumour vessels and B) tumour growth. Illustration by Dr. Esther Bridges. 151
Figure 5.1: A schematic diagram of mouse Notch1 glycosylation sites. 155
Figure 5.2: Relative expression profile of A) MFng, B) LFng and C) RFng in different cell types in the cardiovascular system as predicted by NextBio. 158
Figure 5.3: Relative quantity of A) MFng and B) LFng in 10ng RNA in a panel of tumour and endothelial cell lines compared to HUVEC 160
Figure 5.4: Fringe expression profile in HUVEC and HMEC-1 cells 161

Figure 5.5: QPCR showing transcript level of A) MFng, B) LFng, and C) RFng in HMEC-1 after 8hr of Notch stimulation on BSA, rhDLL4- and rrJAG1 coated plate. ..162
Figure 5.6: Expression profile of Manic Fringe (MFng), Lunatic Fringe (LFng) and Radical Fringe (RFng), JAG1 and PECAM1 in paired renal studies clear normal versus cell renal cell carcinoma (CCRCC), as compiled by Oncomine. 164
Figure 5.7: QPCR showing expression of A) MFng, B) LFng and C) CD31 in paired normal renal and CCRCC tumours..... 165
Figure 5.8: QPCR showing correlation of A) DLL4, B) JAG1, C) MFng and D) LFng with CD31 expression in CCRCC tumours. 166
Figure 5.9: QPCR showing correlation of A) JAG1 and DLL4, B) MFng and DLL4, C) MFng and JAG1, D) LFng and DLL4, E) LFng and JAG1 and F) LFng and MFng expression in CCRCC tumours. 167
Figure 5.10: QPCR showing relative expression of MFng, LFng, DLL4, JAG1 and CD31 normalised to β- ACTIN in CCRCC tumours. 168
Figure 5.11: QPCR confirming A) MFng over-expression in U87 and B) stable knockdown in HMEC-1. 170
Figure 5.12: Validation of Fringe antibody on A) U87 and B) HMEC-1 cytospun cells. 171
Figure 5.13: Validation of Fringe antibody on A) U87 and B) HMEC-1 formalin-fixed paraffin-embedded (FFPE) cells..... 172
Figure 5.14: Fringe (red) and CD31 (green) immunofluorescence on selected CCRCC tumours. 174
Figure 6.1: Illustration demonstrating the mechanisms that effect Notch signalling and their subsequent influence on tumour vasculature. 188

Table of Tables

Table 1.1: The role of mammalian DLL4 and JAG1 Notch ligands in angiogenesis 9
Table 3.1: Comparison between HUVEC and HMEC-1 as an angiogenic model..... 58
Table 3.2: Summary of effects of DLL4- and JAG1-Notch signalling on *in vitro* angiogenic assays compared to control EV (for over-expressing cells) or Scrambled (for siRNA gene suppression cells). 87
Table 5.1: MFng and LFng gene expression relative to β-actin in CCRCC clinical tumours 174

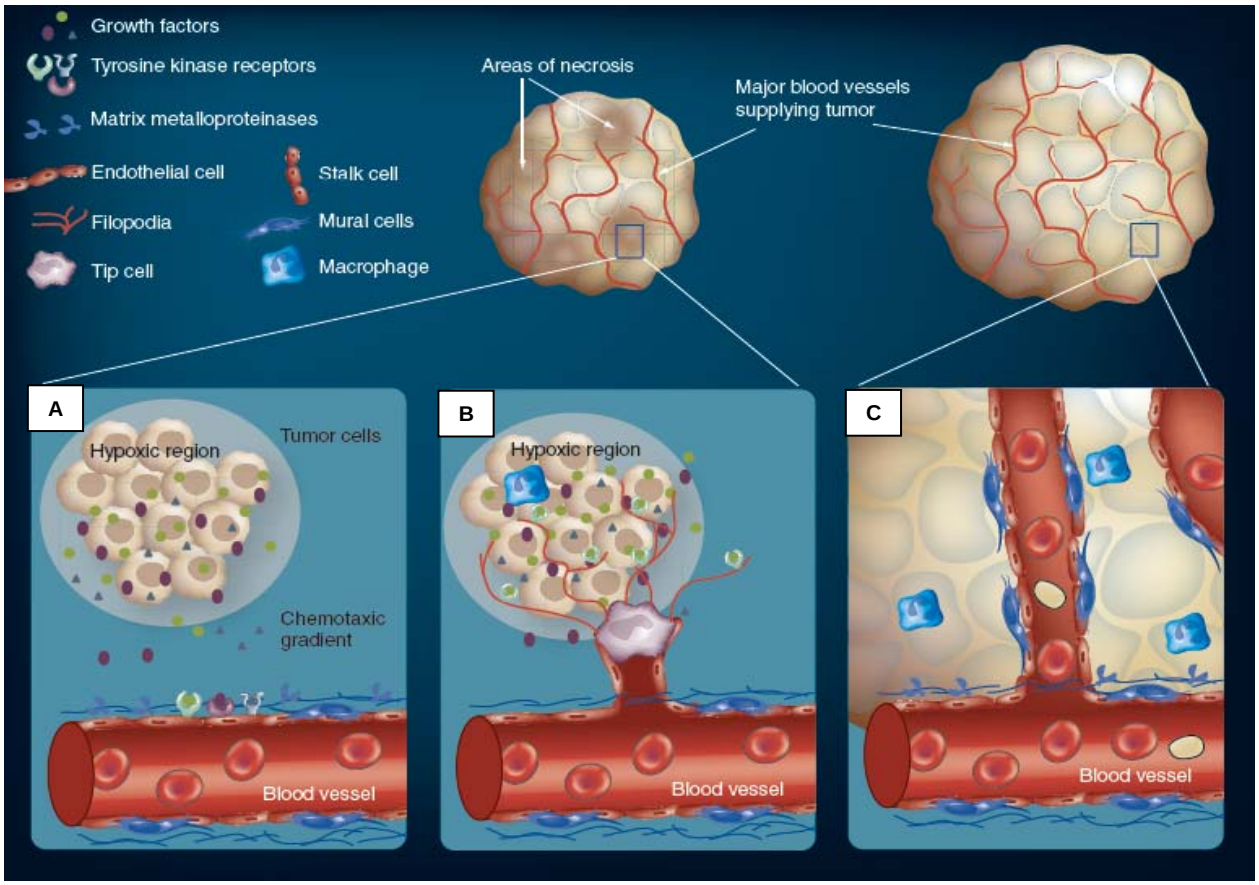
1 Introduction

The growth of new blood vessels, termed angiogenesis, is a morphogenetic process that is central to tumour growth and metastasis. Cells in the core of a tumour with a volume greater than $2mm^3$ can trigger angiogenic switch due to lack of oxygen and nutrients. Ultimately this increases the supply of nutrients and O_2 to the tumour, thereby supporting tumour growth and progression The concept of attacking tumours by cutting off their blood supply was first described in the early 1970s (Folkman 1971) and since then much effort has been put into identifying and targeting the key pathways regulating angiogenesis. It has subsequently been observed that tumour angiogenesis utilises at least some of the angiogenic signalling pathways that are required during vascular development. Growth factors, including vascular endothelial growth factor (VEGF; also known as VEGF-A) secreted by tumour cells and basic fibroblast growth factor (bFGF; also known as FGF2) secreted by tumour fibroblasts, activate angiogenic signalling pathways.

The Notch signalling pathway is a conserved ligand-receptor cascade that plays a role in guiding a variety of cell fate decisions (Artavanis-Tsakonas et al. 1999; Bolos et al. 2007). Notch signalling has been found to be a key pathway involved in modulating the response to an angiogenic stimulus during both vascular development and postnatal angiogenesis. This introduction will compare Notch signalling in vascular development and disease, specifically focusing on two key Notch ligands, Delta-like (DLL)4 and Jagged1 (JAG1), as well as their role in tumour growth. Cross-talk of the Notch pathway with other signalling pathways will also be reviewed.

1.1 Formation of new blood vessels

During early embryonic development, the *de novo* vessel formation from angioblasts forms the primitive vascular plexus in a process termed vasculogenesis. Physiological angiogenesis is essential for the reproduction, repair and development of blood vessels from existing blood vessels. Primarily the process of angiogenesis involves stimulation of endothelial cells that line the luminal surface of the blood vessel (Figure 1.1 A). Endothelial cells release proteases, for example matrix metalloproteinases, which breakdown the surrounding basal extracellular membrane. Endothelial cells penetrate through the extracellular membrane and enter the underlying tissue. This sprouting process is spearheaded by leading endothelial tip cells that migrate along the chemotaxic gradient towards the source of the angiogenic stimuli (Figure 1 B)(Gerhardt 2008). Tip cells produce long dynamic filopodia studded with tyrosine kinase receptors that enable cells to probe the environment for directional cues. These tip cells display a non-proliferative, highly motile and tubeless phenotype. Endothelial stalk cells follow the tip cells, proliferate and migrate in response to the environmental cues. The stalk cells also become polarised and co-ordinate the formation of the vascular lumen (Kamei et al. 2006; Iruela-Arispe and Davis 2009) and establish adherens tight junctions (Dejana et al. 2009) to maintain the integrity of the new sprout, in the later stages of angiogenesis (Figure 1.1 C). Matrix remodelling and a new basement membrane is generated as the vessel matures (Iruela-Arispe and Davis 2009). The new blood vessel is further stabilised by the recruitment of mural cells, such as pericytes (von Tell et al. 2006).



Bridges, Oon and Harris, 2011 (Future Oncology, in press)

Figure 1.1: Process of angiogenesis in tumours.

The formation of new blood vessels summarised into three basic steps: A) stimulation of endothelial cells by pro-angiogenic factors secreted by tumour cells in response to hypoxia results in the degradation of basement membrane; B) activated endothelial cells then sprout towards stimulus, the direction of the growing blood vessel being guided by the tip cell, C) with the maturation of new blood vessels involving the generation of a new basement membrane and recruitment of pericytes. As a result increased tumour growth is supported.

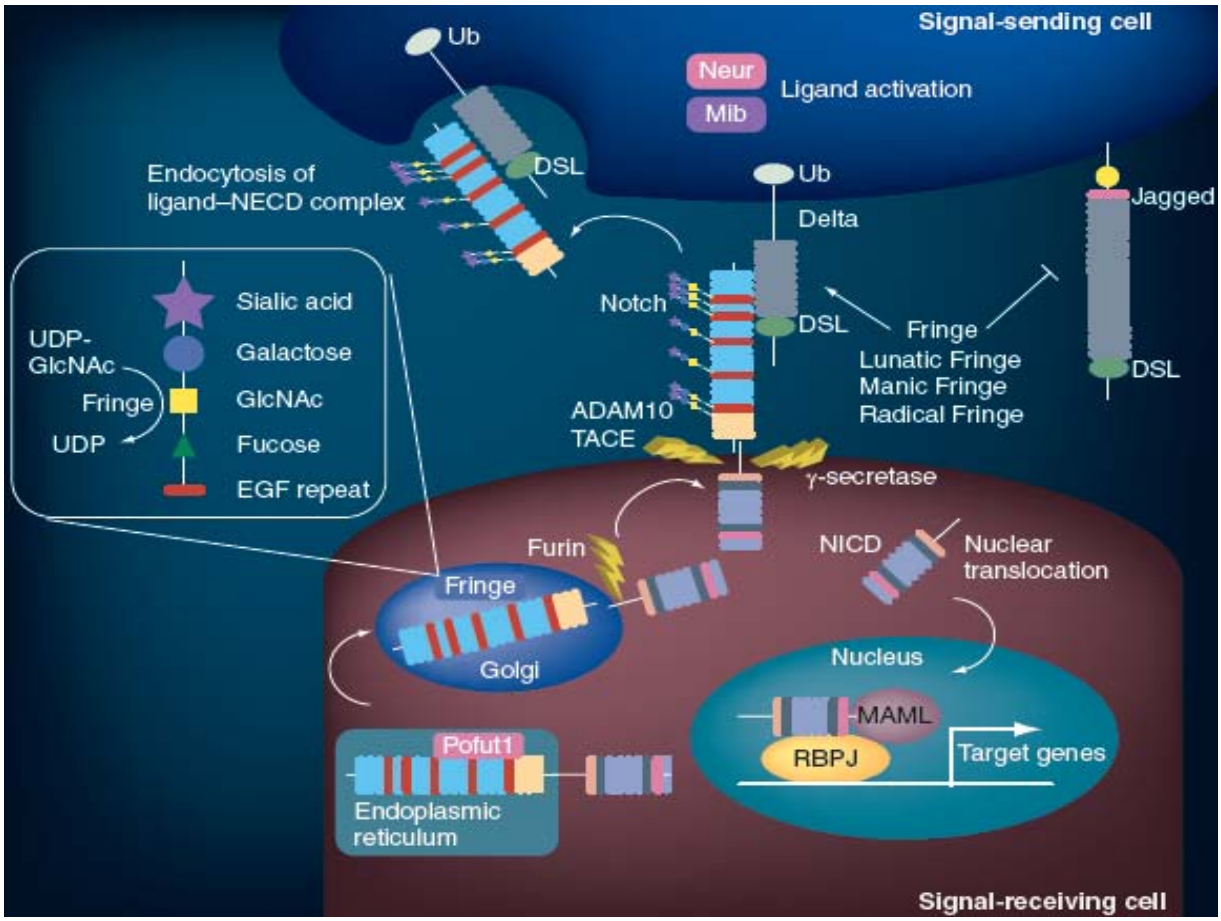
Angiogenesis is dependent on a finely tuned equilibrium between anti-angiogenic and pro-angiogenic molecules. The angiogenic switch within tumours occurs when the pro-angiogenic stimulus is stronger than that of the anti-angiogenic resistance (Hanahan and Folkman 1996; Bergers and Benjamin 2003). Of all the pro-angiogenic molecules the most prominent and best characterised is the VEGF pathway. VEGF was among the first identified pro-angiogenic proteins executing a key function in all stages of angiogenesis, depicted in Figure 1.1 (Gerhardt 2008). The VEGF receptor (VEGFR)-1 (Flt1), VEGFR-2 (KDR, Flk1) and VEGFR-3 (Flt4) are transmembrane receptor tyrosine kinases that dimerise and become activated on ligand binding, activating signalling cascades involving ERK1/2 and AKT (Olsson et al. 2006). VEGFR-2 is prominently expressed in tip cells and in response to the presence of VEGF, promotes the polarised expression of tip cell filopodia, enabling endothelial cell guidance along the angiogenic signal gradient (Gerhardt 2008). The VEGFR-1 is thought to modulate VEGFR-2 signalling by acting as a decoy receptor, sequestering VEGF from VEGFR-2 (Kappas et al. 2008). A recent study has demonstrated a role of VEGFR3 in sprouting angiogenesis, in response to VEGF-C (Tammela et al. 2008). This is further supported by Benedito and colleagues (2009) who have demonstrated that decreased expression of VEGFR3 in tip cells suppressed sprouting. In response to the presence of VEGF the newly formed blood vessel are then stabilised through the recruitment of mural cells like pericytes and vascular smooth muscle cells (Gerhardt and Betsholtz 2003; Bergers and Song 2005; Gaetani et al. 2010).

1.2 The classical Notch signalling pathway

The Notch family of ligands and receptors are type I transmembrane proteins (Figure 1.2). In mammals, there are four known Notch receptors (Notch1, Notch2, Notch3 and Notch 4) (Kopan and Ilagan 2009; Pratt et al. 2010). The Notch receptors consist of a signal peptide, an extracellular domain implicated with ligand interaction, a transmembrane domain that is involved in receptor activation and an intracellular signalling domain. An important structural characteristic of these receptors is the presence of epidermal growth factor repeats at the extracellular domain where Notch signalling is activated. The Notch receptor is pre-cleaved by furin-like convertase and further modified by Fringe in the Golgi to produce a fully functional receptor, before it is targeted to the plasma membrane as a heterodimer, held together by non-covalent interactions. Five Notch ligands have been identified to date, Jagged1 (JAG1), Jagged2 (JAG2), Delta-like (DLL-) 1,3 and 4 which bind to the epidermal growth factor repeat of the Notch receptor through the Delta/ Serrate/ Lag2 (DSL) domain.

Notch signalling is dependent on close cell-to-cell contact. The 'canonical' Notch signalling pathway (Kopan and Ilagan 2009; Pratt et al. 2010), summarised in Figure 1.2, is initiated when the extracellular domain of the Notch ligand expressed on the surface of the signalling cell engages with the extracellular domain of the Notch receptor expressed on the neighbouring cell (the receiving cell). Upon binding to the ligand, the Notch receptor in signal-receiving cells undergoes a conformational change, which triggers the proteolytic activation of the receptor. The Notch receptor is sequentially cleaved, firstly by a metalloprotease of the ADAM (a disintegrin and metalloprotease) family, for example ADAM 10 or the TNFα converting enzyme (Brou et al. 2000; Mumm et al. 2000). The extracellular domain of the receptor is endocytosed by the signalling cell. This primes the

remaining Notch receptor for additional proteolytic cleavage within the transmembrane domain by γ-secretase, which leads to the release of the notch intracellular domain into the cytoplasm of the signal receiving cell. The liberated notch intracellular domain is then translocated into the nucleus and interaction with the transcriptional repressor factor CSL (named after mammalian CBF1/RBP-Jκ, drosophilia Su(H), and C.elegans Lag1) converts CSL to a transcriptional activator (Jarriault et al. 1995; Schroeter et al. 1998). Mastermind-like coactivators are also recruited (Petcherski and Kimble 2000; Wu et al. 2000; Wu et al. 2002; Nam et al. 2006). This results in induction or down regulation of various downstream targets of Notch signalling. The best characterised downstream targets include the basic helix-loop-helix family of transcriptional repressors, the Hairy and Enhancer of Split (HES-1, -5, -7) and Hes-related (HEY-1, -2, -L) protein families (Iso et al. 2003).



Bridges, Oon and Harris, 2011 (Future Oncology, in press)

Figure 1.2: The Notch signalling pathway, which is mediated by a series of proteolytic events.

The notch receptor is O-fucosylated at the epidermal growth factor domains by POFUT1 in the endoplasmic reticulum which is required for Notch trafficking, pre-cleaved in the Golgi by furin-like convertase and further modified by Fringe, which is essential in the activation of notch signalling. The heterodimeric receptor is targeted to the plasma membrane where it undergoes cleavage by ADAM 10/ TACE at the extracellular site. The ligand-Notch extracellular domain complex is then endocytosed by the neighbouring cell rendering further cleavage of the receptor by gamma-secretase at the intracellular site. The liberated Notch intracellular domain is translocated into the nucleus to bind to CSL/RBP-Jκ, and the MAML co-activator which results in the regulation of notch target genes. Fringe has been shown to potentiate Delta-Notch but inhibit Jagged-Notch signalling. Key: POFUT1= Protein O-fucosyltranferase, DSL=Delta Serrate Lag2, NECD=Notch extracellular domain, NICD=Notch intracellular domain, CSL= CBF1/RBP-Jκ, Drosophilia Su(H), and ***Caenorhabditis elegans*** Lag1, MAML=Master mind like, TACE=TNF-alpha converting enzyme, Neur=Neuralised, Mib=Mind bomb

1.3 The regulation of new blood vessels during development

The Notch signalling pathway is involved in many biological processes, such as cell fate specification, differentiation, proliferation, apoptosis, migration and angiogenesis (Artavanis-Tsakonas et al. 1999; Bolos et al. 2007). The mammalian expression of Notch ligands and receptors varies both spatially and temporally, which influences the fate of the cell when Notch signalling is activated. Notch signalling plays a critical role during the proper construction of the vascular system by cross talking with other signalling pathways, as well as angiogenesis (Lawson et al. 2001; Hofmann and Iruela-Arispe 2007; Hurlbut et al. 2007). Several components of the Notch pathway are expressed in the vasculature: Notch1, Notch3, Notch4 receptors and DLL1, DLL4, JAG1, JAG2 ligands. Of particular interest are the ligands DLL4 and JAG1, which are implicated in tumour angiogenesis (Table 1.1). Evidence of a role of Notch components in the formation and stabilisation of blood vessels is provided by *in vivo* studies modulating the expression of the Notch receptor or ligand during development. The primary vascular plexus in mice begins remodelling approximately around embryonic day (E) 9.5-E11.5, leading to the establishment of arteries and veins. During early mouse embryogenesis, DLL4 is the first Notch ligand to be expressed in a robust manner followed by JAG1 (Iso et al. 2003). DLL4 is expressed in the heart as well as in the endothelium of blood vessels (Mailhos et al. 2001; Gale et al. 2004). Haploinsufficiency for DLL4 in mice led to embryonic death at E10.5 due to vascular defects and disrupted basement membrane around the aorta (Gale et al. 2004; Krebs et al. 2004; Benedito et al. 2008). DLL4 null mice displayed more severe embryonic vascular defects and embryonic death was observed at E9.5 (Duarte et al. 2004). Excessive non-productive angiogenesis has also been reported in zebrafish and mice retina model following loss of DLL4 expression (Gerhardt 2008).

Table 1.1: The role of mammalian DLL4 and JAG1 Notch ligands in angiogenesis

Sites of expression	Role in angiogenesis	Effect of expression	Effect following loss of expression	References
DLL4				
Endothelial cells	Arterial specification Tip and stalk cell differentiation during angiogenesis	↓Proliferation ↓Migration ↓Sprouting	↑Sprouts ↑Proliferation	(Krebs et al. 2000; Villa et al. 2001; Liu et al. 2003; Gale et al. 2004; Krebs et al. 2004; Hellstrom et al. 2007; Hodkinson et al. 2007; Leslie et al. 2007; Lobov et al. 2007; Siekmann and Lawson 2007; Suchting et al. 2007; Benedito et al. 2008; Harrington et al. 2008; Trindade et al. 2008; Schadler et al. 2010)
Vascular smooth muscle cells	Smooth muscle differentiation and maturation	Modulates matrix production, assembly, cell adhesion	-	
JAG1				
Endothelial cells	Arterial specification Tip and stalk cell differentiation during angiogenesis	↓Proliferation ↑Sprouts ↑Migration	↓Sprouts ↓Proliferation	(Krebs et al. 2000; Villa et al. 2001; Zeng et al. 2005; Benedito et al. 2009; Liu et al. 2009)
Vascular smooth muscle cells	Smooth muscle differentiation and maturation	Modulates matrix production, assembly, cell adhesion	↓Vascular smooth muscle cell coverage	

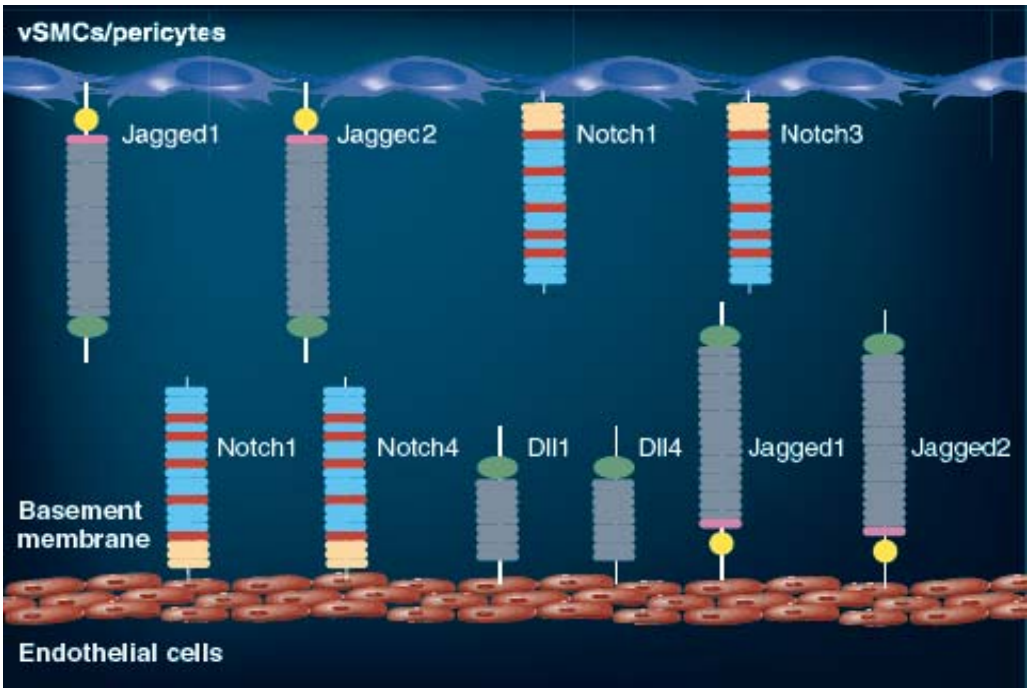
JAG1 expression can be found expressed in the endothelium of blood vessels, as well as in vascular smooth muscle cells. Similarly, mice with global or endothelium specific knockout of JAG1 display embryonic lethality at E11.5, with reported less elaborate vascular networks

and smaller vessels, as well as a significant reduction of sprouting angiogenesis and vessel branching being observed (Xue et al. 1999; High et al. 2008; Benedito et al. 2009). Additionally, loss of JAG1 expression in endothelial cells resulted in a significant reduction in the coverage of vascular smooth muscle cells on the arteries in a retinal angiogenesis model (Benedito et al. 2009) and in mouse embryos (Xue et al. 1999; High et al. 2008; Benedito et al. 2009). Combining these data together suggests that JAG1 expressed in endothelial cells can induce Notch signalling in neighbouring vascular smooth muscle cells (and *vice-versa*), and may be important for maturing blood vessels, a paradigm uncovering the activation of Notch signalling between different cell types.

The Notch receptors are also critically important for the proper construction of the vascular system. In mice Notch1 and Notch4 is expressed within and around the developing vasculature, though Notch1 and Notch4 are found predominantly expressed in arterial endothelial cells by E13.5 (Krebs et al. 2000; Limbourg et al. 2005). Global knockout of Notch1 resulted in embryo death at E11.5, due to profound failure of blood vessel to form organised vascular networks (Krebs et al. 2000). While Notch4 mutants are viable and develop normally, the Notch1/Notch4 double mutants contribute to embryonic lethality and more severe vascular defects, indicating that Notch1 and Notch4 are partially redundant (Krebs et al. 2000; Krebs et al. 2004). Interestingly, when the activated Notch4 NICD was over-expressed defective angiogenesis was also observed, which resulted in embryonic death (Uyttendaele et al. 2001). Such studies indicate the importance of having a temporal and spatial localised activation of the Notch signalling pathway in regulating normal vasculature development. Mice with a double knockout of HEY-1 and HEY-2 also died during early embryonic development, due to the vascular plexus remodelling defects and arterial venous differentiation defects (Fischer et al. 2004). It is clear then that the proper regulation of the

Notch pathway is critically important for the construction of a functional vascular system during embryogenesis in mammals.

Further studies have also demonstrated that Notch signalling is indispensible in post-natal angiogenesis (Takeshita et al. 2007). Notch1 is found broadly expressed in many tissues, including the vascular endothelium, and in mural cells such as the vascular smooth muscle cells and pericytes (Krebs et al. 2000; Hofmann and Iruela-Arispe 2007; Peault et al. 2007). Notch3 is predominantly expressed in vascular smooth muscle cells, whereas Notch4 expression becomes restricted to vascular endothelial cells (Krebs et al. 2000; Peault et al. 2007; Murphy et al. 2008). Similarly, DLL1, DLL4 and JAG1, JAG2 are the predominant ligands in the endothelium (Villa et al. 2001; Hofmann and Luisa Iruela-Arispe 2007; Sorensen et al. 2009); JAG1 and JAG2 are expressed in the vascular smooth muscle cells (Hofmann and Iruela-Arispe 2007; High et al. 2008) (Figure 1.3).



Bridges, Oon and Harris, 2011 (Future Oncology, in press)

Figure 1.3: Distribution of predominant ligands and receptors, which play an important role in tumour angiogenesis.

Notch signalling is activated through cell-to-cell contact. Ligands can bind to receptors in the same cell type (vascular smooth muscle cells/pericyte-vascular smooth muscle cells/pericyte or endothelial cell- endothelial cell) or different cell type (eg. vascular smooth muscle cells/pericyte- endothelial cell).

1.4 Role of Notch signalling in tumour biology

Notch signalling is also important in various pathological states. The tumourigenic property of Notch is usually associated with ligand up-regulation, expression of active Notch receptors or modulation of pathways that regulate Notch signalling, as discussed further in the following sections.

1.4.1 Aberrant expression of Notch ligands and receptors in solid tumours

Deregulation of the Notch3 pathway in the vascular system leads to hereditary vascular disorders, such as CADASIL (cerebral autosomal dominant arteriopathy with subcortical infarcts and leukoencephalopathy) which causes abnormality in the vascular smooth muscle cells and result in blood vessel damage, causing migraines and other impairments of normal brain function (Arboleda-Velasquez et al. 2005; Louvi et al. 2006). Mutations in JAG1 cause Alagille syndrome, an autosomal dominant vascular disorder in humans. Patients with Alagille syndrome may have a narrowing pulmonary arteries or diaplay abnormalities of the carotid arteries which can lead to serious heart problems or stroke (Oda et al. 1997; Kamath et al. 2004; High et al. 2008).

Overall, aberrant gain or loss of Notch signalling components has also been linked to multiple human diseases and cancers, including T-cell acute lymhoblastic leukaemia/lymphoma, breast, colon, ovarian, osteosarcoma, squamous cell carcinoma, glioma and lung cancer (Dang et al. 2000; Pece et al. 2004; van Es et al. 2005; Bolos et al. 2007; Reedijk et al. 2008; Ferrando 2009; Rao et al. 2009; Tammam et al. 2009; Wang et al. 2009; Westhoff et al. 2009; Gaetani et al. 2010; Harrison et al. 2010; Hijioka et al. 2010; Jung et al. 2010; Kamstrup et al. 2010; Li et al. 2010; Rose et al. 2010; Wustehube et al. 2010; Zhang et al. 2010; Zhao et al. 2010). In particular, DLL4 has been found expressed in glioblastoma, colon cancer, renal cancer, breast cancer and Ewing's Sarcoma (Oishi et al. ; Mailhos et al. 2001; Patel et al. 2005; Noguera-Troise et al. 2006; Ridgway et al. 2006; Hellstrom et al. 2007; Li et al. 2007; Scehnet et al. 2007; Hoey et al. 2009; Jubb et al. 2009; Schadler et al. 2010). JAG1 has been found expressed in cervical, head and neck cancer, breast, prostate and colon cancer (Guilmeau et al. ; Veeraraghavalu et al. 2004; Reedijk et al. 2005; Veeraraghavalu et al. 2005;

Zeng et al. 2005; Baliko et al. 2007; Ramdass et al. 2007; D'Souza et al. 2008; Benedito et al. 2009; Pannequin et al. 2009; Rodilla et al. 2009; Lin et al.). Evidence of activated Notch signalling was found within gliomas (Shih and Holland 2006) and in over 50% of human breast cancers evaluated (Pece et al. 2004). Notch activation in tumour cells promotes survival and proliferation (e.g. (Radtke and Raj 2003)). Additionally Notch activation in tumour endothelium can regulate tumour angiogenesis (e.g. (Reedijk et al. 2005; Zeng et al. 2005; Funahashi et al. 2008)), progression and invasion (Pang et al. 2010). This can be illustrated by examining the correlation of Notch ligands and receptors with markers of proliferation (e.g. Ki67), markers of apoptosis (TUNEL) and patient outcome in various solid tumours. For example, expression of Notch1 and/or JAG1 in the tumour compartment was associated with a poor survival outcome in breast cancer (Reedijk et al. 2005; Dickson et al. 2007; Reedijk et al. 2008), head and neck squamous cell carcinoma (Gu et al. 2010; Lin et al. 2010) and colon cancer (Reedijk et al. 2008; Sancho et al. 2010; Sikandar et al. 2010). Notch1 and JAG1 expression was found to influence tumour cell survival, proliferation (Purow et al. 2005; Reedijk et al. 2005; Stylianou et al. 2006; Harrison et al. 2010; Ling et al. 2010; Yao et al. 2010), and growth (Guilmeau et al. 2010). Notch1 and Notch4 have recently been shown to positively correlate with poor prognostic factors in breast cancer, such as node status and tumour grade (Stylianou et al. 2006; Harrison et al. 2010; Ling et al. 2010; Yao et al. 2010). However, Notch1 may act as a tumour suppressor in some cancer types, including pancreatic ductal adenocarcinoma, thyroid cancer cells and lung adenocarcinoma (Dotto 2008; Xiao et al. 2009; Eliasz et al. 2010; Hanlon et al. 2010).

A variety of studies have also focused on the expression profile of the Notch components in the vasculature compartment within tumours and compared differences in expression in normal healthy tissue. DLL4 expression was found up-regulated in tumour vasculature

compared to normal vessels (Mailhos et al. 2001; Li et al. 2010; Schadler et al. 2010), for example, DLL4 expression in blood vessels in clear cell renal tumours (Mailhos et al. 2001) was higher than normal kidney tissue (Patel et al. 2005) and correlated with vessel maturation (Patel et al. 2006). DLL4 was also expressed in the endothelium of colon cancer but not the normal mucosa (Mailhos et al. 2001; Jubb et al. 2009). DLL4 expression in the colon vasculature endothelium was not associated with a poor outcome in patients, however, it was strongly associated with VEGF and hypoxia markers, which do correlate with poor outcome (Jubb et al. 2009). While DLL4 is robustly expressed in tumour vasculatures, DLL4 was also detected in perinecrotic areas of 20% of human glioblastoma samples by *in situ* hybridisation (Li et al. 2007). Although the other Notch ligands have been less studied in terms of tumour vasculature, DLL1 has been reported to be associated with tumour angiogenesis (Urs et al. 2008). DLL4 was upregulated in the vasculature of human xenograft tumours (Mailhos et al. 2001; Noguera-Troise et al. 2006), linking the role of DLL4-Notch signalling in pathological angiogenesis within preclinical models. However, over expression of DLL4 in tumour cells does not always correlate with increased xenograft (mouse BL41 and human MOPC315) tumour growth (Segarra et al. 2008). The difference in results might reflect the cell type used (Segarra et al. 2008), for example enhanced tumour growth was observed in the U87 glioblastoma cell line that over expressed DLL4 in another study (Li et al. 2007).

1.5 Mechanisms that effect Notch signalling and their subsequent influence on tumour vasculature

Notch signalling is dependent on cell-cell contact and therefore changes in the function or expression of the ligands or receptors can modify the magnitude of Notch signalling in the

signal receiving cell. Additionally, Notch signalling could be induced in endothelial cells by either neighbouring stromal cells, tumour cells, or cells from distant parts of the tumour.

1.5.1 Fringe can modulate Notch signalling pathway in cells

Notch signalling is regulated by post-translational modification events, such as glycosylation of the extracellular domain of both the receptor and the ligands, which can then affect the ability of the Notch receptor and ligands to interact (Moloney et al. 2000; Acar et al. 2008). Three mammalian Fringe homologues encode a glycosyltransferase that transfers N-acetylglucosamine (GlcNAc) to fucose on Notch epidermal growth factor repeats: Lunatic fringe (LFng), Radical fringe (RFng) and Manic fringe (MFng) (Johnston et al. 1997). To answer questions pertaining to the role of Fringe in angiogenesis, a comprehensive study was carried out to study the effect of global LFng double knock-down in a mouse retinal model and subsequently demonstrated for the first time that Fringe mediates the differential regulation of DLL4- and JAG1- Notch signalling in physiological angiogenesis (Benedito et al. 2009). They reported increased angiogenesis, enhanced endothelial coverage and increased tip cell number in LFng deficient retinas (P4) compared to controls. *In situ* hybridisation for MFng in normal P6 retinas showed high expression of the protein in venules, arterioles and front tip, indicating the abundance of Fringe expression in endothelial cells.

Currently few studies have investigated the role of the Fringe enzymes in tumour biology. MFng has been found to be up-regulated by EWS/FLI1, a fusion gene found in Ewing's sarcoma, which subsequently promoted cellular transformation in NIH3T3 cells in severe combined immunodeficiency disease mice (May et al. 1997; Baliko et al. 2007). A recent study has shown that LFng is up-regulated in human colon adenocarcinoma through

activation of Notch signalling (Reedijk et al. 2008). In contrast, the activation of Notch in cervical cancer is dependent on JAG1, which has been modified by MFNG to negatively regulate notch signalling (Veeraraghavalu et al. 2004), indicating that Notch signalling in different tumour backgrounds can result in promoting different phenotypes. It would be of interest to see if further studies demonstrate aberrant expression of the Fringe in tumour endothelium and the subsequent influence on Notch signalling and tumour vasculature.

1.5.2 Tumour associated growth factors produced by tumour, stromal and inflammatory cells can induce Notch ligand expression in endothelial cells.

The environment within tumours, resulting in the presence of growth factors, can greatly influence the expression of Notch ligands and Notch signalling (Figure 1.1). This in turn mediates pathological angiogenesis. Hypoxic (low levels of oxygen) areas within the tumour, caused by a deficient vascular supply, is a hallmark of cancer and one of the major stimuli to initiate angiogenesis (Fraisl et al. 2009). Hypoxia leads to the up-regulation of hypoxia inducible factors (HIF)-1α, HIF-2α, which are critical regulators of pro-angiogenic signals, such as VEGF (Ikeda et al. 1995; Blancher et al. 2000; Maxwell and Ratcliffe 2002). Various growth factors secreted by tumour cells can recruit different cell types to the tumour, including tumour associated stromal fibroblasts and inflammatory cells. Both tumour associated fibroblasts and inflammatory cells can in turn secrete a variety of growth factors, that can also stimulate tumour angiogenesis and growth (Sparmann and Bar-Sagi 2004; Orimo et al. 2005); these growth factors include TGFβ and PDGFB.

The emerging picture is that the VEGF pathway acts as a central driver for angiogenesis, whereas Notch signalling helps to shape the response appropriately. In order to ensure a stable

blood vessel is formed endothelial cells adopt different phenotypes (i.e. tip or a stalk cell phenotype) during the stages of angiogenesis (Figure 1.1).

Notch signalling, in particular DLL4-Notch interaction, enables the selection and discrimination between the tip cells and the stalk cells, during the early sprouting phase of both physiological and pathological angiogenesis (Phng and Gerhardt 2009). Investigations have revealed that it is the tip endothelial cell that predominantly expresses DLL4 (Claxton and Fruttiger 2004). DLL4 expression is up-regulated in endothelial cells that are cultured under hypoxic conditions (Patel et al. 2005; Diez et al. 2007) and by various growth factors, including VEGF and bFGF (Liu et al. 2003; Patel et al. 2005; Patel et al. 2006; Seo et al. 2006; Williams et al. 2006; Lobov et al. 2007; Gerhardt 2008; Hayashi and Kume 2008). Blockade of VEGF in tumour bearing mice resulted in a rapid and profound reduction in DLL4 expression in tumour blood vessels (Noguera-Troise et al. 2006).

Following stimulation with VEGF, for example, and subsequent induction of DLL4 expression, DLL4-Notch signalling can be induced in the neighbouring signal receiving cell (Figure 3 A). DLL4-Notch signalling results in the transcriptional inhibition of both VEGFR2 and its co-receptor NRP-1 in the signal receiving cell (Taylor et al. 2002; Williams et al. 2006; Harrington et al. 2008). Notch signalling also up-regulates the expression of both the soluble and full-length forms of the VEGF decoy receptor VEGFR1 (Harrington et al. 2008). As a consequence the signal receiving cell is unable to form a tip cell phenotype in response to VEGF and differentiates towards a stalk cell phenotype, whereas the signal sending cell forms a tip cell phenotype (Williams et al. 2006). When DLL4-Notch signalling is blocked then all endothelial cells can act indiscriminately to the VEGF stimulus and the majority of

cells form tip cells with filopodia (Gerhardt 2008; Phng and Gerhardt 2009). Sprouting, branching and fusion of endothelial tubes also become dramatically increased.

Endothelial cell proliferation can also be restricted following DLL4-Notch signalling (Harrington et al. 2008). For example, VEGF dependent proliferation in neighbouring cells is blocked by notch signalling, by reducing phosphorylation of ERK1/2 and AKT after VEGF stimulation (Liu et al. 2003), and cells become growth arrested in the G0/G1 phases of the cell cycle (Noseda et al. 2004; Williams et al. 2006). Notch signalling can also aid endothelial cell survival by inducing the expression of the anti-apoptotic protein BCL-2 (MacKenzie et al. 2004). A recent study has also shown that Notch activates the expression of VEGFR3, which responds to VEGF-C to protect endothelial cells from apoptosis (Shawber et al. 2007). The resulting picture from these studies is that DLL4-Notch signalling in particular functions in an anti-angiogenic capacity by restricting the development of new sprouts by reducing the tip cell phenotype in endothelial cells, as well as promoting a quiescent and mature vascular phenotype.

In a FGF expressing mammary cell line Mm5MT cells it was found that JAG1 expression was elevated (Funahashi et al. 2008). Crosstalk between Wnt and Notch signalling pathways through beta-catenin mediated up-regulation of Notch components, including DLL4 and JAG1 (Katoh 2006; Wang et al. 2007; Coant et al. 2010; Corada et al. 2010; Yamamizu et al. 2010). Growth factors have also been shown to modulate the expression of various Notch ligands in the same cell. For instance, TNFα up-regulated JAG1 expression but reduced DLL4, thus promoting tumour angiogenesis (Sainson et al. 2008). However, it is not completely clear what specific cellular events are stimulated by JAG1, which appears to have different effects on the vasculature to those observed for DLL4. JAG1 is strongly expressed in

the stalk cells, whereas DLL4 is expressed predominantly in tip cells. JAG1 antagonised DLL4-Notch signalling during sprouting angiogenesis in a mouse retina model, thereby enhancing angiogenesis (Benedito et al. 2009). The difference between DLL4 and JAG1 Notch signalling highlights the importance of these ligands in tumour angiogenesis and will be investigated in this thesis.

1.5.3 Interaction with neighbouring vascular cells, tumour cells and inflammatory cells

Expression of Notch ligands and receptors is not restricted to endothelial cells. Research has indicated that tumour and tumour associated stromal cells can also express various ligands, which can subsequently induce Notch signalling in tumour endothelial cells. DLL4 expression was also found induced by interleukin-6,-8 in non-endothelial stromal cells, by signalling through the STAT3/JAK pathway (Sparmann and Bar-Sagi 2004; Suzuki et al. 2006). Similarly, JAG1 ligand expressed on non-endothelial cells has recently been identified as having a role in tumour angiogenesis, as suggested by an extensive analysis of head and neck squamous cell carcinomas (Zeng et al. 2005). JAG1 expression was induced in head and neck squamous cell carcinoma tumour cells by growth factors, following the activation of mitogen activated protein kinase (MAPK) pathway (Zeng et al. 2005). This was reflected in *in vitro* work done on primary endothelial cell cultures where JAG1/Notch4 signalling was also found to be regulated in a MAPK dependent manner (Kiec-Wilk et al. 2010). JAG1 expressing tumour cells were able to signal to neighbouring endothelial cells and thereby contribute to tumour neovascularisation and tumour growth in mice (Zeng et al. 2005); in contrast, loss of JAG1 in these tumour cells inhibited the pro-angiogenic effects of head and neck squamous cell carcinoma.

Cross-talk between endothelial cells and tumour cells, promoting Notch signalling and therefore angiogenesis has implications for tumour progression. The angiogenic switch is an event that has been well documented to support tumour growth and progression. However tumour angiogenesis has also been linked to tumour dormancy and outgrowth (more extensively covered in recent reviews (e.g. (Aguirre-Ghiso 2007; Moserle et al. 2009; Almog 2010)). Tumour dormancy is a protracted stage during tumour progression where the tumours become occult and asymptomatic and can remain in this stage for years before progressing into more aggressive tumours. These tumours are often found devoid of angiogenic capacity (Aguirre-Ghiso 2007).

Various growth factors secreted by tumour cells can recruit inflammatory cells as well as mural cells such as pericytes and vascular smooth muscle cells. Tumour endothelial cells expressing JAG1 could also assist in the recruitment of vascular smooth muscle cells and pericytes, which help maintain the integrity of the blood vessel (von Tell et al. 2006). Studies have demonstrated JAG1 is expressed in vascular smooth muscle cells (Villa et al. 2001; Prakash et al. 2002) and recently expression of DLL4 in vascular smooth muscle cells within Ewing's Sarcoma tumours has been described (Schadler et al. 2010). Therefore vascular smooth muscle cells expressing JAG1 recruited to the tumour have also the potential to influence the developing vasculature within the tumour. Constitutive mutant Notch3 receptor expression can promote enlarged vessels with a reduced number of pericytes or vascular smooth muscle cells in mice (Wang et al. 2008) Additionally, CADASIL patients with mutant Notch3 receptor, although it is unclear if the CADASIL mutations reflect receptor gain or loss of function, also have vessels lacking pericytes, resulting in the deficiencies in arteriole formation (Louvi et al. 2006). DLL4 signalling in tumour models can also modulate the

recruitment of pericytes, affecting blood vessel lumen size (Li et al. 2007; Scehnet et al. 2007). One could conclude that pericytes may function to regulate blood vessel lumen size and blood supply to tumours.

It is evident that tumour stroma cells can interact with tumour cells to contribute to tumourigenesis and angiogenesis through mediation of chemokines and growth factors (Bingle et al. 2002; Leek et al. 2002; Sivridis et al. 2002; Lin and Karin 2007). Tumour-associated-macrophages accumulate in poorly vascularised thus hypoxic areas and surrounding tumour vessels (Negus et al. 1997; Leek et al. 1999; Murdoch et al. 2004; Ohno et al. 2004) and usually correlate with poor prognosis (Bingle et al. 2002; Lewis and Pollard 2006; Lin and Karin 2007). Although notch signalling is implicated in development and tumourigenesis, its functional role in macrophage associated angiogenesis remains to be dissected. Fung et al., 2007 have reported that DLL4 and Notch3 are expressed in macrophages (Fung et al. 2007). DLL4 from co-cultured cells induced notch signalling on macrophages, promoted the activation of MAPK, Akt and NF-kB pathways and increased the expression of DLL4 through a positive feedback loop, coroborating that seen in VEGF-Notch signalling in endothelial cells (Ridgway et al. 2006).

This chapter was adapted from:

Bridges, E.*, **Oon. C**.*, and Harris, A.. *Notch regulation of tumour angiogenesis.* (Future Oncology, in press) * Joint first authorship

1.5.4 Research aims

This project aims to investigate the different effects of DLL4 and JAG1 Notch signalling in tumour angiogenesis.

Chapter 2 describes the materials and methods used in this project.

Chapter 3 studies the effects of DLL4- and JAG1-Notch signalling in endothelial cells *in vitro*.

Chapter 4 investigates the effects of mDLL4 and mJAG1 over-expression on tumour growth and angiogenesis in mouse U87 xenograft model.

Chapter 5 aims to study the expression profile of Fringe in endothelial cells and the pattern of expression in clear cell renal cell carcinoma (CCRCC).

Chapter 6 discusses the overall results of the differential role of DLL4- and JAG1- Notch signalling *in vitro* and *in vivo*, and the expression pattern of Fringe in CCRCC.

2 Methodology

2.1 Materials

2.1.1 Chemicals

Chemicals were purchased from Sigma (Dorset) unless stated otherwise.

2.1.2 Cell Lines

Human umbilical vein endothelial cells (HUVEC) were isolated from umbilical cords (Women's Centre, John Radcliffe Hospital, Oxford) Ethics code: 09/H0606/68, NHS Blood and Transplant, Oxford Centre Tissue Bank). Immortalised human dermal microvascular endothelial cell line (HMEC-1) was obtained from Dr. Richard Sainson (Medimmune, UK). U87 glioblastoma cells were purchased from Cancer Research UK's Cell Services (London). Cell lines over-expressing empty vector (EV) murine DLL4 (mDLL4) and murine JAG1 (mJAG1) were obtained from Dr. Ji-Liang Li (Oxford, UK).

2.1.3 Cell culture reagents

HUVEC up to passage 6 were cultured in M199 medium (Invitrogen) supplemented with 10%(v/v) foetal calf serum (FCS) (PAA laboratories, Austria), 50 μg/ml endothelial cell growth supplement (ECGS; BD Biosciences, Oxford), 5 IU/ml heparin (Sigma-Aldrich, USA), 100 IU/ml penicillin, 100 μg/ml streptomycin and 2 mM glutamine (Invitrogen).

U87 cell lines were maintained in Dulbecco's Modified Eagle's Medium (DMEM) (Invitrogen) supplemented with 10% FCS, 2 mM glutamine and 100 units/ml Pen/Strep (PAA laboratories, Austria). HMEC-1 were grown in MCDB-131 culture medium supplemented with 10% FCS and 40 μM glutamine, 100 U/ml penicillin, 100 μg/ml streptomycin 10 mM L-glutamine, 10 ng/ml epidermal growth factor (Sigma), and 1 μg/ml hydrocortisone (BD Biosciences, Heidelberg, Germany).

Cell transfection was carried out using OptiMEM reduced serum media with Glutamax-1 (Invitrogen). Adherent cells were detached from culture plates using Trypsin/EDTA (PAA laboratories, Austria).

All cell lines were cultured and maintained on tissue-culture grade polystyrene plasticwares (BD Biosciences). These include 100 mm dishes, 75 cm^2 flasks, 25 cm^2 flasks, 6-well plates and 24-well plates.

2.1.4 Real-time PCR primers and probes

The following primer-probe sets were designed using the Probe Library Assay Design Centre website (Roche Applied Science, Burgess Hill). The primers were synthesised by Invitrogen, and the Probe Library was purchased from Roche Applied Science.

Gene	Forward 5′–3′	Reverse 5′–3′	Probe #
GAPDH	AGCCACATCGCTCAGACAC	GCCCAATACGACCAAATCC	60
hACT	GAGGAGGCACCGGTAAATG	GTCACTCACTGGGACATAGGC	81
JAG1	GAATGGCAACAAAACTTGCAT	AGCCTTGTCGGCAAATAGC	42
HEY1	CGAGCTGGACGAGCCCAT	GGAACCTAGAGCCGAACTCA	39
HEY2	GTACCATCCAGCAGTGCATC	AGAGAATTCAGGGCATTT	60
DLL4	CCCTGGCAATGTACTTGTGAT	TGGTGGGTGCAGTAGTTGAG	23
MFNG	TTCCAGGACCAGGGAACA	AGTCTCTCCTGGAGGCCTTT	26
LFNG	GCGCCACAAGGAGATGAC	GCCGAGCAGTTTGTGATGA	81
RFNG	ACAGCCCCCTCTTCCACT	CCCCATGCCTCAAGGTAAC	80
mACT	AAGGCCAACCGTGAAAAGAT	GTGGTACGACCAGAGGCATAC	56
mDLL4	AGGTGCCACTTCGGTTACAC	GGGAGAGCAAATGGCTGATA	106
mJAG1	TGGCCGAGGTCCTACACTT	GCCTTTTCAATTATGCTATCAG	22
mHEY1	CATGAAGAGAGCTCACCC	CGCCGAACTCAAGTTTCC	17

2.1.5 Small interfering RNAs

The following small interfering RNAs (siRNAs) were designed using the siDESIGN Center website (Dharmacon, Lafayette, USA) and synthesised by Eurogentec (Southampton). siRNA

oligonucleotides were re-suspended in annealing buffer (100 mM NaCl, 50 mM Tris, pH 7.5-8.0). Working solutions (20 μM) of siRNA were stored at -20°C, and stocks (100 μM) were stored at -80°C.

Gene	Sense (3' to 5')	Antisense (3' to 5')
Scrambled control	UCUGAAAAGCACGCUUGAC	GUCAAGCGUGCUUUUCAGA
siDLL4 Duplex1	CAACUAUGCUUGUGAAUGU	ACAUUCACAAGCAUAGUUG
siDLL4 Duplex2	ACACAAACCAGAAGAAGGA	UCCUUCUUCUGGUUUGUGU
siJAG1 Duplex1	AUCUUAUGAGGGAUUUACG	CGUAAAUCCCUCAUAAGAU
siJAG1 Duplex2	AACAGGACAAACAAACAGG	CCUGUUUGUUUGUCCUGUU

2.1.6 Antibodies

The following primary antibodies were used for Western blotting (WB) and immunohistochemistry/immunofluroescence (IHC/IF).

Protein	Company	Monoclonal (M) or Polyclonal (P)	Secondary	Dilution
hβ-Actin	Sigma (A1978)	M	Anti-mouse	1:1000 (WB)
hLC3	Nanotools (5F10)	M	Anti-mouse	1:2000 (WB)
hPARP	Cell Signalling Technology (9542)	P	Anti-rabbit	1:1000 (WB)
hHIF1α	BD Bioscience (610958)	M	Anti-mouse	1:1000 (WB)
hN1 ICD	Cell Signalling Technology (4147)	P	Anti-rabbit	1:500 (WB)
h/mDLL4	ABCAM (AB7280)	P	Anti-rabbit	1:500 (WB) 1:100 (IF)
hDLL4 (C-20)	Santa Cruz Biotechnology (SC18640)	P	Anti-goat	1:100 (IF)
h/mJAG1	Cell Signalling Technology (2620)	M	Anti-rabbit	1:1000 (WB) 1:100 (IF)
hGFP	Abcam (AB290)	P	Anti-rabbit	1:1000 (WB)
hMFNG (C-20)	Santa Cruz Biotechnology (SC8236)	P	Anti-goat	1:100 (IF)
mCD31	Acris (BM4086)	M	Anti-rat	1:100 (IHC)
hCD31	DAKO (M0823)	M	Anti-mouse	1:50 (IF)
mCD34	Serotec (MCA1825)	M	Anti-rat	1:250 (IHC)
hMIB1	Dako (M7240)	M	Anti-mouse	1:50 (IHC)
mNG2	Chemicon (AB5320)	P	Anti-rabbit	1:200 (IF)
hCAIX M75	A kind gift from Dr. J. Pastorek, (Bratislava)	M	Anti-mouse	1:50 (IHC)

KEY: Human (h), mouse (m)

WB: Secondary antibodies against mouse, goat or rabbit immunoglobulin conjugated to horseradish peroxidase (HRP) were obtained from Dako (Ely).

IF: Alexa-Fluor fluorescent dyes were purchased from Invitrogen.

2.1.7 Molecular weight markers

Rainbow marker (GE Healthcare, Chalfont St Giles) was used to determine the molecular weight of proteins from 10 to 250 kDa for Western blotting.

2.1.8 Matrigel basement membrane matrix

BD Matrigel™ Basement Membrane Matrix was obtained from BD Biosciences (UK). Matrigel was thawed overnight at 4°C on ice prior to use.

2.1.9 Lentiviral particles

copGFP Control Lentiviral Particles: sc-108084, Control shRNA Lentiviral Particles: sc-108080 or Manic Fringe shRNA Lentiviral Particles: sc-39493-V were purchased from Santa Cruz Biotechnology (Germany).

2.1.10 Mouse model

Female BALB/c mice with severe combined immune deficiency (SCID) were purchased from Harlan UK (Bicester) and housed in the animal facility, Oxford. All animal procedures were performed by qualified technicians under Home Office licence. Bevacizumab was obtained from Genentech (San Francisco, USA) while DBZ was purchased from Syncom (Groningen, the Netherlands). Anti-DLL4 blocking antibody was obtained from MedImmune (USA).

2.1.11 Over-expressing cell line

U87 over-expressing murine DLL4 (U87 mDLL4), murine JAG1 (mJAG1) and Manic Fringe (U87 MFng) cell lines were kind provision from Dr. Ji-Liang Li, Oxford. The cDNA coding for full length murine DLL4, murine JAG1 or human MFng was cloned into LZRSpBMN-linker-IRES-EGFP retroviral vector and transduced into U87 cells as described previously (Li et al. 2007).

2.2 General laboratory methods

2.2.1 Isolation of HUVEC

HUVECs were isolated from fresh human umbilical cords by infusion with 0.2% collagenase (Worthington Biochemical Corporation, Lakewood, USA) in PBS. Briefly, a 21-gauge Safety-Lok blood collection needle (BD Biosciences) was inserted into the umbilical vein and clamped in place with a haemostat. 50 ml PBS solution was injected into the umbilical vein through the needle to remove blood clots. Next, 10 ml warm collagenase solution was carefully injected into the umbilical vein with a syringe, with the bottom end of the umbilical

cord clamped with another haemostat. The cord, filled with collagenase, was then submerged in PBS and incubated at 37°C for 15 minutes. After incubation, the bottom haemostat was removed and the collagenase solution containing dissociated HUVEC was collected in a 30 ml Sterilin tube (Barloworld Scientific, Stone). The tube was centrifuged at 160 g for 4 minutes, and the pellet was re-suspended in 5 ml HUVEC culture medium and plated in a 25 cm^2 culture flask. Freshly isolated HUVEC were designated passage 0 (P0). HUVEC up to passage 6 were used in experiments.

2.2.2 Mammalian cell culture

2.2.2.1 General culture conditions

Cells were cultured and maintained in incubators at 37°C and atmosphere containing 5% CO_2.

2.2.2.2 Recovery of cryo-preserved cells

Medium for cell culture was warmed up in water bath at 37°C. For HUVECs cell culture, flasks were pre-coated with 0.2% gelatin in PBS for 10 minutes. Cryo-preserved cells in vials were then retrieved from liquid nitrogen and thawed immediately in water bath at 37°C before centrifuged at 160 g for 4 minutes to remove dimethyl sulfoxide (DMSO) residue used for cryo-preserving cells. The cell pellet was then resuspended in the appropriate medium and plated in 75 cm^2 culture flasks and incubated at 37°C.

2.2.2.3 Subculturing

All cell lines were routinely split 1 in 3. Cells were sub-cultured at 90-100% confluence. Prior to use, cell culture medium, PBS and trypsin/EDTA solutions were pre-incubated in water bath at 37°C. Medium was aspirated from flasks and rinsed with PBS. Trypsin/EDTA was added to lift cells from flasks followed by addition of appropriate medium to deactivate trypsin once cells have detached.

The cell suspension was then transferred to a 20 ml Sterilin tube and centrifuged at 160 g for 4 minutes. The cell pellet was then re-suspended in an appropriate volume of medium and plated out.

2.2.2.4 Cell counting

Cell suspension (400 µl) was diluted in 19.6 ml ISOTON diluent (Beckman Coulter, High Wycombe), and the cell number per millilitre of the original cell suspension was measured using a Z2 Coulter Counter (Beckman Coulter).

2.2.2.5 Cell cryo-preservation

Cells were trypsinised and centrifuged and re-suspended in freezing solution containing 90% FCS and 10% DMSO. Cells in freezing solution were dispensed into Corning 2 ml round-bottom cryogenic vials (Fisher Scientific, Loughborough). Vials were cooled slowly

overnight at -80^{o}C and transferred to liquid nitrogen the day after for long-term storage.

2.2.3 RNA extraction and analysis

2.2.3.1 RNA extraction from cultured cells

All RNA work was performed using filtered and aerosol-resistant pipette tips, sterile microcentrifuge tubes and DEPC-treated water. RNA extraction from cultured cells was performed using TRI Reagent according to the manufacturer's protocol. Briefly, cell culture medium was aspirated, and the cell monolayer was washed with PBS. After PBS was removed, an appropriate volume of TRI Reagent was added (1 ml per 100 mm dish, or 150 µl per well of a 6-well plate). Cells were then scraped with a Costar cell scraper (Fisher Scientific) to facilitate lysis. The cell lysate was then transferred to 1.7 ml microcentrifuge tubes (Axygen Scientific, Union City, USA). RNA samples may be stored at -80°C, otherwise RNA extraction was performed immediately.

Five minutes after cell lysis, 0.2 ml chloroform per 1 ml TRI reagent was added to the samples. Samples were then vortexed for 15 seconds, incubated at room temperature for 10 minutes, and then centrifuged at 12,000 g for 15 minutes at 4^{o}C. The centrifugation separated the mixture into three phases, and the top aqueous phase containing RNA was transferred into a new microcentrifuge tube. To the new tube, 0.5 ml isopropanol per 1 ml TRI reagent was added and mixed. After standing at room temperature for 5 minutes, the samples were centrifuged at 12,000 g for 10 minutes at 4^{o}C. After centrifugation, an RNA pellet formed at the bottom of the tube. Pellets were then washed with 1 ml 75% ethanol per 1 ml TRI reagent, vortexed, and centrifuged at 12,000 g for 5 minutes at 4^{o}C. The supernatant was removed and

the pellet was air-dried for 10 minutes. RNA was re-suspended in 25µl of DEPC-treated water and stored at -80°C.

2.2.3.2 RNA extraction from tumour samples

RNA extraction from tumour samples was performed using the RNAeasy Protect mini kit (Qiagen). Briefly, a piece of tumour sample weighing approximately 30 mg was removed with a scalpel and crushed in liquid nitrogen using a mortar and pestle. 600 µl Buffer RLT was added to lyse the disrupted tissue and homogenized using a QIAshredder homogenizer, centrifuged for 2 mins at 10,000 g. Supernatant from each tube was removed by pipetting and transferred to a new microcentrifuge tube. 1 volume of 70% ethanol was added to the cleared lysate and mixed by pipetting. 700 µl of sample were transferred into RNeasy spin column and centrifuged for 15 s at 10,000 g. 700 µl Buffer RW1 was added to RNeasy spin column to wash the column membrane and centrifuged for 15 s at 10,000 g. 500 µl Buffer RPE was added to the column and centrifuged twice, initially for 15 s and then for 2 mins at 10,000 g. Samples were then reconstituted with 35 µl RNase-free water onto membrane into a new microcentrifuge tube and centrifuged for 1 min at 10,000 g and stored at -80°C.

2.2.3.3 RNA quantification

RNA was quantified using the ND-1000 spectrophotometer (NanoDrop Technologies). RNA-40 presets were used. The absorption of 1 O.D. is approximately equivalent to 40 µg/mL of RNA. RNA concentration, in ng/µl, equals 40 times the absorbance at 260 nm, or A260.

2.2.3.4 Reverse transcription

Reverse transcription was performed using the High Capacity cDNA Reverse Transcription Kit (Applied Biosystems, Warrington). Briefly, 1 μg of RNA was diluted in 71 μl of DEPC-treated water in a 0.2 ml thermo-tube (ABgene, Epsom). To the RNA sample, 10 μl 10x RT Buffer, 10 μl 10x Random Primers, 4 μl 25x dNTP mixture, and 5 μl MultiScribe Reverse Transcriptase was added, making the final volume 100 μl. The sample was then incubated at 25^{o}C for 10 minutes, 37^{o}C for 2 hours, and 4^{o}C for up to 12 hours before use. The cDNA concentration is taken to be 10 ng/μl (1 μg per 100 μl) assuming 100% efficiency of reverse transcription.

2.2.3.5 Real-time quantitative PCR

Real-time PCR quantitative (qPCR) was performed using the Exiqon system (Roche Applied Science) (Mouritzen et al., 2003). Briefly, a master mix for each gene to be tested was prepared containing the following: 12.5 μl ABsolute QPCR Mix (ABgene), 1 μl forward primer (10 μM), 1 μl reverse primer (10 μM), 0.25 μl probe from the Probe Library (Roche Applied Science), and 0.25 μl DEPC-treated water. Reactions were prepared in 0.1 ml tubes by a CAS-1200 robot (Corbett Research, Cambridge). In triplicates, 15 μl master mix was added to each reaction tube, followed by 10 ng cDNA in 10 ml. Upon completion of the robot run, reaction tubes were capped and placed in the 72-well rotor of a Rotor-Gene RG-3000 qPCR thermocycler (Corbett Research). The samples were then incubated at 50°C for 2 minutes followed by 95°C for 10 minutes to activate the Taq polymerase in the QPCR Mix. Afterwards, the cDNA samples went through 40 cycles of amplification at 95°C for 15

seconds followed by 60°C for 1 minute.

Two housekeeping genes (HKGs) were used to normalise the expression of genes of interest (GOIs). Glyceraldehyde-3-phosphate dehydrogenase (GAPDH) was used for cDNA derived from all cell lines as it was consistently expressed at the same level under normoxia. However, GAPDH expression is regulated by hypoxia (Escoubet et al. 1999), thus human or mouse β-actin (hACT or mACT) was used for cDNA derived from tumours (Castello et al. 2002). Data were analyzed using the comparative Ct method (Livak and Schmittgen, 2001). Briefly, the threshold cycle (Ct) values for each GOI and HKG were converted to raw expression values by performing the operation 2^{-Ct}. The raw expression value of each GOI was then divided by that of the HKG to account for different amounts of cDNA in each sample. Finally, the normalised values were then rescaled to set the expression in the control sample to 1. Error propagation was calculated throughout the operations, and final results were reported as mean ± standard error of the mean (SEM) to reflect the triplicate measurements.

2.2.4 Protein extraction and analysis

2.2.4.1 Protein extraction from cultured cells

Protein extraction from cultured cells was performed using urea lysis buffer which consists of 10% glycerol, 10 mM Tris-HCl (pH 6.8), 5 mM dithiothreitol, 1% sodium dodecyl sulphate (SDS) and 8 M urea. Briefly, medium was removed from cultured cells and rinsed with PBS on ice. To each 100 mm dish of cells, 1 ml of the lysis buffer and 10 μl of Protease Inhibitor

Cocktail were added. Cells were then scraped off with a cell scraper, and cell lysates transferred to microcentrifuge tubes. Protein lysates were stored at -20^{o}C.

2.2.4.2 Western blotting

Protein was quantified using NanoDrop ND-1000 spectrophotometer using absorbance at 280nm (Thermo Scientific, Surrey, UK).

Western blotting of protein samples was performed using the NuPAGE® Bis-Tris Pre-Cast Gels (Invitrogen). All reagents and apparatuses were obtained from Invitrogen. Protein samples (25 μg) were diluted in lysis buffer to a volume of 19.5 μl, and 7.5 μl 4x LDS Sample Buffer and 3 μl 10x Reducing Agent were added. The samples were then heated at 70^{o}C for 10 minutes and loaded into NuPAGE 10% Bis-Tris gels in an XCell SureLock Mini-Cell, and filled 1x NuPAGE® MOPS SDS Running Buffer containing 500 μl Antioxidant. Gels were run at a constant voltage of 150 V for 50 minutes.

Proteins were then transferred from the gel to an Immobilon-PVDF transfer membrane (Millipore, Watford). Both the membrane and the gel were sandwiched between six layers of filter paper, with the membrane between the gel and the anode. The membrane and filter paper had been pre-soaked in transfer buffer (25 mM Tris base, 192 mM glycine, 15% methanol). The transfer assembly was placed in a semi-dry transfer apparatus (WEP, Seattle, USA). Protein was transferred at a constant current of 130 mA per gel for 50 minutes.

Non-specific binding sites on the membrane were blocked for 1 hr at room temperature in blocking solution (5% milk powder, 0.1% Tween-20 in PBS). After blocking, the membrane was probed with a primary antibody in blocking solution overnight at 4^{o}C. The membrane

was then washed in PBS with 0.1% Tween-20 three times for 10 minute each. Next, the membrane was probed with an appropriate HRP-conjugated secondary antibody in blocking solution for 1 hour at room temperature. Following this step, the membrane was again washed as before. Finally, the membrane was covered with Enhanced Chemiluminescence (ECL) reagent (GE Healthcare) for 1 minute and placed in a film cassette. In a dark room, the membrane was exposed to ECL Hyperfilm (GE Healthcare) for 10 seconds, 1 minute, 10 minutes or longer as needed, and the films were then developed using an X-ray film processor (Xograph, Tetbury).

2.2.4.3 Densitometry analysis

Densitometry analysis was done on Image J by calculating the relative density of each peak which corresponds well with the size and darkness of each band in the western blot, and normalised to the standard (First lane) and the loading control (β-Actin).

2.2.5 Websites

Genome Browser: http://genome.ucsc.edu/

NCBI: http://www.ncbi.nlm.nih.gov/

Oncomine: https://www.oncomine.org/resource/login.html

NextBio: http://www.nextbio.com/b/nextbio.nb

Probe Library Assay Design Center:

http://www.roche-applied-science.com/sis/rtpcr/upl/adc.jsp

PubMed: http://www.ncbi.nlm.nih.gov/entrez/query.fcgi

siDESIGN™ Center: http://www.dharmacon.com/sidesign/

2.3 Experimental methods

2.3.1 RNA interference

HiPerfect (QIAGEN) was used for siRNA transfection into cells. Briefly, $2x10^5$ HMEC-1 cells per well were seeded in a 6-well plate and cultured in complete medium at 37°C, 5% CO_2 overnight. The transfection volume was 2 ml per well, and the optimum siRNA concentration was 20 nM (siDLL4) and 5 nM (siJAG1). On the day of transfection, 2 µl of the siDLL4 or 0.5 µl siJAG1 working solution (20 µM) was added to 98 µl of OptiMEM in a round-bottom tube (for each well). A scrambled control siRNA was used to control for non-specific RNAi-related effects. Next, 12 µl of HiPerfect was added to the diluted siRNA and mixed by pipetting up and down 5 times. Solutions were incubated for 10 minutes at room temperature to allow formation of transfection complexes. 100 µl of the complexes were added drop-wise onto the cells in 2ml complete medium, gently swirling the plate to ensure uniform distribution of transfection complexes. Cells were then incubated under their normal growth conditions until analysis of gene silencing was performed.

2.3.2 Lentiviral transduction

Lentiviral particles (copGFP Control Lentiviral Particles: sc-108084, Control shRNA Lentiviral Particles: sc-108080 or Manic Fringe shRNA Lentiviral Particles: sc-39493-V) were purchased from Santa Cruz Biotechnology Inc, and stored at -80°C. Each vial contains

200 µl viral stock containing 1 x 10^6 infectious units of virus (IFU), sufficient for 10- 20 transductions. HMEC-1cells were plated at $1x10^5$ in a 12-well plate 24 hours prior to viral infection and incubated overnight. On the following day, media was replaced with 1 ml of Polybrene/ media mixture (5 µg/ml) per well to increase efficiency of transduction. Lentiviral particles were thawed at room temperature and mix gently prior to use. Cells were infected by adding 20 µl shRNA Lentiviral Particles to the culture, swirling the plate gently to mix and incubated overnight. copGFP Control Lentiviral Particles were used for measuring transduction efficiency. On the next day, culture medium was replaced with 1 ml of complete medium without Polybrene and incubated overnight. Cells were then split 1:3 and further incubated for 48 hours in complete medium. Selection of stable clones expressing the shRNA were done using 0.2 µg/ml Puromycin dihydrochloride to kill the non-transduced cells. Culture medium was replaced with fresh puromycin-containing medium every 3-4 days, until resistant colonies could be identified. Pooled colonies were used in my experiments.

2.3.3 Coating plates with recombinant DLL4 or JAG1 protein

Prior to experiment, tissue culture plates were coated with 0.2% gelatine (w/v) in PBS containing 1 µg/mL BSA, 1 µg/mL rhDLL4 (R&D Systems), 2.6 µg/mL rhJAG1-Fc (R&D Systems) or 2.6 µg/mL rrJAG1-Fc (R&D Systems), each was equivalent to 18nM protein. The plates were then incubated at 4^oC for 24 hours. Plates were pre-warmed to 37^oC and the coating solution were aspirated before seeding 2 x 10^5 HUVEC or HMEC-1 per well in 6-well plates.

2.3.4 *In vitro* angiogenic assays

2.3.4.1 *In vitro* cell proliferation count

Cells were seeded onto 6-well plates at 2 x 10^5 cells per well and incubated in the CO_2 incubator at 37^{o}C. Cells were counted everyday over five days using the Z2 Coulter Counter (Beckman Coulter).

2.3.4.2 Hanging drop assay

HMEC-1 cells were suspended in culture medium containing 0.2% (w/v) carboxymethylcellulose and seeded in non-adherent 60-microwell minitrays (Sigma) overnight. Spheroids of defined size and cell number (500 cells/spheroid) were generated overnight, after which they were embedded into Matrigel in a 24-well plate and allowed to polymerize (30 minutes), then 1 ml complete media with DMSO control or DBZ (200nM) was added on top of the gel. Pictures were taken on Day 1, Day 3 and Day 6 at 10× magnification using an Axiovert 100M microscope (Zeiss, Jena, Germany). Capillary sprouting was assessed by measuring the average length of three longest sprouts per spheroid (Korff and Augustin 1999) and sprout coverage area originating from 15 randomly selected spheroids per well on Day 3 when sprouting was most eminent, using Image J.

2.3.4.3 Network formation assay

Full Matrigel matrix (BD Biosciences) was added to wells (60 µl/well of a 96-well plate) and allowed to polymerize for 2hr at 37 °C. 2x10^4 of HMEC-1 cells were resuspended in 100 µl media with DMSO control or DBZ (200 nM) and cultured on the polymerised Matrigel.

Endothelial networks from DMSO control or DBZ treated groups were photographed 1 field per well at 8hr. Number of nodes (branch points) and polygons (honeycomb formation) from a total of 6 wells per condition were captured using Axiovert 100M microscope (Zeiss, Jena, Germany) quantified.

2.3.4.4 Scratched wound assay

Briefly, 0.5 million HMEC-1 cells were grown on 12-well plate pre-labeled with a traced line, for 24hr. Physical wound was introduced with a 10µl pipette tip on the confluent monolayer. Endothelial cell migration was quantified by measuring the width of the cell-free zone (distance between the edges of the injured confluent monolayer) at 6hr, 12hr and 24hr after scratch was initiated with a 10µl pipette tip. Areas of scratch were captured using Axiovert 100M microscope (Zeiss, Jena, Germany) and quantified on Image J.

2.4 Immunostaining

For all staining, omission of primary antibody was used as the negative control.

2.4.1 Preparation of sections

Frozen and formalin fixed paraffin embedded (FFPE) cytospin cells/ tissue sections were processed and sectioned to 4 microns in thickness onto X-tra slides by Helen Turley (NDCLS, University of Oxford) and Graham Steers (NDCLS, University of oxford).

Frozen sections were fixed in acetone for 10 minutes at room temperature, while FFPE slides were dewaxed and rehydrated as follows:

Twice in Citroclear for 5 minutes each, twice in 100% ethanol for 5 minutes each, once with 50% ethanol for 5 minutes and final rinse in PBS with 20 seconds agitation. Antigen retrieval was carried out in TRIS/EDTA pH 9.0 or 0.01mM Citrate pH6.0, heated to 125^{o}C and 15-20 lb pressure for 2 minutes in a Decloaker Chamber (Biocare Medical cat No: DC2002). Endogenous peroxidise activity was blocked with 0.03% hydrogen peroxide for 20 minutes using the DAKO CheckMate EnVision Detection Kit.

2.4.2 Staining protocols

2.4.2.1 Immunohistochemistry

CAIX (and CD34 double staining)

Slides were antigen retrieved in the decloaker with TRIS/EDTA pH 9.0 and peroxidase blocked for 20 minutes. Primary CAIX rabbit polyclonal antibody (1:100, a kind gift from Dr. J. Pastorek, Bratislava) was added for 1hr, then rinsed in PBS for 5 minutes followed by Anti rabbit polymer IMMPRESS Reagent (Vector Labs) for 30 minutes, and then rinsed in PBS 5 minutes. Visualisation of CAIX was achieved by applying diaminobenzidine substrate (DAB) for 8 minutes and further rinsed in PBS. For CAIX single staining, slides were counter stained with hematoxylin and mounted in Aquamount. Otherwise, primary CD34 rat polyclonal antibody (1:250) (Serotec) was added and incubated overnight at 4^{o} C. On the following day, slides were rinsed in PBS for 5 minutes followed by incubation with Envision secondary antibody rabbit/mouse HRP (DAKO) for 30 minutes, and finally the Grey developer (Peroxidase substrate kit, Vectorlab) for 8 minutes. Slides were counter stained with hematoxylin (Sigma), mounted in Aquamount (BDH, UK) and visualised under a light microscope.

MIB1

Slides were antigen retrieved in decloaker in 0.01mM Citrate pH 6.0 and peroxidase blocked for 20 minutes. Primary MIB1 mouse monoclonal antibody (1:50) (DAKO) was added and left to incubate at room temperature for 1 hr. Slides were counter stained with hematoxylin (Sigma), mounted in Aquamount (BDH, UK) and visualized under a light microscope.

2.4.2.2 Immunofluorescence

DLL4 and JAG double staining in HUVEC and HMEC-1

Briefly, cells were seeded onto glass slips in 6-well plates at 2 x 10^4 cells per well and incubated overnight. The cells were rinsed briefly in PBS and fixed with 4% formaldehyde in PBS for 15 minutes at room temperature followed by rinsing three times in PBS for five minutes each. Cells were permeabilised with ice-cold 100% methanol and incubated for 10 minutes at –20°C before final rinse in PBS for 5 minutes. Following blocking of nonspecific binding with 5% BSA in PBS for 1hr, sections were incubated with primary antibody for 1hr at room temperature. The endothelial cells were then incubated with goat anti-DLL4 C-20 (1:100, Santa Cruz Biotechnology Inc) and rabbit anti-JAG1 (1:100, Cell Signalling Technology). Incubation of endothelial cells with only secondary antibody without primary antibody was used as a negative control. After 10-min washes in PBS, cells were incubated with secondary antibody Alexa-Fluor 546 donkey anti-goat (0.5 µg/mL, Molecular Probe, Invitrogen) and Alexa-Fluor 488 donkey anti-rabbit (0.5 µg/mL, Molecular Probe, Invitrogen) for an hour at room temperature. Cells were then washed three times in PBS before mounting with fluorescent mounting medium with DAPI (Vectashield) and visualised under the fluorescent microscope.

DLL4 and JAG1 staining in over-expressing cells

Briefly, cells were seeded onto glass slips in 6-well plates at 3 x 10^5 cells per well and incubated overnight. The cells were rinsed briefly in PBS and fixed with 4% formaldehyde in PBS for 15 minutes at room temperature followed by rinsing three times in PBS for 5 minutes each. Cells were permeabilised with ice-cold 100% methanol and incubated for 10 minutes at

–20°C before final rinse in PBS for 5 minutes. Following blocking of nonspecific binding with 5% filtered goat serum in PBS for 1hr, sections were incubated with primary antibody for 1hr at room temperature. The endothelial cells were then incubated with rabbit anti-DLL4 (1:50, ABCAM) or rabbit anti-JAG1 (1:100, Cell Signalling Technology). Incubation of endothelial cells with only secondary antibody without primary antibody was used as a negative control. After 10-min washes in PBS, cells were incubated with secondary antibody Alexa-Fluor 488 goat anti-rabbit IGg (0.5 μg/mL, Molecular Probe, Invitrogen) for an hour at room temperature. Cells were then washed three times in PBS before mounting with fluorescent mounting medium with DAPI (Vectashield) and visualised under the fluorescent microscope.

MFng staining on cytospin cells and CCRCC tumour sections

Cytospin from U87 and HMEC-1 control cells in suspension were mounted onto slides by Helen Turley (NDCLS, University of Oxford) and fixed in acetone for 10 minutess at room temperature. CCRCC tumour sections were obtained from the NCDLS tumour archive (Oxford).

Following blocking of nonspecific binding with 5% BSA in PBS for 1hr, sections were incubated with primary antibody. Omission of primary antibody served as a negative control for staining. In CCRCC tumours, Fringe colocalisation was assessed by double staining with goat anti-human Manic Fringe C-20 (1:100, Santa Cruz Biotechnology) and mouse anti-human CD31 (JC 70A) (1:50, DAKO) and left at 4^{o}C overnight. U87 EV, U87 MFng, HMEC-1 SCR and HMEC-1 shMFng cell pellets were used as controls for the Fringe antibody. On the following day, slides were rinsed in PBS briefly followed by incubation with secondary antibody, Alexa Fluor 647 donkey anti-goat IgG and Alexa Fluor 488 rabbit anti-

mouse IgG, both at 1:200 dilution. Slides were mounted in fluorescent mounting medium with DAPI (Vectashield) and visualised under a fluorescent microscope.

Vessel and pericyte staining and quantification

U87 mDLL4 and U87 mJAG1 xenograft tumours were provided by Dr. Ji-Liang Li (Cancer Research UK, Oxford). For immunofluorescent staining, 4-μm cryo-sections were fixed in acetone for 10 minute and dried in air for 1hr. Following blocking of nonspecific binding with 5% BSA in PBS for 1hr, sections were incubated with primary antibody for 1hr at room temperature. Endothelial cells (ECs) were stained with rat anti-mouse CD31/PECAM (2 μg/mL, Clone ER-MP12, Acris GmBH). Pericyte coverage around the vessel was assessed by staining with the pericyte marker NG2 (1:200, Chemicon). After rinsing with PBS, sections were incubated with secondary antibody Alexa-Fluor 594 goat anti-rabbit or Alexa-Fluor 488 goat anti-rat (0.5 μg/mL, Molecular Probe, Invitrogen). Fluorescent microscopy images were acquired for five randomly chosen fields per tumour section. Vessel density corresponds to the percentage of each field occupied by a CD31-positive signal (as determined by the percentage of black pixels per field after transforming the RGB pictures into binary files using Image J). Vessel number is determined by the number of continuous CD31-positive structures per field. Vessel size quantification is relative to the average number of pixels per continuous CD31-positive structure. Percentage of pericyte coverage was calculated from the total number of NG2 positive stained cells that co-localise with the vessels over total vessel numbers.

Vessel perfusion

Frozen sections were fixed in acetone for 10 minute and air dried for 1 hr. Following blocking of nonspecific binding with 5% BSA in PBS for 1hr, sections were incubated with CD31/PECAM (2 μg/mL, Clone ER-MP12, Acris GmBH) rat anti-mouse monoclonal antibody for 1hr at room temperature. After rinsing with PBS, sections were incubated with Alexa-Fluor 488 goat anti-rat (0.5 μg/mL, Molecular Probe, Invitrogen) and Streptavidin Alexa Fluor 594 conjugate (1:100, Invitrogen) to enhance the signal for biotinylated tomato lectin. Images were taken focused on areas with vessels (tumour hot spot) to determine percentage perfusion in existing vessels. Percentage of perfusion was calculated as the percentage area positive for tomato lectin compared to the CD31 positive area via set threshold and conversion into binary files, as described above.

DLL4 / JAG1 and CD31 double staining

Frozen sections were fixed in acetone for 10 minute and air dried for 1hr. Following blocking of nonspecific binding with 5% BSA in PBS for 1hr, sections were incubated with rat anti-mouse monoclonal CD31/PECAM antibody (2 μg/mL, Clone ER-MP12, Acris GmBH) and rabbit anti-mouse/human DLL4 (1:100, ABCAM) or rabbit anti mouse/human JAG1 (1:100, Cell Signalling Technology) for 1hr at room temperature. Slides were then rinsed with PBS, and sections were incubated with Alexa-Fluor 488 goat anti-rat (0.5 μg/mL, Molecular Probe, Invitrogen) and Alexa-Fluor 594 goat anti-rabbit (0.5 μg/mL, Molecular Probe, Invitrogen). Fluorescent microscopy images were acquired for five randomly chosen fields per tumour section.

2.5 Mouse models

Six- to eight-week-old female BALB/c SCID mice (Harlan Sprague Dawley, Inc., Indiana) were injected subcutaneously with 100 μl cell suspension containing $1x10^7$ U87 empty vector (EV), U87 murine DLL4 (mDLL4) or U87 murine JAG1 (mJAG1) cells, together with 100 μl Matrigel (BD Biosciences). Each treatment group consisted of five mice. Tumour growth was monitored two to three times per week by measuring the length (L), width (W) and height (H) of each tumour with a calliper. Tumour volumes (V) were then calculated from the formula ($V = 1/6 \times \pi \times L \times W \times H$). Pimonidazole (Hydroxyprobe-1) (2mg) and Biotinylated Lycopersicon Esculentum (Tomato) Lectin (1 μg/μl) were injected intravenously into each mouse via the lateral vein 30 minutes before euthanasia. When the tumour reached the maximum size permitted by the Home Office license, the mouse was sacrificed and the tumour excised. Half the tumour was frozen in liquid nitrogen for RNA isolation, and the other half fixed in formalin for immunohistochemical analysis.

Treatments with PBS (control), DBZ (5.4 mmol/kg), bevacizumab (10 mg/kg) or both were given intraperitoneally every three days, starting from Day 7, when the tumours reached the size of $150mm^3$ until the mice were sacrificed. All protocols were carried out under Home Office legislation (Li et al. 2007).

In the preliminary experiment to study the effect of specific anti-DLL4 blockade on U87 tumours, protocol for animal work remained the same with the exception that mice number were increased from five to seven per group in the U87 EV and U87 mJAG1 xenograft tumours. Treatment with 5mg/kg anti-DLL4 antibody or PBS (control) was given twice a week until mice were sacrificed.

2.6 Statistical methods

The statistical analysis and graphing software Excel (Microsoft, USA) and Prism (GraphPad, USA) were used to analyse all data. The Student's t-test (parametric) or the Wilcoxon test (non-parametric) was used to compare mean values between two data sets. The analysis of variance (ANOVA) test was used to compare mean values among three or more data sets, and the Bonferroni's post-test was used to compare any two data sets among the three or more sets. Kruskal Wallis test with Dunn's post-test comparison was employed to analyse more than two sets of non parametric data. The ANOVA F- test was used to assess significance between two curve fits. Kaplan-Meier survival curves was used to analyse the percentage survival of mice. Curve comparison was performed using the log rank test. Correlation coefficient- Spearman rank correlation was used to compare non-parametric data. Statistical significance was indicated in the figures by *, where $P<0.05$, and**, where $P<0.01$. All error bars depict SEM.

3 Effect of DLL4 and JAG1 on Notch signalling *in vitro*

3.1 Introduction

DLL4 and JAG1, are the predominant Notch ligands in the endothelium (Villa et al. 2001; Hofmann and Iruela-Arispe 2007). While DLL4 has been described as a negative modulator of angiogenesis (Noguera-Troise et al. 2006; Ridgway et al. 2006; Hellstrom et al. 2007), JAG1 has been associated with pro-angiogenic endothelial cells *in vitro* and *in vivo* (Zeng et al. 2005; Sainson et al. 2008; Benedito et al. 2009). The opposite effects of DLL4 and JAG1 on vasculature highlights the importance of these ligands and further studies are needed to better understand the role of DLL4 and JAG1 in the regulation of angiogenesis.

This chapter aims to study the effects of DLL4 and JAG1 on notch signalling in endothelial cells at both the transcript and functional level. Endothelial cells are commonly used in various *in vitro* model systems to study the complexity of angiogenic cascade. Two endothelial cells types, human microvascular endothelial cells (HMEC-1) and human umbilical vein endothelial cells (HUVEC) have been shown in *in vitro* models to mimic the angiogenic activities of endothelial cells *in vivo* (Ades et al. 1992; Bouis et al. 2001). HMEC-1 cells are a well characterised immortalised cell lines (Xu et al. 1994; Bonnefoy et al. 2001) compared to the HUVEC primary endothelial cells that have a limited life-span and display characteristics that differ in batches due to their multi-donor origin (Jaffe et al. 1973).

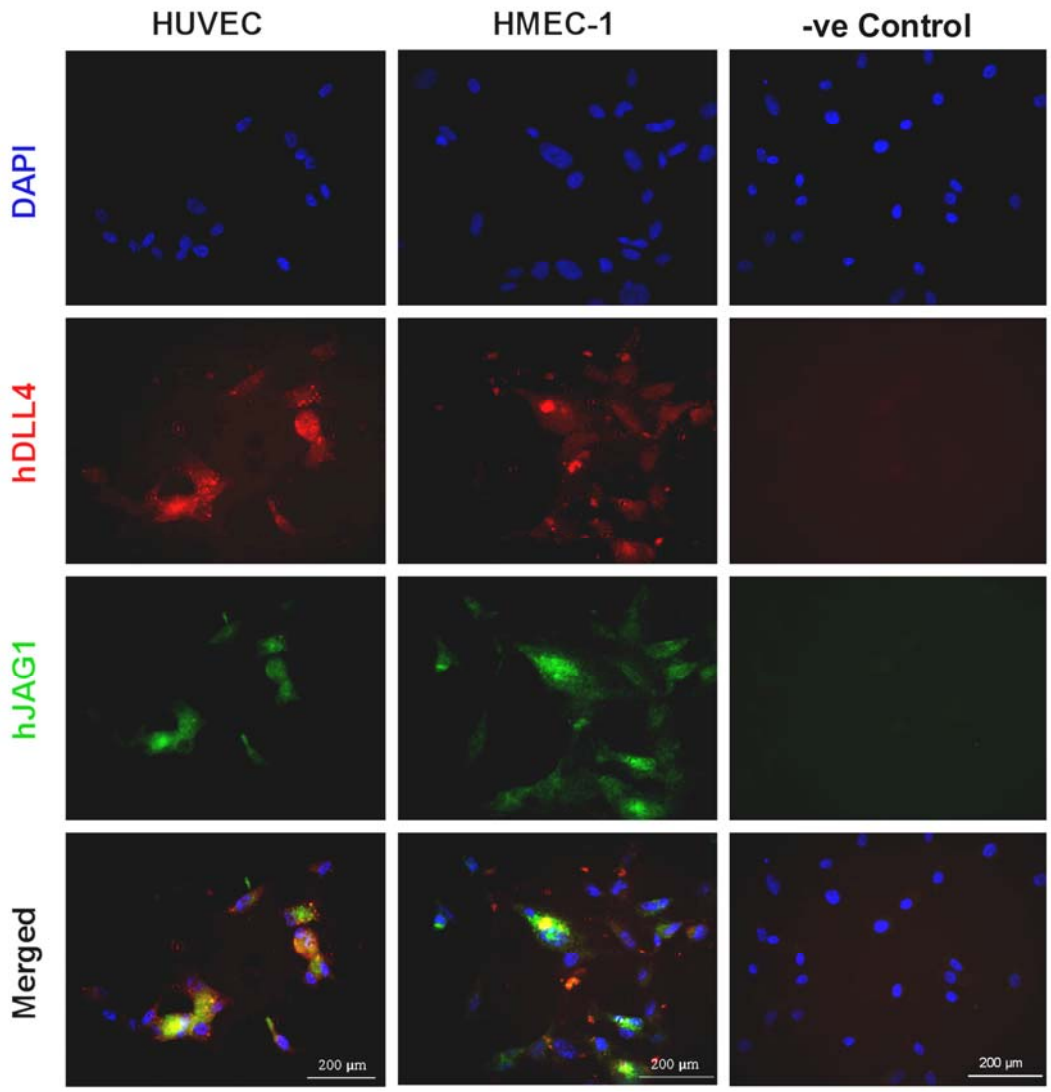
Two approaches were used to achieve the aim of this chapter. Firstly, HUVEC and HMEC-1 were stimulated with exogenous DLL4 or JAG1 recombinant proteins at different concentrations and time points to activate Notch signalling. The differences and advantages of

using HMEC-1 over HUVEC as an *in vitro* angiogenic model to study the effects of DLL4 and JAG1 in endothelial cells will also be discussed. The expression of DLL4 and JAG1 were manipulated in HMEC-1 by generating HMEC-1 over-expressing murine DLL4 (mDLL4) or murine JAG1 (mJAG1). Expression of basal DLL4 and JAG1 was silenced by siRNA targeted in HMEC-1 to study the functional roles of DLL4 and JAG1. HMEC-1 mDLL4 and HMEC-1 mJAG1 cells were used to study the effects of DLL4 and JAG1 on proliferation, migration, network formation and sprout coverage. Similarly, these angiogenic assays were performed on DLL4 or JAG1-silenced HMEC-1. Dibenzazepine (DBZ), a γ-secretase inhibitor was used to inhibit Notch signalling.

3.2 DLL4 and JAG1 were expressed in HUVEC and HMEC-1 cells

HUVEC and HMEC-1 were stained and blotted for DLL4 and JAG1 to examine the basal expression of the ligands in these endothelial cells at low confluency (Figure 3.1) when minimal Notch activation was initiated. Both ligands were basally expressed in HUVEC and HMEC-1, with the DLL4 being the most abundant expressed ligand in HUVEC compared to HMEC-1 (Figure 3.1 B). Interestingly, immunofluorescence staining with anti- JAG1 and anti-DLL4 antibody (both corresponded to the intracellular region of JAG1 and DLL4 respectively) revealed cytoplasmic localisation of JAG1 in HUVEC (Figure 3.1 A), whereas JAG1 and punctate DLL4 were observed persistently compartmentalised within the cytoplasm and exhibited nuclear positivity in a number of both cell types (Figure 3.1 A). Co-localisation of both JAG1 and DLL4 was more prominently observed in HUVEC compared to HMEC-1 cells (Figure 3.1 A).

A.


HUVEC
HMEC-1
-ve Control
DAPI
hDLL4
hJAG1
Merged
200 µm
200 µm
200 µm

B.

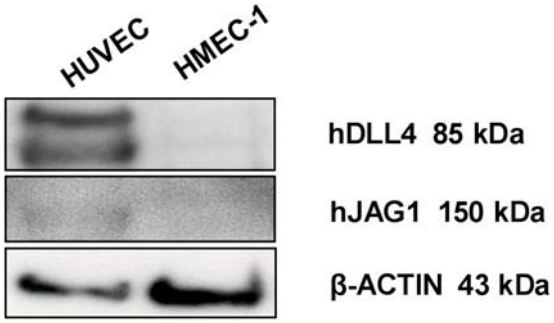

HUVEC
HMEC-1
hDLL4 85 kDa
hJAG1 150 kDa
β-ACTIN 43 kDa

Figure 3.1: A) DLL4 and B) JAG1 protein expression in HUVEC and HMEC-1 at low confluency.

A) Double staining for DLL4 and JAG1 in HUVEC and HMEC-1. Both antibodies recognise the intracellular region of each ligand. DAPI functions as a nuclear stain. Omission of primary antibody was used in negative control. B) Western blotting for DLL4 and JAG1 expression in HUVEC and HMEC-1. β-ACTIN was used as loading control. Figures are representatives of 2 independent experiments.

3.3 Exogenous ligands can activate Notch signalling in HUVEC and HMEC-1

In keeping with previous work, it was recently shown that DLL4 immobilised onto plates could activate Notch signalling (Williams et al. 2006; Harrington et al. 2008) and up-regulate the expression of DLL4 and JAG1 in HUVEC (Harrington et al. 2008). In order to understand the difference between the two ligands in the regulation of Notch signalling, cellular Notch signalling was activated using recombinant protein immobilised onto plates. Recombinant proteins consisting of the extracellular domain were used at the same molarity of 18nM, a working concentration which is equivalent to 1μg/ml of rhDLL4 (Ridgway et al. 2006; Williams et al. 2006) or 2.6 μg/ml of rrJAG1 proteins.

A preliminary experiment was carried out using HUVEC with control Bovine Serum Albumin (BSA-), recombinant human DLL4 (rhDLL4-), recombinant human JAG1 (rhJAG1-) and recombinant rat JAG1 (rrJAG1-) coated plates to determine the efficacy of rrJAG1 compared to rhJAG1 which has recently become available on the market. BLAST sequence of the rrJAG1 extracellular domain against that of rhJAG1 revealed a 96.7% homology between the two species.

Results demonstrate that the JAG1 and DLL4 ligands activated Notch signalling in the endothelial cells with DLL4 being more potent. However, at the same molarity, rhJAG1 was less potent compared to rrJAG1 in regulating the HEY1 and HEY2 Notch target genes and DLL4 downstream target gene at 8hr (Figure 3.2).

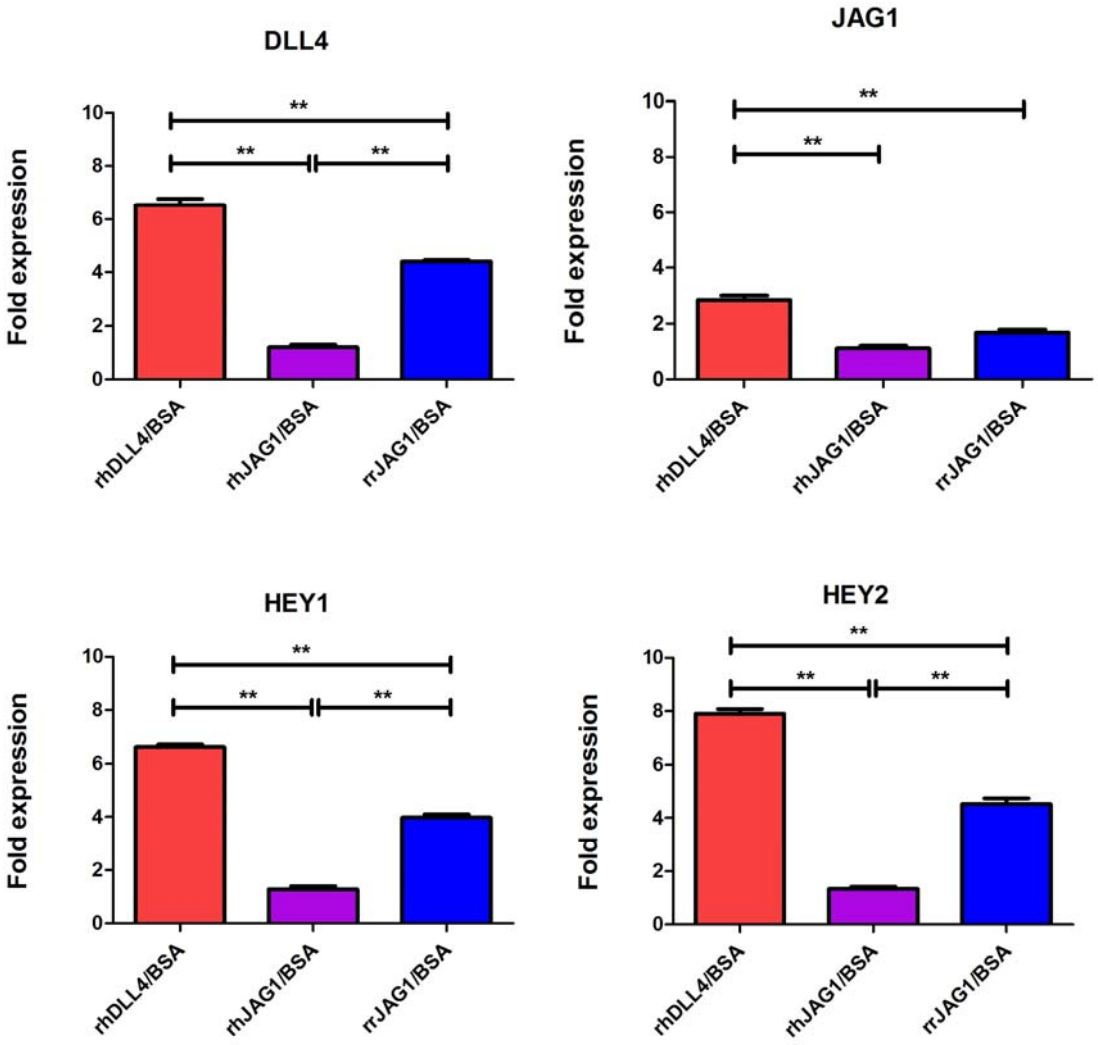


Figure 3.2**:** Exogenous activation of Notch signalling in HUVEC

mRNA expression of DLL4, JAG1, HEY1 and HEY2 in HUVEC following 8hr stimulation with BSA, rhDLL4, rhJAG1 or rrJAG1. Graphs are representatives of n=2, with the other replicate sharing a similar trend but with different degree of activation due to HUVEC donor variation. (**P<0.01, ANOVA with Bonferroni's post-test). Error bars represent SEM.

The lower potency of rrJAG1 in inducing the Notch downstream genes (Figure 3.2) prompted a preliminary dose response study to determine the optimal effect of both rhDLL4 and rrJAG1 recombinant proteins using six different protein concentrations (16, 8, 2, 0.25, 0.0625, 0.016 µg/ml) on coated plate compared to BSA to study the induction of Notch downstream genes, DLL4 and HEY1 at 8hr. Both recombinant proteins increased DLL4 and HEY1 expression in a dose dependent manner, with rrJAG1 being less effective compared to rhDLL4 (Figure 3.3 A and B). 1µg/ml rhDLL4 and 2.6 µg/ml of rrJAG1 proteins (18 nM equivalence) were the minimum working concentrations (and thus cost effective) that effectively activate Notch signalling.

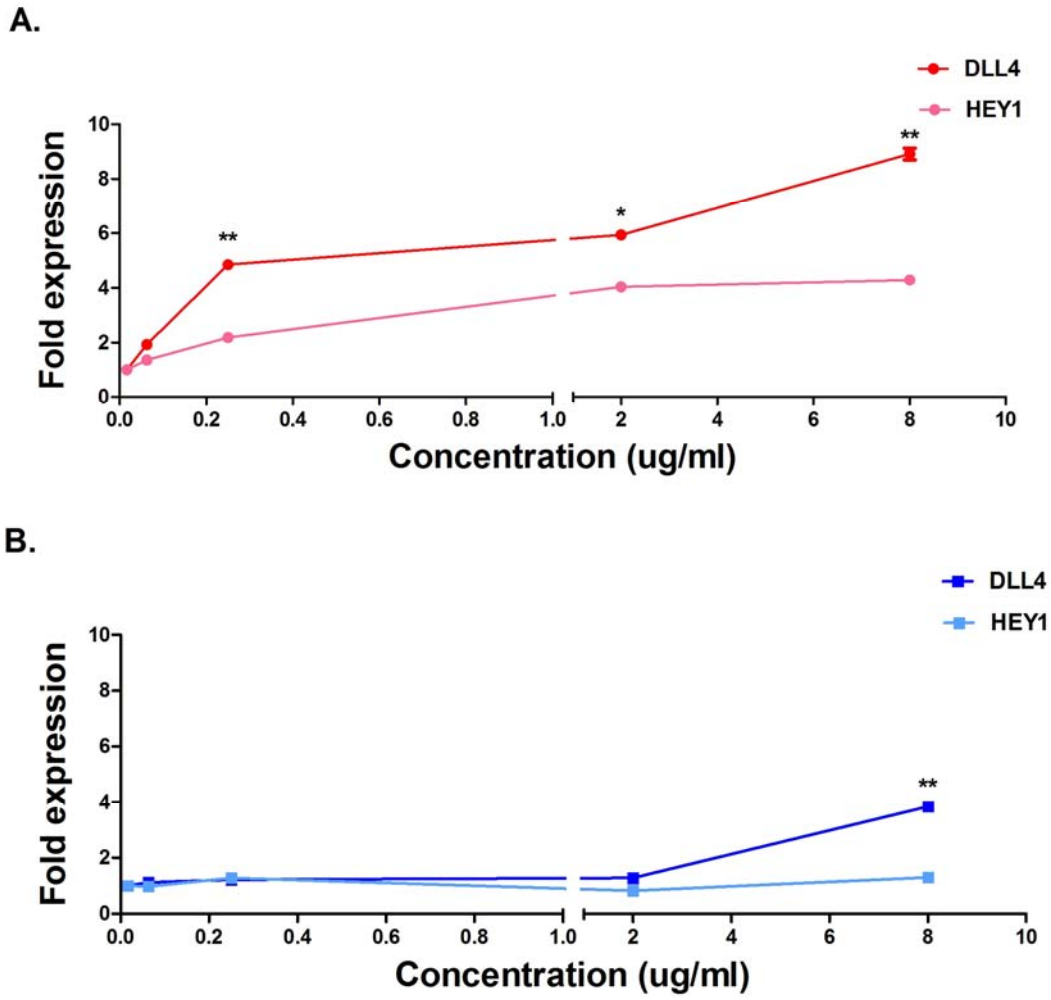


Figure 3.3: QPCR showing dose curve of A) rhDLL4/BSA and B) rrJAG1/BSA on DLL4 and HEY1 downstream gene expression in HUVEC at 8hr.

A series of rhDLL4 and rrJAG1 dilutions were tested on HUVEC. Graphs are representatives of n=1 from preliminary experiment (*P<0.05, **P<0.01, Student's t-test at each time point). Error bars represent SEM.

To overcome the variety in the expression of downstream Notch targets arising from multi donor source of HUVEC (for example DLL4 gene expression varied from 10 folds to 30 fold upon Notch activation on rhDLL4 coated plates in three independent experiments, data not shown), I looked for another alternative cell line. HMEC-1 has been used in angiogenic assays. After comparing the two cell lines (see Table 3.1), I decided to use HMEC-1 for future assays.

Table 3.1: Comparison between HUVEC and HMEC-1 as an angiogenic model

HUVEC	**HMEC-1**
Primary endothelial cell line isolated from human umbilical vein	An immortalized human dermal microvascular endothelial cell line transfected a PBR-322-based plasmid containing region for simian virus 40 and large T antigen (Ades et al. 1992)
Limited lifespan, undergo senescence at passages 8-10	Show no signs of senescence even after 95 passages (Ades et al. 1992)
Display characteristics that differ due to multi donor origin (Bouis et al. 2001)	Negate inconsistency associated with primary isolation (Lidington et al. 1999)
Laborious to isolate and requires more rigid care and growth media (10% FCS)	Require less stringent growth medium and can grow in absence of serum passaged 35 times without senescence (Ades et al. 1992)
Low proliferative rate thus need lentiviral transduction to over-express or knockdown gene expression	Easier manipulation for gene over-expressing or silencing

HMEC-1 was tested on recombinant rhDLL4 and rrJAG1 coated plates for 8hr, 24hr and 48hr to study the expression profile of the Notch target and downstream genes compared to that of HUVEC cells (Figure 3.4). Both rhDLL4 and rrJAG1 regulated the Notch target and downstream genes, in a similar manner over a time course, however to a lesser magnitude than following HUVEC stimulation by rrJAG1 (Figure 3.4 A). In HMEC-1, both rhDLL4 and rrJAG1 were equally capable of up-regulating DLL4, JAG1, HEY1, and HEY2 (Figure 3.4 B)

making HMEC-1 a good model to compare the effects of each ligand. Notch activation in HUVEC could be observed as early as 8 hours when DLL4, JAG1 and HEY1 expression were peaked; HEY2 expression however was highest at 24 hours. In contrast, DLL4 and JAG1 expression continued to increase over time whereas HEY1 and HEY2 peaked at 8hr in HMEC-1. An interesting observation was made whereby rhDLL4 stimulation was found to induce DLL4 expression, particularly so in HUVEC (approximately 10 folds at 8hr) compared to HMEC-1 (approximately 5 fold at 48hr). Stimulation by rrJAG1 also induced DLL4 but barely induced JAG1 expression in HUVEC (Figure 3.4 A). Both rhDLL4 and rrJAG1 were equally effective in up-regulating DLL4 gene expression with time. Similarly, induction of JAG1 gene expression by rhDLL4 and rrJAG1 was also observed in HMEC-1 at transcript level, with no significant difference in strength of activation between the two ligands. (Figure 3.4 B). Student t-test was carried out to compare the significance between rhDLL4 and rrJAG1 at the peaked time point (8hr for DLL4 and HEY1, 24hr for HEY2) in HUVEC, while no significance was observed between rhDLL4 and rrJAG1 regulation of downstream and target genes in HMEC-1. However, in HMEC-1 both rhDLL4 and rrJAG1 were equally potent in regulating the Notch target and downstream genes.

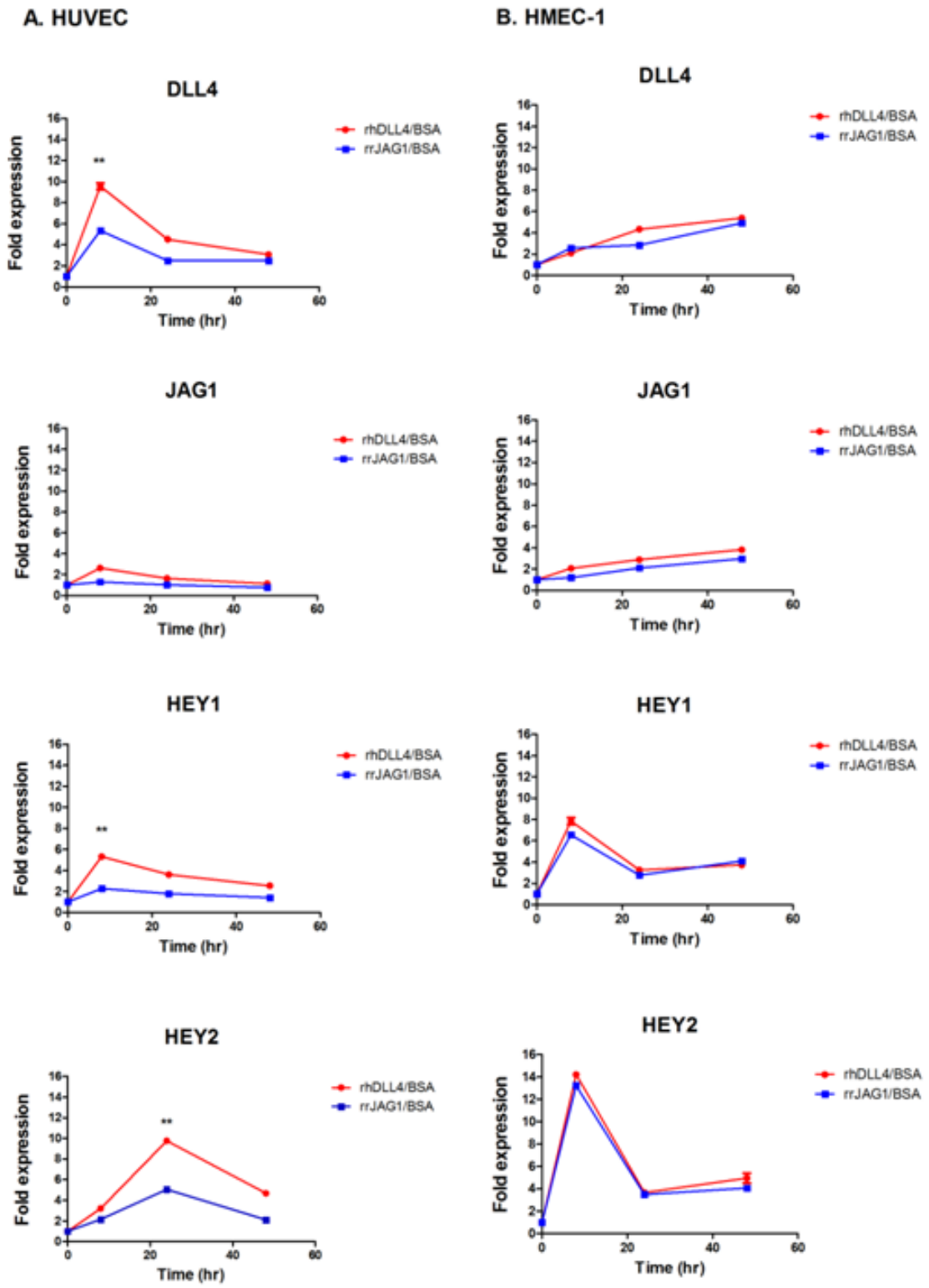


Figure 3.4**:** Downstream target gene expression profile in A) HUVEC and B) HMEC-1 stimulated with rhDLL4 (1 µg/ml) or rrJAG1 (2.6 µg/ml) over a time course.

QPCR was used to determine changes in the expression of DLL4, JAG1, HEY1 and HEY2 (**P<0.01, Student's t-test at peak experiment time point). Graphs are representatives of n=3 independent experiments.

Western blot using antibodies against DLL4, JAG1 and Notch1 Val1744 (N1 ICD) was carried out on HUVEC and HMEC-1 cell lysates to assess their expression at 8hr, 24hr and 48hr post Notch activation on BSA-, rhDLL4- and rrJAG1 plates. The protein expression profile for these genes was very different in both HUVEC (Figure 3.5) and HMEC-1 cells (Figure 3.6). Densitometry semi-quantitative analysis was carried out on Image J on a representative western blot to compare DLL4, JAG1 and N1 ICD protein expression compared to β-actin. Ideally, densitometry analysis should be carried out for all three blots, however due to experimental batch differences, a representative analysis is shown.

In HUVEC, rhDLL4 induced DLL4 expression at 8hr, 24hr and 48hr (Figure 3.5 A and B), in line with QPCR (Figure 3.4 A). rrJAG1 did not appear to induce DLL4 (Figure 3.5 A and B) even though QPCR showed a slight increase at transcript level (Figure 3.4 A). rrJAG1 induced JAG1 protein expression at 8hr and 24hr compared to BSA controls (slight increase was observed in QPCR at these time points, but not evident at 48hr) because cells were confluent (Figure 3.5 A and C), as JAG1 protein expression is positively dependent on cell confluency (Kawano et al. 2002). rhDLL4 also induced JAG1 expression at all time points studied compared to the BSA samples (Figure 3.5 A and C). N1 ICD was strongly induced by rhDLL4 in HUVEC compared to BSA samples (Figure 3.5 A and C). rrJAG1 also induced N1 ICD, but not to the same magnitude as DLL4 at all time points (Figure 3.5 A and D). This ties in with the lower potency of rrJAG1 to induce downstream target genes of Notch signalling compared to rhDLL4 by QPCR (Figure 3.4 A).

In HMEC-1, confluency increased DLL4 protein expression in BSA samples (Figure 3.6 A and B). QPCR results showed up-regulation of DLL4 expression at transcript level over time by rrJAG1 and rhDLL4 (Figure 3.4 B) which was represented in changes of the DLL4 protein

expression (Figure 3.6 A and B). rhDLL4 and rrJAG1 did induced JAG1 protein expression at 8hr compared to BSA control (Figure 3.6 A and C). JAG1 protein expression increased with confluency over the time course, as revealed in BSA samples (Figure 3.6 A and C). Confluency increased N1 ICD protein expression in BSA samples at 24hr, but level remained the same possibly due to maximal Notch activation (Figure 3.6 A and D). rhDLL4 induced N1 ICD expression more than rrJAG1 in HMEC-1, relative to BSA samples over time.

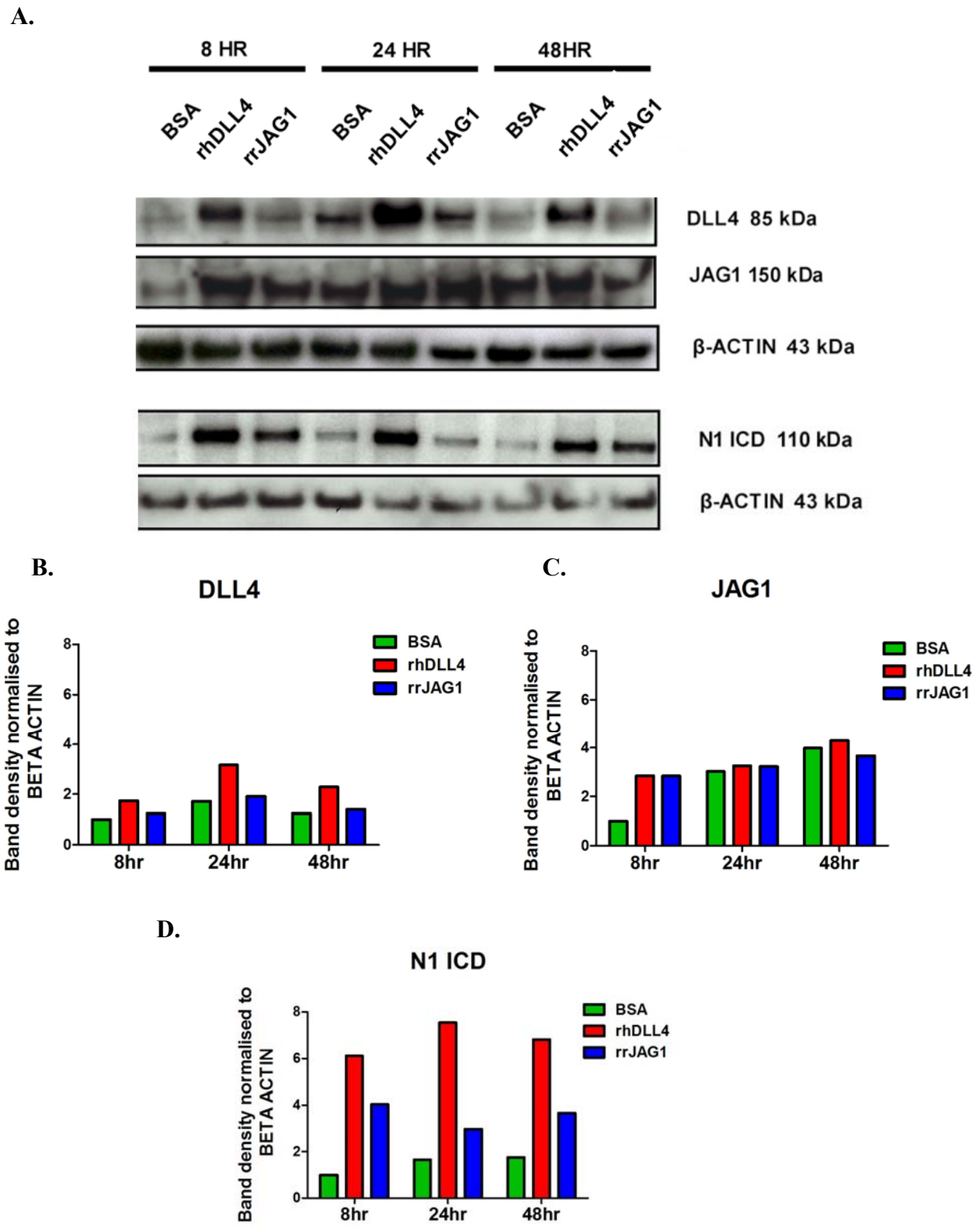


Figure 3.5: Protein expression profile of DLL4, JAG1 and N1 ICD upon Notch activation

HUVEC cells stimulated with BSA, rhDLL4 or rrJAG1 over a time course on by A) western blotting and densitometry analysis of B) DLL4, C) JAG1 and D) N1 ICD protein expression. β-ACTIN was used as loading control. Figure and graphs are a representative of n=3 independent experiments

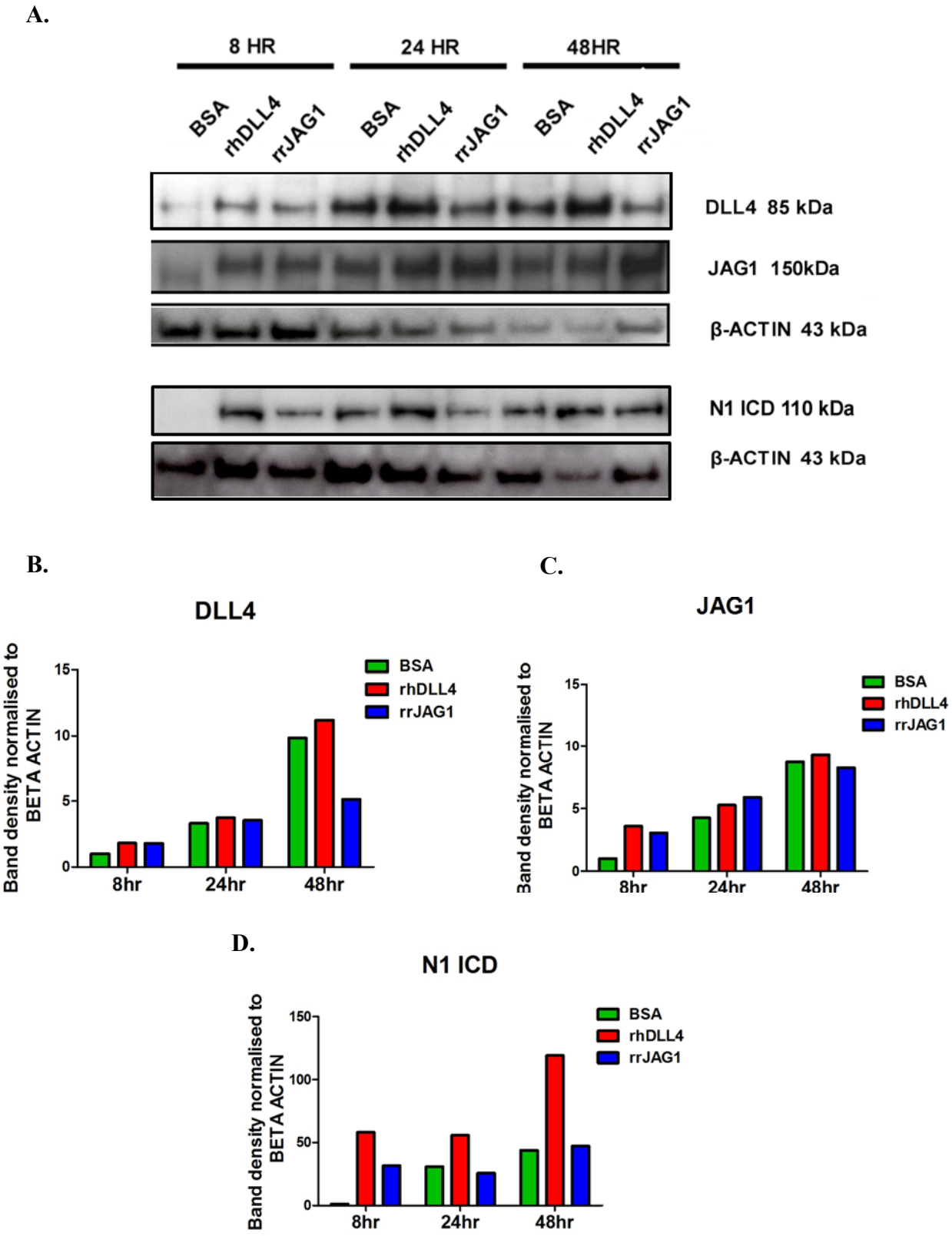


Figure 3.6: Protein expression profile of DLL4, JAG1 and N1 ICD upon Notch activation

HMEC-1 cells stimulated with BSA, rhDLL4 or rrJAG1 over a time course on by A) western blotting and densitometry analysis of B) DLL4, C) JAG1 and D) N1 ICD protein expression. β-ACTIN was used as loading control. Figure and graphs are a representative of n=3 independent experiments.

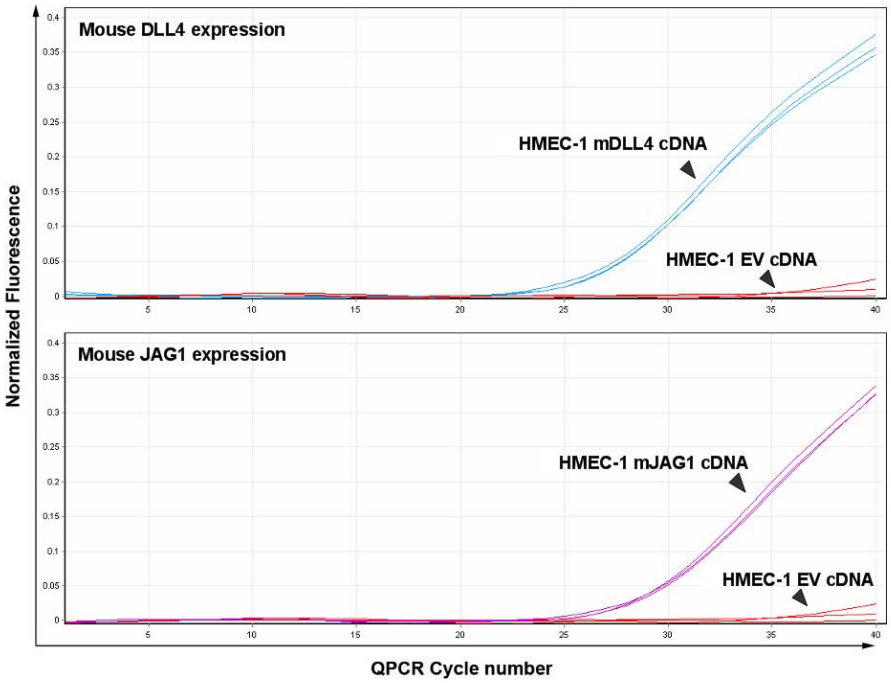
3.4 Characterisation of HMEC-1 mDLL4 and HMEC-1 mJAG1

HMEC-1 over-expressing murine DLL4 (mDLL4), murine JAG1 (mJAG1) or control HMEC-1 cells (EV) were kindly provided by Dr. Ji-Liang Li (Oxford). HMEC-1 cells were transduced with an LZRSpBMN-linker-IRES-EGFP retroviral vector encoding for full length mDLL4, mJAG1 or empty vector (EV). These cell lines were first characterised to confirm ligand over-expression by quantitative PCR (QPCR) and western blot.

3.4.1 mDLL4 and mJAG1 were up-regulated in HMEC-1 over-expressing cell line

To confirm successful retroviral transduction of mDLL4 or mJAG1 into HMEC-1 cells, RNA was harvested and subjected to QPCR. Murine DLL4 and murine JAG1 genes were both detectable in the expressing cell line at mRNA level (Figure 3.7 A), as well as on the protein level (Figure 3.7 B) compared to empty vector (EV). The antibodies used to probe for protein recognise both the human and mouse Notch ligands. Green Fluorescent Protein (GFP) expression from the vector indicated successful transduction of EV, mDLL4 and mJAG1 into HMEC-1 with similar expression levels between JAG1 and DLL4 (Figure 3.7 B).

A.



B.

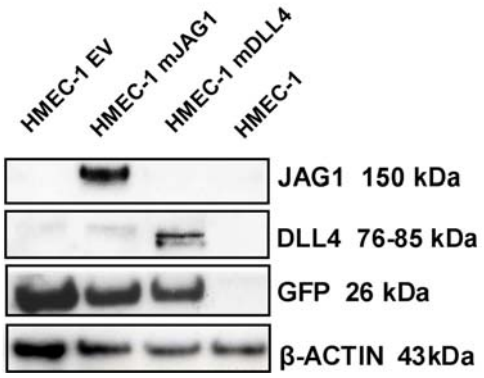


Figure 3.7: Expression of mDLL4 and mJAG1 in HMEC-1 mDLL4 or HMEC-1 mJAG1 over-expressing cells respectively at both the A) transcript level and B) protein level, indicating successful retroviral transduction.

Representative figures for QPCR and western blot, n=2 independent experiments. β-ACTIN was used as loading control.

3.4.2 mDLL4 and mJAG1 activation of Notch signalling up-regulated downstream and Notch target genes in HMEC-1

To determine if the mDLL4 and mJAG1 being expressed was functional and capable of activating Notch signalling in neighbouring cells, RNA was isolated for QPCR to examine the expression of DLL4, JAG1, HEY1 and HEY2. mDLL4 increased the expression of DLL4 in a feed forward mechanism as also shown by others (Caolo et al. 2010). Induction of HEY1 and HEY2 was higher in mDLL4 compared to mJAG1 over-expressing cells. Both mDLL4 and mJAG1 equally up-regulated the expression of JAG1 (Figure 3.8).

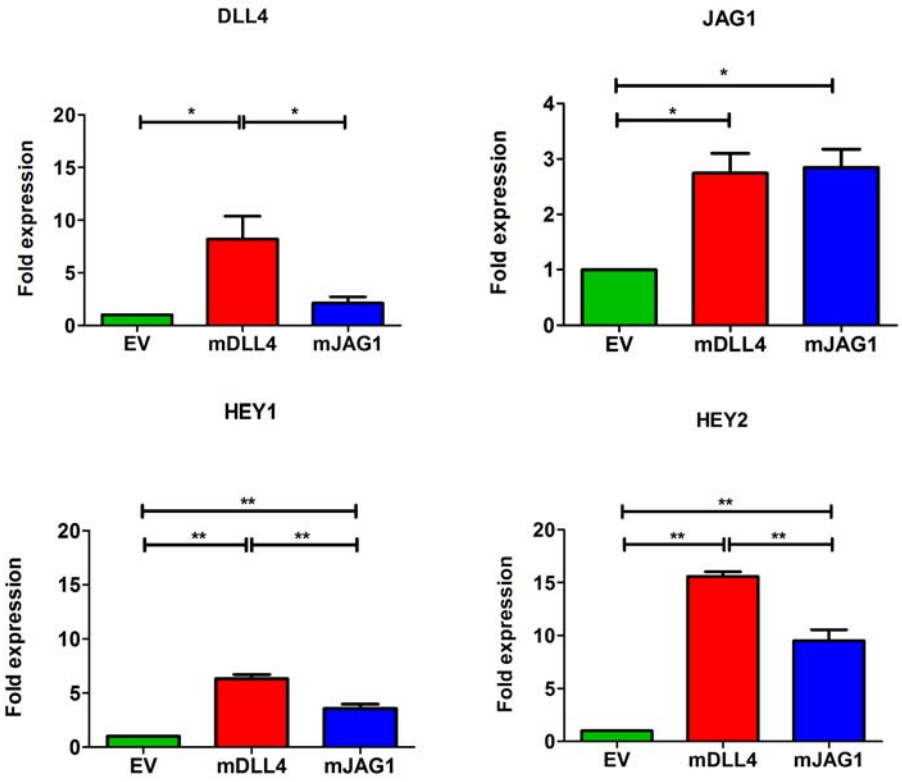


Figure 3.8: The up-regulation of downstream and target genes in over-expressing cell lines.

Real-time PCR was used to measure the expression of DLL4, JAG1, HEY1 and HEY2 (*P<0.05, **P<0.01, ANOVA with Bonferroni's post-test, n=3). Error bars represent SEM.

3.5 Activation of Notch signalling did not affect cell proliferation in HMEC-1 cells

Endothelial cell proliferation is an important feature of the sprouting process in angiogenesis. The effects of DLL4 and JAG1 ligands on endothelial cell proliferation was assessed by determining changes in cell number.

Over-expression of either mDLL4 or mJAG1 in HMEC-1 cells did not affect cell number over 6 days compared to EV cells (Figure 3.9).

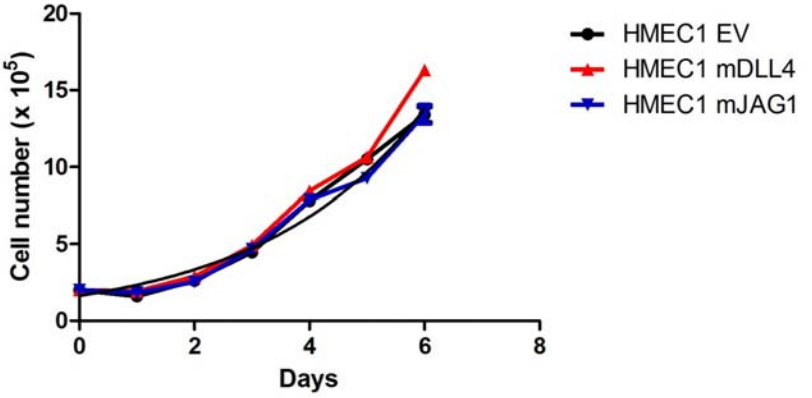


Figure 3.9**:** mDLL4 and mJAG1 did not affect HMEC-1 cell number relative to EV cells.

Statistics analysis (F test) revealed no significant differences. Error bars represent SEM (n=3).

3.6 Role of mDLL4 and mJAG1 in angiogenesis

As no single model can capture the whole array of complexity associated with angiogenesis, several assays with increasing intricacy were employed to address a few aspects of angiogenesis which are known to be modulated by DLL4- and JAG1- Notch signalling: cell proliferation, cell migration, network formation and capillary outgrowth. A standard

concentration of 200nM of DBZ was used in selectedexperiments to effectively inhibit Notch signalling (van Tetering et al. 2009), as indicated by diminished expression of activated N1 ICD (Figure 3.10).

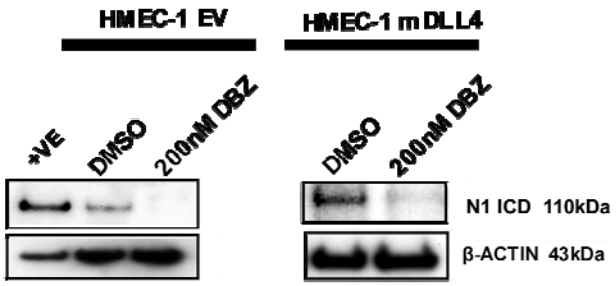


Figure 3.10**:** DBZ (200nM) inhibited Notch signalling in HMEC-1 EV and HMEC-1 mDLL4 at 8hr.

HMEC-1 mDLL4 was used as a positive control (+VE) for activated N1 ICD. β-ACTIN was used as loading control. Figure is a representative of n=2 independent experiments.

3.6.1 Both mDLL4 and mJAG1 increased HMEC-1 cell motility

A scratch wound assay was utilised to study the effect of mDLL4 and mJAG1 on endothelial cell migration, HMEC-1 cells were grown to confluence in a 12-well plate and scraped with a sterile 10µl pipette tip to create a cell-free zone (0hr). Cells were rinsed twice with PBS before images were acquired at 0hr. The rate of cells moving into the artificially generated space to close this wound was used to quantify cell migration. Data was presented as the percentage area of cell-free zone relative to 0hr. Both mDLL4 and mJAG1 promoted cell migration as indicated by increased rate by which the cells close the wound (Figure 3.11).

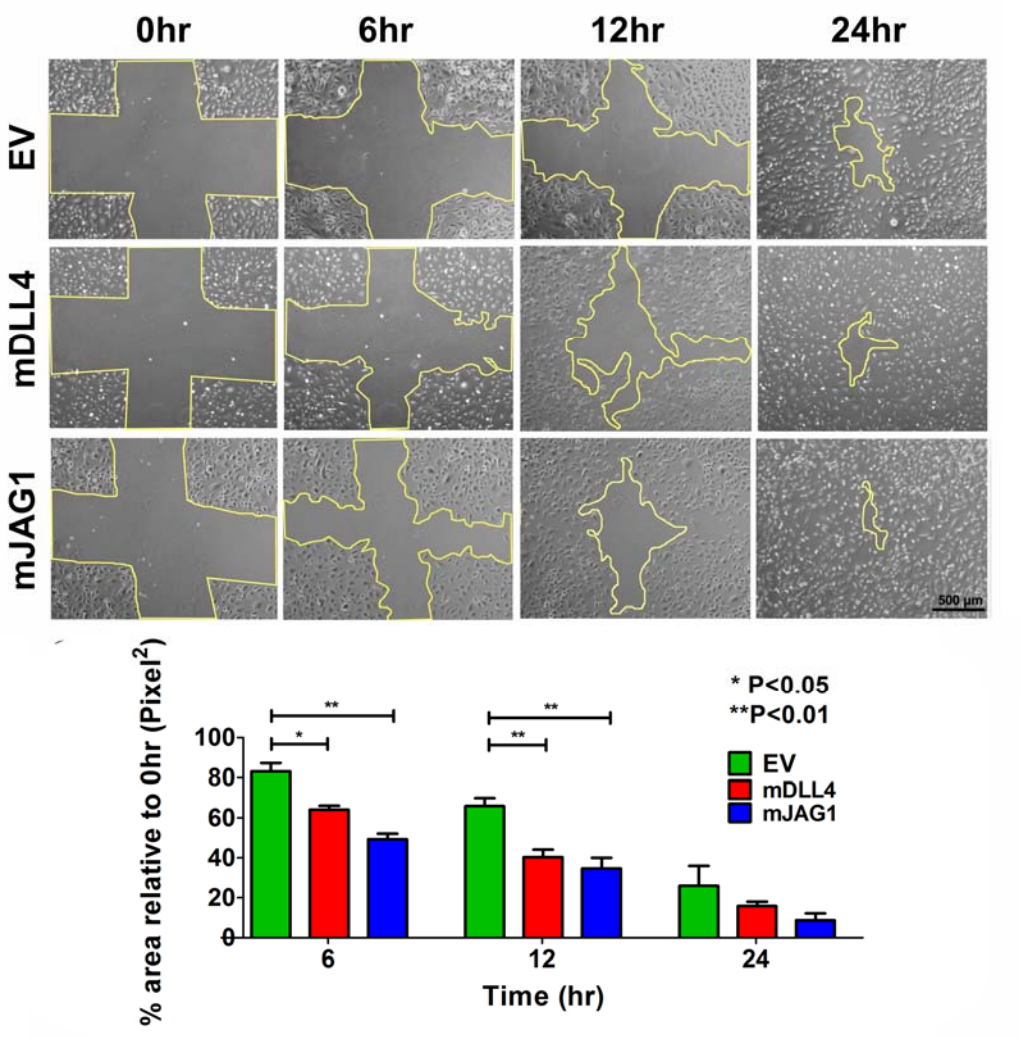


Figure 3.11**:** mDLL4 and mJAG1 promoted HMEC-1 cell migration.

Endothelial cell migration was quantified by measuring the width of the cell-free zone (distance between the edges of the injured confluent monolayer) over a time course after the wound was made in confluent cells. Areas of scratch were captured and quantified in Image J. Statistics analysis (*P<0.05, **P<0.01, ANOVA with Bonferroni's post-test, n=5 independent experiments). Error bars represent SEM.

3.6.2 mDLL4 and mJAG1 had different effects on network formation

The Matrigel network formation assay can model the reorganization stage of angiogenesis. To elucidate the role of DLL4 and JAG1 in forming a tube-like network, HMEC-1 over-

expressing mDLL4 or mJAG1 were placed on polymerized Matrigel to promote the formation of tube-like structures. In this assay, cells initially attach to the matrix, then migrate towards each other, organize and form a network. Network formation was quantified by calculating the number of nodes which are the branch points of any three or more connecting capillary-like structures (Ward et al. 2010) and the number of closed polygons (Ramachandran et al. 2009) on average per field of view in two-dimensional microscope images of the 96 well plate.

HMEC-1 mDLL4 had markedly reduced number of nodes and closed polygons while HMEC-1 mJAG1 formed network with increased branch points and polygons. Inhibition of Notch signalling with DBZ increased node numbers in mDLL4 over-expressing cells (Figure 3.12)

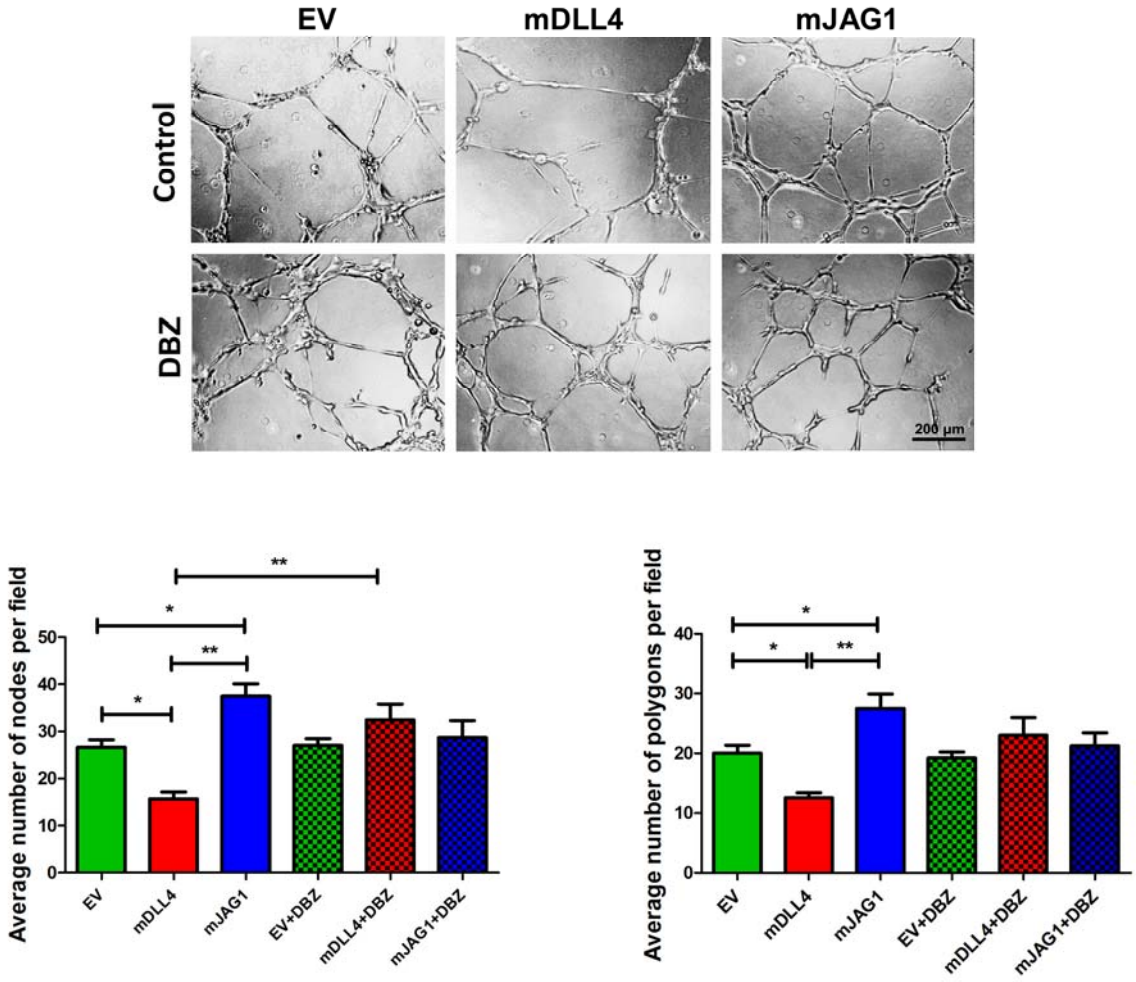


Figure 3.12**:** mDLL4 reduced number of nodes and polygons whereas mJAG1increased number of nodes and polygons on the Matrigel assay after 8hr, relative to EV control.

DBZ (200 nM) was used to inhibit Notch signalling. Number of nodes (branch points) and polygons (honeycomb formation) from a total of 6 wells per experiment were quantified. Statistics analysis (*P<0.05, **P<0.01, ANOVA with Bonferroni's post-test, n=3 independent experiments). Error bars represent SEM

3.6.3 mDLL4 and mJAG1 elicited different effects on sprouting

Embedding endothelial spheroids into Matrigel (the hanging drop assay) provides a three-dimensional (3D) assay modelling the complexity of the sprouting angiogenesis, by the invasion into the extracellular matrix and differentiation of the tip and stalk cell leading to the

formation of complex 3D tubes. To form the endothelial spheroids, HMEC-1 cells over-expressing mDLL4, mJAG1 and control EV were suspended in droplets of medium, where they developed into articulate 3D aggregates overnight, after which they were embedded into Matrigel. Sprouts emerging from endothelial cell spheroids formed capillary like structures, which were most apparent and easy to quantify at Day 3 (Figure 3.13). The influence of mDLL4 and mJAG1 on HMEC-1 spheroid sprouting was assessed by measuring the average length of the three longest sprouts per spheroid (Korff and Augustin 1999) and the area covered by the sprouts originating from 15 randomly selected individual spheroids per well, using Image J.

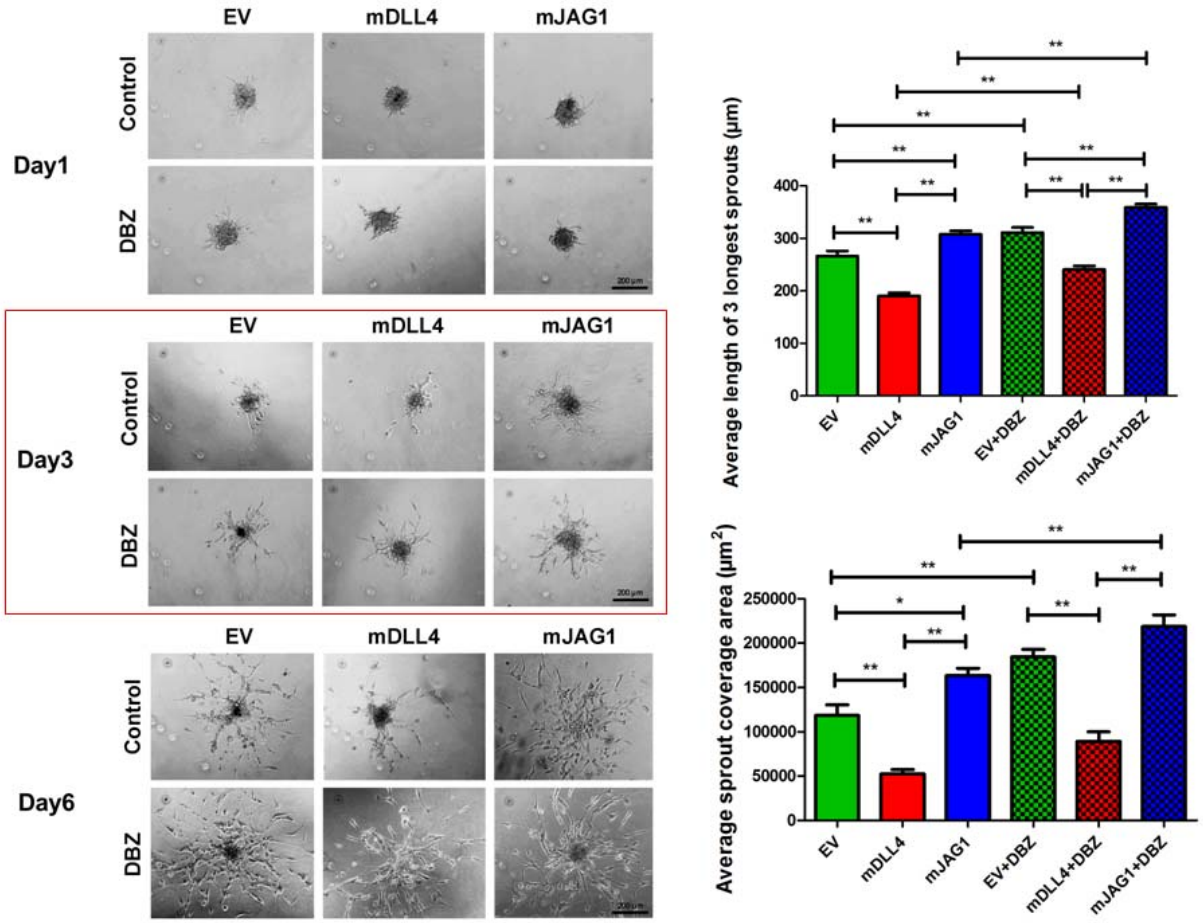


Figure 3.13**:** A) Effect of mDLL4 and mJAG1 on sprouting in HMEC-1 spheroids over a time course and B) changes quantified on Day3.

Images for an average of 15 spheroids per condition were acquired at Day1, Day 3 and Day 6. Coverage and average length of 3 longest sprouts at Day 3 were quantified with Image J. Statistics analysis (*P<0.05, **P<0.01, ANOVA with Bonferroni's post-test, n=3 independent experiments). Error bars represent SEM.

A larger figure for the HMEC-1 EV, mDLL4 and mJAG1 spheroids at Day 3 is shown in Figure 3.13.1.

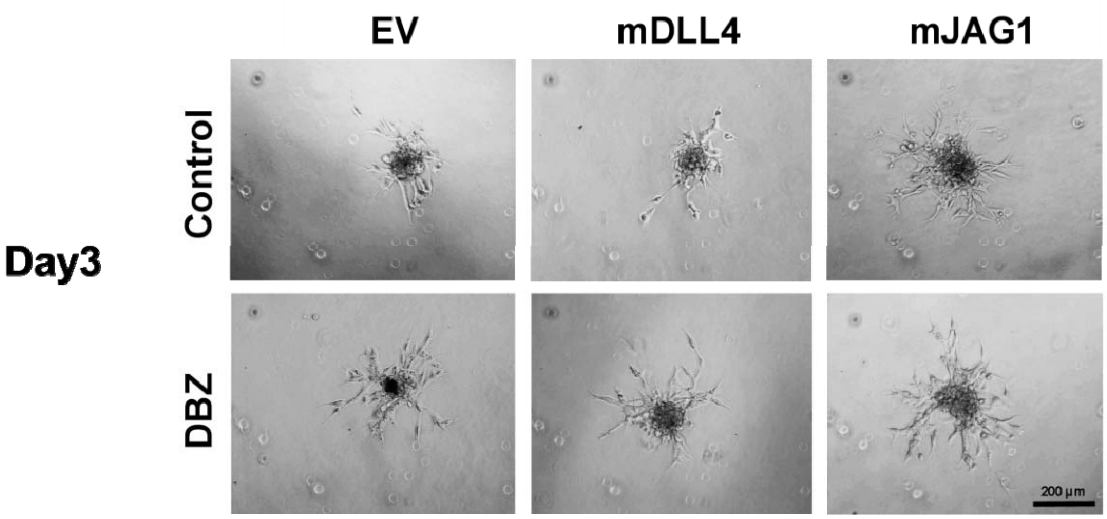


Figure 3.13.1**:** Effects of mDLL4 and mJAG1 on sprouting in HMEC-1 spheroids at day 3.

In contrast to mDLL4 cells which had decreased sprout lengths and overall sprout coverage area, mJAG1 cells promoted sprouting (Figure 3.13). Blocking Notch signaling with DBZ on the other hand increased sprouting in EV, mDLL4 and mJAG1 spheroids.

3.7 Role of endogenous DLL4 and JAG1 ligands in angiogenesis

While over-expressing full length DLL4 and JAG1 ligands in endothelial cells enabled assessment of their functional roles in angiogenic assays, it may not be physiologically or biologically relevant as over-expression of ligands constitutively activates Notch signalling. As DLL4 and JAG1 are robustly expressed in endothelial cells, the role of each ligand modulating features of angiogenesis was also studied through loss-of-function experiments, involving knocking down of DLL4 or JAG1 by small interfering RNAs (siRNAs) in HMEC-1 cells on angiogenic functional assays. HMEC-1 cells were transfected with scrambled (Scr), DLL4 or JAG1 siRNA (siDLL4 or siJAG1 respectively). DLL4 and JAG1 gene knockdown

were maintained at approximately 60% (Figure 3.14) and 70% (Figure 3.15) respectively over a period of 6 days on both the mRNA (determined by QPCR) and protein levels (assessed by western blot and immunofluorescence staining).

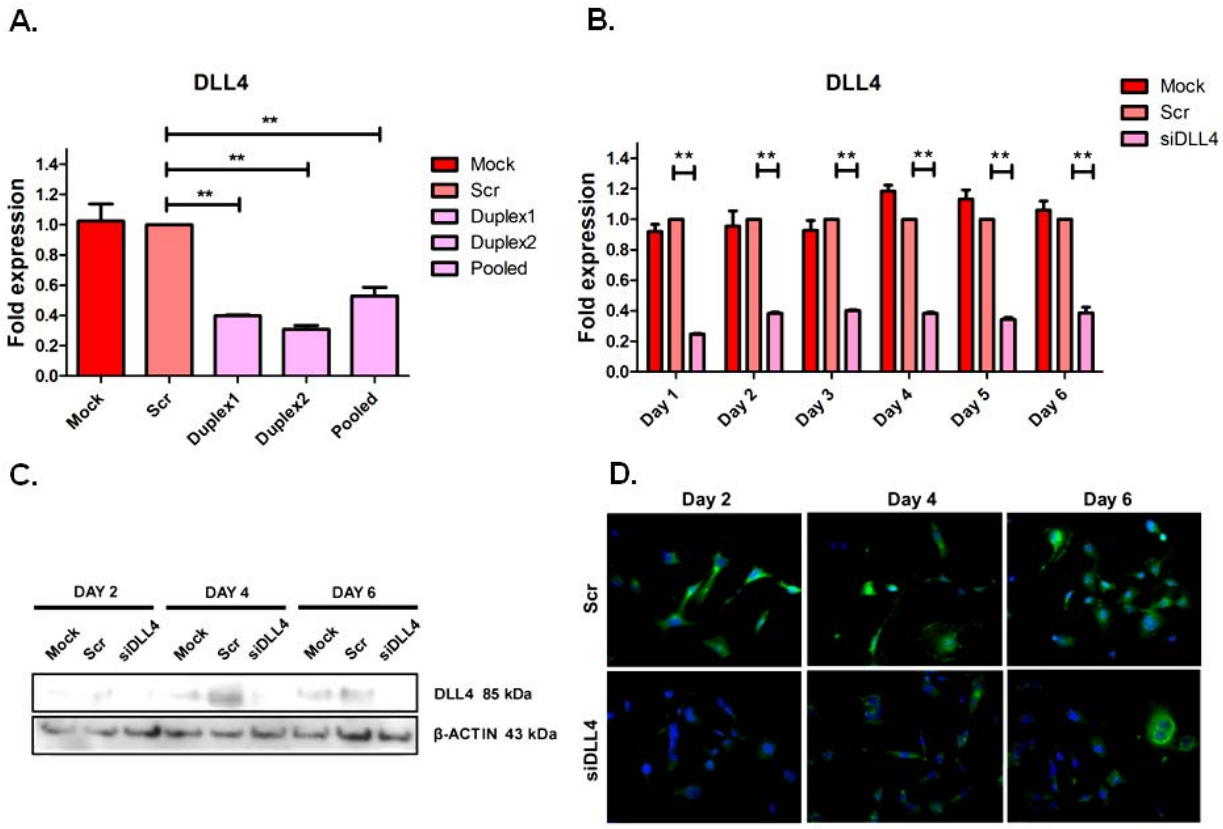


Figure 3.14**:** Confirmation of successful knockdown of DLL4 expression on the mRNA level A) by two different siRNA duplexes (20nM) and B) over a time course, as well as reduction of DLL4 protein expression over a time course using Duplex 2, confirmed by C) western blot and D) immunofluorescence, compared to Scrambled (Scr) control.

A representative figure for QPCR, western blot and immunofluorescence is shown (n=2 independent experiments). Statistics analysis (**P<0.01, ANOVA with Bonferroni's post-test). Error bars represent SEM.

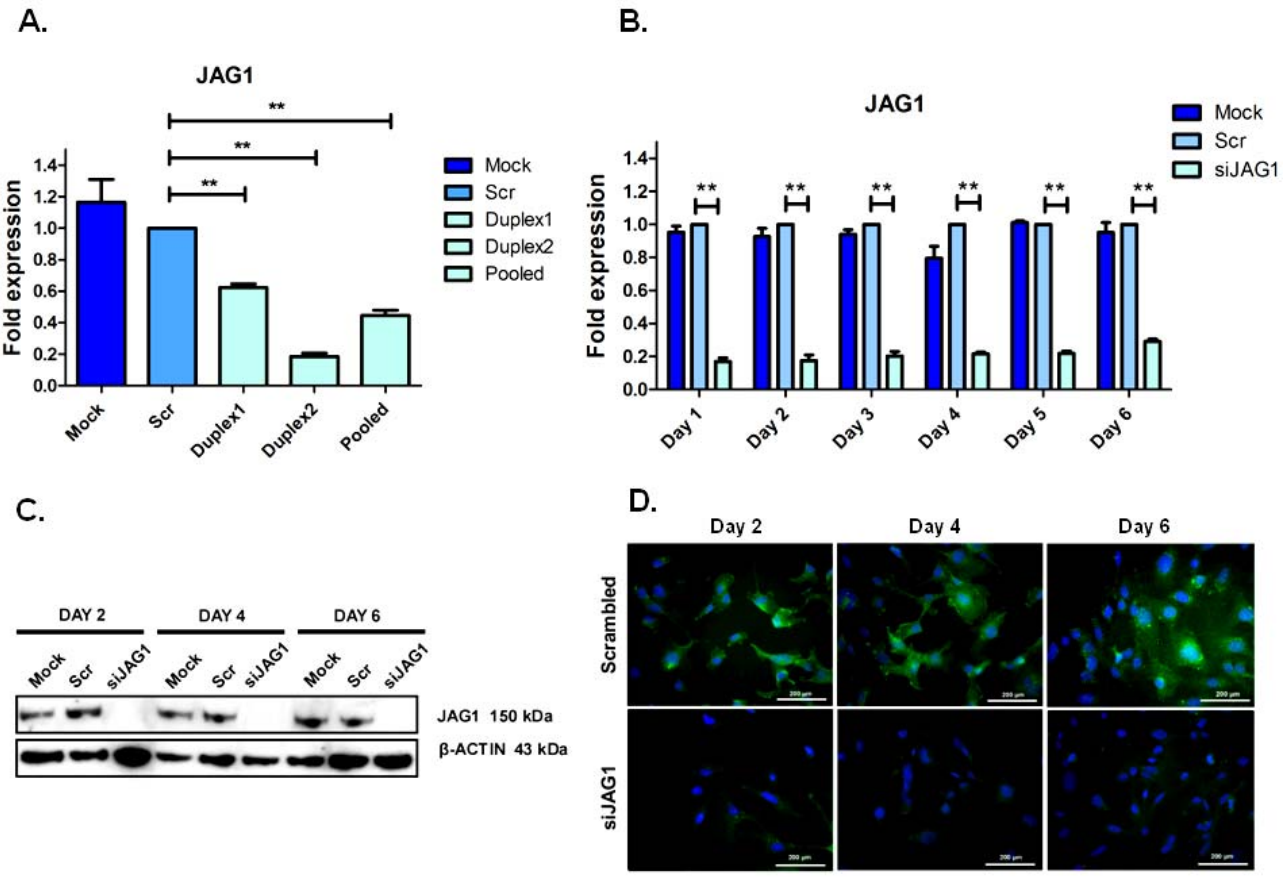


Figure 3.15**:** Confirmation of successful knockdown of JAG1 expression on the mRNA level A) by two different siRNA duplexes (5nM) and B) over a time course, as well as reduction of DLL4 protein expression over a time course using Duplex 2, confirmed by C) western blot and D) immunofluorescence, compared to Scrambled (Scr) control.

A representative figure for QPCR, western blot and immunofluorescence is shown (n=2 independent experiments). Statistics analysis (**P<0.01, ANOVA with Bonferroni's post-test). Error bars represent SEM.

3.7.1 Silencing either DLL4 or JAG1 in HMEC-1 reduced cell number *in vitro*

While over-expression of mDLL4 and mJAG1 had no effect on HMEC-1 cell count, it was observed that siRNA suppression of either DLL4 or JAG1 decreased cell number over time (Figure 3.16).

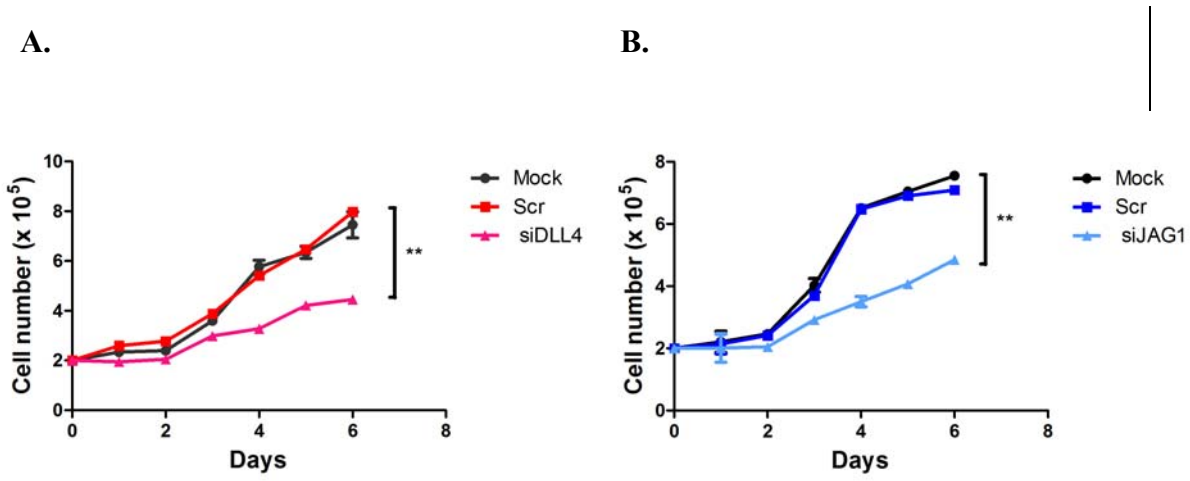


Figure 3.16**:** Both A) DLL4 and B) JAG1 knockdown reduced HMEC-1 cell number compared to the Scrambled (Scr) and Mock growth curves.

Day of siRNA transfection is indicated as Day 0. Data are shown as mean ± SEM of duplicate wells from the representative results of three independent experiments. ANOVA F test (**P<0.01). Error bars represent SEM.

3.7.2 Silencing either endogenous DLL4 or JAG1 inhibited cell migration

To assess the role of endogenous DLL4 and JAG1 ligands in mediating cell migration, HMEC-1 cells were treated with siRNAs for DLL4 or JAG1 and plated onto a 12 well plate and grown to confluency. Experiment was carried out as described previously. Silencing DLL4 and JAG1 individually with small interfering RNA reduced cell migration at 24hr compared to the Scr control cells (Figure 3.17).

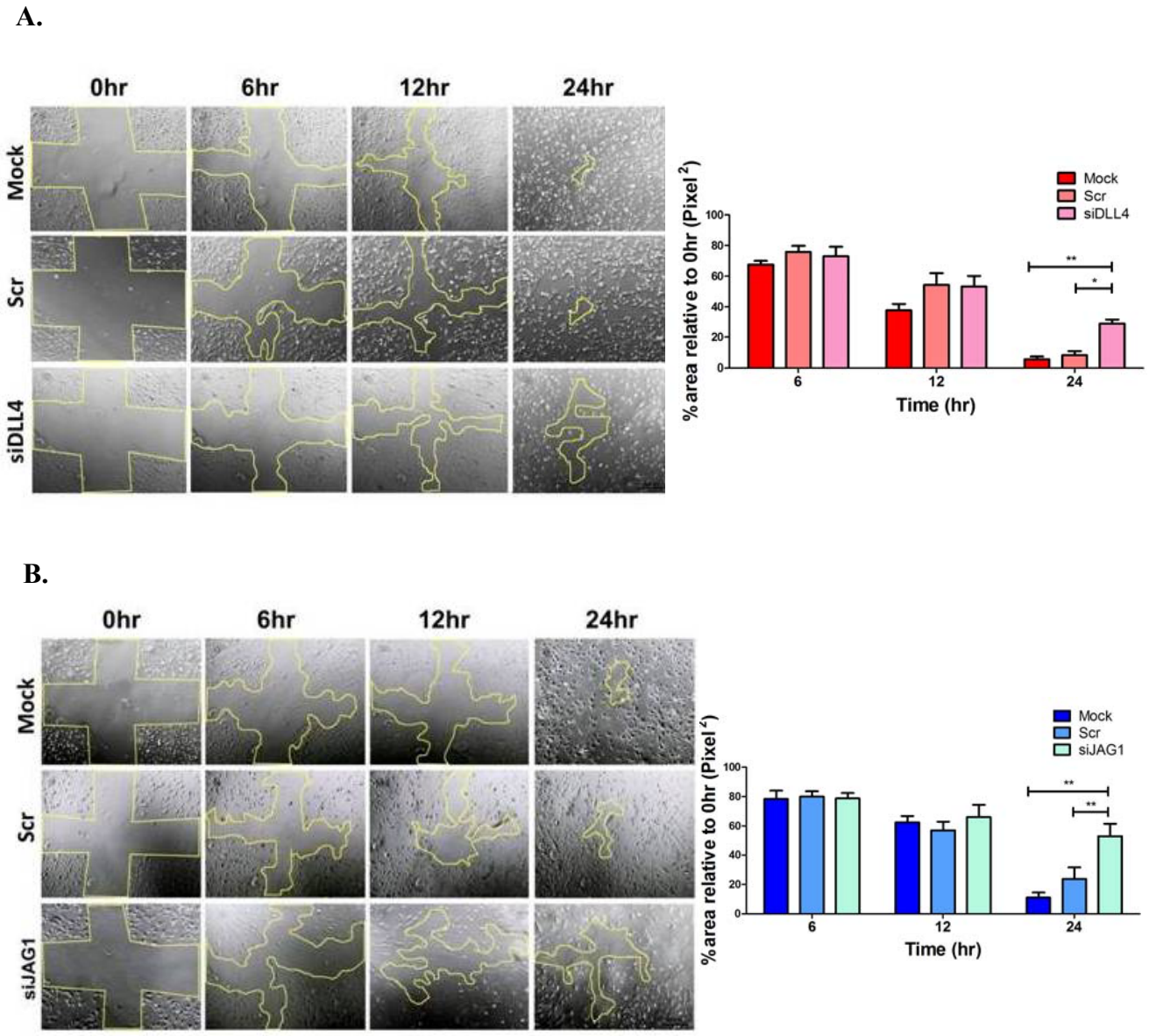


Figure 3.17**:** Silencing of either A) DLL4 or B) JAG1 hampered migration of HMEC-1 cells.

Effect of DLL4 or JAG1 knockdown on migration was quantified by measuring the width of the cell-free zone (distance between the edges of the injured confluent monolayer) over a time course after the wound was made in confluent cells. Areas of scratch were quantified in Image J. Statistics analysis (*P<0.05, **P<0.01, ANOVA with Bonferroni's post-test, n=5 independent experiments). Error bars represent SEM.

3.7.3 Silencing either DLL4 or JAG1 had different effects on HMEC-1 network formation

HMEC-1 endothelial cell network formation was assessed on matrigel assay as previously described. Interestingly, silencing DLL4 inhibited the formation of network on Matrigel, whereas silencing JAG1 did not affect the formation of nodes or polygons compared to Scrambled (Scr) cells (Figure 3.18). However, blocking Notch signalling with DBZ (200nM) did not reverse the network phenotype observed for either siDLL4 cells (Figure 3.18 A) or for the siJAG1 cells (Figure 3.18 B).

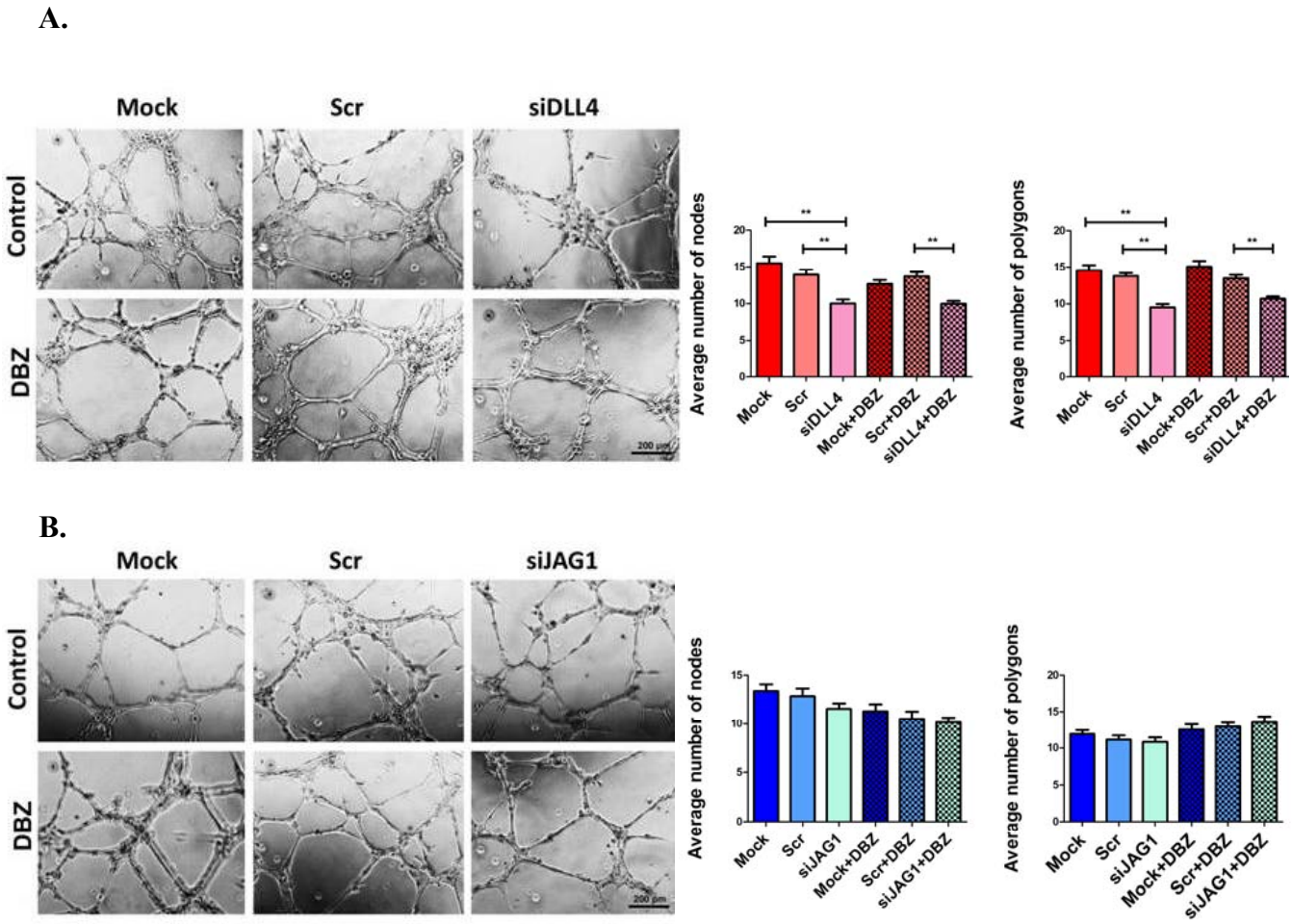


Figure 3.18**:** Effect of A) DLL4 or B) JAG1 siRNA in HMEC-1 cells on network formation.

Endothelial networks from DMSO control or DBZ (200nM) treated groups were photographed 1 field per well at 8hr. Number of nodes (branch points) and polygons (honeycomb formation) from a total of 6 wells per experiment were quantified. Statistics analysis (*P<0.05, **P<0.01, ANOVA with Bonferroni's post-test, n=3 independent experiments). Error bars represent SEM.

3.8 Silencing endogenous DLL4 or JAG1 had opposite effects on sprouting

To examine the role of endogenous DLL4 and JAG1 ligands in modulating sprouting, DLL4 or JAG1 expression was silenced in HMEC-1 cells and embedded into Matrigel as endothelial spheroids and quantified as previously described for the hanging drop assay.

When DLL4 and JAG1 expression was knocked down following siRNA transfection, siDLL4 and siJAG1 displayed opposite effects in the hanging drop assay. Upon assessment of sprout length and coverage area at Day 3, siDLL4 significantly increased sprouting and coverage (Figure 3.19), while siJAG1 decreased sprout length and coverage area (Figure 3.20). Treatment with DBZ (200nM) increased sprouting in the Scrambled (Scr) spheroids (Figure 3.19 and Figure 3.20) and reversed the effect of JAG1 suppression by increasing sprouting (Figure 3.20).

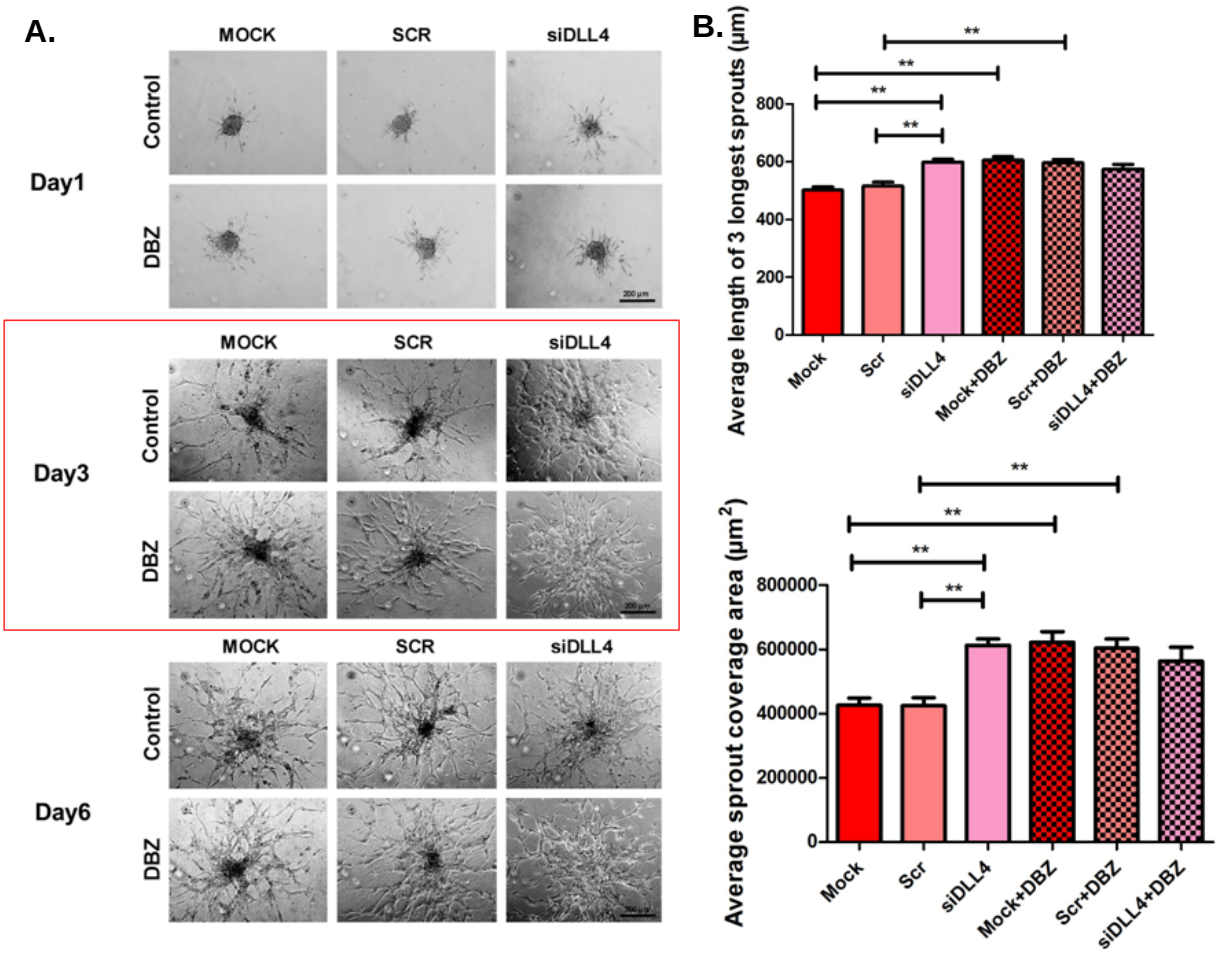


Figure 3.19**:** Effect of DLL4 suppression on HMEC-1 sprouting.

24 hours post transfection, Mock, Scrambled (Scr) and siDLL4 spheroids were embedded into full Matrigel and treated with DBZ (200nM) over a time course. A) Images for 15-20 spheroids per condition were acquired at Day1, Day 3 and Day 6. B) Spheroid sprout coverage and average length of 3 longest sprout were quantified at Day 3. Statistics analysis (**P<0.01, ANOVA with Bonferroni's post-test, n=3 independent experiments). Error bars represent SEM.

A larger representative figure for the effects of DLL4 suppression and JAG1 suprression on HMEC-1 sprouting at Day 3 is shown in Figure 3.19.1 and Figure 3.20.1 respectively.

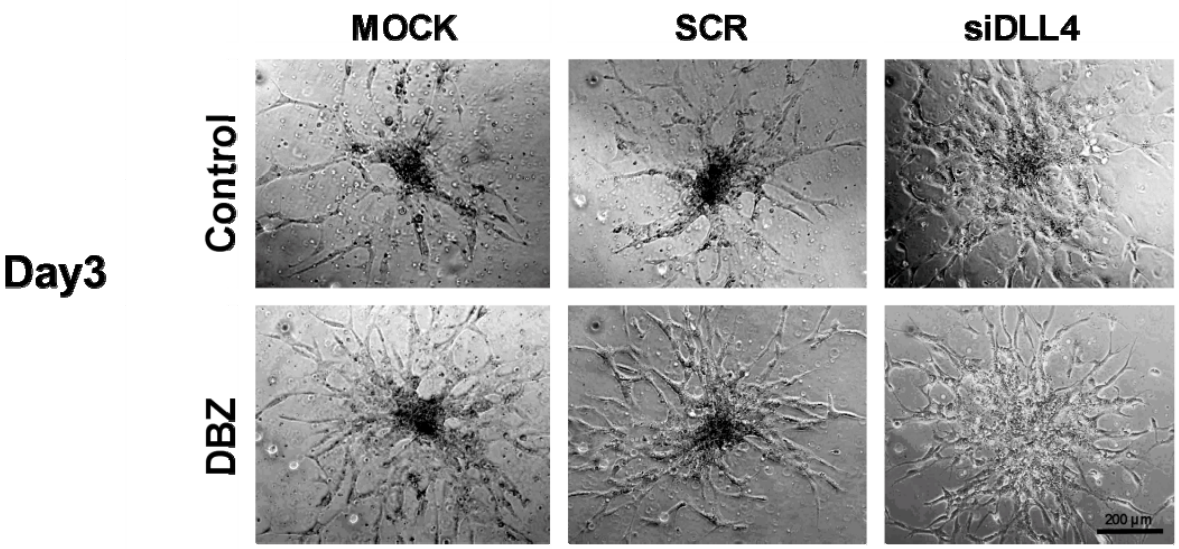


Figure 3.19.1**:** Effect of siDLL4 on sprouting in HMEC-1 spheroids at Day 3.

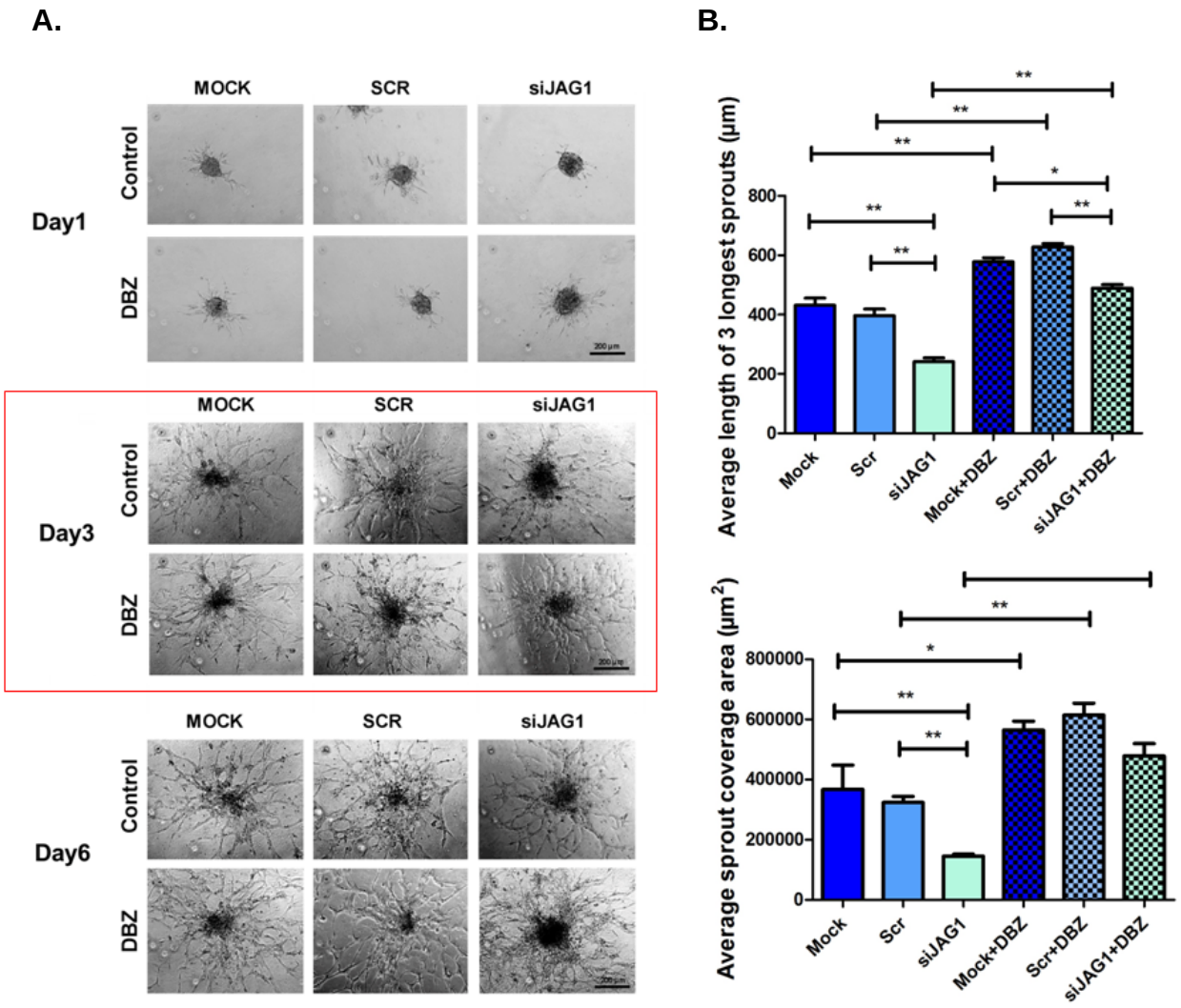


Figure 3.20**:** Effect of JAG1 suppression on HMEC-1 sprouting.

24 hours post transfection, Mock, Scrambled (Scr) and siJAG1 spheroids were embedded into full Matrigel and treated with DBZ (200nM) over a time course. A) Images for 15-20 spheroids per condition were acquired at Day1, Day 3 and Day 6. B) Spheroid sprout coverage and average length of 3 longest sprout were quantified at Day 3. Statistics analysis (**P<0.01, ANOVA with Bonferroni's post-test, n=3 independent experiments). Error bars represent SEM.

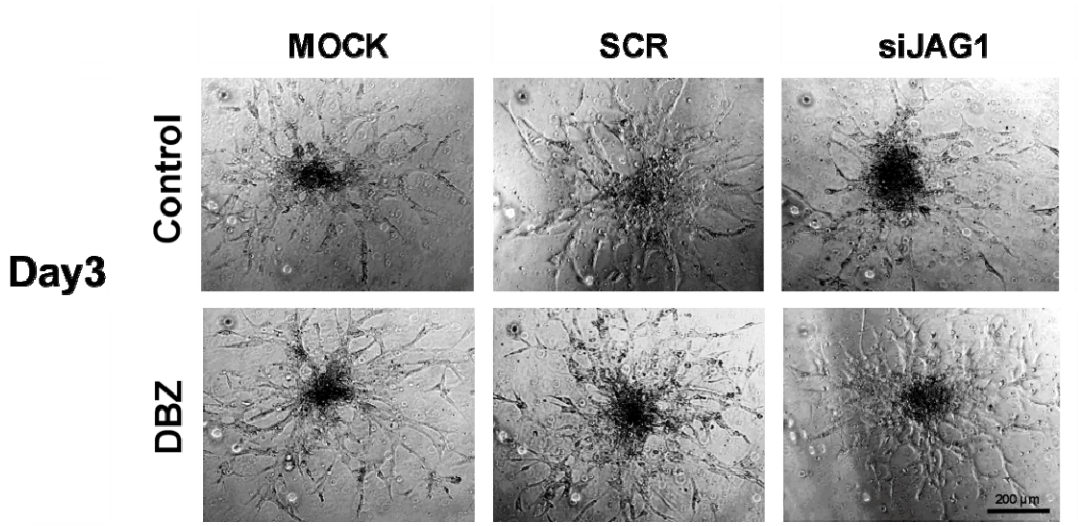


Figure 3.20.1**:** Effect of siJAG1 on sprouting in HMEC-1 spheroids at Day 3.

The subsequent effects of DLL4 and JAG1 over-expression or knockdown with siRNA on cell number, cell migration, network formation and sprouting are summarised in Table 3.2.

Table 3.2: Summary of effects of DLL4- and JAG1-Notch signalling on *in vitro* angiogenic assays compared to control EV (for over-expressing cells) or Scrambled (for siRNA gene suppression cells).

	Cell Count Assay	**Migration Scratch Assay**	**Matrigel Assay**	**Hanging Drop Assay**
HMEC-1 over-expressing mDLL4 or mJAG1	No difference	Both mDLL4 and mJAG1 promoted cell migration	mDLL4 reduced formation of nodes and polygons mJAG1 increased node numbers and polygons	mDLL4 decreased sprouting mJAG1 increased sprouting
DLL4 or JAG1 siRNA in HMEC-1	Suppression of either ligand reduced cell number	Suppression of either ligand reduced cell migration	siDLL4 reduced number of nodes and polygons siJAG1 had no effect on node numbers and polygons	siDLL4 increased sprouting siJAG1 decreased sprouting

3.9 Discussion

Basal expression pattern of DLL4 and JAG1 in HUVEC and HMEC-1

DLL4 and JAG1 are expressed in HUVEC and HMEC-1. Immunofluorescence staining with anti- JAG1 and anti-DLL4 antibody which corresponded to the intracellular region of the ligands revealed cytoplasmic localisation of JAG1 in HUVEC (Figure 3.1 A), whereas JAG1 and punctate DLL4 expression were observed within the cytoplasm and exhibited nuclear positivity in a number of both cell types (Figure 3.1 A). Co-localisation of both JAG1 and DLL4 was more prominently observed in HUVEC compared to HMEC-1 cells (Figure 3.1 A), indicating spatial and temporal Notch activation in the two cell lines. Co-localisation also suggests a positive correlation between the two ligands, possibly through the up-regulation of JAG1 by DLL4 (Harrington et al. 2008). There is emerging evidence for a functional role of the intracellular domain (ICD) of DSL ligands. DSL proteins have been demonstrated to be subjected to the proteolytic cleavages, first in the extracellular region by TACE, followed by intermembranous cleavage mediated by a presenilin-dependent γ-secretase activity, resulting in the liberated intracellular domains which then localise to the nucleus (Bland et al. 2003; LaVoie and Selkoe 2003; Six et al. 2004; Hiratochi et al. 2007), implicating a novel intrinsic signalling pathway dependent on the DSL ligand. Thus, nuclear localisation of DLL4 ICD and JAG1 ICD suggests a further role in gene expression through association with transcriptional complexes, for example DLL1 ICD has been demonstrated to bind to Smad transcription factors involved in TGF-β/ Activin signalling (Hiratochi et al. 2007). Thus, it would be interesting to screen for transcription factors that bind to the DLL4 ICD and JAG1 ICD by immunoprecipitation for DLL4 ICD and JAG1 ICD nuclear proteins, followed by hybridisation on transcription factor arrays.

Effects of DLL4 and JAG1 on downstream target genes

This project was initially carried out to elucidate the role of DLL4 and JAG1 in angiogenesis *in vitro* and to discover differences in their regulation of Notch activity. I initially concentrated on known downstream signalling pathways to compare their effectiveness. In HUVEC (Figure 3.4 A) and HMEC-1 (Figure 3.4 B), DLL4 up-regulated DLL4 expression (Shawber et al. 2003; Ridgway et al. 2006), while modest up-regulation of JAG1 was observed upon stimulation with rrJAG1 at the transcript level. Interestingly, the downstream target genes DLL4, JAG1, HEY1 and HEY2 were up-regulated by both DLL4 and JAG1 with DLL4 being more potent than JAG1 in activating Notch signalling through Notch1 cleavage in HUVEC (Figure 3.4 A and Figure 3.5 A and D) but both displayed equal potency at the transcript level in HMEC-1 (Figure 3.4 B). In HUVEC, the induction of DLL4 by rrDLL4 peaked at 24hr (Figure 3.5 B) due to DLL4 protein synthesis, in consistent with 8hr peak induction at transcript level (Figure 3.4 A). In HMEC-1, DLL4 was up-regulated by rrDLL4 over time (Figure 3.6 B) in line with QPCR data (Figure 3.4 B). However, protein expression for JAG1 did not correlate with the transcript level in both cell lines (Figure 3.5 A and Figure 3.6 A), possibly due to post-translational modification or the long half life of JAG1 protein (24hr) (Rodilla et al. 2009). In HMEC-1, cell confluency increased Notch activation through cell to cell contact to increase the expression of DLL4, JAG1 and N1 ICD (Figure 3.6 B and D), as also observed in other studies in HUVEC (Benedito et al. 2009). However in HUVEC, only JAG1 expression was increased with increased cell density (Kawano et al. 2002) (Figure 3.5 C), possibly due to donor effect as this was observed in other replicates. Altogether, these highlight the differences in the expression of downstream target genes in response to Notch stimulation in HUVEC and HMEC-1.

Ideally human JAG1 and human DLL4 proteins should be used to activate Notch signalling in human endothelial cells. However rhJAG1 appears to be less effective compared to rrJAG1 in Notch regulation on downstream genes. It is unclear why this is the case but these may be a problem with the purification and stability of the rhJAG1 protein. The differences observed could be due to the existence of His tag at the C terminus of the rrJAG1 but not on the rhJAG1 recombinant protein which may have altered the protein folding and stability. It was decided that the studies should proceed with rrJAG1 as it has a 96.7% homology with rhJAG1.

Interestingly, constitutive expression of mDLL4 in HMEC-1 up-regulated DLL4 gene expression through feed-forward mechanism (Figure 3.8) as also observed in DLL4- eGFP-transfected human cardiac microvascular endothelial cells (HCMVEC) (Caolo et al. 2010). The activation of DLL4, HEY1 and HEY2 genes was stronger in mDLL4 cells compared to mJAG1 cells (Figure 3.8), unlike that observed on protein coated plate (Figure 3.4 B). This could be due to the constitutive expression of mDLL4 which further up-regulates its expression (approximately 10 folds) (Figure 3.8) compared to transient stimulation on rhDLL4 plate (approximately 5 folds) (Figure 3.4 B), saturating the system and increasing dominance of Notch activation through DLL4 ligand compared to activation through JAG1 ligand.

The differences in the strength of activating Notch signalling between the two ligands were also observed by others in HUVEC (Benedito et al. 2009) and lymphatic endothelial cells (LEC) (Emuss et al. 2009). It has been suggested that the difference seen in gene expression between rrJAG1 and rhDLL4 could be due to the modulation of Notch signalling by fringe

which in general favours DLL-Notch signalling over JAG-Notch signalling (Shimizu et al. 2001; Benedito et al. 2009; Kato et al. 2010; Marklund et al. 2010).

Effects of DLL4 and JAG1 on cell number

Over-expressing mDLL4 or mJAG1 in HMEC-1 cells did not affect cell number over time. The overall cell number can be influenced by the balance of cell proliferation and the magnitude of cell death, and other factors such as adhesion. Notch activation modulates cell cycle regulation by inducing cell cycle arrest (Noseda et al. 2004; Sarmento et al. 2005; Georgia et al. 2006; Jia et al. 2007; Riccio et al. 2008; Emuss et al. 2009; Shen et al. 2010). It was previously found that activated Notch4 did not affect proliferation of simian virus 40 (SV40) large T antigen-transformed endothelial cells (HMEC-1) (Leong et al. 2002) by binding to retinoblastoma gene product (Rb) and affecting downstream gene expression related to cell cycle progression (Sherr 2000). Considering that Notch1 and Notch4 are abundantly expressed in the vasculature (Krebs et al. 2000), the activation of Notch signalling in HMEC-1 is very likely to be through Notch1 (as shown in Figure 3.6 A and D) and Notch4 (Leong et al. 2002), contributing to the redundancy of mDLL4 and mJAG1 effects on cell proliferation.

On the other hand, siRNA knockdown of DLL4 and JAG1 respectively decreased cell count compared to Scrambled control cells. A few reasons could account for this observation. The reduction in cell could be due to increased cell death due to loss of endogenous DLL4 or JAG1 expression in HMEC-1. Both DLL4 and JAG1 have been shown to sustain cell survival in different cell types (Jundt et al. 2002; Liu et al. 2003; Purow et al. 2005; Androutsellis-Theotokis et al. 2006; Rosati et al. 2009; Liu et al. 2010). Notch activation can lead to

suppression of apoptosis in a variety of cancer cell lines (Jundt et al. 2002) through different mechanisms, including the inhibition of p53, as well as the activation of the PIK3/AKT pathway (Sade et al. 2004; Kim et al. 2007; Palomero et al. 2007; Meurette et al. 2009). Inhibition of JAG1 by RNA interference has been shown to induce apoptosis and inhibit proliferation in glioma cell line (Purow et al. 2005) and prostate cancer cells (Wang et al. 2010), and disrupt cell cycle progression through G1/S in breast cancer cells (Cohen et al. 2010). DLL4 down-regulation inhibited HUVEC cell proliferation by inducing cell cycle arrest through increasing p21 expression but only induced apoptosis in HUVEC following serum and growth factor deprivation (Patel et al. 2005). These suggest that DLL4 and JAG1 are essential to sustain cell survival.

Accurate assessment of viable cell number and cell proliferation is an important requirement to study the effects of the ligands in endothelial cell growth. Cell counting assay determines number of healthy cells in culture but cannot distinguish between actively dividing cells or quiescent cells. Alternatively, staining cells with trypan blue enables evaluation of proportion of viable cells to dead cells by measuring the capacity of cells with uncompromised membrane integrity to exclude the dye. Cell proliferation on the other hand measures the number of cells that are dividing in culture. Measurement of DNA synthesis as a marker for proliferation can be done by incorporating cell DNA with labelled DNA precursors (3H-thymidine or bromodeoxyuridine) which is proportional to the amount of cell division taking place in the cell culture. Cell cycle and cell death analysis can be performed using propidium iodide and Annexin V on a flow cytometer or by measuring the expression of cell cycle regulators p21, p27 and p53 or apoptosis markers, cleaved PARP and activated Caspase 3 on western blots, ELISA or immunohistochemistry to further elucidate the contributing factor to decreased cell number.

Effects of DLL4 and JAG1 on cell migration

Cell migration requires defined endothelial cell polarity and adhesion which involves the expression of integrins and cadherins. Notch signalling can positively modulate cell adhesion through the integrin pathway (Leong and Karsan 2006; Hodkinson et al. 2007; Karsan 2008). Both mDLL4 and mJAG1 increased HMEC-1 cell motility compared to the control EV in the migration scratch assay (Figure 3.11). This observation is contradictory to findings from other studies which demonstrated that DLL4 negatively regulated cell migration in HUVEC (Trindade et al. 2008; Williams et al. 2008) while JAG1 promoted HUVEC cell migration (Chigurupati et al. 2007). However, these differences could be explained by the different types of endothelial cells used, for example the transformation of HMEC-1 with large T antigen which may have affected the Notch signalling pathway, for example by increasing the expression of Notch1, as observed in mesothelial cells transformed with SV40 (Bocchetta et al. 2003). Activation of Notch1 has been shown to increase β1 integrin affinity (Karsan 2008) which is required for cell adhesion and endothelial cell polarity (Zovein et al. 2010) thus promoting endothelial cell motility. Delta-like 1 has recently been shown to have a role in cell adhesion in mast cells (Murata et al. 2010), thus DLL4 may have a function as a cell adhesion molecule in endothelial cells which explains the increase in migratory effect in mDLL4 over-expressing cells.

Conversely, silencing either DLL4 or JAG1 ligand expression decreased cell migration in scratch assay (Figure 3.17), as observed in HUVEC (Patel et al. 2005), ovarian endothelial cells (Lu et al. 2007), and prostate cancer cells (Wang et al. 2010). Therefore, removing the endogenous DLL4 or JAG1 ligands could affect the downstream expression of cadherins and integrins which caused cells to lose their ability to adhere to each other or to the plate. The

decrease in cell migration could also be due to decreased cell proliferation or increased cell death as previously discussed, however this is unlikely as the cell number of DLL4 and JAG1 suppressed cells is not significantly different within the first two days for gene knockdown compared to Scrambled (Scr) (Figure 3.16). Furthermore, the scratch assay was performed within 24hr time frame thus proliferation could not account as a factor as the doubling time for HMEC-1 cells is 28.6 hr (Tacker and Okorodudu 2004). As future work, it would have been interesting to confirm the phenotype observed in HUVEC as well as on other endothelial cell types. Further endothelial migration studies in response to growth factors to mimic that in *in vivo* can be done on Boyden chamber assay which holds the advantage of generating gradients of soluble factors to assess chemotactic migration of endothelial cells compared to the conventional scratch assay.

Effects of DLL4 and JAG1 on network formation

The ordinary Matrigel tube formation assay reflects the potency of endothelial cells to adhere, migrate and to arrange into a complex interconnecting network. Endothelial cell adhesion and migration is chiefly mediated through binding of integrin cell surface receptors to the extracellular matrix ligands which serves to anchor cells to their matrix (Fujiwara et al. 2004; Carlson et al. 2008; Qin and Zhang 2010) and similar to cadherin signalling, integrin can mediate cell-cell and cell-matrix communication (Wu and Sheibani 2003). HMEC-1 mDLL4 had reduced network formation by reducing number of nodes and polygons while HMEC-1 mJAG1 enhanced network formation by doing the opposite. This is consistent with other published literatures using HUVEC (Williams et al. 2006; Chigurupati et al. 2007; Trindade et al. 2008) (Figure 3.12). However, the effect of stronger activation of Notch signalling by mDLL4 in HMEC1 cells (Figure 3.8) can be blocked by DBZ as indicated by the increased

number of nodes in mDLL4 cells but not in mJAG1 cells. The transition from quiescent phenotype to a proliferative and migratory phenotype often depends on the balanced production of stimulatory and inhibitory effects. This balance may be differentially regulated by DLL4 and JAG1, for example the crosstalks between Notch signalling and other signalling pathways such as the VEGF, MAPK and Wnt pathways which have lately been elucidated to influence cell adhesion (Hutchings et al. 2003; Wu and Sheibani 2003; Nelson and Nusse 2004) could account for the different effect of DLL4 and JAG1 on network formation.

While siRNA suppression of DLL4 led to decreased network formation (Figure 3.18 A), it was intriguing as to why DBZ did not have any effect on blocking Notch signalling when DLL4 or JAG1 expression was reduced. Though there is a possibility of DBZ treatment not fully working, this is highly unlikely as the same results were observed in 3 independent experiments and often done in parallel with other angiogenic assays in which DBZ treatment had worked. In order to confirm the results, experiments should be repeated using fresh DBZ stock in HMEC-1 and other endothelial cell types. Further questions were raised regarding why silencing of JAG1 expression did not influence network formation (Figure 3.18 B). All these together raised speculation regarding the importance of DLL4 and its possibility of being a dominant ligand to activate Notch signalling in endothelial cells, at least in the HMEC-1 model. Fringe, which potentiates DLL- Notch signalling (Visan et al. 2006; Stanley and Guidos 2009; Yuan et al. 2011) but inhibit JAG- Notch signalling (Kato et al. 2010; Marklund et al. 2010; Visan et al. 2010) could be an important player for the observed effect in HMEC-1 cells which express Fringe in abundance, this will be discussed further in Chapter Five.

The endothelial spheroids stabilise the cells (Korff and Augustin 1998) and allow steps of angiogenesis to be studied. In the hanging drop assay, over-expression of mDLL4 decreased sprouting potency, while JAG1 exerted an opposite phenotype (Figure 3.13). These support existing *in vitro* and *in vivo* data which revealed DLL4 to be a negative regulator of angiogenesis (Leslie et al. 2007; Li et al. 2007; Lobov et al. 2007; Trindade et al. 2008) and JAG1 to be pro-angiogenic (Zeng et al. 2005; Benedito et al. 2009). Blocking Notch signaling with DBZ on the other hand increased sprouting in EV, mDLL4 and mJAG1 spheroids (Figure 3.13), implying DLL4 is the dominant ligand in basal conditions and the default position on global inhibition is similar to absence of DLL4 effect. This was also observed *in vivo* when DLL4-Notch signalling was inhibited (Noguera-Troise et al. 2006; Ridgway et al. 2006; Garber 2007; Thurston et al. 2007). However, we cannot rule out that the significantly reduced sprouting observed in the mDLL4 expressing cells even in the presence of DBZ could possibly be affects of DLL4 independent of Notch cleavage as mounting literature has shown that endocytosis of Notch ligands could trigger a set of signalling cascade in the signal sending cell to further activate bidirectional signalling (Six et al. 2004; Popovic et al. 2011). An additive effect of increased sprouting was observed in mJAG1 cells when overall Notch signalling was blocked, this may be due to occurrence of initial sprouting stimulated by JAG1 before the addition of DBZ.

Suppression of either ligand in the HMEC-1 spheroids led to the reversed observation obtained for the over-expressing ligand model (Figure 3.19 and Figure 3.20) in the hanging drop assay. siDLL4 significantly increased sprouting (Figure 3.19), while siJAG1 decreased sprout length and coverage area (Figure 3.20). Treatment with DBZ increased sprouting in the Scrambled (Scr) spheroids (Figure 3.19 and Figure 3.20). Furthermore, DBZ could reverse the effect of JAG1 suppression by increasing sprouting. These observations are in agreement with

Benedito and colleagues work (2009) who hypothesised that JAG1 antagonizes DLL4-Notch signalling in cells expressing Fringe. If indeed it is true, then silencing JAG1 would further amplify the effect of DLL4-Notch signalling as observed in the reduction of sprout length and coverage area (Figure 3.20). In supporting the hypothesis that DLL4 may be the more important or dominant ligand in triggering Notch signalling, reducing JAG1 expression augmented DLL4-Notch signalling which was then blocked with DBZ which led to increased sprouting compared to untreated spheroids (Figure 3.20). Taken together, these results reveal the role of JAG1 as a positive regulator of sprouting while DLL4 as a negative regulator of angiogenesis. To further elucidate the role of DLL4 and JAG1 as well as the relationship between the two ligands, blocking specific ligand induced Notch signalling with anti-DLL4 or anti-JAG1 blocking antibody should be included in this experiment as future work. *In situ* staining for DLL4, JAG1, HEY1 and HEY2 Notch target genes expression on these spheroids should also be performed to study the pattern of expression as a subsequent effect of these ligand over-expression or knockdown in endothelial cells.

The differences observed between the effects of DLL4 and JAG1 in network formation and hanging drop assay suggest that there may be a different set of genes regulated differently by DLL4 and JAG1 leading to the phenotype observed. Therefore, global gene analysis to compare DLL4 and JAG1 activated Notch signalling in endothelial cells may shed light and reveal potential pathways involved, thus delineating new downstream genes which might be differentially regulated by the two ligands. This has been carried out and the results are currently being interpreted. The basis of the enhanced sprouting found with global inhibition of Notch signalling remains to be explained, but could be due to enhanced signalling via VEGFR2 or 3, which are suppressed by Notch signalling. It will be of interest to use blocking antibodies to the receptors and ligands to investigate this further.

The differences between HMEC-1 and HUVEC may reflect the actual heterogeneity of endothelial cells arising from different vascular origins, but it is likely that HMEC-1 cells differ to that of HUVEC due to the steps taken to produce an immortalised cell line, in particular those promoting cell growth (Lidington et al. 1999). Endothelial cells from different blood vessels and microvascular endothelial cells from different tissues have been shown to possess distinct and characteristic gene expression profiles (Chi et al. 2003). Therefore, extra caution should be implemented when choosing the type of endothelial cells for experiments, as the resulting outcome cannot be generalised to endothelium of different vascular beds. As such future work includes comparing a variety of endothelial cell lines derived from different vascular origins.

4 Effects of DLL4 and JAG1 over-expression on xenograft tumours

4.1 Introduction

Central to tumour growth, angiogenesis is a multifaceted process involving matrix degradation, endothelial cell proliferation, migration, sprouting and recruitment of mural cells. Angiogenesis is regulated by angiogenic molecules produced by the malignant cells or tumour stroma within the tumour microenvironment (Bergers and Benjamin 2003; Hicklin and Ellis 2005). Notch signalling can be activated in endothelial cells following contact between stromal cells, endothelial cells and tumour cells. Both DLL4 and JAG1 are implicated in tumour angiogenesis, with a high abundance of DLL4 expression found in the endothelium of tumour blood vessels (Mailhos et al. 2001; Gale et al. 2004; Noguera-Troise et al. 2006), while JAG1 is more highly expressed in tumour cells (Veeraraghavalu et al. 2004; Reedijk et al. 2005; Veeraraghavalu et al. 2005; Zeng et al. 2005; Baliko et al. 2007; Ramdass et al. 2007; D'Souza et al. 2008; Pannequin et al. 2009; Rodilla et al. 2009; Guilmeau et al. 2010; Lin et al. 2010) and mural cells (Hofmann and Luisa Iruela-Arispe 2007; High et al. 2008). These ligands have opposing effects on vessel formation. DLL4 has been shown to inhibit sprouting resulting in fewer but better perfused blood vessels which promoted tumour growth (Noguera-Troise et al. 2006; Ridgway et al. 2006; Li et al. 2007; Scehnet et al. 2007). JAG1 on the other hand has been shown to be able to signal to tumour endothelium to promote angiogenesis and tumour growth via the MAP kinase pathway (Zeng et al., 2005).

While studies in the recent years have focused on the effects of DLL4 on tumour growth and vascularisation, very little is known about JAG1- Notch signalling in tumour angiogenesis and its influence on tumour growth and progression. Therefore, this chapter seeks to study the different effects of DLL4 and JAG1 on xenograft tumour growth and vasculature, as well as the effects of treatments on the downstream Notch target genes. Glioblastoma multiformes, often very highly vascularised (Kleihues et al. 2002) are the most aggressive tumours among tumours of the central nervous system with the poorest clinical prognosis (Shih and Holland 2006). Notch signalling has been shown to play an essential role in the formation of gliomas (Kanamori et al. 2007; Hulleman et al. 2009; Gaetani et al. 2010). Previous work done in our lab has shown that DLL4 expression is up-regulated in endothelial cells and is detected in perinecrotic areas in 20% of human glioblastoma samples using *in situ* hybridisation (Li et al. 2007). JAG1 expression on the other hand is elevated in glioblastoma, both at the transcript and protein level and influenced glioma cell survival and proliferation (Purow et al. 2005). Hence, these ligands were over-expressed in the U87 human glioblastoma cell line U87 to study the effect of DLL4 and JAG1 on tumour growth and vessel formation *in vivo*.

Tumour cells and other components in the tumour microenvironment secrete VEGF to promote angiogenesis. Bevacizumab is a monoclonal antibody (mAb) which binds human VEGF thus inhibiting the direct tumour effect on new vessel formation, normalize vessels and cause tumour vessels to regress as also shown by my colleagues (unpublished data) and others (Willett et al. 2004; Jain 2005; Myers et al. 2010).

In vivo work was carried out by Dr. Ji-Liang Li (Oxford) and Dr. Esther Bridges (Oxford). Briefly, SCID mice were implanted subcutaneously with control U87 cells (U87 EV), murine DLL4-expressing U87 cells (U87 mDLL4) or murine JAG1-expressing cells (U87 mJAG1)

and treated with bevacizumab, an anti-VEGF monoclonal antibody (mAb). To mimic the clinical setting in which anti-tumour therapies are often initiated only after diagnosis of cancer, anti-VEGF treatment was administrated when the tumour reached 150mm^3 in size. Dibenzazepine (DBZ), a γ-secretase inhibitor was used to inhibit Notch signalling. The effects of DBZ and bevacizumab (mAb) on Notch signalling in tumour and stromal cells were confirmed by assessing the expression of human Hey1 (hHEY1) and murine Hey1 (mHEY1) by QPCR. The hairy/enhancer of split family of helix-loop-helix (bHLH) transcription factors (HES and HEY) are known targets of the Notch signaling pathway. HES1 and HEY1 expression have been identified in human gliomas and the U87 cell line (Li et al. 2007; Hulleman et al. 2009; Chen et al. 2010; Gaetani et al. 2010).

To address the mechanism of tumour growth and resistance, the vessel density and morphology of tumour neovasculature were assesed by immunostaining for the endothelial marker CD31 and pericyte marker NG2. Additional histopathology staining included MIB1 which is an antibody against the Ki-67 proliferation marker, Carbonic anhydrase IX (CA9), marker of hypoxia as well as hematoxylin and eosin (H&E). DLL4 and JAG1 staining was also carried out to study the expression pattern on xenograft tumours following DLL4 and JAG1 over-expression, DBZ and bevacizumab treatments.

4.2 Characterisation of U87 cell lines

U87 over-expressing murine DLL4 (U87 mDLL4), murine JAG1 (U87 mJAG1) or control U87 cells (U87 EV) were kindly provided by Dr. Ji-Liang Li (Oxford). These cell lines were first characterised to ensure successful transduction and ligand expression by quantitative real-time PCR (qPCR), western blot and immunofluorescence. The effect of mDLL4 and mJAG1 on U87 apoptotic cell death was also studied by subjecting cells to 0.1% oxygen (hypoxia) and serum starvation followed by western blotting for PARP cleavage, a nuclear poly (ADP-ribose) polymerase which is cleaved by Caspase-3 during apoptosis. The effect of mDLL4 and mJAG1 on U87 cell proliferation was also investigated.

4.2.1 mDLL4 and mJAG1 were successfully transduced into the U87 cell line

Murine DLL4 gene and murine JAG1 genes were both detectable in the relevant transfected cell line by QPCR (Figure 4.1 A). Western blotting and immunocytofluorescence revealed that mDLL4 and mJAG1 proteins were abundantly expressed in U87 mDLL4 and U87 mJAG1 respectively (Figure 4.1 B and C) confirming the success of transduction. Antibodies used for immunofluorescence corresponded to the extracellular region of mDLL4 protein and the intracellular region of mJAG1. mJAG1 displayed predominantly cytoplasmic expression (Figure 4.1 C) whereas mDLL4 expression was observed in the cytoplasm and in the nucleus of a number of cells (Figure 4.1 C).

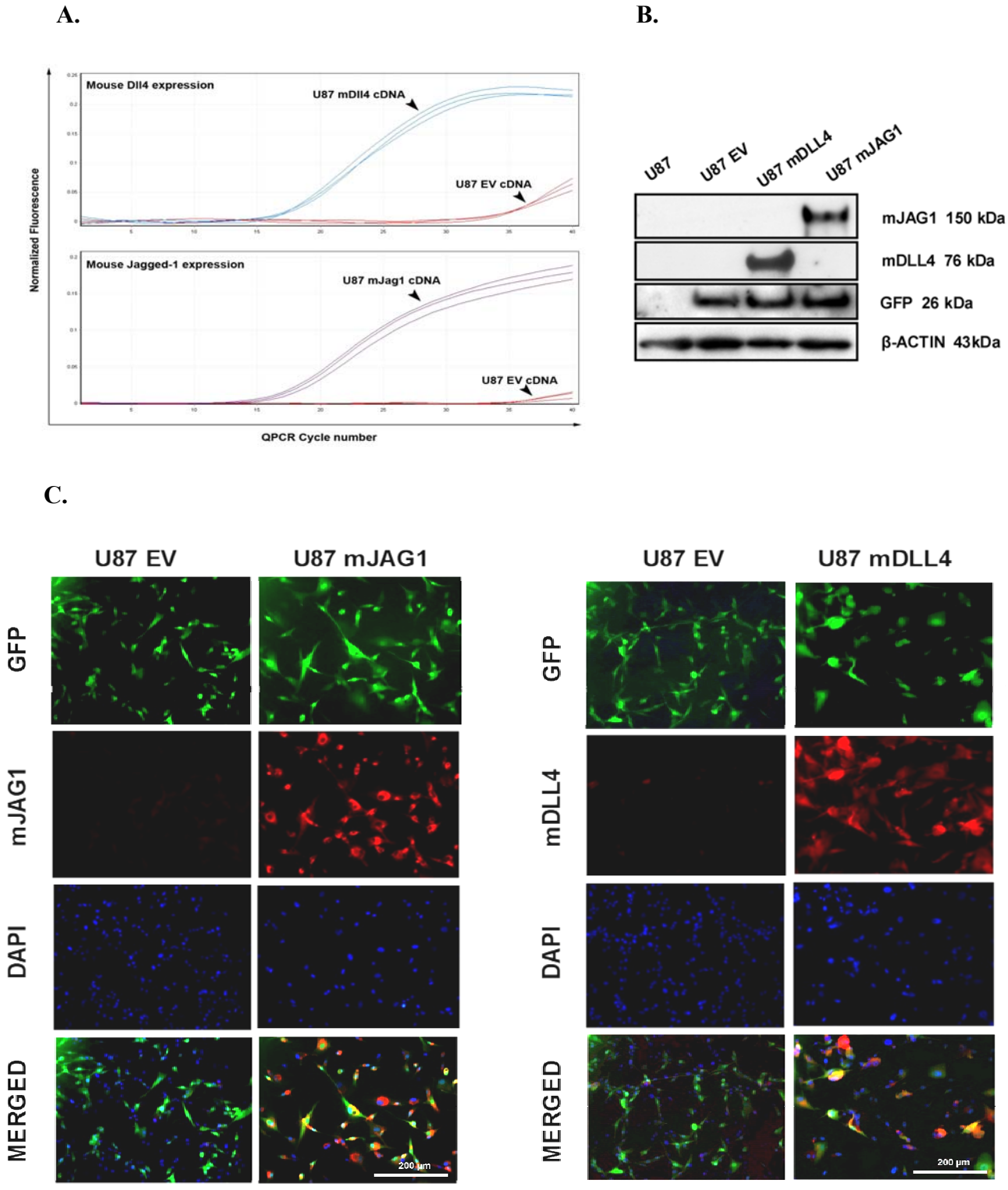


Figure 4.1: Expression of mDLL4 and mJAG1 in U87 transduced with mDLL4 and mJAG1 respectively at both A) the transcript and (B-C) protein level confirmed successful retroviral transduction.

A) QPCR was used to confirm the expression of murine DLL4 and murine JAG1. B) mDLL4 and mJAG1 protein expression in transduced cells β-ACTIN was used as loading control. C) Immunofluorescence staining for mDLL4 and mJAG1 was carried out with anti- DLL4 (corresponding to extracellular region of DLL4) and anti- JAG1 (corresponding to intracellular region of JAG1) antibodies. QPCR, western blot, and immunofluorescence are a representative of n=3 independent experiments.

QPCR was carried out to assess the ability of the murine ligands to activate Notch signalling by binding to Notch receptors on neighbouring cells. U87 expressing mDLL4 and mJAG1 up-regulated the expression of these Notch target genes suggesting that the ligands are capable of initiating Notch signalling (Figure 4.2), and confirming functional expression of mDLL4 and mJAG1. Both mDLL4 and mJAG1 were equally effective in inducing Notch signalling, for instance in the up-regulation of HEY1 and HES1, enabling comparison of functionality the ligands in regulating vasculature *in vivo*.

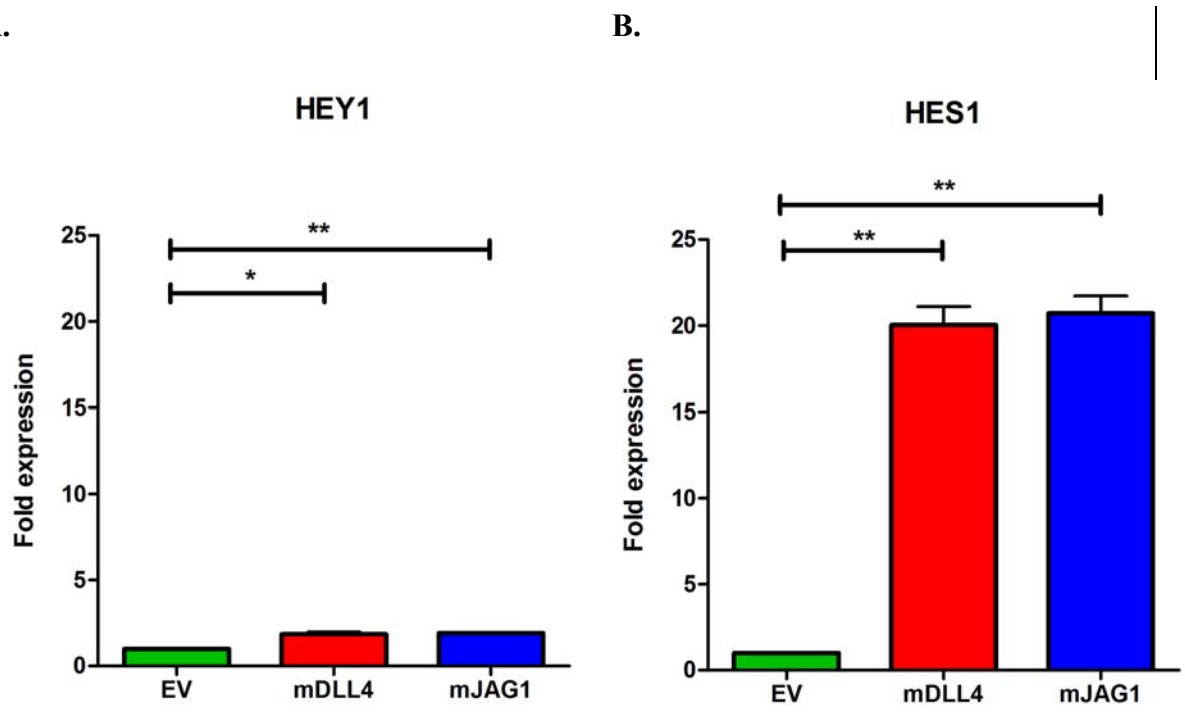


Figure 4.2: Up-regulation of A) HEY1 and B) HES1 in mDLL4 and mJAG1 expressing U87 cells, indicating activation of Notch signalling on neighbouring cells.

QPCR was used to quantify the gene expression of A) HEY1 and B) HES1. QPCR (**P<0.01,*P<0.05, ANOVA with Bonferroni's post-test, n=3 independent experiments). Error bars represent SEM.

4.3 Both mDLL4 and mJAG1 reduced U87 cell proliferation but did not affect apoptotic cell death in U87 cells *in vitro*

The U87 EV, mDLL4 and mJAG1 cell lines were counted daily over a five day period to assess proliferation. Both mDLL4 and mJAG1 reduced U87 cell proliferation (Figure 4.3 A) which is consistent with previous work done in the lab where U87 cells over-expressing human DLL4 were found to decrease in number (Li et al. 2007).

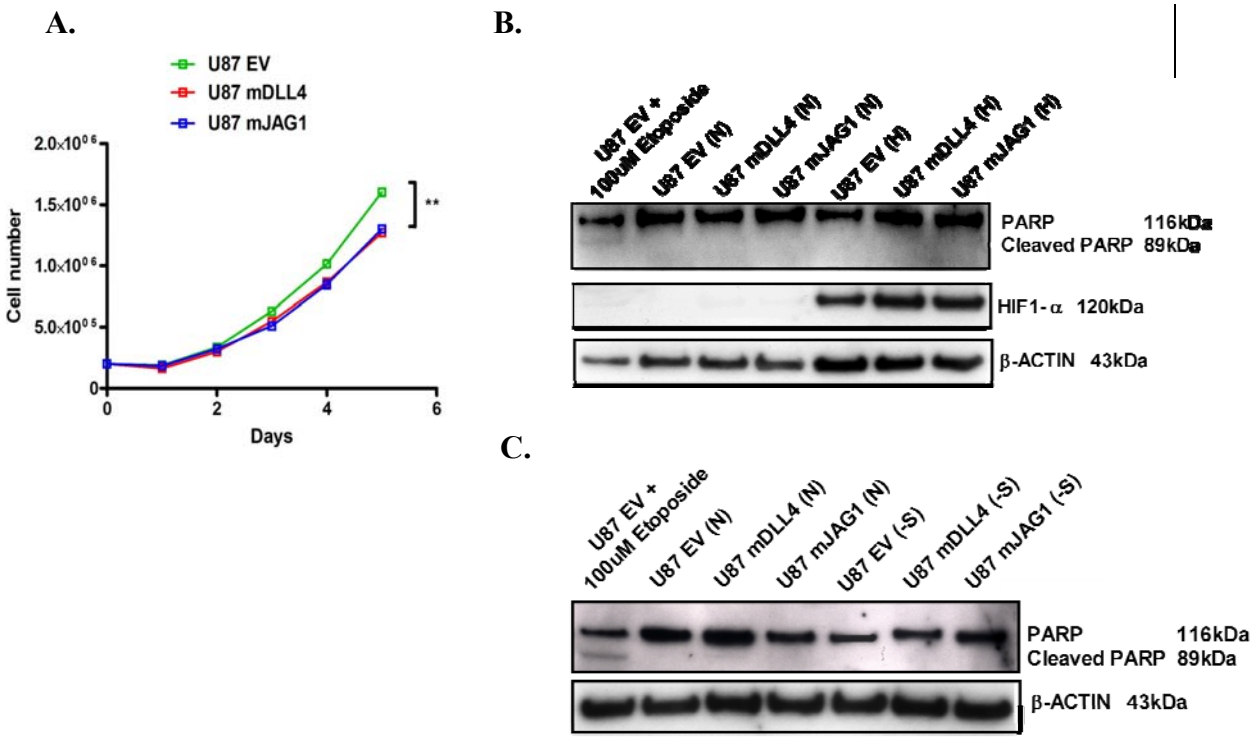


Figure 4.3**:** mDLL4 and mJAG1 over-expressed in U87 A) decreased cell number and (B-C) U87 cells were resistant to apoptosis in normoxia (N), 0.1% hypoxia (H) and under serum starvation (-S) for 72hr *in vitro*.

A) Cells were trypsinised and counted using cell counter daily over a period of 5 days. Analysis was done using ANOVA F test (**P<0.01), n=3 independent experiments. Error bars represent SEM. A representative figure is shown. B) Cells were treated with 100 μM Etoposide (positive control), subjected to normoxia or 0.1% oxygen (hypoxia) or serum starved for 72hr. Western blotting was carried out to check the expression of cleaved PARP and HIF1-α. β-ACTIN was used as loading control. A representative western blot is shown (n=3).

To mimic the tumour microenvironment, U87 EV, U87 mDLL4 and U87 mJAG1 cells were exposed to hypoxia and serum starvation for 72hr. U87 EV cells were treated with 100uM Etoposide (Chen et al. 2007; Hussein et al. 2011) to induce apoptosis as positive control (Figure 4.3 B and C). Up-regulation of HIF1-α expression which accumulates under hypoxic conditions was observed in U87 cells which were subjected to 0.1% oxygen tension for 72hr. U87 EV cells were found to be resistant to apoptosis under normoxia, 0.1% hypoxia and under serum starvation, consistent with other studies (Wu et al. 2004; Gong and Agani 2005; Lefranc et al. 2005; Azad et al. 2008). mDLL4 and mJAG1 did not exert any apoptotic effect under the growth conditions utilized. The reduction of cell number by mDLL4 and mJAG1 in U87 cells *in vitro* was therefore not due to increased apoptotic cell death but could be caused by cell cycle arrest or possibly through Notch induction of epithelial-mesenchymal transition (EMT) which downregulates the cell adhesion molecule E-cadherin {Larue, 2005 #949}

4.4 Both mDLL4 and mJAG1 decreased mouse survival by promoting xenograft tumour growth *in vivo*

Activation of Notch signalling in U87 xenograft tumours by mDLL4 and mJAG1 promoted tumour growth and reduced mice survival. Consistent with previous work done by my

colleagues on hDll4, mDLL4 and mJAG1 enhanced tumour growth *in vivo* compared to EV (Li et al. 2007) (Figure 4.4).

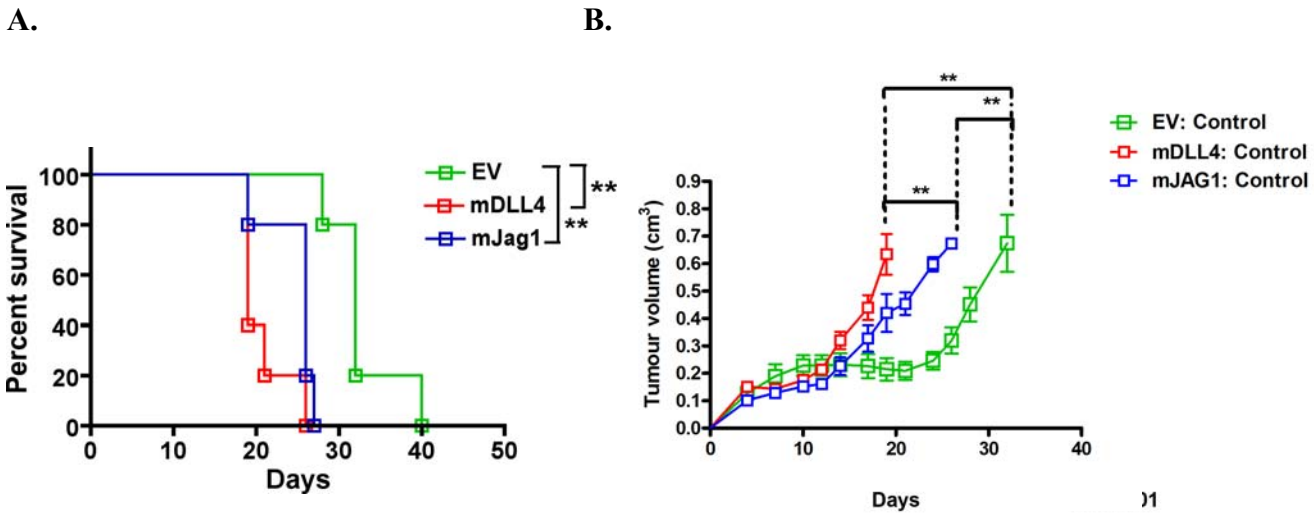


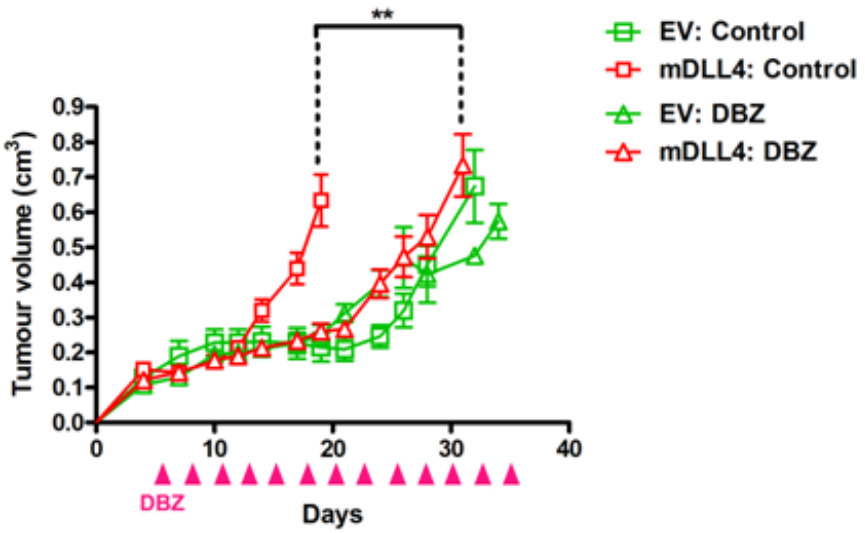
Figure 4.4**:** A) Percentage mice survival was compiled on a Kaplan-Meier survival plot. B) Both mDLL4 and mJAG1 promoted U87 xenograft tumour growth.

A) Each group consisted of 5 mice. Figure was kindly provided by Dr. Ji-Liang Li. B) Data was analysed using ANOVA F test (**P<0.01). Error bars represent SEM.

4.5 DBZ eradicated the effects of mDLL4 and mJAG1 on tumour growth

To assess if inhibiting the Notch signalling pathway reversed the effect of the Notch ligands on tumour growth, DBZ (8.1 mmol/kg), a γ-secretase inhibitor was administered once every 3 days, starting from day 7 (Figure 4.5). Treatment with DBZ successfully inhibited the mDLL4 and mJAG1 growth induction back to U87 EV level.

A.



B.

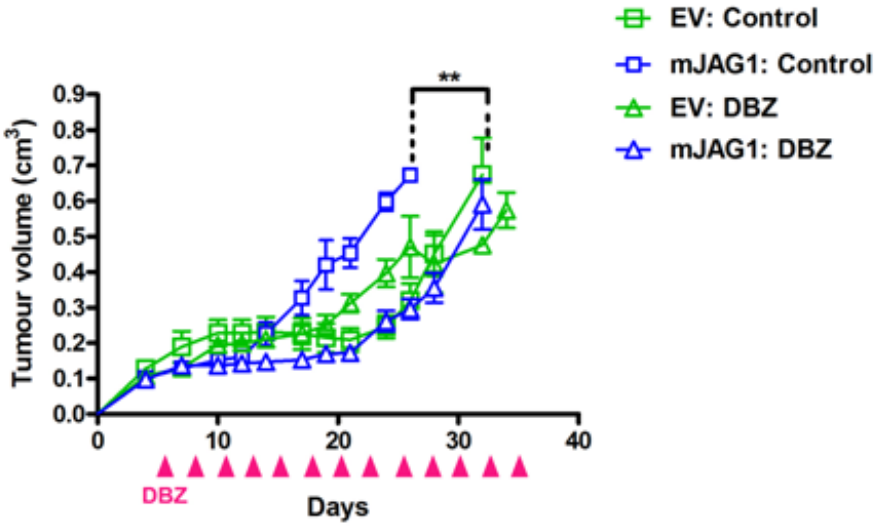


Figure 4.5**:** Tumour growth curves of A) U87 mDLL4 and B) U87 mJAG1 compared to U87 EV, treated with DBZ (8.1 mmol/kg) or PBS (control).

Each group consisted of 5 mice, ANOVA F test (**P<0.01). Error bars represent SEM.

Changes in mRNA expression of human and murine HEY1 were used to determine the activation of Notch signalling in tumour cells and in tumour stromal respectively because signalling could occur between different cell types *in vivo*. mDLL4 up-regulated hHEY1 ($P<0.01$) but the up-regulation was not significant for mJAG1 (Figure 4.6 A). mDLL4 and mJAG1 up-regulated mHEY1 ($P<0.05$) (Figure 4.6 B) more than hHEY1 (Figure 4.6 A). mJAG1 seemed to up-regulate mHEY1 better than mDLL4, although it was not significant (Figure 4.6 B). DBZ, either as a single or combined treatment with bevacizumab (mAb) inhibited Notch signalling by down-regulating both hHEY1 ($P<0.01$) and mHEY1 ($P<0.01$) in the mDLL4 and mJAG1 over-expressing U87 xenograft tumours (Figure 4.6 A and B). Interestingly, treatment with bevacizumab in the EV group decreased hHEY1 expression ($P<0.01$) (Figure 4.6 A) but appeared to increase mHEY1 expression (Figure 4.6 B) compared to untreated, even though it was insignificant. Bevacizumab did not affect hHEY1 expression in mDLL4 and mJAG1 groups (Figure 4.6 A). However, treatment with bevacizumab decreased mHEY1 expression in mJAG1 tumours compared to untreated mJAG1 tumours.

A. **B.**

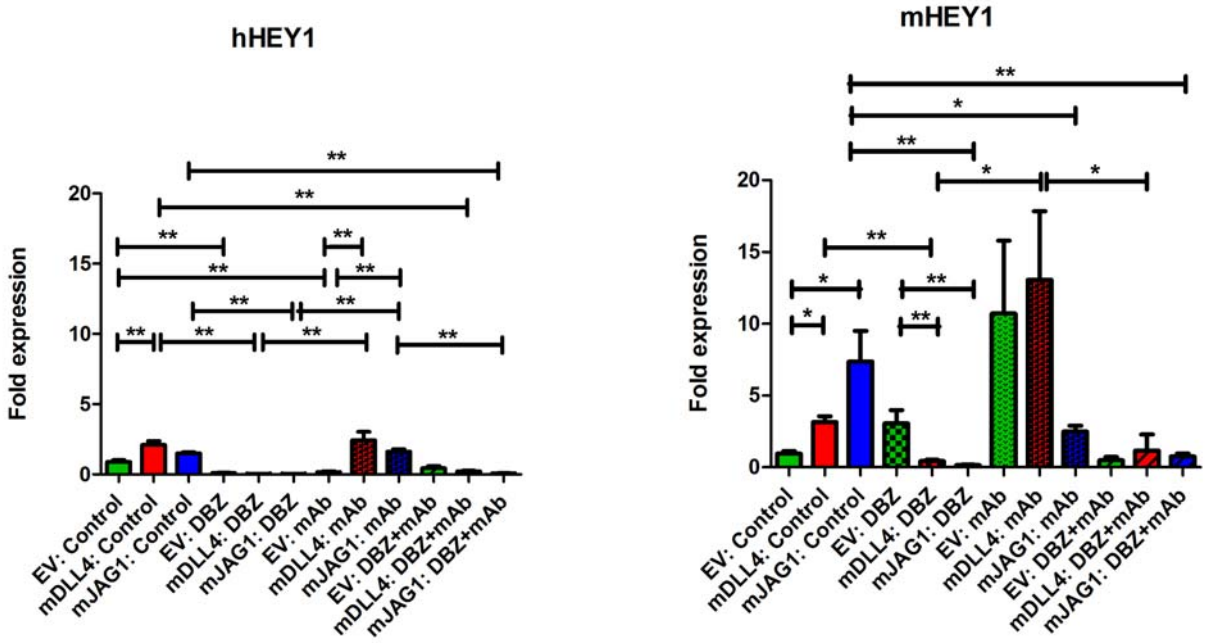


Figure 4.6**:** Assesment of A) human HEY1 (hHEY1) and B) murine HEY1 (mHEY1) Notch target genes in xenograft tumours.

Each group consisted of 5 mice. **P<0.01, *P<0.05, ANOVA with Bonferroni's post-test, n=5 mice. Bars represent SEM.

4.6 DLL4-Notch signalling mediated tumour resistance to VEGF inhibition

To assess the interplay between Notch signalling and the VEGF pathway, tumour growth curves of U87 EV and U87 mDLL4 treated with DBZ (8.1 mmol/kg), bevacizumab (mAb) (10mg/kg) or PBS (control) are shown in Figure 4.7 A. All treatments were started at Day 7. mDLL4 promoted U87 tumour growth compared to EV (P<0.01) (Figure 4.7 A). DBZ treatment slightly delayed control tumour (EV) growth (EV: Control; EV: DBZ) (4 days)

(Figure 4.7 A and Figure 4.7 C), although not significantly, suggesting that Notch signalling has a role in the growth of the tumours and is sensitive to DBZ treatment in U87 tumours. This was confirmed by DBZ down-regulation of hHEY1 (Figure 4.6 A). DBZ reversed mDLL4 tumour growth and growth was similar to that for U87 EV xenograft tumours ($P<0.01$) (Figure 4.7 A and Figure 4.7 C). mDLL4- Notch inhibition was also confirmed by down-regulation of hHEY1 (Figure 4.6 A). Bevacizumab treatment of control tumours (EV) significantly delayed tumour growth compared to untreated ($P<0.01$) (Figure 4.7 A).However, expression of mDLL4 resulted in tumours that were more resistant to anti-VEGF therapy as indicated by the shorter delay between mDLL4: control and mDLL4: mAb (5 days) tumours compared to that in control tumours (EV: control; EV: mAb) (14 days) ($P<0.01$) (Figure 4.7 A and Figure 4.7 B). Combined DBZ and bevacizumab treatment was additive in mDLL4 tumour group ($P<0.01$) but no further effect was observed in EV tumour group (Figure 4.7 A).

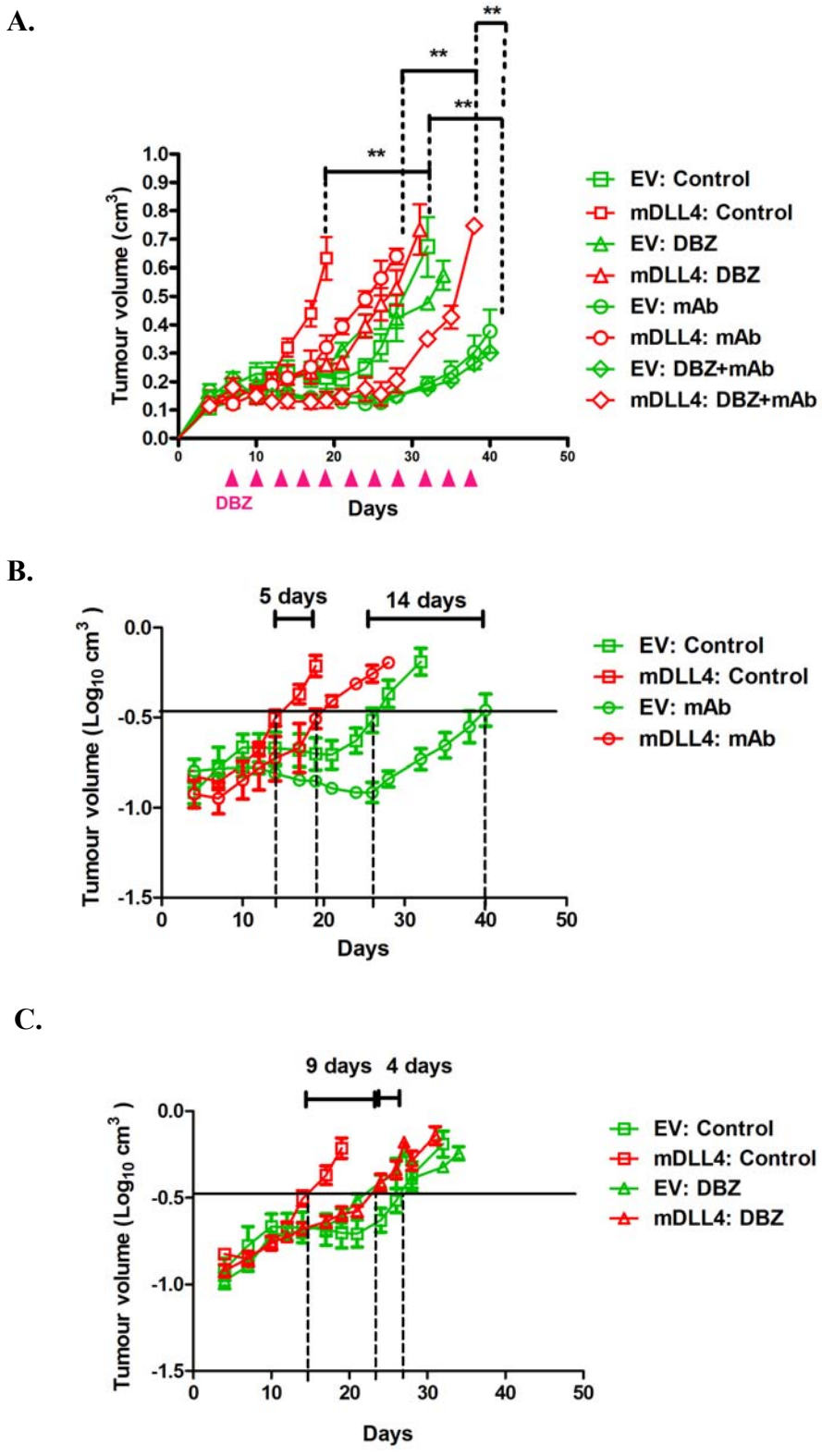


Figure 4.7**:** A) Overall tumour growth curves of U87 EV and U87 mDLL4 treated with DBZ (8.1 mmol/kg), bevacizumab (mAb) (10mg/kg) or PBS (control), B) linear plot of tumour volume for U87 EV and U87 mDLL4 treated with bevacizumab (mAb) (10mg/kg) or PBS

(control) and C) linear plot of U87 EV and U87 mDLL4 treated with DBZ (8.1 mmol/kg) or bevacizumab (mAb) (10mg/kg).

Each group consisted of 5 mice, ANOVA F test, non linear regression (**P<0.01). Error bars represent SEM.

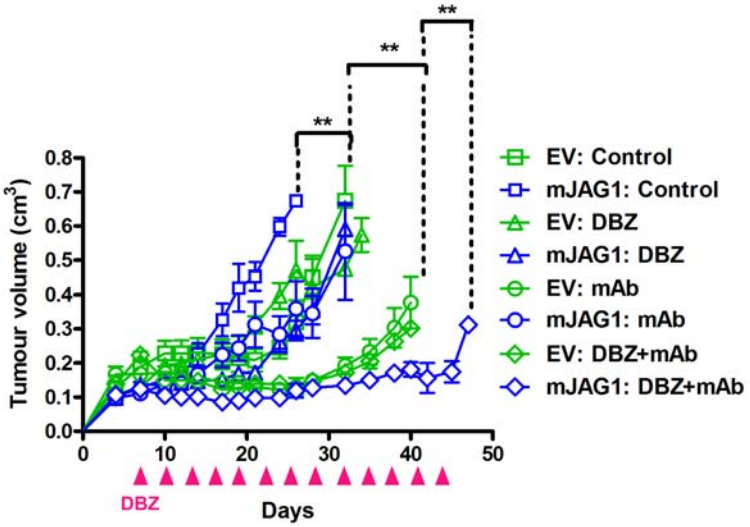
However, there was still some resistance to DBZ treatment in U87 mDLL4 tumours with treatment unable to bring tumour growth back to control levels. This is unlikely to be due to DBZ not working properly as it is fully effective in the mJAG1 xenograft model (Figure 4.8). Total inhibition of Notch signalling and delayed tumour growth has been observed in our U87 human DLL4 xenograft model.

4.7 JAG1-Notch signalling also mediated tumour resistance to VEGF inhibition

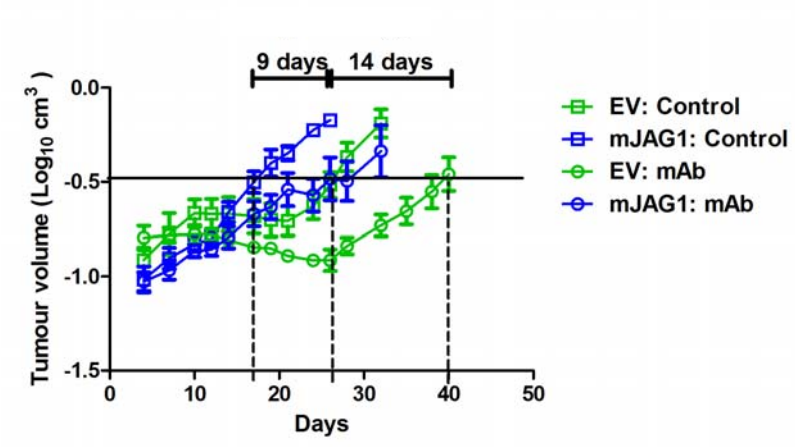
The tumour growth curves of U87 EV and U87 mJAG1 treated with DBZ (8.1 mmol/kg), bevacizumab (mAb) (10mg/kg) or PBS (control) are shown in Figure 4.8. All treatments commenced at Day 7. DBZ treatment slightly delayed control tumour (EV) growth (EV: Control; EV: DBZ) (4 days) (Figure 4.8 A and Figure 4.8 C). Similarly, mJAG1 promoted U87 tumour growth compared to EV (P<0.01) (Figure 4.8 A). DBZ inhibited JAG1-Notch signalling as indicated by down-regulation of hHEY1 (Figure 4.6 A) and reversed mJAG1 tumour growth similar to that for U87 EV xenograft tumours (P<0.01) (Figure 4.8 A and Figure 4.8 C). Bevacizumab treatment significantly delayed tumour growth in control EV and mJAG1 group respectively, compared to untreated (P<0.01) (Figure 4.8 A). However, mJAG1 contributed to relatively higher resistance to bevacizumab (mJAG1: control; mJAG1: mAb) (9 days) compared to control tumour (EV: control; EV: mAb) (14 days) (P<0.01) (Figure 4.8 B)

Interestingly in the bevacizumab treated group, JAG1-Notch signalling was fully reversed upon DBZ treatment (EV: mAb; mJAG1: DBZ+mAb) compared to that in U87 mDLL4 model (EV: mAb; mDLL4: DBZ+mAb) ($P<0.01$) (Figure 4.8 A). The *in vitro* work demonstrated that DLL4 could have a dominant position over JAG1, making DLL4 a very important ligand in up-regulating the Notch target genes and possibly the downstream resistance pathways. This may explain why DBZ is more effective in inhibiting the enhanced tumour growth.

A.



B.



C.

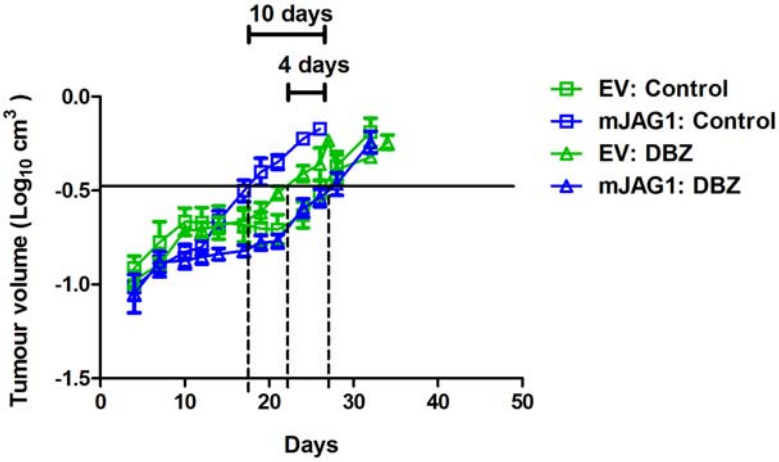


Figure 4.8: tumour growth after treatment with DBZ or bevacizumab or both simultanously

A) Overall tumour growth curves of U87 EV and U87 mJAG1 treated with DBZ (8.1 mmol/kg), bevacizumab (mAb) (10mg/kg) or PBS (control), B) linear plot of tumour volume for U87 EV and U87 mJAG1 treated with bevacizumab (mAb) (10mg/kg) or PBS (control) and C) linear plot of U87 EV and U87 mJAG1 treated with DBZ (8.1 mmol/kg). Each group consisted of 5 mice, ANOVA F-test, non linear regression (**P<0.01). Error bars represent SEM.

4.8 mDLL4 and mJAG1 produced different vascular phenotypes in U87 xenograft sections with decreased pericyte coverage.

To assess the effect of mDLL4 and mJAG1 on tumour vasculature, immunofluorescence staining was carried out to stain for vessels, using CD31 (Pusztaszeri et al. 2006) and pericytes (NG2) (Ozerdem et al. 2001; Fukushi et al. 2004) (Figure 4.9 A). Field images focused on vascularised areas representative of each tumour. Vessel density and vessel size induced by DLL4 and JAG1 were quantified on Image J via set threshold and conversion to binary (Figure 4.9 B and C). NG2 proteoglycan coverage was calculated as the percentage of NG2-positive vessels compared to the number of CD31-positive vessel (Figure 4.9 D).

mDLL4 signalling produced fewer (P<0.05) (Figure 4.9 A and B) but larger vessels (P<0.01) (Figure 4.9 A and C) whereas mJAG1 signalling increased vessel number when compared to control EV (P<0.01) (Figure 4.9 A and B). Both tumour types had reduced pericyte coverage when compared to EV (P<0.01) (Figure 4.9 A and D). Treatment with DBZ increased vessel numbers in EV and mDLL4 groups (P<0.01) (Figure 4.9 A and B) but significantly decreased vessel size in EV, mDLL4 and mJAG1 groups (P<0.01) (Figure 4.9 A and C). Pericyte coverage was also significantly increased in mDLL4 and mJAG1 groups upon inhibition of Notch signalling (P<0.01,) (Figure 4.9 A and D). Administration of bevacizumab reduced

vessel density in EV, mDLL4 and mJAG1 groups ($P<0.01$) (Figure 4.9 A and B) and significantly reduced vessel size in the mDLL4 group (mDLL4: PBS; mDLL4 :mAb) ($P<0.01$,) (Figure 4.9 A and C). The percentage of pericyte coverage in tumours treated with both DBZ and bevacizumab was similar to that in tumours treated with DBZ (Figure 4.9 A and D).

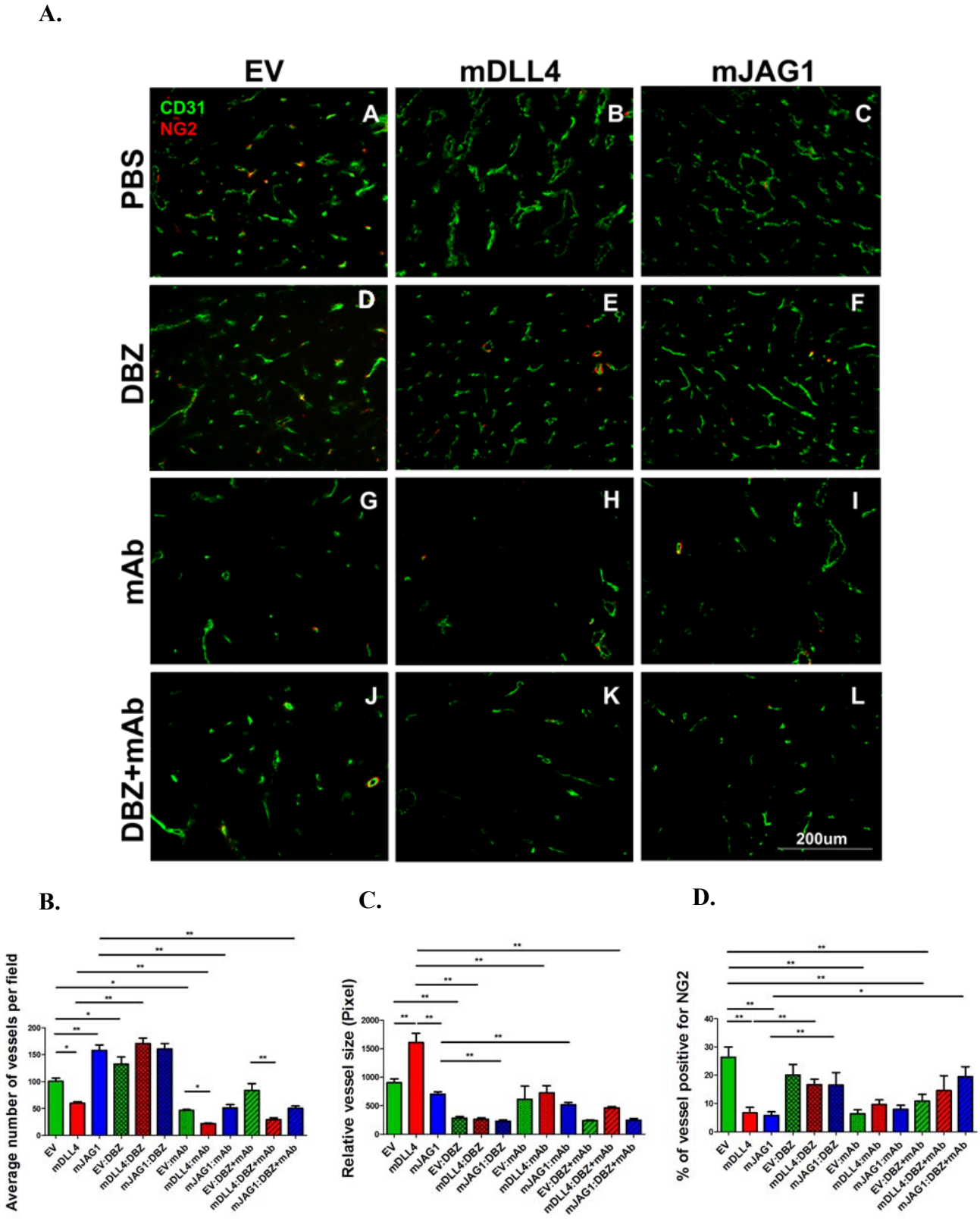


Figure 4.9**:** A) Immunofluorescence staining for vessels, CD31 (green); pericytes, NG2 (red) and merged images (yellow) to show vascular phenotypes in xenograft models and

quantification of B) vessel number C) relative vessel size and D) percentage of pericyte coverage on vessels in U87 xenograft sections.

Fluorescent microscopy images were acquired for five randomly chosen fields per tumour section. Data are presented as mean ± SEM (n=5 tumours). Statistics test: *P<0.05 and **P<0.01, ANOVA with Bonferroni's post-test.

Enlarged graphs for vessel number and pericyte quantification are shown in Figure 4.9.1.

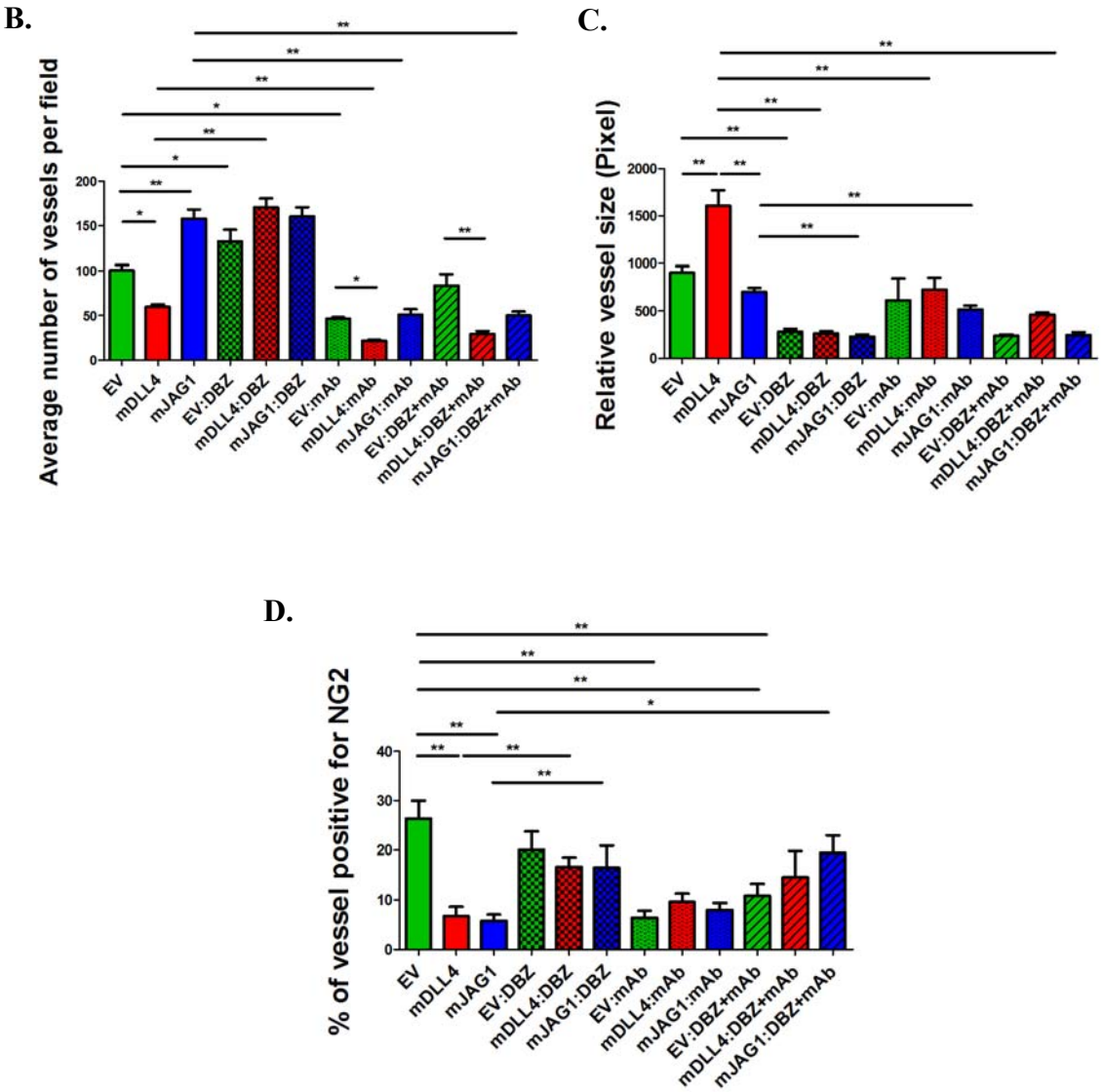


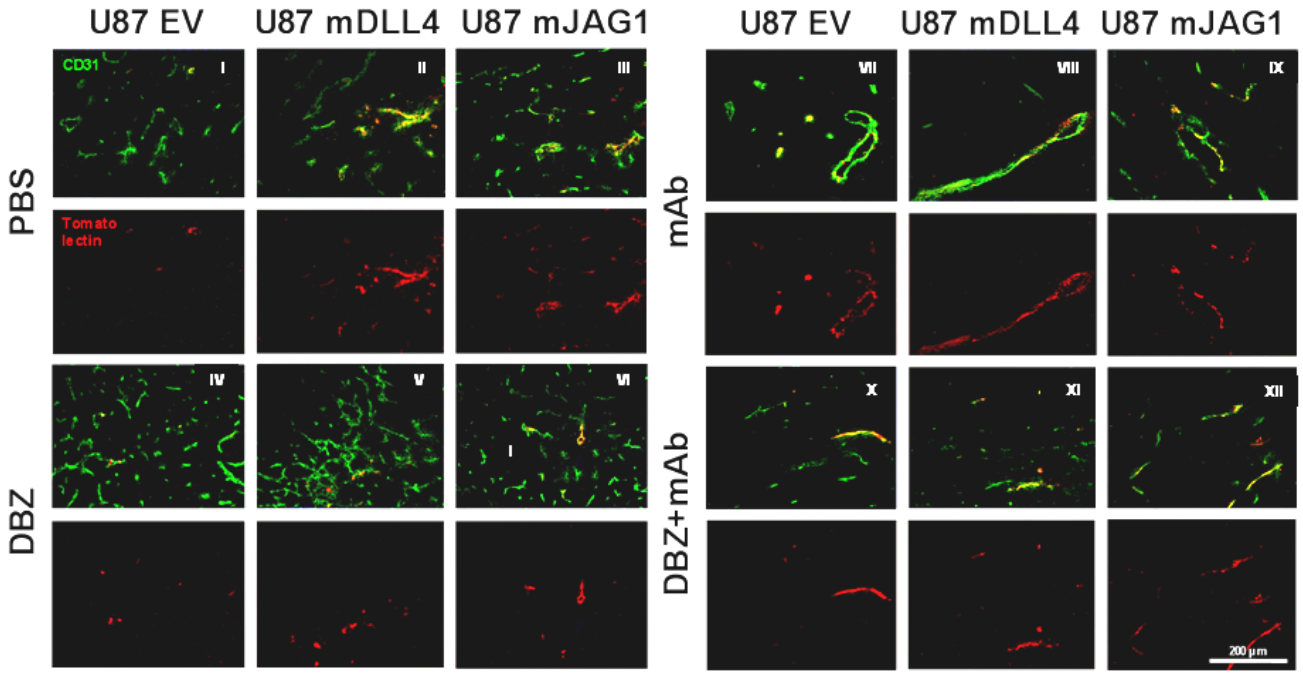
Figure 4.9.1: Quantification of B) vessel number C) relative vessel size and D) percentage of pericyte coverage on vessels in U87 xenograft sections.

Data are presented as mean ± SEM (n=5 mice). Statistics test: *P<0.05 and **P<0.01, ANOVA with Bonferroni's post-test.

4.9 Both mDLL4 and mJAG1 increased vessel perfusion in U87 xenograft tumours

In order to investigate the effects of mDLL4 and mJAG1 and anti-VEGF treatment on tumour vessel perfusion, Biotinylated Lycopersicon Esculentum (Tomato) Lectin (1 µg/µl) was injected intravenously into each mouse via the lateral vein 30 minutes before euthanasia. Frozen sections were double stained for CD31 (vessel marker) and Streptavidin to enhance the signal for biotinylated tomato lectin. Images were taken focused on areas with vessels (tumour hot spot) to determine percentage perfusion in existing vessels. Tomato lectin perfusion technique relies on the specific binding to the cell surface N-acetylglucosamine oligomers on vascular endothelial cells, thereby defining perfused vessels (Debbage et al. 1998). The presence of vessels was confirmed by colocalization with CD31. Percentage of perfusion was calculated as the percentage area positive for tomato lectin compared to the CD31 positive area.

A.



B.

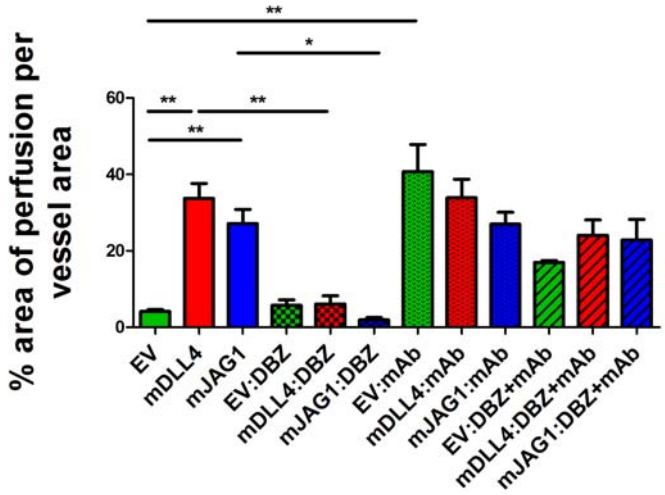


Figure 4.10**:** A) Immunofluorescence staining for vessels using CD31(green) and biotinylated tomato lectin (red) to measure vessel perfusion, merged images show colocalization of tomato lectin on vessels (yellow) and B) quantification of percentage area perfusion per vessel area.

Data are presented as mean ± SEM (n=5 mice). Statistics test: *P<0.05 and **P<0.01, ANOVA with Bonferroni's post-test.

Both mDLL4 and mJAG1 over-expression in U87 tumours resulted in increased vessel perfusion ($P<0.01$) compared to control EV (Figure 4.10) which was also observed by my colleagues in the U87 hDLL4 model. Treatment with DBZ reversed the effect of Notch signalling by decreasing perfusion in these groups ($P<0.01$). Anti-VEGF treatment with bevacizumab mAb resulted in an increase in vascular perfusion in EV but did not affect perfusion in mDLL4 and mJAG1 models.

4.10 DLL4 was highly expressed in tumour vessels

In order to evaluate the expression of DLL4 in these xenograft tumours, DLL4 immunostaining was carried out on frozen sections using an anti mouse and human DLL4 antibody and visualised under fluorescence microscope at a consistent threshold. DLL4 was abundantly expressed in U87 xenograft tumour vasculature (Figure 4.11 I-III) (Noguera-Troise et al. 2006; Patel et al. 2006; Ridgway et al. 2006; Li et al. 2007; Segarra et al. 2008; Jubb et al. 2009; Jubb et al. 2010). DLL4 expression was also very high in tumours over-expressing mDLL4, once again confirming the transduction of mDLL4 in U87 cells, and tumour vessels (Figure 4.11 II, V, VIII, XI). DLL4 expression in the vessels was diminished with DBZ treatment (Figure 4.11 IV and VI). Reduction of DLL4 expression in vessels was not prominent in U87 mDLL4 tumours treated with DBZ. (Figure 4.11 V). Bevacizumab profoundly pruned the vessels leaving behind surviving vessels which expressed high levels of DLL4 in control tumours (Figure 4.11 VII) and tumours over-expressing mDLL4 (Figure 4.11 VIII). Less DLL4 expression was observed in the vasculature of U87 mJAG1 treated with bevacizumab (Figure 4.11 IX).

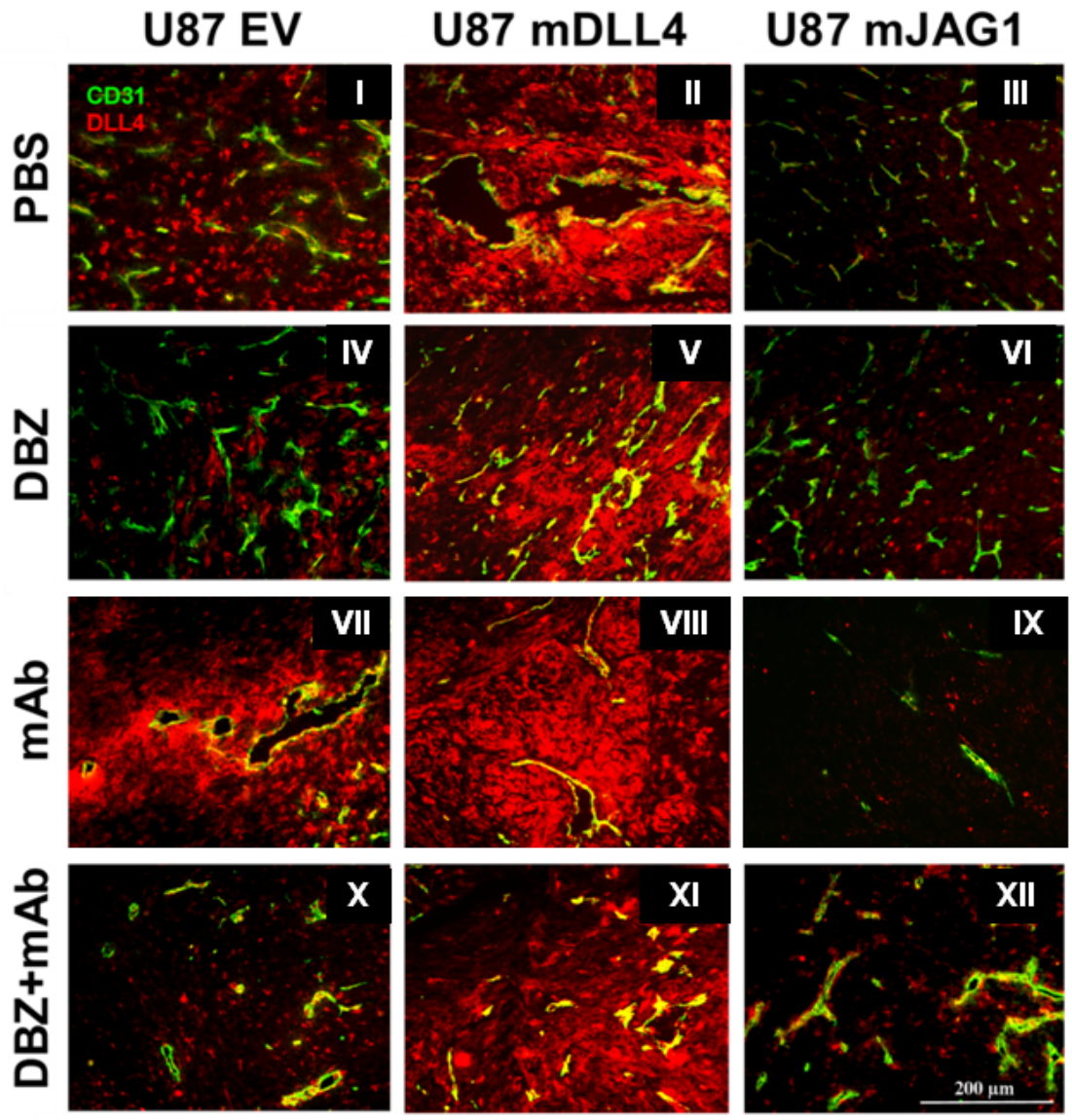


Figure 4.11: DLL4 expression in U87 xenograft tumours**.**

Double staining for DLL4 (red) and CD31 (green). Colocalization is shown in yellow. Each group consisted of 5 mice.

Interestingly, DLL4 expression was also present in the tumour cells and/or stromal of control (EV) and mJAG1 tumour. In control tumours, this staining was decreased by DBZ treatment (Figure 4.11 IV) but highly up-regulated after bevacizumab treatment (Figure 4.11 VII). In U87 mJAG1 tumours, this staining was also increased after bevacizumab treatment (Figure 4.11 IX). Work is ongoing to establish the cell type responsible for the DLL4 expression.

4.11 mDLL4 increased JAG1 expression in vessels and tumour cells and stroma

To study the effect of mDLL4 and mJAG1 on JAG1 expression, JAG1 expression was analysed in the xenograft sections via immunostaining using an anti human and mouse JAG1 antibody, as described in Materials and Methods section, followed by visualisation at a set threshold under fluorescence microscope. JAG1 was found expressed weakly in the vessels, although not obvious in the merged figure. (Figure 4.12 I). Notably, JAG1 expression intensified in the U87 mDLL4 tumours cells/ stroma (Figure 4.12 II). JAG1 was abundantly expressed in U87 over-expressing mJAG1 tumours ratifying transduction efficacy (Figure 4.12 III, VI, IX, XII). Inhibition with DBZ resulted in abated JAG1 intensity in mDLL4 tumours (Figure 4.12 V) while anti-VEGF treatment with bevacizumab mAb had no effect on JAG1 expression in the tumours (Figure 4.12 VII-IX).

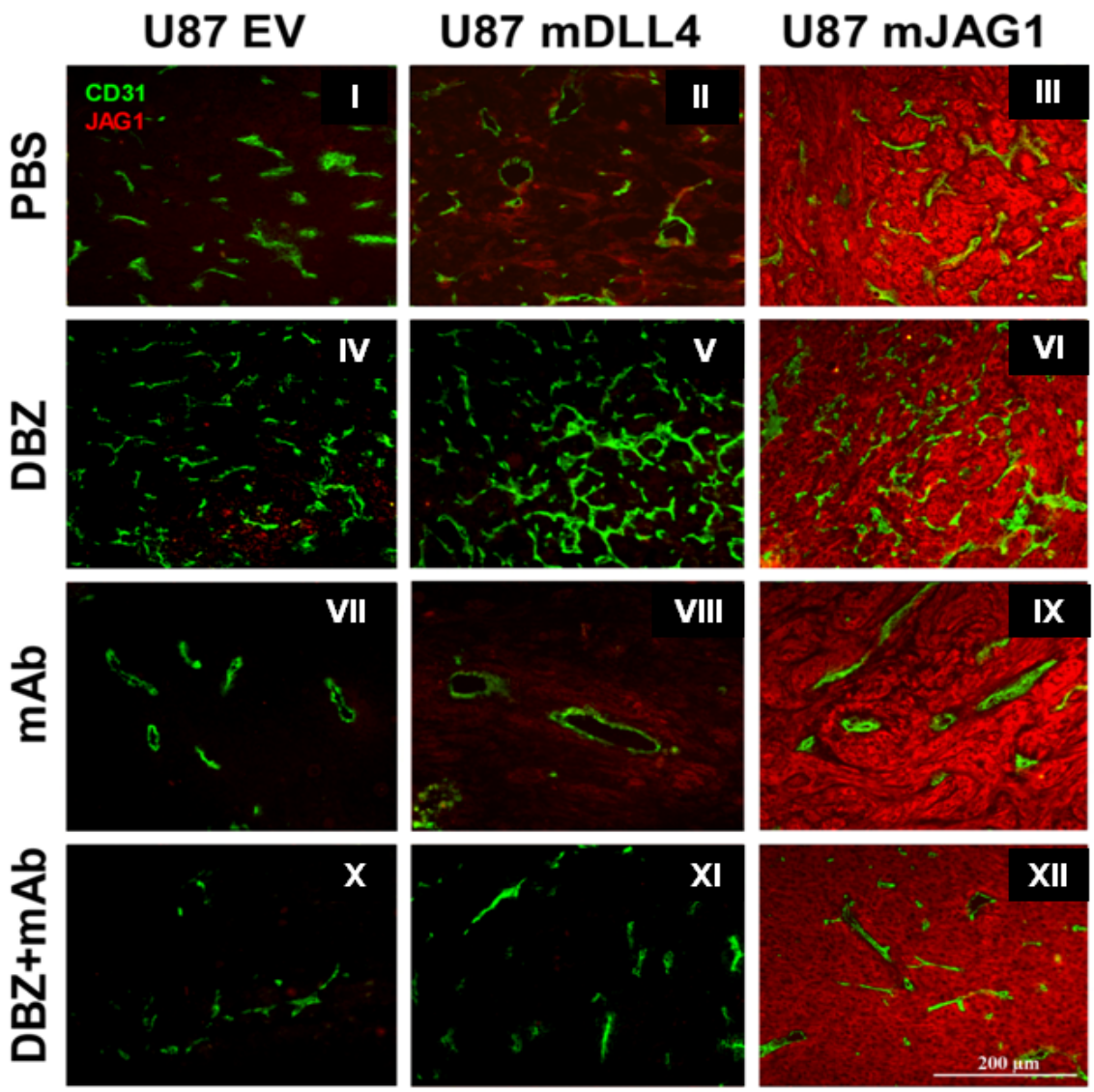


Figure 4.12: JAG1 expression in xenograft tumours

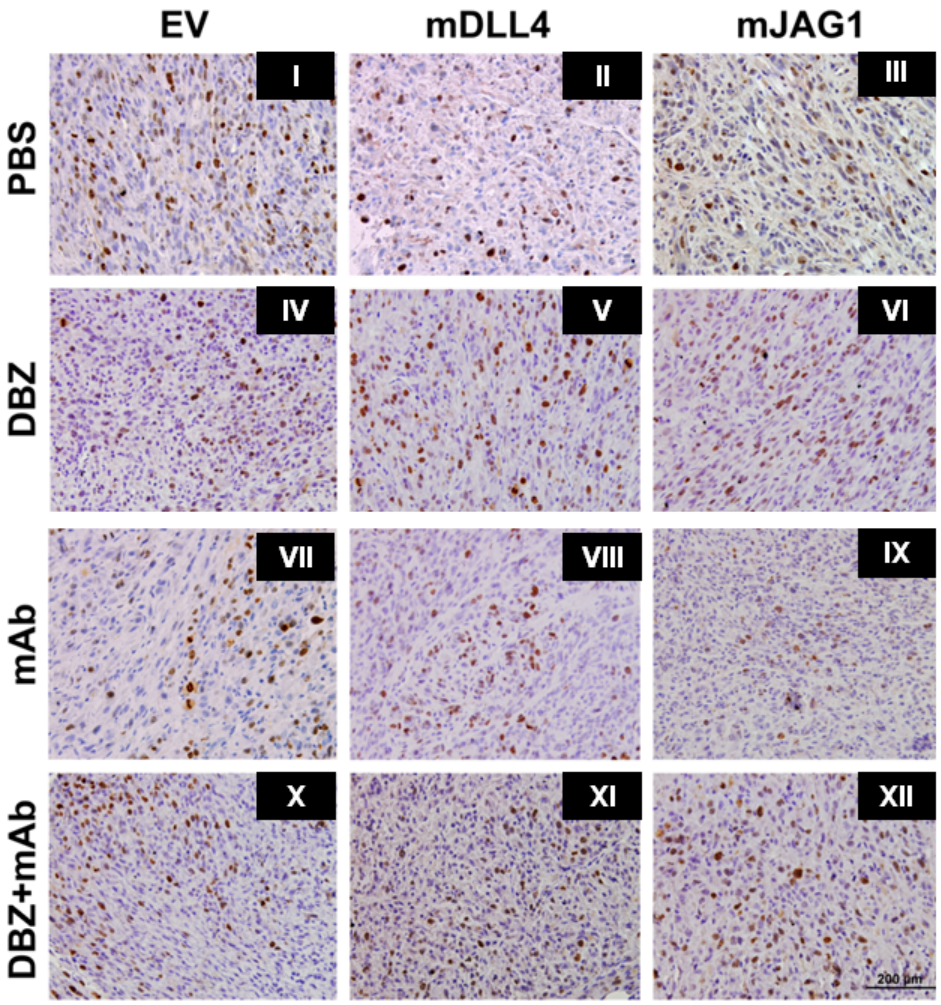
Double staining for JAG1 (red) and CD31 (green). Colocalization is shown in yellow. Each group consisted of 5 mice.

4.12 Tumour cell proliferation was unaffected by mDLL4 and mJAG1 expression

The growth of tumours depends on the balance between the cell proliferation and cell death. To determine if mDLL4 and mJAG1 had any proliferative effect in xenograft tumours, Formalin-Fixed, Paraffin-Embedded (FFPE) sections were stained with the Ki-67 proliferative marker (MIB1) antibody and scored by a pathologist (Dr. Adrian Jubb) using Image J software. The analysis involved performing colour deconvolution on immunohischemistry slides to calculate the number of Ki-67 positive nuclei (brown) and total nuclei (blue). Proliferation index was presented as the ratio of total number of brown stains over total number of blue stains.

Overall, mDLL4 and mJAG1 over-expression in U87 tumour cells had no effect on cell proliferation. Treatment with DBZ or bevacizumab had little effect on number of cells proliferating with the exception of mAb treatment of EV and mJAG1 tumours. Although this decrease has reached significance, there is no apparent decrease in proliferation in the DBZ/bevacizumab combination treatment suggesting that this result may not be accurate. This is probably due to random variation in a small number of samples and analyses and could be assessed in repeat experiments.

A.



B.

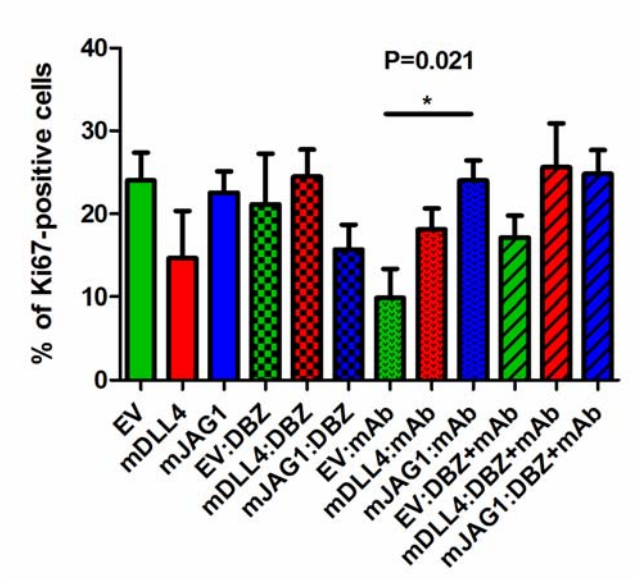
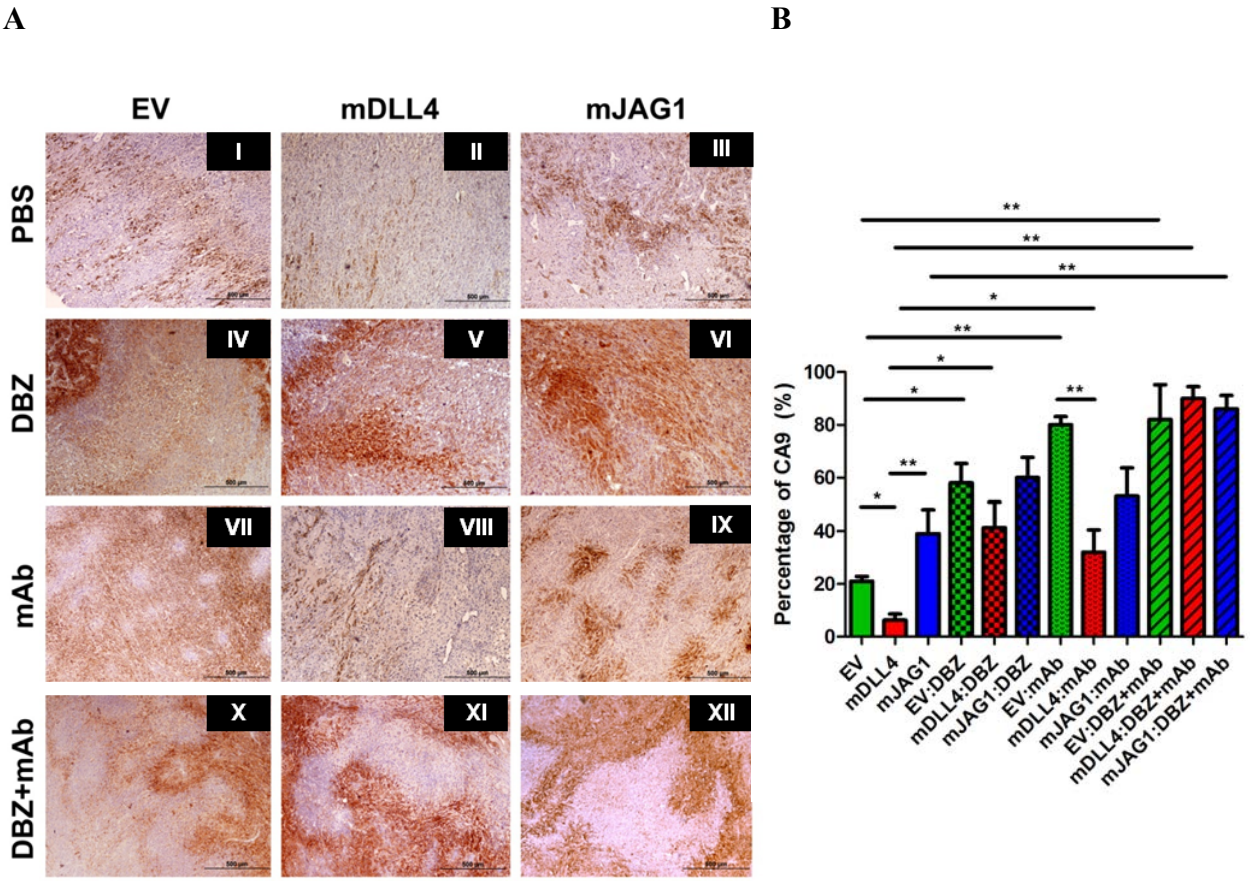


Figure 4.13: A) Histopathology staining for MIB1 in xenograft tumours and B) proliferation index of xenograft tumours.

A) Immunohistochemistry staining for MIB1 was carried out and visualised under normal light microscope. B) Data was plotted on a histogram with SEM and analysed with ANOVA (n=5 mice). Statistical test: *P<0.05, ANOVA with Bonferroni's post-test.

4.13 mDLL4 but not mJAG1 decreased tumour hypoxia

To investigate the dynamics of hypoxia, tumour FFPE sections were stained for endogenous hypoxia marker, CAIX and scored as the percentage of CAIX per section with the help of Dr. Adrian Jubb. In consistent with previous work (Li et al. 2007), mDLL4 significantly diminished CAIX expression in U87 xenograft tumours compared to control EV (P<0.05) (Figure 4.14). This effect was reversed when Notch signalling was blocked with DBZ treatment rendering the tumours more hypoxic in EV and mDLL4 groups (Figure 4.14 IV and V). Both of these groups had an increase in hypoxia with either DBZ (Figure 4.14 IV and V) or bevacizumab treatment (Figure 4.14 VII and VIII) with an additive effect seen in the mDLL4 tumours (Figure 4.14 XI). In contrast, expression of mJAG1 did not reduce CAIX expression compared to the control EV tumours (Figure 4.14 III). Treatment of this group with DBZ (Figure 4.14 VI) or bevacizumab (Figure 4.14 IX) did not significantly affect the level of CAIX expression compared to untreated mJAG1 tumours (Figure 4.14 III). However, DBZ and bevacizumab co-treatment appeared to be working in synergy to increase tumour hypoxia (P<0.01) (Figure 4.14 X-XII). Dual staining for CAIX (brown) and CD34 (grey) revealed weaker CAIX staining around bigger and perfused vessels in mDLL4 tumours in Figure 4.14 C.



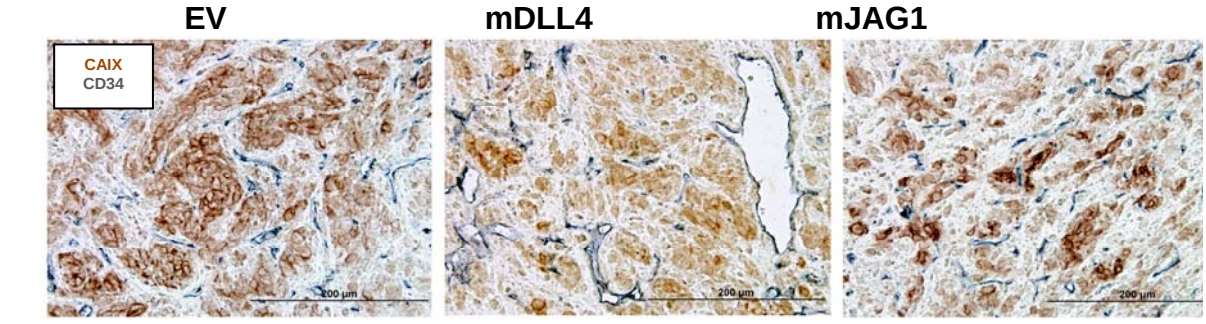


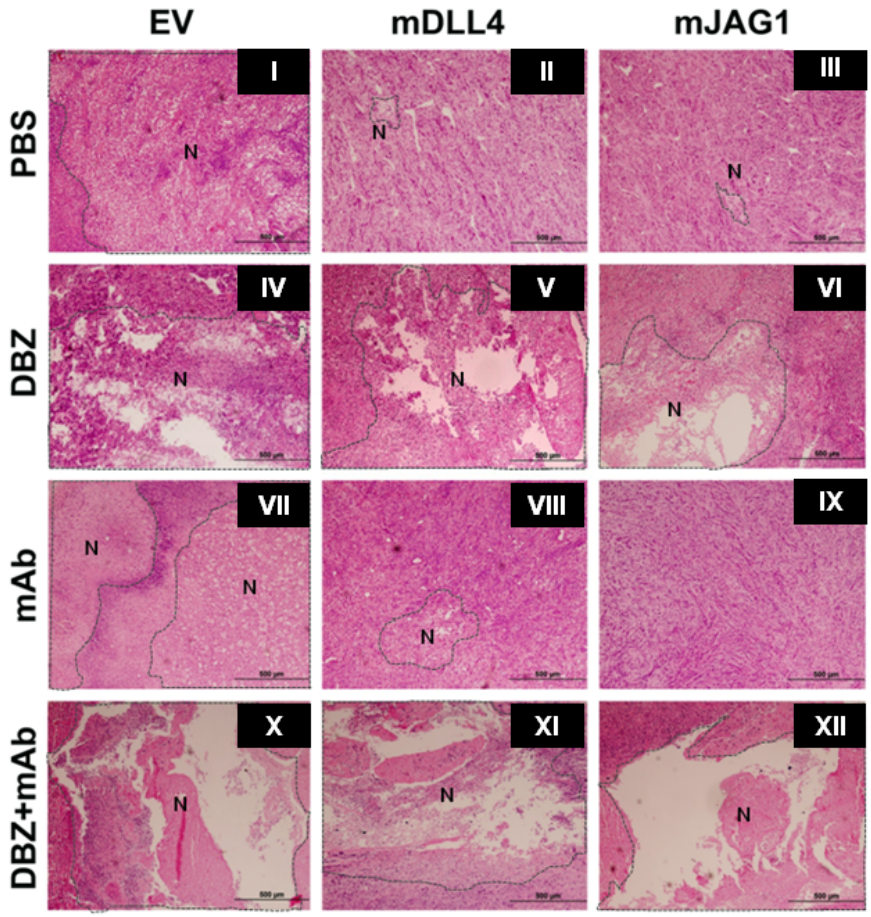
Figure 4.14: A) Histopathology staining for intratumoural hypoxia using Carbonic anhydrase IX (CAIX) on xenograft tumours and B) hypoxia index of xenograft tumours and C) dual staining for CAIX (brown) and vessels (CD34) (grey).

A) Immunohistochemistry staining was carried out and visualised under a normal light microscope. B) Data was plotted on a histogram with SEM and analysed with ANOVA (n=5 mice). Statistical test: *P<0.05, ANOVA with Bonferroni's post-test.

4.14 mDLL4 and mJAG1 decreased tumour necrosis which contributed to tumour growth

Tumour cell death is often evaluated by the passive process of necrosis and the active process of apoptotic cell death. Terminal deoxynucleotidyl transferase dUTP nick end labeling (TUNEL) staining were initially carried out to assess apoptosis in the xenograft tumours. However TUNEL failed to discriminate between necrosis and apoptosis (Grasl-Kraupp et al. 1995), thus quantification was compromised due to the highly necrotic areas in some of the sections. Immunostaining for activated Caspase-3 was then performed but scoring was arduous and not reproducible due to high levels of neutrophil infiltration which stained positive for Caspase-3 (O'Neill et al. 2000; Daigle and Simon 2001). H&E staining allows an overview of the tissue structure, enabling identification of necrotic areas on the tumour sections, as characterised by lighter pink staining of loose cells, while severe necrosis caused the necrotic cells to fall off while being sectioned (shown empty as white background in Figure 4.15).

A.



B.

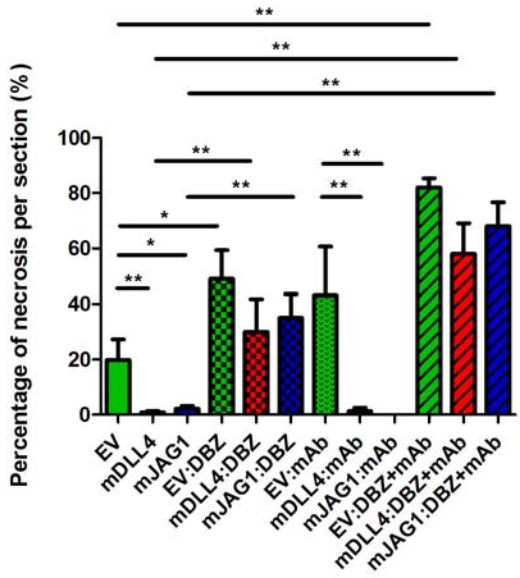


Figure 4.15: A) Hematoxylin and eosin (H&E) staining on xenograft tumours and B) necrosis index of xenograft tumours.

A) Immunohistochemistry staining for H&E was carried out and visualised under normal light microscope. Necrotic areas were identified (enclosed within dotted lines) and marked as N. B) Data was plotted on a histogram with SEM and analysed with ANOVA (n=5 mice). Statistical test: *P<0.05, ANOVA with Bonferroni's post-test.

Both mDLL4 and mJAG1 significantly reduced the percentage of tumoural necrosis (P<0.05) (Figure 4.15 II and III), while treatment with DBZ obviated the effect by increasing necrosis (Figure 4.15 IV-VI). Anti-VEGF treatment with bevacizumab increased necrosis in control tumour (VII). However, percentage necrosis was decreased in mDLL4 and mJAG1 tumours compared to EV within the bevacizumab treated group (Figure 4.15 VII-IX). Co-treatment with DBZ and bevacizumab enhanced necrosis in all groups (Figure 4.15 X-XII).

4.15 Preliminary experiment: Blocking DLL4-Notch signalling delayed tumour growth in U87 xenograft tumours

To examine the interplay between JAG1 and DLL4 in promoting tumour growth, a preliminary experiment was carried out using a specific anti-DLL4 monoclonal blocking antibody which recognises human and murine DLL4 to block the Notch signalling pathway in U87 tumours over-expressing mJAG1. Briefly, anti-DLL4 antibody (5mg/kg) was administered into mice twice a week. Blocking DLL4-Notch signalling effectively delayed tumour growth in the U87 EV control tumour group (P<0.01). Although the same effect was observed within mJAG1 over-expressing tumours when DLL4-Notch signalling was inhibited (P<0.01), the delay appears smaller in the mJAG1 group compared to EV group.

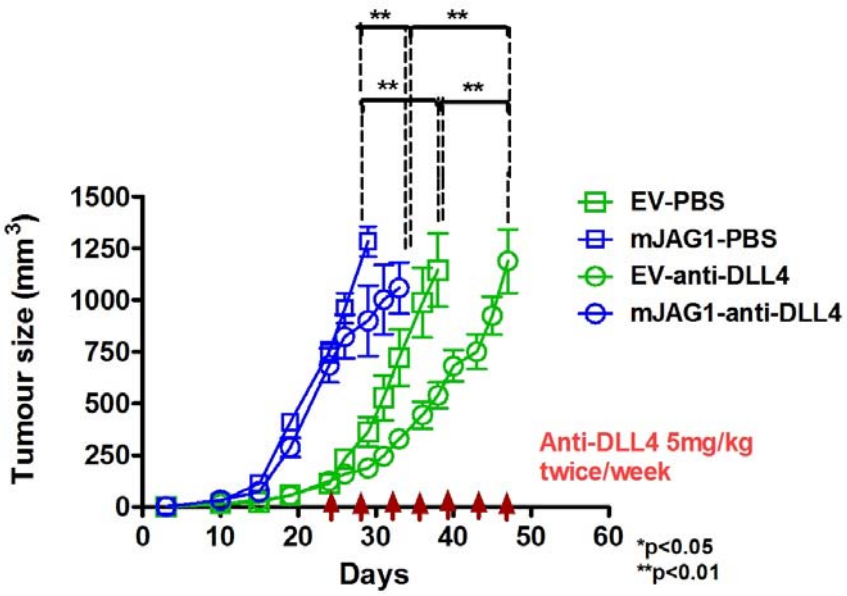


Figure 4.16**:** Preliminary results: Tumour growth curves of U87 EV and U87 mJAG1 treated with 5mg/kg anti-DLL4 antibody or PBS (control).

Each group of xenograft tumours consisted of 7 replicates. Data was analysed using ANOVA F test (**P<0.01) to test the significance between each group. Figure was kindly provided by Dr. Ji-Liang Li.

4.16 Discussion

Effects of mDLL4 and mJAG1 on downstream Notch target genes

In vitro, both mDLL4 and mJAG1 upregulated the HES1 and HEY1 Notch target genes, with up-regulation of HES1 was higher than HEY1 due to its ubiquitous expression in endothelial, perivascular and non vascular cells (Benedito et al. 2009) whereas HEY1 expression is more restricted to the vessels (Fischer et al. 2002), thus making HES1 a better Notch indicator gene. However, interplay between the Notch ligands and the Notch receptors in the stroma and tumour cells was observed *in vivo*. mDLL4 up-regulated hHEY1 (P<0.01) but induction was

not significant for mJAG1 (Figure 4.6 A), possibly due to feed forward mechanism of mDLL4 to up-regulate itself thus enhancing Notch signalling (Caolo et al. 2010). Both mDLL4 and mJAG1 up-regulated mHEY1 ($P<0.05$) (Figure 4.6 B) more than hHEY1 (Figure 4.6 A), implying more efficient Notch activation within the same ligand-receptor species, in this case murine ligands activating murine Notch receptors in the stroma, or cell type differences. Moreover, HEY1 expression is more associated with cardiovascular system (Fischer et al. 2002), as such this accounts for the higher induction of mHEY1 possibly in the vessels compared to hHEY1. mJAG1 appeared to be more potent than mDLL4 is the up-regulation of mHEY1, although this was insignificant (Figure 4.6 B). This could be due to high level of hypoxia in mJAG1 tumours, as indicated by CAIX expression (Figure 4.14 A III). Secretion of human and mouse VEGF upregulates DLL4 or HIF-1α (Diez et al. 2007; Chen et al. 2010) which triggers further Notch activation leading to up-regulation of mHEY1.

DBZ, either as a single or combined treatment with bevacizumab (mAb) inhibited Notch signalling by down-regulating both hHEY1 ($P<0.01$) and mHEY1 ($P<0.01$) in the mDLL4 and mJAG1 over-expressing U87 xenograft tumours (Figure 4.6 A and B). Treatment with bevacizumab in the EV group decreased hHEY1 expression ($P<0.01$), which could be explained by pruning of vessels expressing mDLL4, thus decreasing stroma- tumour Notch signalling (Noguera-Troise et al. 2006) (Figure 4.6 A). Unexpectedly, bevacizumab appeared to increase mHEY1 expression in EV group compared to untreated (Figure 4.6 B), but it was not significant. This could be due to bevacizumab being a humanised anti-VEGF antibody which is ineffective in sequestering stromal murine VEGF, causing some residual effects and maintaining vessels but clearly still marked pruning.

Bevacizumab did not affect hHEY1 expression in mDLL4 and mJAG1 groups (Figure 4.14 A). However, treatment with bevacizumab decreased mHEY1 expression in mJAG1 tumours compared to untreated mJAG1 tumours. This could be due to the big SEM deviation in mHEY1 expression observed within the mJAG1 control group as well as the EV, mDLL4 and mJAG1 tumour groups treated with bevacizumab (Figure 4.6 B). This could be explained by the technical variability during tumour cutting for RNA extraction. A small piece of tumour was used to be representative, however tumours can be heterogenous and the degree of necrosis and the minority distribution of stromal components compared to tumour cells could account for the big variation between groups. The regulation of other downstream Notch target genes such as HES1 which is more ubiquitously expressed in vessels and non vascular cells will be studied.

Vasculature effects

Both mDLL4 and mJAG promoted U87 xenograft tumour growth through different vasculature phenotypes. mDLL4 appeared to be more effective in promoting U87 tumour growth compared to mJAG1 (Figure 4.4 B) which may be explained by the up-regulation of DLL4 expression by mDLL4 thus enhancing Notch signalling more than mJAG1 in U87 tumours as also supported by the *in vitro* results in endothelial cells and others (Ridgway et al. 2006; Caolo et al. 2010) suggesting the importance of DLL4 as the more dominant ligand in Notch signalling compared to JAG1 at the functional level as also shown in the previous chapter. mDLL4 decreased vessel number but harboured bigger vessels, similar to the phenotype observed with hDLL4 (Li et al. 2007), while JAG1 increased tumour angiogenesis. The pro-angiogenic effect of JAG1 was also observed in mouse retinal model (Benedito et al. 2009) and head and neck squamous cell carcinoma tumour model (Zeng et al. 2005).

Pericyte coverage

Both mDLL4 and mJAG1 tumour types had reduced pericyte coverage compared to EV control. Similar results were also observed when tumours were double-stained for CD31 and α-SMA, which is a marker for matured pericytes found on big developed vessels (Jockovich et al. 2007) (data not shown). Pericytes are perivascular cells that envelope the blood vessels to provide support and stabilize the vascular tubes. The degree of pericyte coverage is often associated with the stability of blood vessels and is critical for the development of a functional vascular network (Chantrain et al. 2006). The increased vessel perfusion induced by mDLL4 and mJAG1 could be associated with more stable vessels, through a yet unknown mechanism that does not require pericyte recruitment. This may involve the crosstalk between Notch signalling and the Wnt signalling pathway through the up-regulation of the Notch-regulated ankyrin repeat protein, Nrarp by DLL4 (Phng et al. 2009) and beta–catenin by JAG1 (Rodilla et al. 2009) which has recently been shown to play a role in vessel stability (Phng et al. 2009).

Another explanation for the reduction of pericyte coverage in mDLL4 and mJAG1 over-expressing tumours could be through the stromal derived factor-1A (SDF-1A)/CXCR4 axis in which PDGF-BB induced pericytes are recruited by SDF-1A chemotaxis gradient (Song et al. 2009). DLL4 (Williams et al. 2008) and JAG1 (unpublished preliminary result) can down-regulate CXCR4 in endothelial cells therefore this could thus hamper pericyte recruitment to the vessels.

While many studies reported JAG1 to positively regulate vSMC coverage (Doi et al. 2006; Wu et al. 2008; Benedito et al. 2009), Morrow and colleagues demonstrated Notch signalling to inhibit aortic SMC differentiation through an RBP-Jκ/Hey-dependent mechanism (Morrow

et al. 2005). Over-expression of constitutively active Notch intracellular (IC) receptors (Notch1 IC and Notch3 IC) resulted in a significant down-regulation of α-actin, myosin, calponin and smoothelin expression, which was significantly diminished after inhibition of Notch-mediated RBP-Jκ/Hey or siRNA suppression of basic helix-loop-helix factors HES gene and HEY genes. This could account for the decrease of pericyte and vSMC coverage in the U87 over-expressing mJAG1 and mDLL4 model, in which active canonical Notch signalling is present, as indicated by the up-regulation of the HEY1 notch target gene (Figure 4.6). Besides, mDLL4 or mJAG1 over-expression in U87 may produce stable and functional vessels, as demonstrated by more perfused vessels that drove tumour growth (Figure 4.10), thus the tumour cells could mimic the role of pericytes.

Recently, comprehensive studies revealed that glioblastoma stem-like cells could differentiate into functional tumour endothelium (Ricci-Vitiani et al. 2010; Wang et al. 2010) and possibly other cell types, for example pericytes and smooth muscle cells. Therefore, it would be interesting to examine the proportion of human or mouse origin cells make up in the vessels and identify the origin of pericytes and vascular smooth muscle cells, whether they were recruited by tumour endothelium or differentiated from glioblastoma stem-like cells. As such, double staining for mouse and human specific CD31 vessel marker should be carried out to identify origin of tumour endothelium.

Vessel perfusion

Vessel perfusion in mDLL4 and mJAG1 tumour groups was improved making the vessels more functional to feed the tumours with oxygen and nutrients (Figure 4.10). This was confirmed by a decrease in intratumoural hypoxia in mDLL4 tumours, indicated by reduced

CAIX expression around bigger and perfused vessels in mDLL4 tumours (Figure 4.14 C). As CAIX expression depends on oxygenation status of the tumour, its protein stability and slow induction can accumulate over long periods of hypoxia (Wykoff et al. 2001). Due to the long half life of CAIX (2-3 days) (Turner et al. 2002; Rafajova et al. 2004), its expression may still be present upon re-oxygenation. Besides blood supply, tumour oxygenation status may also be influenced by cell metabolic demands which could be affected by mJAG1 expression, providing another explanation for tumour growth driven by mJAG1 expression through increased perfusion and reduced necrosis but no effect on CAIX expression was observed. In order to assess an effect of mJAG1 on tumour hypoxia, tumours will be stained for pimonidazole and scored to see if CAIX expression and pimonidazole staining overlap as noted before (Wykoff et al. 2000).

Growth and cell death

Tumour growth is balanced by cell proliferation and cell death. Overall, mDLL4 and mJAG1 did not affect U87 tumour cell proliferation. Notch signalling is well recognised to be important for stem cell regulation in glioblastomas (Hovinga et al. 2010; Stockhausen et al. 2010). Although stem cell activation may reduce proliferation in normal tissues, it would not be expected to reduce growth of tumour cells. In fact we saw reduced proliferation *in vitro* and no difference *in vivo*. However, the induction of a stem cell phenotype *in vivo* could contribute to some of the phenotype, for example enhanced tumour survival under stress, or cells at an earlier stage of differentiation expanded and were less susceptible to hypoxia effects. Preliminary analyses of Caspase3 and TUNEL gave variable results on these samples and were inconclusive. The different effects of mDLL4 and mJAG1 on U87 cell proliferation *in vitro* (Figure 4.3A) and tumour growth *in vivo* (Figure 4.4 B) revealed a stroma-dependent

mechanism for Notch signalling in U87 xenograft tumours. Both mDLL4 and mJAG1 promoted U87 tumour growth in SCID mice suggesting that both ligands expressed on U87 could signal to the surrounding tumour and stromal cells, as revealed by up-regulation of hHEY1 and mHEY1 gene expression by QPCR which was substantially down-regulated upon blocking Notch signalling with DBZ (Figure 4.6). This culminated in a change vasculature formation (Figure 4.9). Taken together, both mDLL4 and mJAG1 increased perfusion in vessels promoting nutrient and oxygen uptake by tumour cells to decrease hypoxia and percent of tumour necrosis (Figure 4.15 II and III) to promote U87 xenograft tumour growth.

Therapeutic intervention- vasculature effects

Upon blocking Notch signalling with DBZ, mDLL4- and mJAG1-Notch signalling to the surrounding tumour and stromal cells were substantially down-regulated as revealed by down-regulation of hHEY1 and mHEY1 (Figure 4.6). The vasculature phenotypes were reversed in EV and mDLL4 tumours when Notch signalling was blocked with DBZ (Figure 4.9 A IV and V). The enhanced vessel density upon blocking Notch signalling with DBZ treatment could be partly due to the increased level of VEGF secreted by tumours and stromal cells under hypoxic conditions (Aiello et al. 1995) which then established a paracrine loop to activate endothelial cell proliferation (Reynolds et al. 2000) to form non functional vessels, which increased hypoxia and induced pericyte proliferation and migration to the vessels.

Ephrin-B2 is a key player in angiogenesis (Liu et al. 2004; Heroult et al. 2006; Kuijper et al. 2007; Djokovic et al. 2010) and arteriogenesis (Korff et al. 2006), thus the size of vessels is associated with Ephrin B2 expression. In co-culture experiments using endothelial cells and either DLL4- or JAG1-expressing cells, DLL4 stimulation but not JAG1 was found to

markedly induce Ephrin B2 expression (Iso et al. 2006), providing explanation for the increase in vessel size observed in mDLL4 tumours (Figure 4.9 B). Inhibition of Notch signalling has been demonstrated to down-regulate the expression of Ephrin B2 (Grego-Bessa et al. 2007) This could account for the reduction of vessel size observed in EV, mDLL4 and mJAG1 groups treated with DBZ (Figure 4.9 B). Endothelial Ephrin-B2 is upregulated by VEGF through the DLL4-Notch pathway (Harrington et al. 2008) and hypoxic stress (Korff et al. 2006). The vessel size in mDLL4 tumours was VEGF dependent, because bevacizumab decreased vessel size in mDLL4 tumours (Figure 4.9 B). This implies that there is a VEGF dependent pathway also independent of Notch signalling regulating Ephrin-B2 (Wang et al. 2010).

Bevacizumab treatment delayed tumour growth for EV, mDLL4 and mJAG1 groups. However, the tumour growth delay period between bevacizumab mAb treated and untreated, within both the mDLL4 and mJAG1 groups, was shorter compared to control tumour (EV). This, suggests resistance mediated by these ligands, which was reversed upon treatment with DBZ as shown by co-treatment in both mDLL4 (Figure 4.7) and mJAG1 (Figure 4.8) groups. Interestingly, combination treatment worked better in both mDLL4 and mJAG1 tumour groups as shown by the significant delayed effect on tumour growth compared to single treatment.

Therapeutic intervention- pericyte effects

In the U87 mDLL4 and mJAG1 tumour models, both ligands decreased pericyte coverage compared to control EV but these phenotypes were reversed upon Notch signalling inhibition with DBZ (Figure 4.9 D). VEGF has been shown to affect recruitment and maintainance of

pericytes (Hagedorn et al. 2004). Blockade of VEGFR2 signalling was associated with a decrease in pericyte proliferation, migration and detachment from vessels (Lin et al. 2011). This could explain why sequestering VEGF with bevacizumab mAb decreased pericyte coverage (EV: mAb; EV:PBS) (Figure 4.9 I and II). Published literatures suggest that pericytes might play a role in resistance to anti-VEGF treatment in tumours (Benjamin et al. 1998; Bergers et al. 2003). However, the percentage of pericyte coverage in tumours treated with both DBZ and bevacizumab were similar to that in tumours treated with DBZ, suggesting that the resistance to bevacizumab observed in mDLL4 and mJAG1 tumours was independent of pericyte coverage. However, all interpretations of results solely depend on the pericyte markers used. Evaluation of pericyte coverage should not be judged based on use of a single marker only. The expression pattern of NG2, α-SMA, desmin, PDGFR-β and RGS5 are different in different models and may not correlate with maturation and quiescence of vessels (Enge et al. 2002; Fruttiger 2002; Bondjers et al. 2003; Gerhardt and Betsholtz 2003; Brey et al. 2004). Following this, it would be interesting to stain tumour sections with desmin, PDGFR-β or RGS pericyte marker to confirm the results. Immunostaining and QPCR for VEGFR2 and PDGF-BB are vital to determine their pattern and level of expression as the relationship between VEGF and PDGF has been implicated in the recruitment of pericytes in blood vessels (Greenberg and Cheresh 2009) although several other factors have also been implicated in pericyte recruitment to tumour vessel wall including sphingosine-1-phosphate, Ang-1, metalloproteinases (Chantrain, 2006) and Ephrin-B2 (Foo et al. 2006; Kuijper et al. 2007), therefore their expression should also be studied.

Therapeutic intervention- perfusion and hypoxia effects

Increased vessel perfusion induced by mDLL4 and mJAG1 was associated with enhanced tumour growth, thus blocking DLL4- and JAG1-Notch signalling with DBZ decreased vessel perfusion (Figure 4.10 II and III) and delayed tumour growth to that of control EV (Figure 4.7 and Figure 4.8). However, the high percentage of perfusion in bevacizumab mAb treated groups did not contribute to increased tumour growth. This discrepancy could be explained by the design of this experiment and analysis of results. Anti-VEGF blocks formation of new vessels and prunes the existing vessels, resulting in reduced vessel density (Figure 4.9 B). This experiment focused on the end point when the effects of mDLL4, mJAG1 and treatments were analysed after the mice were sacrificed. Data was presented as a percentage area of tumour vessels positive for tomato lectin in which those remaining vessels were resistant to bevacizumab treatment in the surviving tumours. Thus the remaining 10% of vessel left after pruning had higher DLL4 expression than in the controls, and perfusion per vessel was increased, but total of number of vessels decreased markedly. Nevertheless, the remaining well perfused vessels could then contribute to tumour re-growth and survival. Tumour vessel normalization with anti-VEGF therapy may present a window for optimum adjuvant drug delivery (Jain 2005; Dickson et al. 2007) in which anti-VEGF confers transient pruning of tumour vessels resulting in improved tumour perfusion (Myers et al. 2010), and this window time point in my experimental model is what I may have missed. For more accurate quantification of vessel perfusion, field images should be acquired randomly to reflect the heterogeneity of vessel types in different groups. Live imaging techniques and ultrasound assessment to monitor changes in the blood vessels over time should also be employed.

mDLL4 decreased CAIX expression compared to EV in U87 xenograft tumours (Figure 4.14 I and II). U87 mJAG1 tumours were more hypoxic compared to U87 mDLL4 tumours (Figure 4.14 III and IV). Even though they had more vessels, the vessels may be less effective but still perfused overall as a result of mismatched heterogenous distribution of perfused and poorly perfused vessels. CAIX expression depends on the HIF-1 pathway, which is up-regulated by hypoxia (Wykoff et al. 2000). Close examination of CAIX expression revealed perinecrotic staining (Figure 4.14 A) that associated with the frequency of CAIX expression in poorly vascularised tumours (Koukourakis et al. 2001). Notch signalling inhibition with DBZ rendered the tumours more hypoxic in EV and mDLL4 groups (Figure 4.14 IV and V). However, the elevated CAIX expression in mJAG1 tumours remained unchanged with DBZ treatment (Figure 4.14 III and VI). Blocking Notch signalling may on one hand reduce JAG1 expression, thus increase oxygenation of remaining vessels, but also decrease endogenous DLL4 expression and counteract this effect. mJAG1 mediated resistance to bevacizumab, such that there was no change in CAIX expression compared to untreated (Figure 4.14 III and IX). Increased CAIX expression was also observed in EV and mDLL4 co-treatment groups compared to untreated (Figure 4.14 X-XII). The sum effects of Notch inhibition and VEGF sequestering on tumour hypoxia in mJAG1 tumours are the same as in EV and mDLL4 tumour groups (Figure 4.14 X-XII).

What is important is the ultimate effect of mDLL4 and mJAG1 on tumour necrosis, in which both ligands significantly reduced tumour necrosis (mDLL4, ($P<0.01$) and mJAG1 ($P<0.05$) (Figure 4.15 I-III)**.** Treatment with DBZ produced non functional vessels which resulted in tumours starved from nutrients and oxygen (Figure 4.15 IV-VI). Bevacizumab treatment in the mDLL4 and mJAG1 groups had little effect on necrosis showing that notch signalling by either ligand protected the vessels from bevacizumab and the consequences of vessel

elimination. Treatment with DBZ and bevacizumab induced the greatest necrosis (Figure 4.15 X-XII) which shows bevacizumab has a substantial effect when used in combination and resistance to its effects is reversed.

Expression patterns of Notch ligands

In vitro, mDLL4 was expressed in the cytoplasm and exhibited nuclear positivity in a number of cells, as also observed by others (Martinez et al. 2009) (Figure 4.1 C) whereas mJAG1 displayed predominantly cytoplasmic expression (Figure 4.1 C). This pattern of expression was also observed in oral squamous carcinoma cells and clear cell renal carcinoma cells (Hijioka et al. 2010; Wu et al. 2011). DSL ligand endocytosis is known for further activation of Notch signalling (LaVoie and Selkoe 2003; Le Borgne et al. 2005; Hansson et al. 2010). Positive cytoplasmic staining for both mJAG1 and mDLL4 (Figure 4.1 C) indicate protein synthesis and possibly endocytosis of the ligands into the cells. The internalised ligands are either targeted for degradation by ubiquitin or recycled to the plasma membrane for activation (Ilagan and Kopan 2007). Localization of mDLL4 extracellular domain in the nucleus (Figure 4.1 C) may indicate nuclear translocation following endocytosis after Notch activation (Bland et al. 2003), suggesting a function for DLL4 in the nucleus, perhaps in modulating transcription. Interestingly, mJAG1 expression was mainly detected in the cytoplasm. This suggests that DLL4 and JAG1 may have different cellular roles, apart from initiating Notch signalling in the neighbouring cells, and may be involved in modulating different pathways involved in angiogenesis.

DLL4 was abundantly expressed in tumour vessels (Figure 4.11) (Mailhos et al. 2001; Noguera-Troise et al. 2006; Li et al. 2010; Schadler et al. 2010). Pruning of vessels by

bevacizumab in control EV tumours which are positive for DLL4 expression (Figure 4.11 I and VII) resulted in reduced DLL4-Notch signalling between endothelial cells and tumour cells (Noguera-Troise et al. 2006), thus down-regulating hHEY1 gene expression (Figure 4.6). The high level of DLL4 expression in the mDLL4 tumour vessels could be a result of positive regulation of Notch signalling by mDLL4 (Figure 4.11 II, V, VIII and XI) (Caolo et al. 2010). However, less DLL4 expression was detected in U87 mJAG1 vessels (Figure 4.11 II and III), suggesting that mDLL4 is a better inducer of Notch signalling than mJAG1, as supported by the *in vitro* work. DLL4 immunofluorescence stained what appeared to be tumour and/or stromal cells on the sections, and increased in DLL4 expression in cells surrounding tumour vessels in control tumours treated with bevacizumab was observed (Figure 4.11 VII). We was hypothesised that the DLL4 expression could be elicited by macrophages (Fung et al. 2007; Sonoshita et al. 2011) which are known to accumulate in hypoxic areas in tumours, particularly so in tumours treated with anti-VEGF therapy (Murdoch et al. 2004) (Figure 4.18). Furthermore, bevacizumab has been shown to induce inflammation in the human choroidal neovascularization membrane (Tatar et al. 2008). Therefore, increases in DLL4 expression seen in the vessels in the control tumours when treated with mAb may be caused by a positive feedback loop (Caolo et al. 2010) where DLL4 positive macrophages signal to the vessels and up-regulate DLL4. Neutrophils have also been shown to play a role in mediating resistance to anti-VEGF in tumours (Shojaei et al. 2007). As such, it is vital to follow up on macrophage and neutrophil infiltration assessment through CD68 and CD11b immunostaining respectively, which is ongoing.

DLL4 has been demonstrated to be induced by hypoxia through HIF-1α (Patel et al. 2005; Diez et al. 2007). The high level of DLL4 expression in EV and mJAG1 tumour vessels within the co-treatment group (Figure 4.11 X and XII) could be the result of increased

hypoxia due to formation of non-functional vessels by DBZ which were then pruned by bevacizumab creating a hypoxic tumour microenvironment. This might then trigger the surrounding mouse stromal cells to express murine VEGF and up-regulate the expression of DLL4 in tumours (Diez et al. 2007), although this could not be determined in this figure as the antibody used recognises both murine and human DLL4. The pattern of murine DLL4 and human DLL4 expression in the xenograft tumours should be assessed using a species specific antibody.

mJAG1 was found to be expressed weakly in tumour vessels (not obvious in merged figures) and increased in expression was observed in vessels and tumour cells or stroma in U87 mDLL4 tumours (Figure 4.12). Taken together, DLL4 appeared to the more predominant ligand in tumour vessels compared to mJAG1. The different levels of expression between DLL4 and JAG1 in the tumour vessels could affect signalling, as since the fine tuning and spatial expression of each ligand expression determines the outcomes of Notch signalling (Hofmann and Luisa Iruela-Arispe 2007; Benedito et al. 2009).

The Notch signalling pathway interacts with other pathways to influence patterning of vasculature, one such pathway is the VEGF pathway (Holderfield and Hughes 2008). VEGFR-2 is highly expressed at the angiogenic front and in response to the presence of VEGF, promotes the polarised expression of tip cell filopodia, facilitating endothelial cell guidance along the VEGF gradient (Gerhardt 2008). The VEGFR-1 is thought to modulate VEGFR-2 signalling in a role as a decoy receptor, sequestering VEGF from VEGFR-2 (Kappas et al. 2008). Apart from the involvement of VEGF-VEGFR2 pathway in angiogenesis, there is emerging evidence that VEGF-C is overexpressed in tumours (Alitalo et al. 2005) and VEGFR3 which up-regulated in tumour vessels is an important player in

angiogenesis via Notch signalling (Tammela et al. 2008). Benedito and colleagues (2009) have recently demonstrated that decreased expression of VEGFR3 in tip cells suppressed sprouting. Thus, JAG1-Notch signalling could promote tumour growth by increasing VEGFR3 expression in angiogenic front. On the other hand, DLL4-Notch signalling has been shown to decrease VEGFR3 expression in endothelial cells and blocking Notch signalling impaired sprouting (Tammela et al. 2008) suggesting that VEGFR3 could modulate the different effects of mDLL4 and mJAG1 on tumour vasculature. As such it would be interesting to examine the expression of VEGF, VEGFR2, VEGFC and VEGFR3 in these tumours. It is likely that these conflicting results of effects of notch signalling on VEGFR3, reflect differences between vessels and vascular beds.

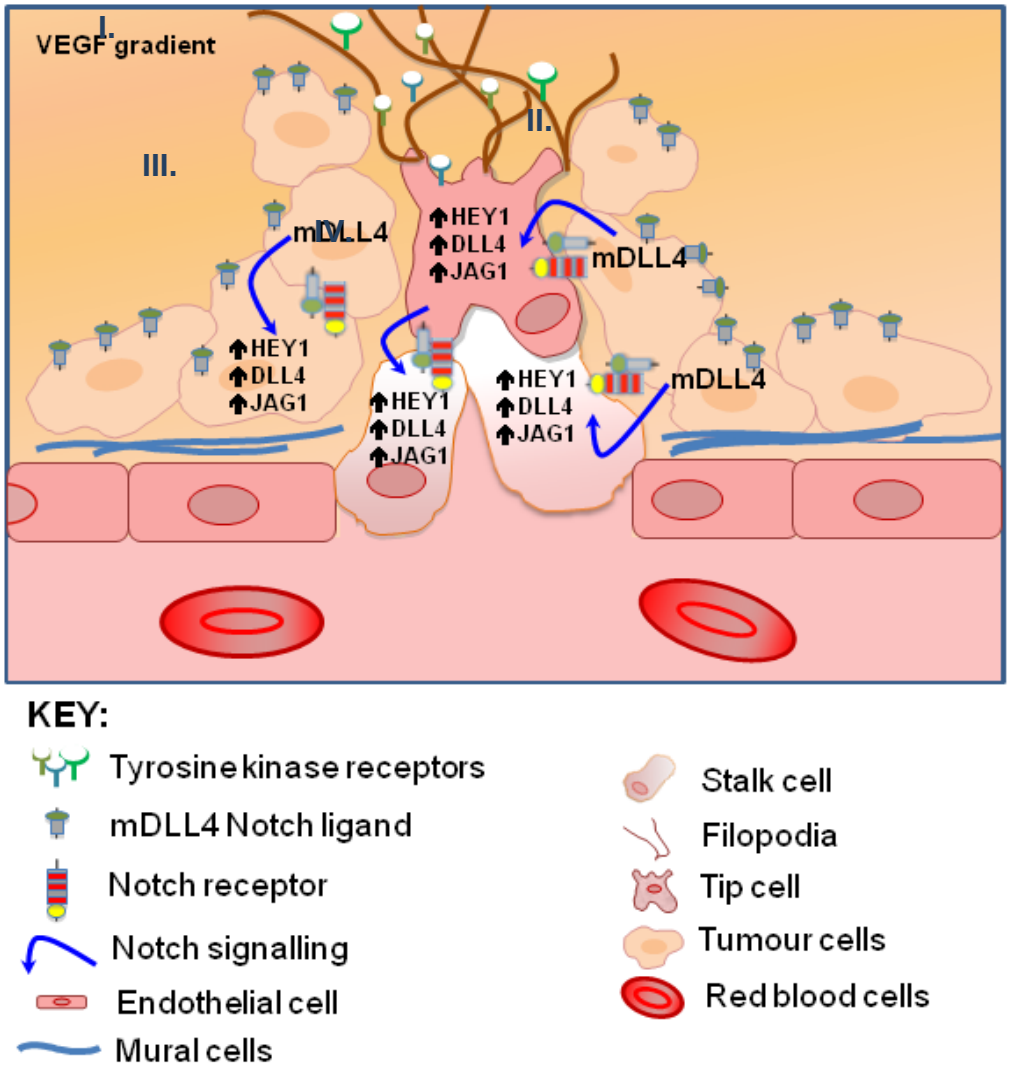
In order to understand the relationship between DLL4 and JAG1 in tumour angiogenesis, anti-DLL4 and anti-JAG1 blocking antibodies should be employed instead of using DBZ which is a general γ-secretase inhibitor which blocks all γ-secretase activities (Augelli-Szafran et al. ; Wong et al. 2004; Beel et al. 2009). Results from a preliminary experiment carried out using a specific anti-DLL4 monoclonal antibody blocking human and mouse DLL4 effectively delayed tumour growth in the U87 EV control tumour group ($P<0.01$) (Figure 4.16), possibly by disrupting functional angiogenesis, consistent with mounting literature (Noguera-Troise et al. 2006; Ridgway et al. 2006; Scehnet et al. 2007; Thurston et al. 2007; Hoey et al. 2009). Although the same effect was observed within mJAG1 over-expressing tumours when DLL4-Notch signalling was inhibited ($P<0.01$), the delay appears smaller in the mJAG1 group compared to EV group because the treatment was started late (Day 25) due to technical difficulties. Ideally, the anti-DLL4 treatment should have started at Day 15 when tumours reached the size of 150 mm^3. However, only 3 treatments of antibody were sufficient to give a statistically significant delay in tumour growth. This data nevertheless implies that DLL4 was

a dominant ligand over JAG1. To confirm this hypothesis the experiment should be repeated and the tumour sections stained for CD31 to see if specific blocking of DLL4-Notch signalling can affect vasculature phenotype.

JAG1 has been shown to antagonize DLL4-Notch signalling in mouse retinal model (Benedito et al. 2009). Therefore, blocking JAG1-Notch signalling in U87 mDLL4 xenograft tumours would be interesting to see if this effect affects tumour growth and vasculature formation.

To summarise the *in vivo* observations, the effects of mDLL4 and mJAG1 on U87 xenograft tumour growth are illustrated in Figure 4.17 and Figure 4.18 respectively.

A.



B.

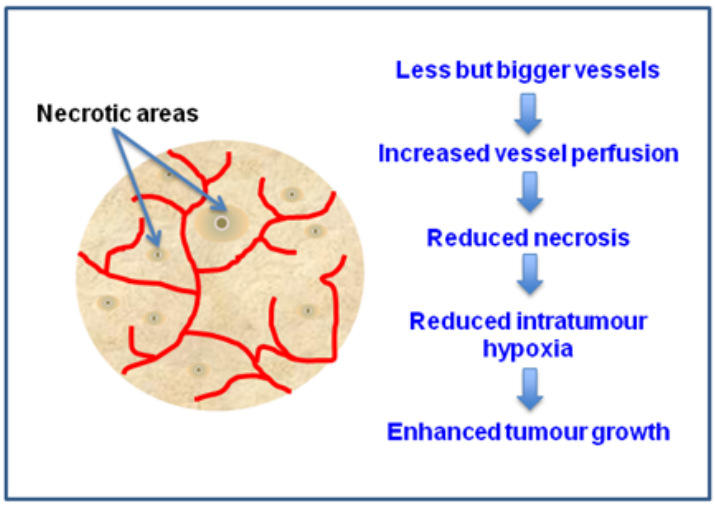


Figure 4.17: Cartoon demonstrating the effects of mDLL4 over-expression on U87 A) tumour vessels and B) tumour growth. Illustration by Dr. Esther Bridges.

A I) Angiogenic sprouting is aided by filopodia in response to VEGF gradient. mDLL4-Notch signalling is promoted in II) vessels and III) tumour by increasing DLL4, HEY1 and JAG1 expression. IV) Signalling from tip cell to stalk cell specifies cell fate contributing to B) development of fewer but well perfused blood vessels, decreased hypoxia and necrosis thus promoting tumour growth.

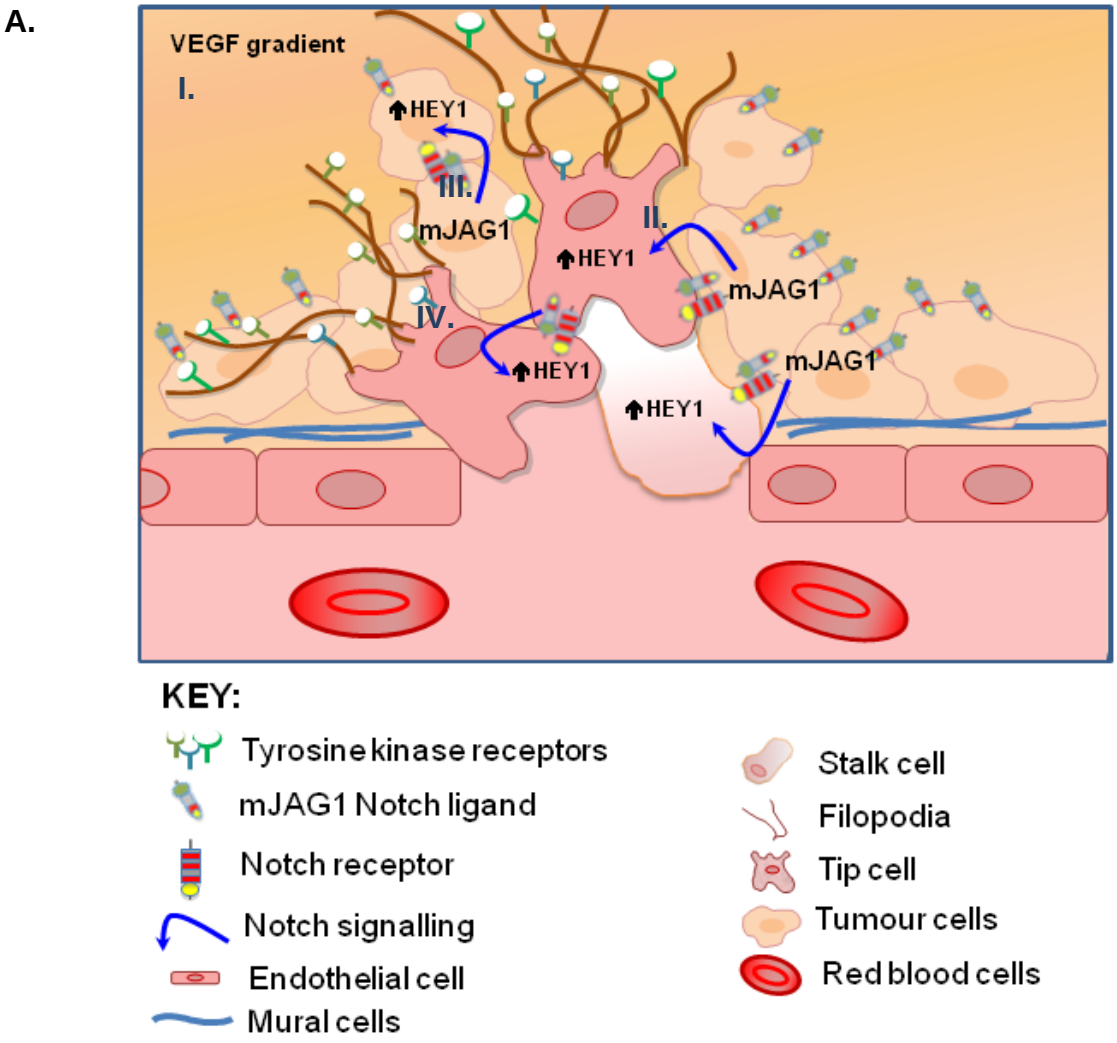


Figure 4.18: Cartoon demonstrating the effects of mJAG1 over-expression on U87 A) tumour vessels and B) tumour growth. Illustration by Dr. Esther Bridges.

A I) Angiogenic sprouting is aided by filopodia in response to VEGF gradient. mJAG1-Notch signalling is promoted in II) vessels and III) tumour by increasing HEY1 expression. IV) Tip cell- stalk cell signalling specifies cell fate contributing to B) development of fewer but well perfused blood vessels, decreased hypoxia and necrosis thus promoting tumour growth.

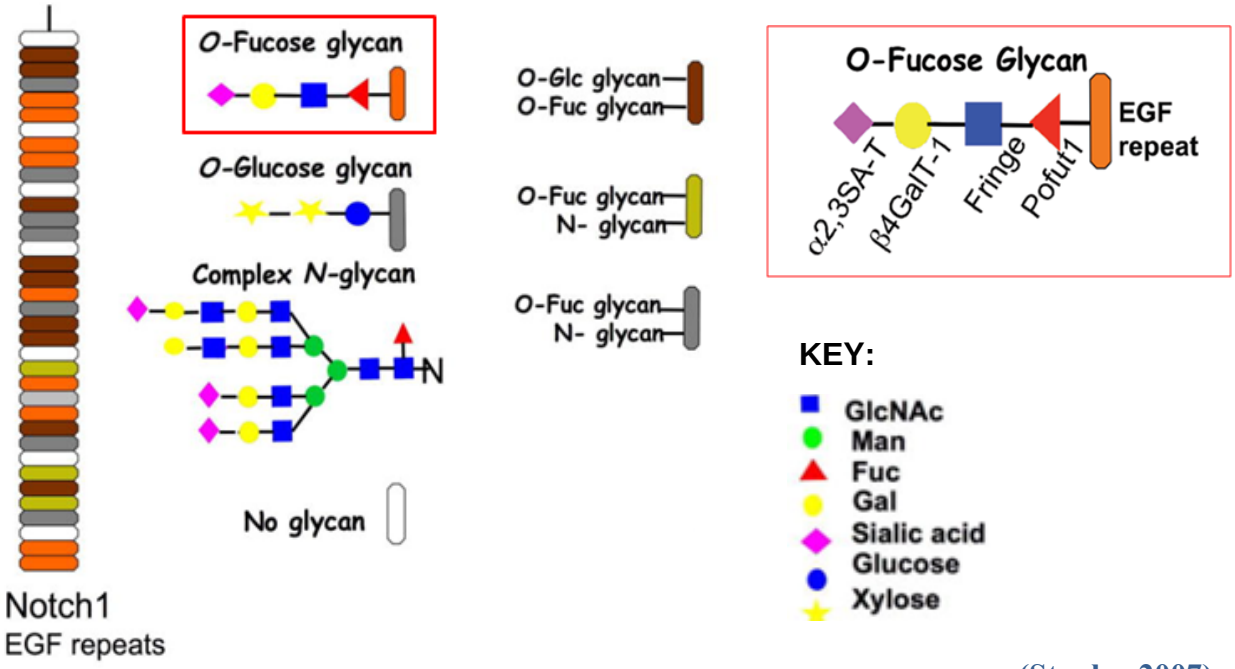
5 Expression profile of Fringe in endothelial cells and tumour

5.1 Introduction

The Notch receptor is a large single-pass transmembrane receptor protein with a large extracellular portion composed of multiple EGF-like repeats. The extracellular domains of Notch1 and Notch2 contain 36 tandem epidermal growth factor-like (EGF) repeats, whereas Notch3 and Notch4 each consists of 34 and 29 EGF-like repeats. EGF-like repeats are identified by the existence of six conserved cysteine residues which form three disulfide bonds. Many of the EGF repeats on the Notch1 receptor contain evolutionarily conserved consensus sites for two forms of glycosylation: *O*-fucose (C2XXXXS/TC3) and *O*-glucose (C1XSXPC2), where X represents any amino acid (Shao et al. 2003), while N-glycans are added at certain AsnXSer/Thr consensus sequons (Stanley 2007) (Figure 5.1).

The discovery of the *Drosophila* Fringe gene (FNG) which regulates Notch signalling by encoding a glycosyltransferase that transfers N-acetylglucosamine (GlcNAc) to fucose on Notch epidermal growth factor like (EGF) repeats (Moloney et al. 2000) has since sparked off interest in the roles of glycans in Notch signalling. In mammals, three Fringe homologues have been characterised: Manic Fringe (MFng), Lunatic Fringe (LFng) and Radical Fringe (RFng) (Johnston et al. 1997). Although secreted product of *Xenopus* gene LFng has been demonstrated to act as signalling molecules to induce mesodermal tissue formation in animal cap assays (Wu et al. 1996), it is reported to localise and act in the Golgi as a glycosyltransferase but not exert its effects outside of the cell in *Drosophila* (Munro and Freeman 2000). This highlights the different effect of spatial Fringe expression in veterbrates and invertebrates.

Although Notch receptor is the main target of Fringe action, Fringe may also elongate O-fucose on the EGF domain of Notch ligands (Panin et al. 2002). However, the effect of Fringe appears to be more critical in the signal receiving cell, whereas co-expression of Fringe and the Notch receptors exerted very little effect on Notch activation (Panin et al. 2002; Benedito et al. 2009). One possibility could be that glycosylation of Notch ligands by Fringe could influence the ability of cells to respond to ligands expressed by neighbouring cells through the autocrine inhibition of Notch activation by Notch ligands, termed as *cis*-inhibition. Fringe has been demonstrated to promote DLL-Notch signalling (Visan et al. 2006; Stanley and Guidos 2009; Yuan et al. 2011) compared to JAG- notch signalling (Kato et al. 2010; Marklund et al. 2010; Visan et al. 2010).



(Stanley 2007)

Figure 5.1: A schematic diagram of mouse Notch1 glycosylation sites.

The extracellular domain of Notch1 has 36 tandem EGF repeats with consensus sites known to be modified by O-fucose glycans, O-glucose glycans, and complex N-glycans. Fringe is a glycosyltransferase that transfers N-acetylglucosamine (GlcNAc) to fucose residue (▲) on the EGF repeat, then the subsequent addition of a galactose (●) and sialic acid (◆) will occur to form a tetrasaccharide glycan.

As the majority of studies have focused on the role of Fringe and Notch signalling in development, very little is known about the functional role of Fringe in the regulation of tumour angiogenesis. This chapter seeks to elucidate the relationship between Fringe and DLL4- and JAG1- Notch signalling in angiogenic tumours, firstly by studying the expression profile of Fringe in endothelial cells and then in tumour samples. A panel of tumour cell lines and endothelial cell lines were screened for the relative expression of MFng and LFng at the transcript level. Eighteen cases of Clear Cell Renal Cell Carcinoma (CCRCC) clinical samples were studied for the expression on MFng and LFng at the transcript level.

Immunofluorescence was carried out to asses if MFng co-localises with the vessels, associated with the high expression in endothelial cells.

5.2 MFng is highly expressed in endothelial cells

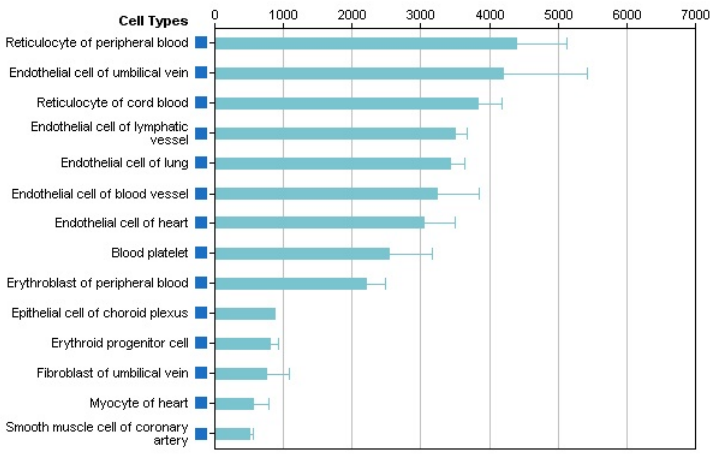
Due to limited information on Fringe and tumour angiogenesis, online cancer microarray compendia were utilised to assess and predict Fringe expression in tumours. A brief interrogation on NextBio and Oncomine, which are online repositories for curated microarray data, predicted abundant MFng expression in the endothelial cells in relative to other cell types in the cardiovascular system (Figure 5.2 A). LFng and RFng were also expressed in the endothelial cells, however their respective expression distribution was not relatively higher in the endothelial cells but rather ubiquitous in all cell types in the cardiovascular system (Figure 5.2 B and C).

To validate the online database data, a panel of nine cancer cell lines and four endothelial cell lines including HUVEC and HMEC-1 were subject to preliminary screening for expression of MFng, LFng and RFng using QPCR. The panel of cell lines included breast cancer cell lines (MDA231,MCF7 and T47D), cervical cancer cell line (HeLa), colorectal cancer cell lines (HCT116, DLD-1and LS174T), glioblastoma cell line (U87), renal cancer cell line (7860) and endothelial cell lines (HBEC-1, EAHY296, HUVEC and HMEC-1).

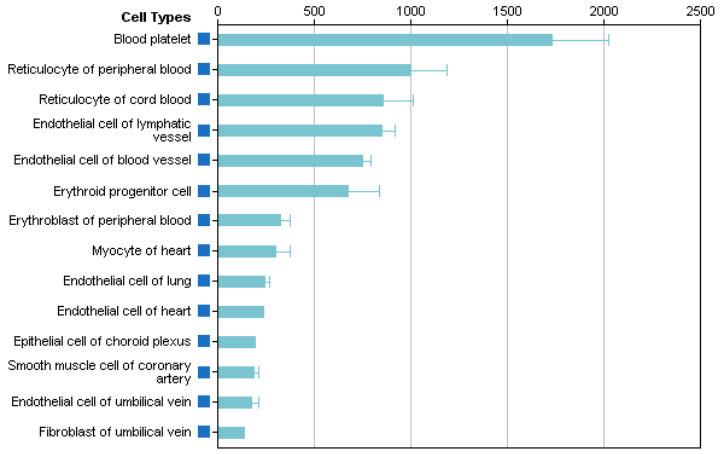
A standard curve was generated by plotting C_t values against the log-transformed concentrations of serial five-fold dilutions of HUVEC cDNA to obtain the relative quantity of Manic Fringe and Lunatic Fringe expression in each cell line. The expression of MFng was relatively higher in the endothelial cell lines compared to the cancer cell lines screened

(Figure 5.3 A). However, relative LFng expression was higher in cancer cell lines, especially in breast adenocarcinoma cell lines compared to the endothelial cell lines (Figure 5.3 B). MFng was most highly expressed in HUVEC and HMEC-1 followed by LFng and RFng (Figure 5.4).

A. MFng



B. LFng



C. RFng

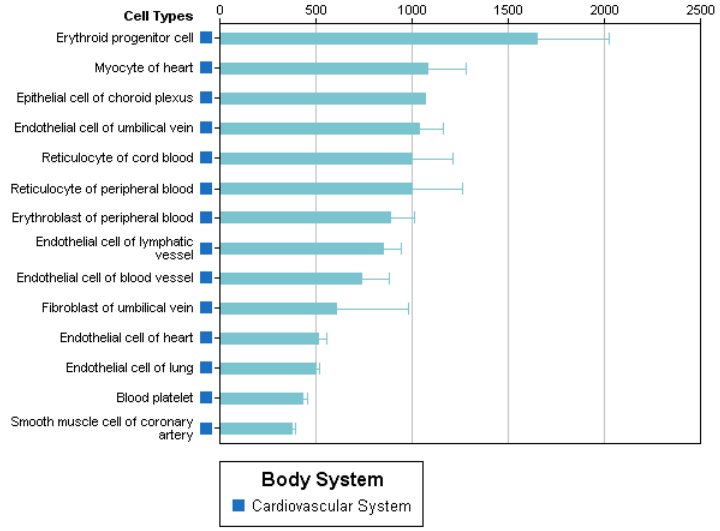
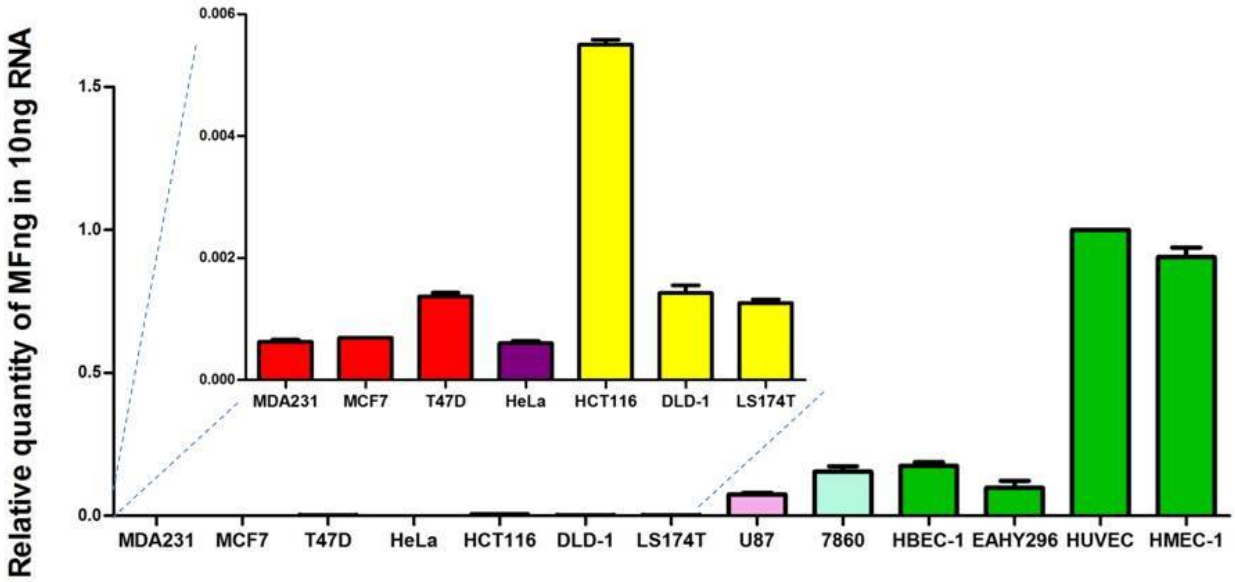


Figure 5.2: Relative expression profile of A) MFng, B) LFng and C) RFng in different cell types in the cardiovascular system as predicted by NextBio.

The NextBio analysis summary contains relative gene expression levels in a given cell type compared to the median expression across all body cell types analysed. The median expression is treated as the normal/control expression level. This study is an accumulation of samples from numerous studies using the Affymetrix Human Genome U133 Plus2 or U133A platforms. Signals from common probesets in these platforms are normalised using quantile normalisation.

A.



B.

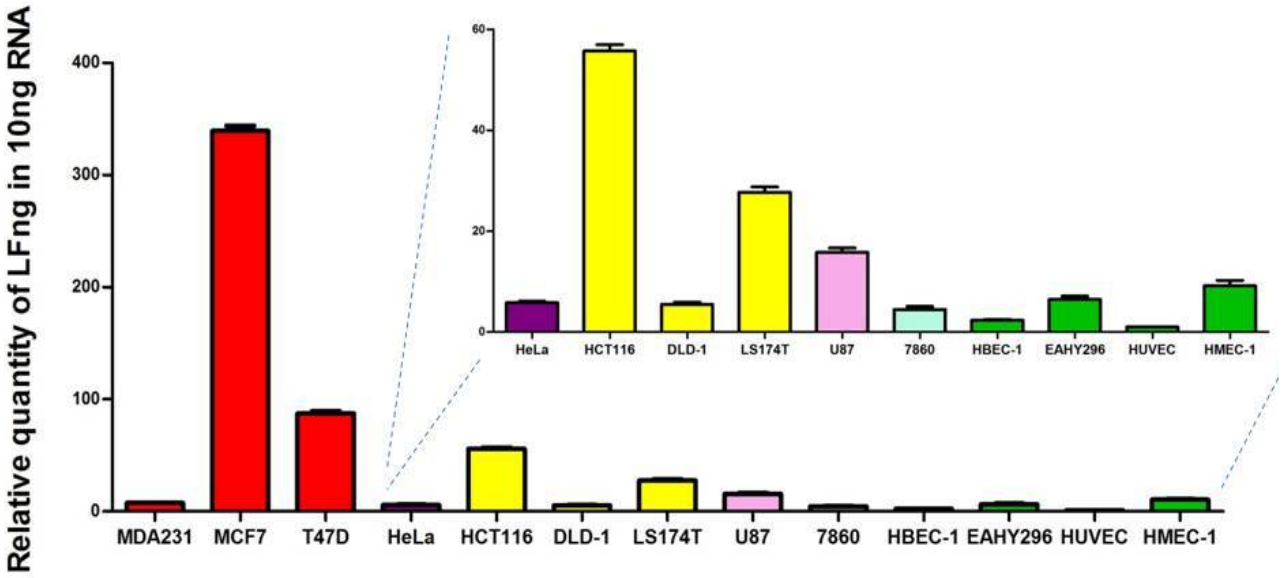


Figure 5.3: Relative quantity of A) MFng and B) LFng in 10ng RNA in a panel of tumour and endothelial cell lines compared to HUVEC.

(A and B) Breast cancer cell lines (red), cervical cancer cell line (purple), colorectal cancer cell lines (yellow), glioblastoma cell line (pink), renal cancer cell line (light blue) and endothelial cell lines (green). Error bars represent SEM. Figure is a representative of (n=1) from a preliminary experiment.

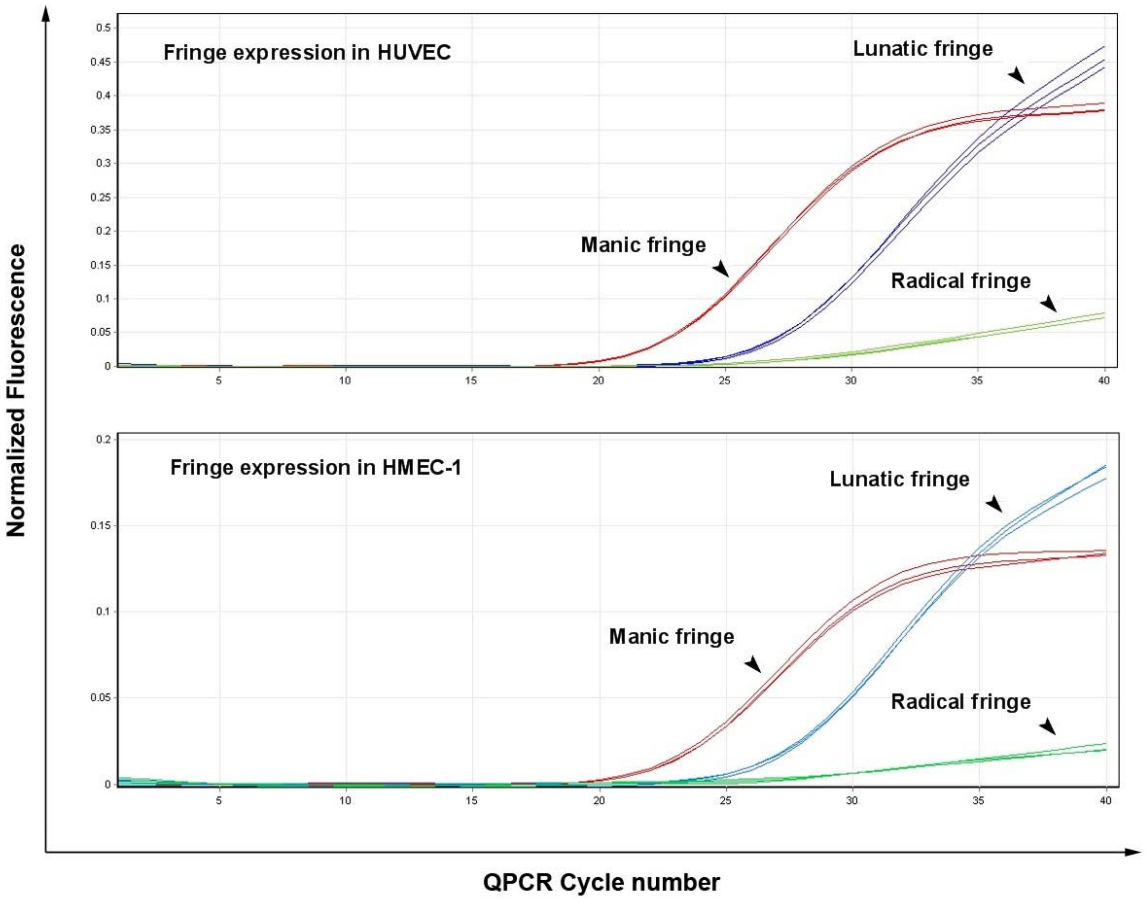


Figure 5.4: Fringe expression profile in HUVEC and HMEC-1 cells.

A representative QPCR figure is shown (n=3 independent experiments).

5.2.1 Notch activation did not affect MFng, LFng and RFng gene expression in HMEC-1

To determine if Notch activation could affect the expression of MFng, LFng and RFng at the transcript level, HMEC-1 cells were plated onto BSA-, rhDLL4- or rrJAG1 coated plates for 8hr, a time point when Notch activation peaks (as shown by the peak induction of HEY1 and HEY2 gene expression in Chapter 3), and subjected to QPCR. Notch stimulation did not have

any effect on Fringe expression, also indicating that they are not Notch downstream genes (Figure 5.5).

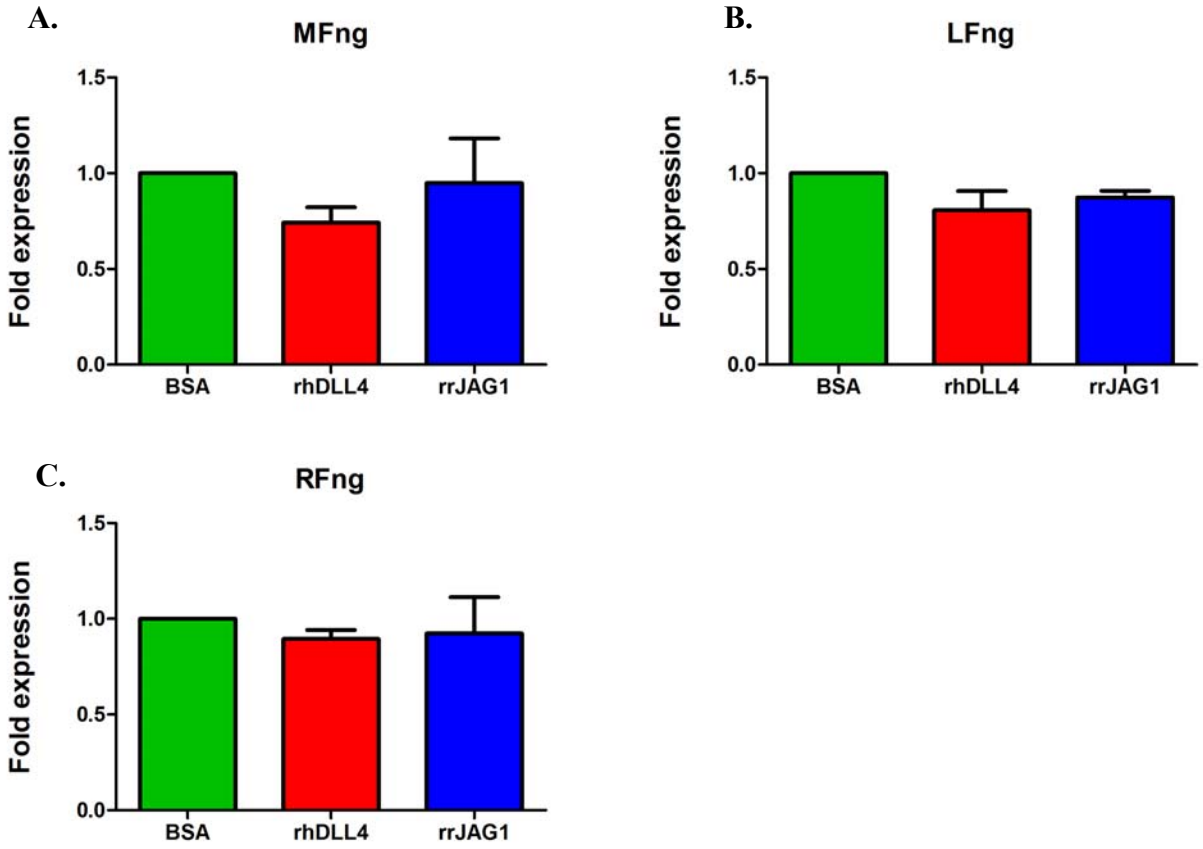


Figure 5.5: QPCR showing transcript level of A) MFng, B) LFng, and C) RFng in HMEC-1 after 8hr of Notch stimulation on BSA, rhDLL4- and rrJAG1 coated plate.

Statistical test: ANOVA, Bonferroni, n=3 independent experiments. Bars represent SEM.

5.3 MFng is expressed in angiogenic tumours

Preliminary data-mining on Oncomine revealed MFng, JAG1 and CD31 over-expression in Clear Cell Renal Cell Carcinoma (CCRCC) compared to normal renal tissues in Gumz_Renal Paired Studies, comprising of 10 clear cell renal cell carcinoma samples, as well as 10 patient-matched normal tissue samples which were analysed on Affymetrix U133A microarray

(Figure 5.6). However, LFng and RFng expression in CCRCC remained unchanged compared to normal renal tissues (Figure 5.6). QPCR was carried out to study the MFng and LFng gene expression and their correlation with DLL4 and JAG1 in 18 CCRCC tumour samples versus normal renal cortex. Up-regulation of MFng ($P<0.05$), LFng ($P<0.01$) and CD31 ($P<0.01$) gene expression were observed in CCRCC tumours compared to normal renal tissue (Figure 5.7). DLL4 and JAG1 expression correlated with CD31 expression ($P<0.01$) in CCRCC tumours (Figure 5.8 A and B). Both DLL4 and JAG1 gene expression correlated with each other in the tumours ($P<0.01$) (Figure 5.9 A). However, there was no significant correlation between the expression of MFng and LFng to that of the vessel marker, PECAM/CD31 (Figure 5.8 C and D) or DLL4 or JAG1 expression (Figure 5.9 B, C, D, E, F) in the CCRCC tumours.

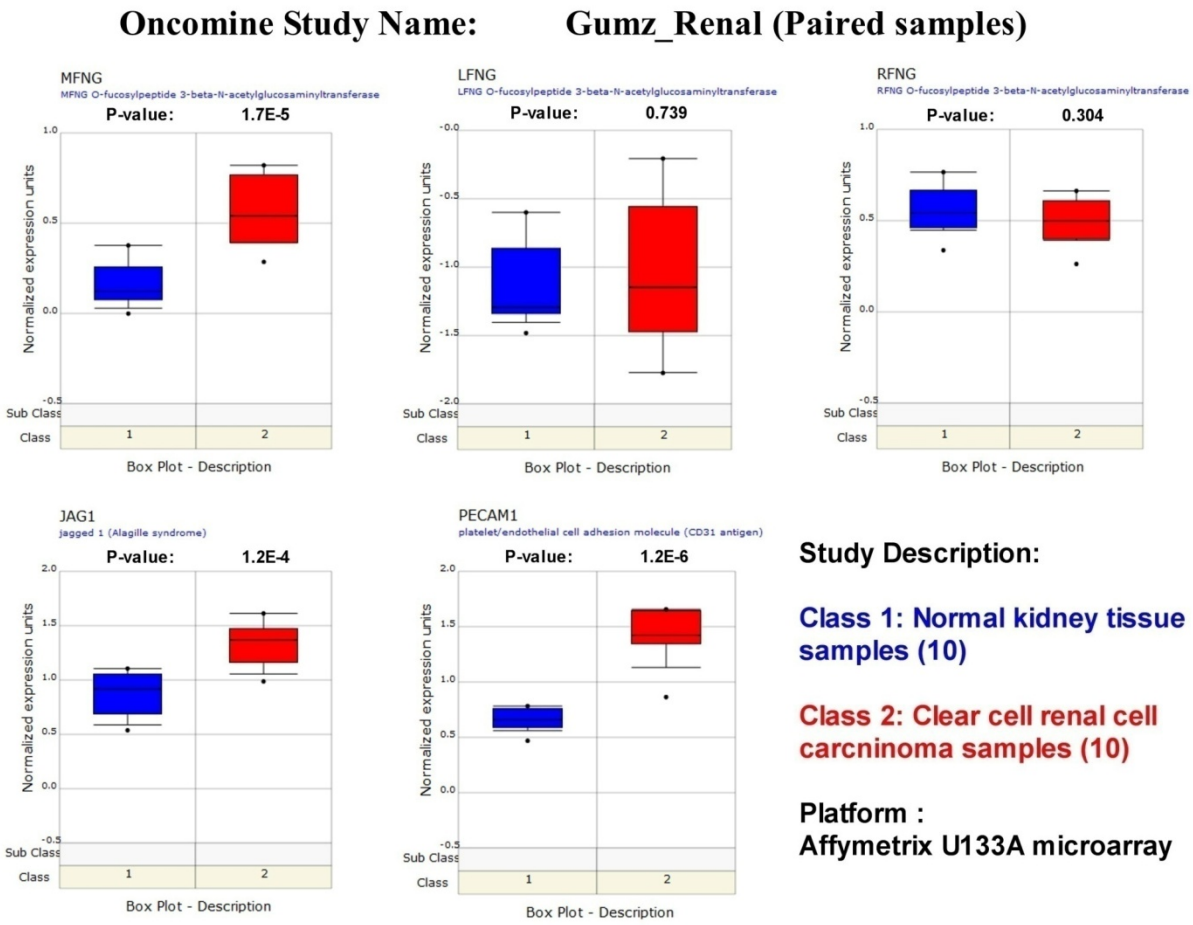


Figure 5.6: Expression profile of Manic Fringe (MFng), Lunatic Fringe (LFng) and Radical Fringe (RFng), JAG1 and PECAM1 in paired renal studies clear normal versus cell renal cell carcinoma (CCRCC), as compiled by Oncomine.

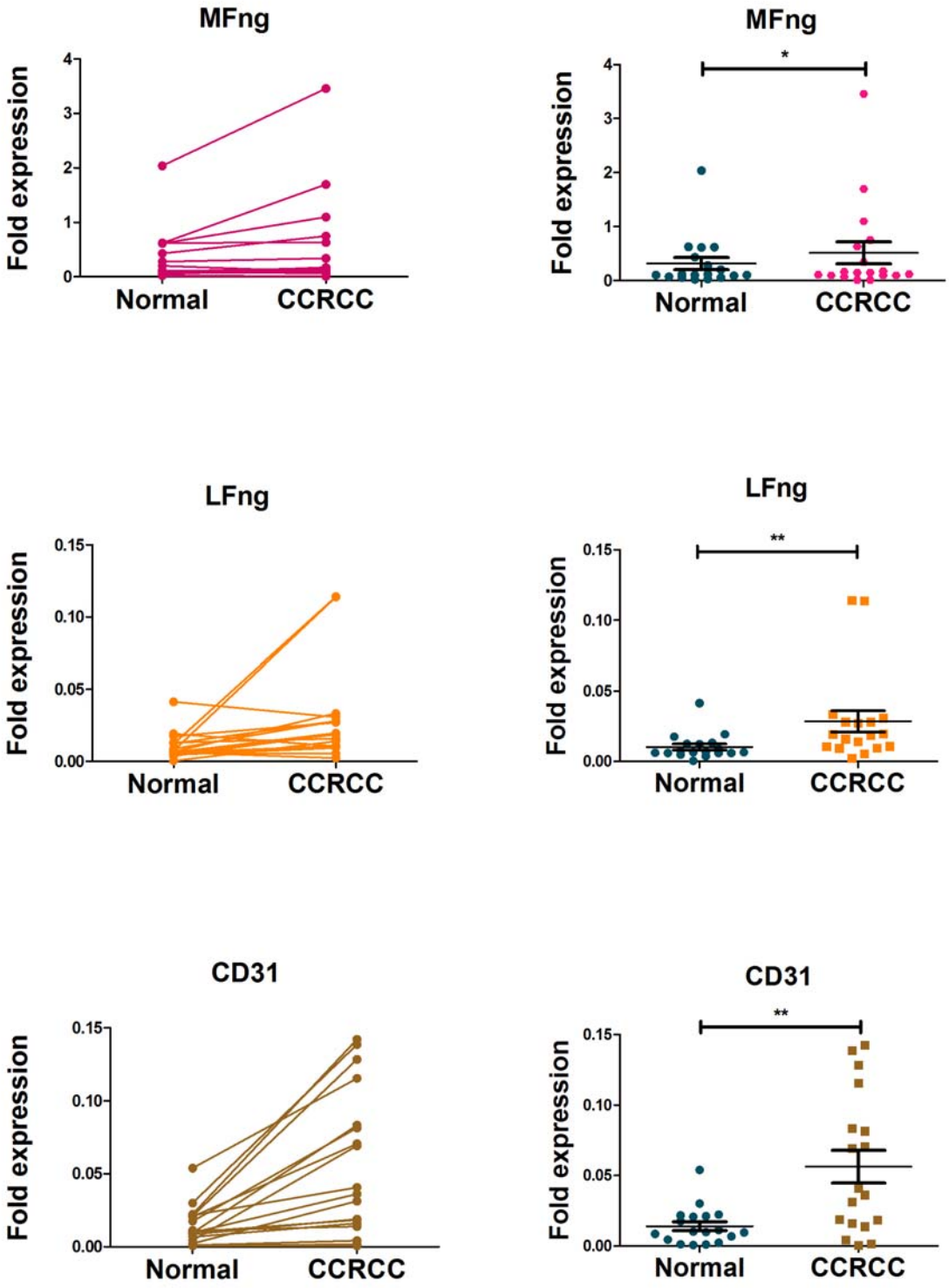


Figure 5.7: QPCR showing expression of A) MFng, B) LFng and C) CD31 in paired normal renal and CCRCC tumours.

RNA from all clinical samples was obtained from Dr. Robert McCormick (Oxford). Statistical test: Wilcoxon matched pairs test, *P<0.05, **P<0.01 (n=18 pairs of CCRCC and normal renal tumours). Bars represent SEM.

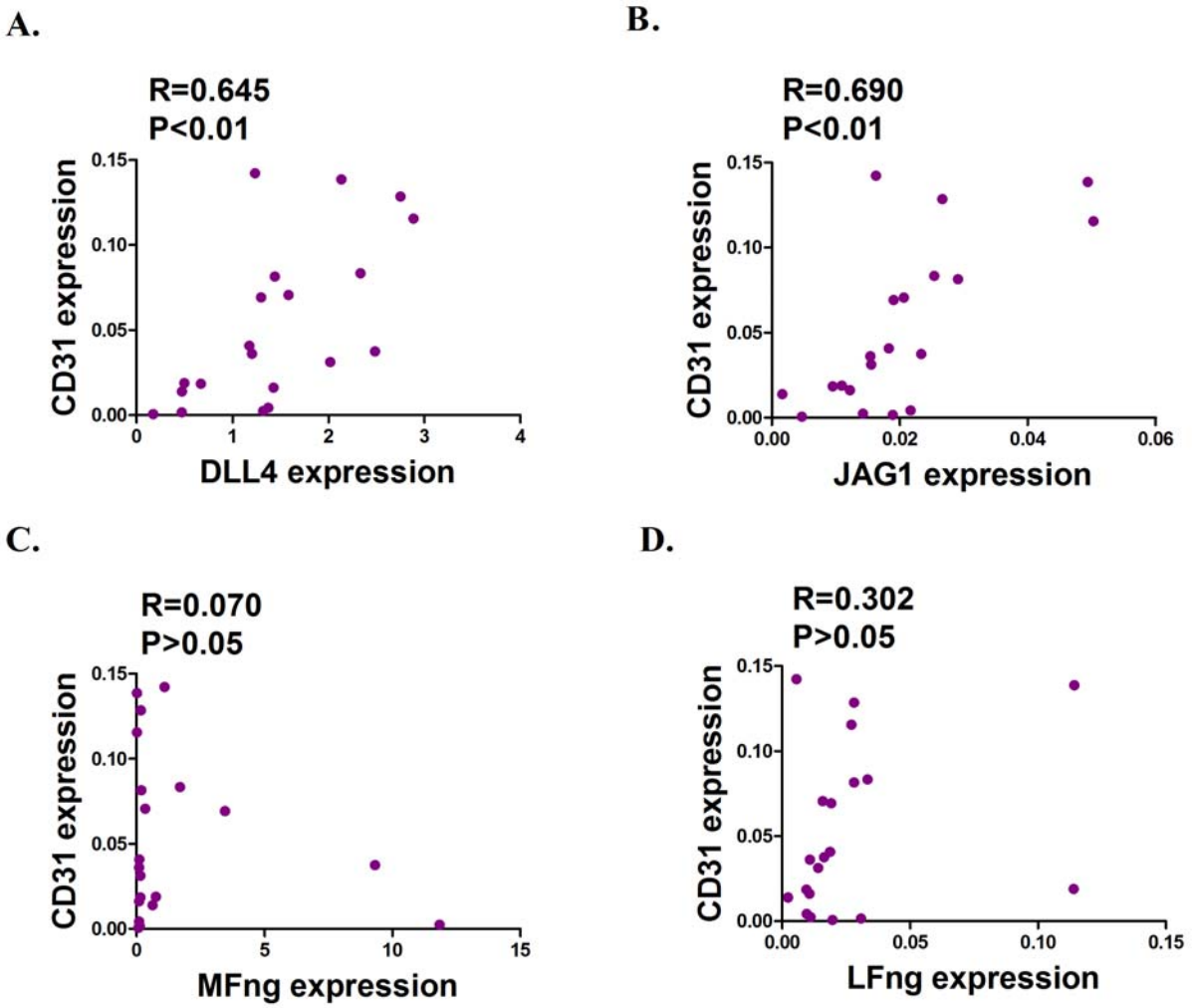


Figure 5.8: QPCR showing correlation of A) DLL4, B) JAG1, C) MFng and D) LFng with CD31 expression in CCRCC tumours.

Statistical test: Spearman nonparametric correlation coefficient (R) , *P<0.05, **P<0.01 (n=18 pairs of CCRCC and normal renal tumours)

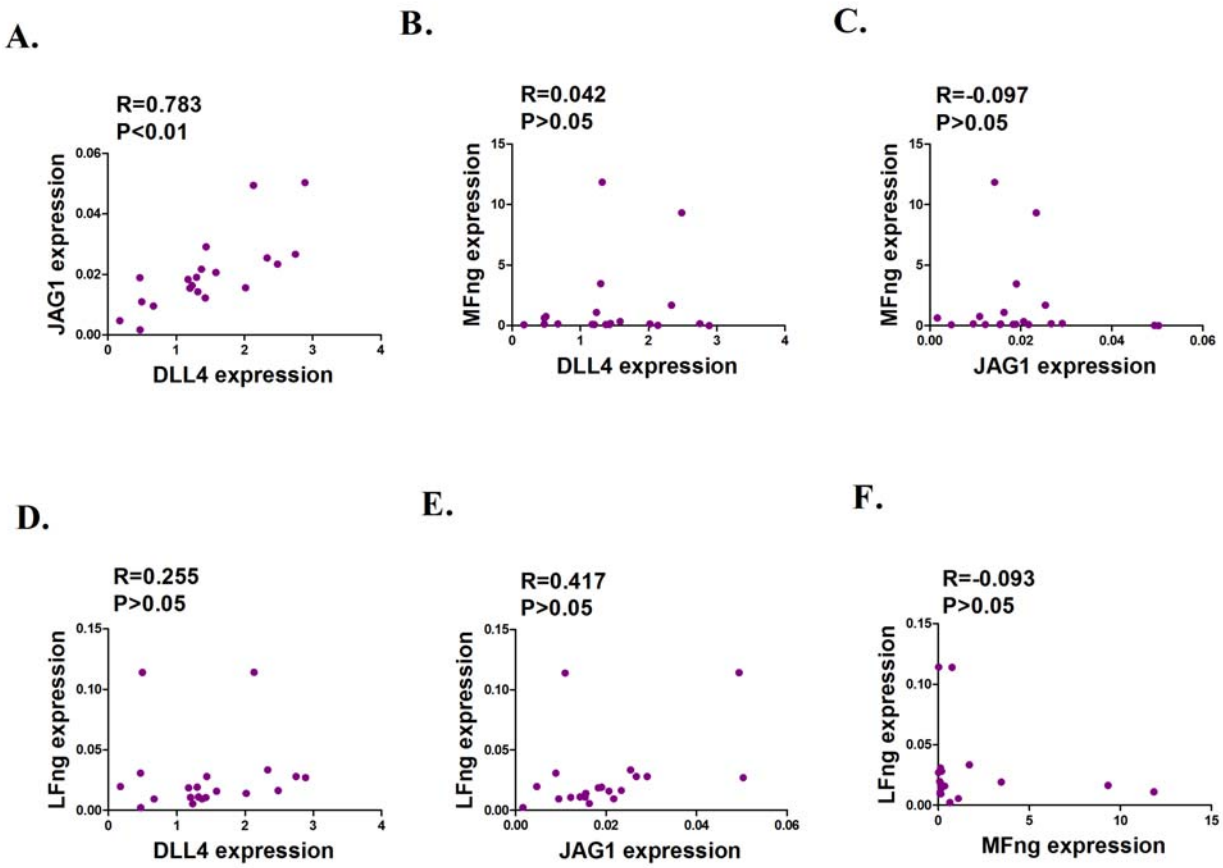


Figure 5.9: QPCR showing correlation of A) JAG1 and DLL4, B) MFng and DLL4, C) MFng and JAG1, D) LFng and DLL4, E) LFng and JAG1 and F) LFng and MFng expression in CCRCC tumours.

Statistical test: Spearman nonparametric correlation coefficient (R) , *P<0.05, **P<0.01 (n=18 pairs of CCRCC and normal renal tumours)

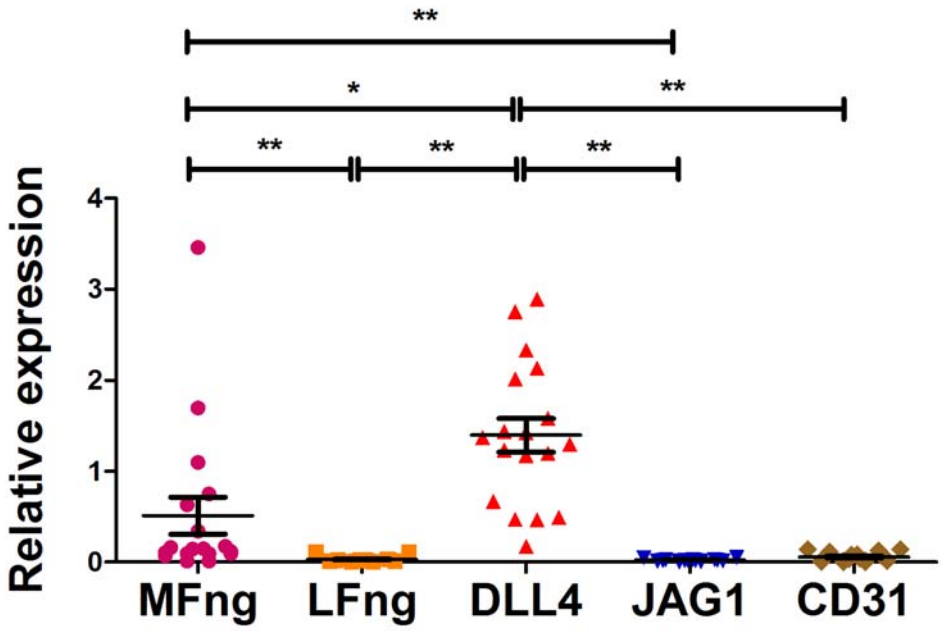


Figure 5.10: QPCR showing relative expression of MFng, LFng, DLL4, JAG1 and CD31 normalised to β- ACTIN in CCRCC tumours.

Statistical test: Kruskal-Wallis, Dunns post-test, *P<0.05, **P<0.01 (n=18 pairs of CCRCC and normal renal tumours). Bars represent SEM.

DLL4 expression was relatively higher compared to MFng, LFng and CD31expression in the CCRCC tumours (Figure 5.10). MFng expression was relatively higher compared to LFng at the transcript level in the tumours (Figure 5.10).

5.4 Fringe expression pattern in CCRCC tumours

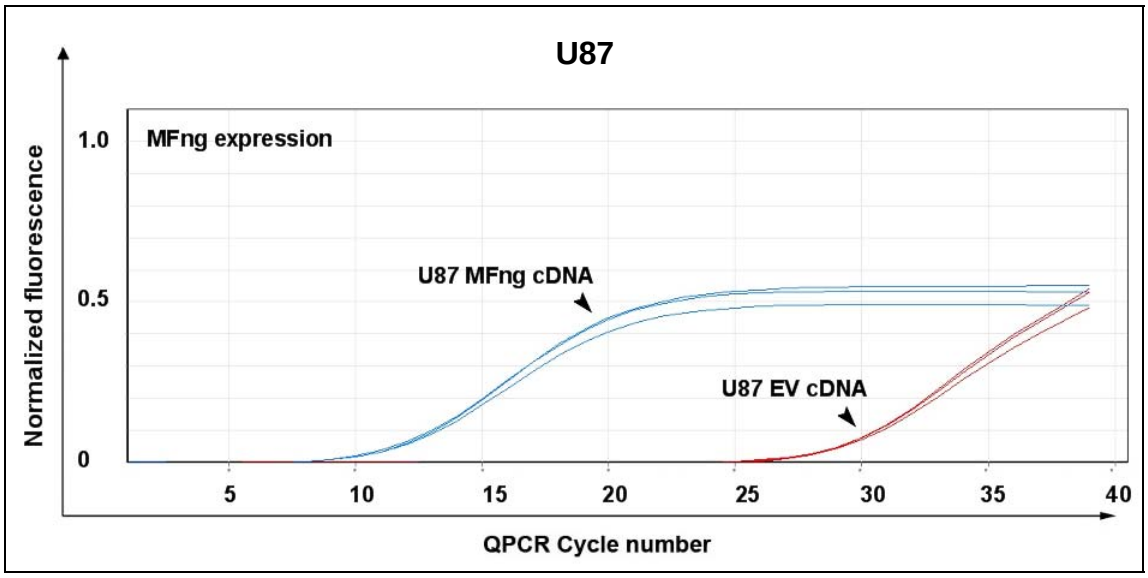
Following prediction of MFng expression in endothelial cells and angiogenic tumours from microarray compendia (Figure 5.2 and Figure 5.6), validated by QPCR data (Figure 5.3 and Figure 5.4), immunostaining was utilised to determine the location of Fringe expression pattern on CCRCC tumours using a Manic Fringe commercial antibody. Due to limited

availability of validated antibody specific for MFng in the market at the time I commenced on my project, I started off by looking into the literature for sources of antibody for immunostaining and western blotting. Although 3 commercial MFng antibodies were purchased, due to time constraint, I only managed to optimise immunostaining using one of the MFng antibodies and this antibody was raised against peptide mapping at the C-terminus of Manic Fringe, which is highly homologous to LFng and RFng. Ideally, I would like to optimise each antibody for staining and this work is still on-going.

5.4.1 Validation of Fringe antibody

MFng expression, being the most prevalent Fringe homolog in endothelial cells was manipulated in two cell lines, one with lower MFng expression (U87) (Figure 5.3 A) to over-express MFng (U87 MFng) and the other with abundant MFng expression (HMEC-1) (Figure 5.3 A) to suppress its expression (HMEC-1 shMFng), with their respective Empty Vector control (U87 EV) and Scrambled control (HMEC-1 shSCR). U87 MFng was a kind gift from Dr. Ji-Liang Li, while HMEC-1 shMFng was generated as described in Materials and Methodology. QPCR revealed up-regulation of MFng in U87 MFng compared to U87 EV and down-regulation of MFng in HMEC-1 shMFng indicating successful transduction (Figure 5.11).

A.



B.

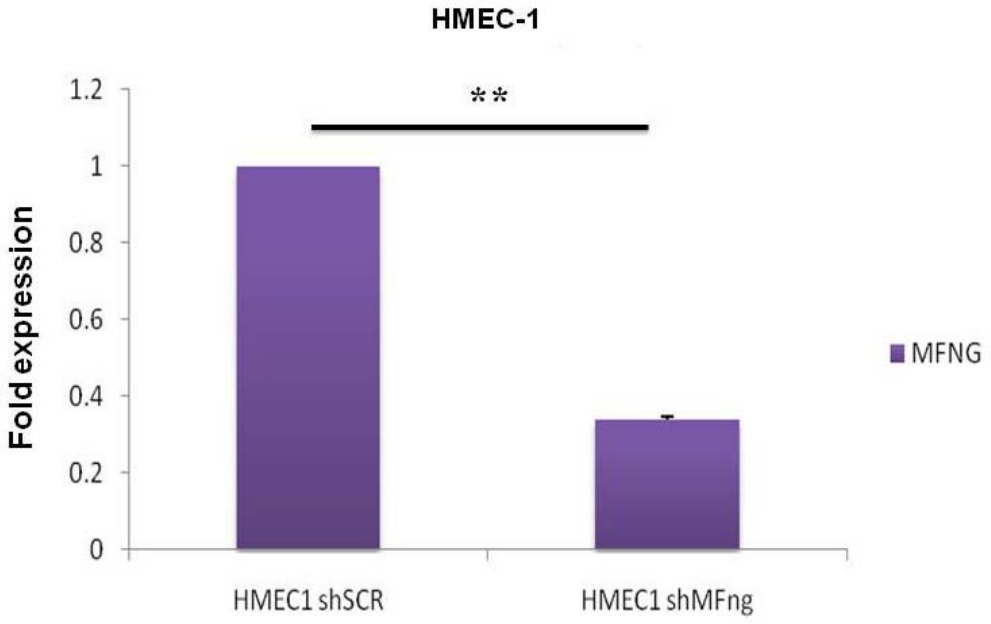


Figure 5.11: QPCR confirming A) MFng over-expression in U87 and B) stable knockdown in HMEC-1.

A) A representative figure from n=3 independent experiments. B) Bars represent SEM from three independent experiments. Statistical test: Student's t-test, **P<0.01, n=3 independent experiments. Bars represent SEM.

In order to validate the binding specificities and the ability to stain for immunofluorescence for colocalization analysis, staining was done on cytospin cells as described in Materials and Methodology. Increased intensity of Fringe expression was observed in U87 MFng compared to U87 EV cells (Figure 5.12 A) while suppression of MFng expression decreased Fringe expression intensity in HMEC-1 shMFng compared to HMEC-1 shSCR (Figure 5.12 B). A similar pattern of expression was observed in (formalin-fixed, paraffin-embedded) FFPE sections of the over-expressing and knockdown cell lines (Figure 5.13 A and B).

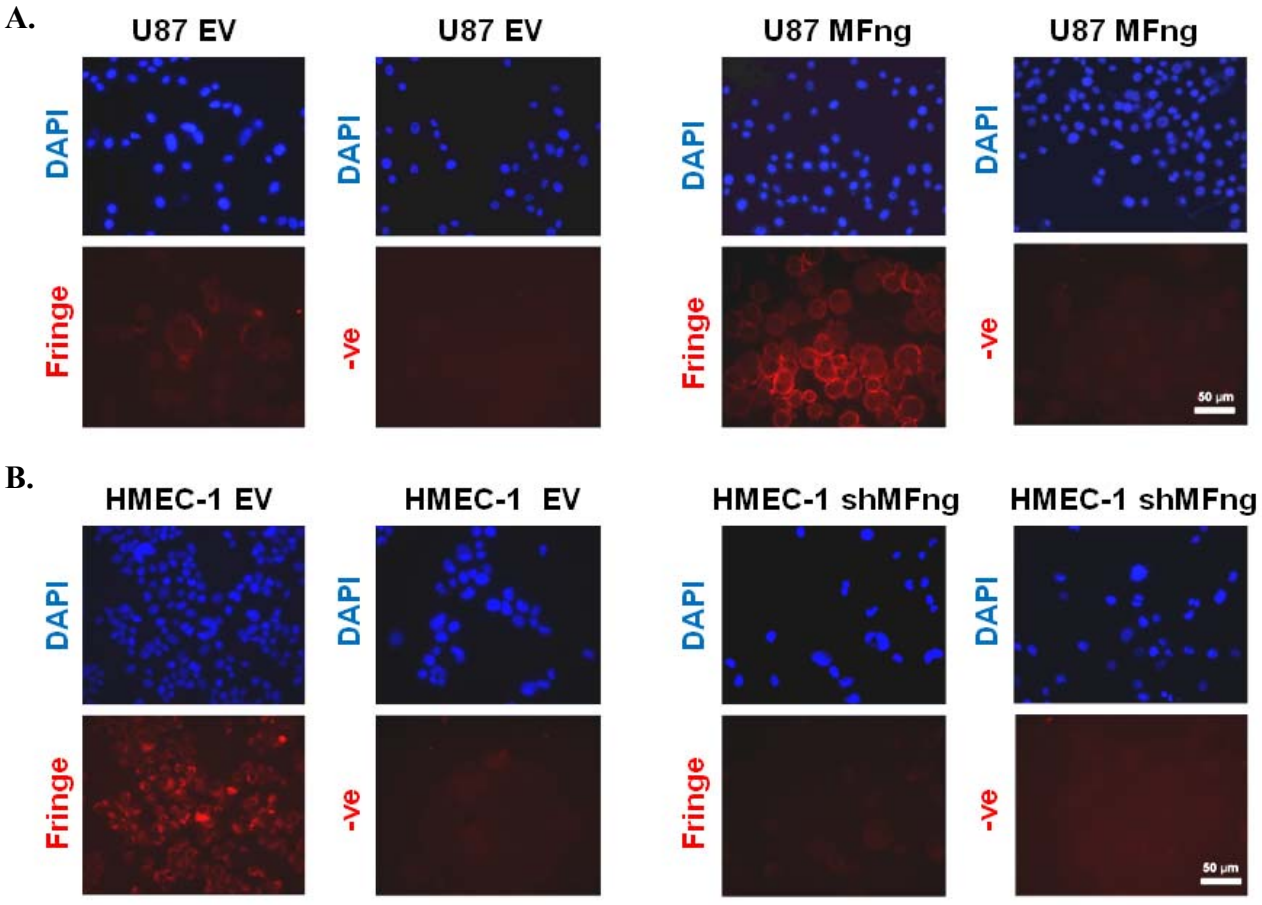


Figure 5.12: Validation of Fringe antibody on A) U87 and B) HMEC-1 cytospun cells.

Negative control staining (-ve) was performed by omission of the primary antibody. A representative figure is shown (n= 2 independent experiments).

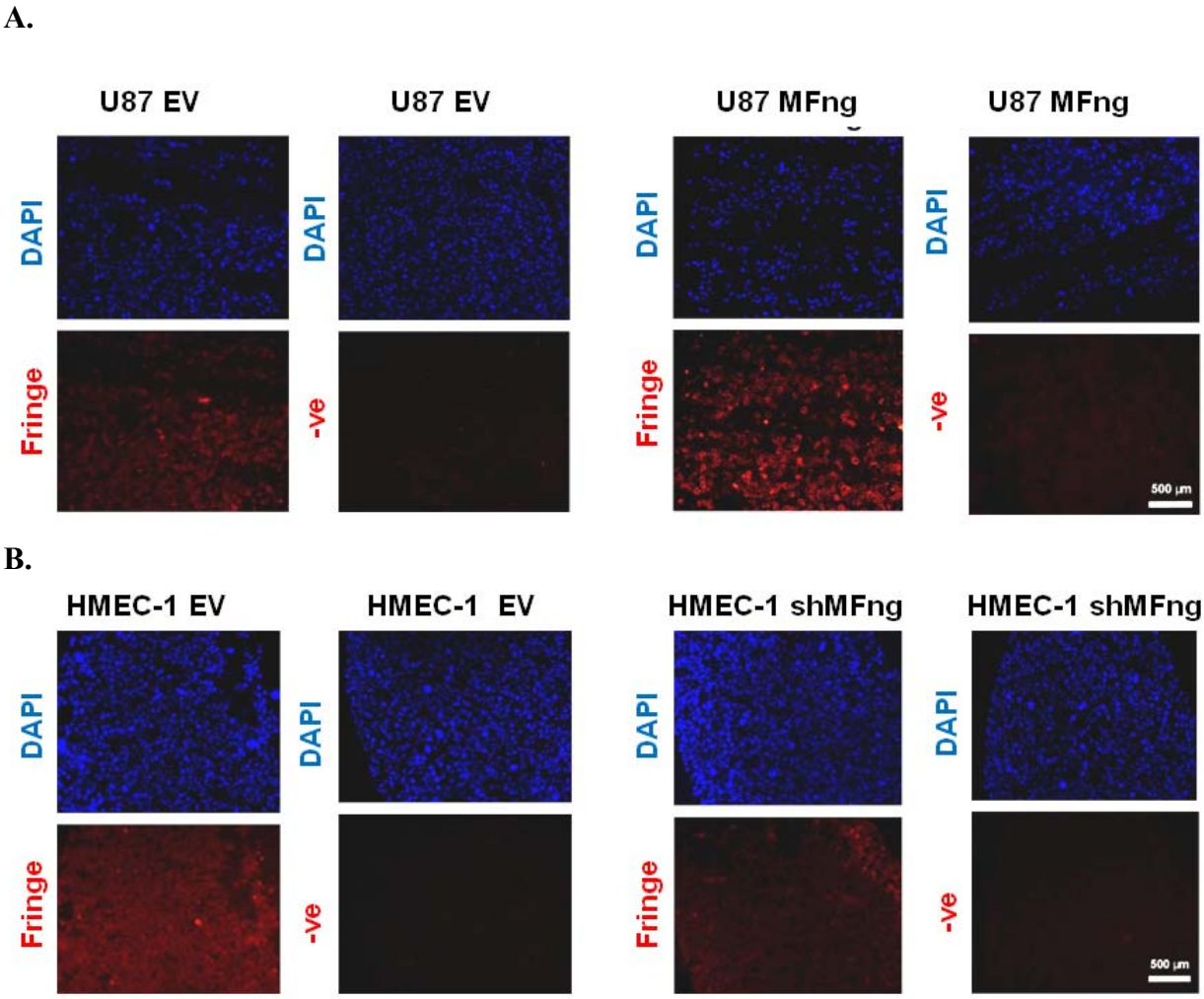


Figure 5.13: Validation of Fringe antibody on A) U87 and B) HMEC-1 formalin-fixed paraffin-embedded (FFPE) cells.

Negative control staining (-ve) was performed by omission of the primary antibody. A representative figure is shown (n= 2 independent experiments).

5.4.2 Fringe was abundantly expressed in CCRCC tumour vasculature

To assess and visualise the expression of Fringe in our renal series. Preliminary immunofluorescent staining was then performed on four clinical CCRCC tumour sections, selected based on their relative MFng gene expression at the transcript level to represent

high, medium and low Fringe expression in tumours (Table 5.1). Fringe was robustly expressed in tumour vessels (Figure 5.14), its expression correlated with the MFng relative expression in the tumours (Table 5.1).

Table 5.1: MFng and LFng gene expression relative to β-actin in CCRCC clinical tumours

Relative gene expression \ Tumour code	JY60	JY66	JY250	JY80
MFng	3.458	0.063	0.012	0.09
LFng	0.019	0.002	0.027	0.01

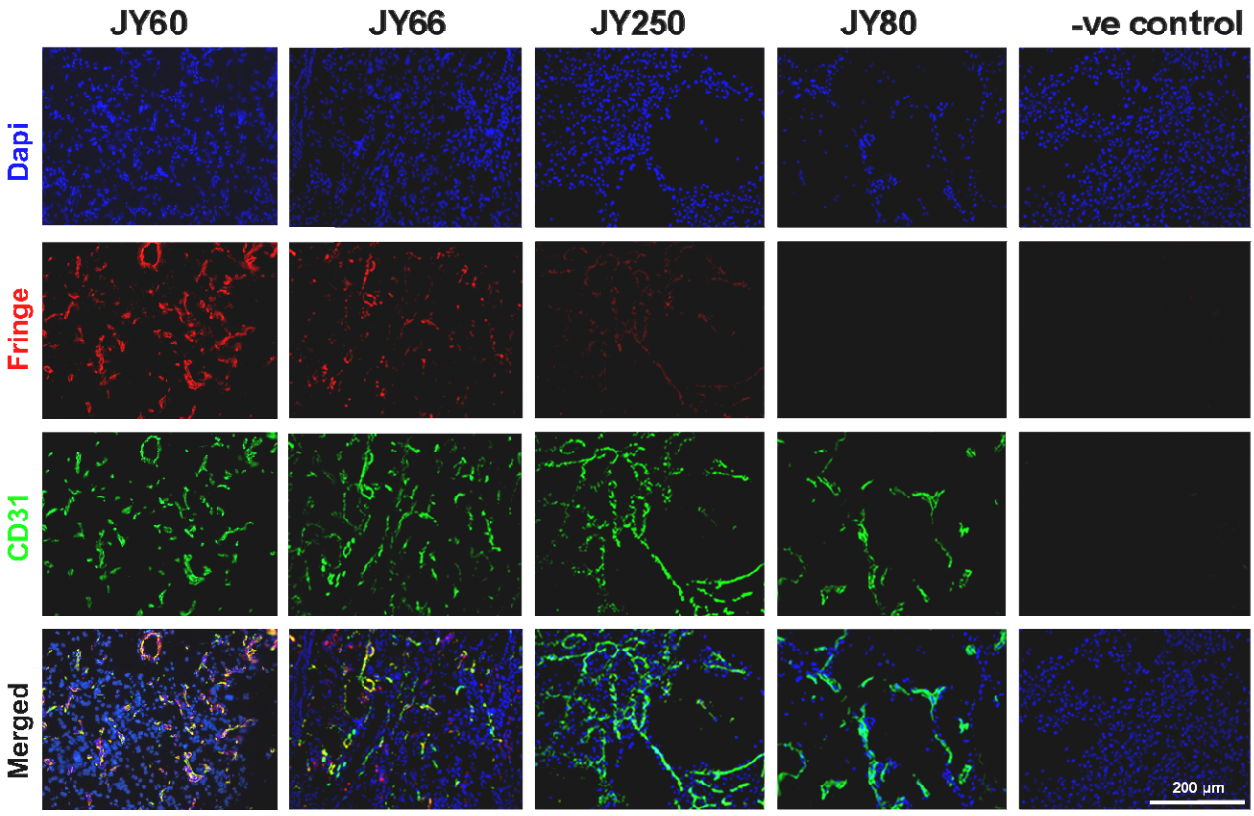


Figure 5.14: Fringe (red) and CD31 (green) immunofluorescence on selected CCRCC tumours.

Immunofluorescence staining was carried out and visualised under fluorescence microscope. Negative control (no primary antibody). Fringe was expressed in vessels (co-localisation shown in yellow).

5.5 Discussion

Preliminary screening of nine cancer cell lines and four endothelial cell lines, including HUVEC and HMEC-1 revealed that MFng expression is abundant in the endothelial cells (Figure 5.3 A and Figure 5.4). While MFng was more highly expressed in the endothelial cells relative to tumour cell lines (Figure 5.3 A), LFng expression was relatively higher in tumour cells lines especially in MCF7 and T47D Estrogen Receptor (ER) positive breast cancer cell lines (Figure 5.3 B). This implies that MFng may have an endothelial specific role. Benedito and colleagues (2009) has previously demonstrated that MFng is highly expressed in the arteries, veins, and capillary endothelial cells in postnatal retinas. They also observed significantly enhanced sprouting in the retinal vasculature in LFng double knockout mice, suggesting that LFng is indispensable in angiogenesis, but did not study MFng or tumour vessels. On the other hand, high expression in ER positive breast cancer cell lines suggest that LFng may play a role in estrogen- ER interaction apart from angiogenesis, as supported by immunostaining of LFng in ovarian granulosa and theca cells of developing follicles (Hahn et al. 2005). Besides, they also found LFng null mice to be infertile, suggesting that LFng is necessary in estrogen signaling. However, this is a preliminary screening at the transcript level and needs to be confirmed at the protein level. We have so far unable to obtain a working antibody for western blot and work is still in progress to optimise commercial antibodies and in-house developed antibody.

The CCRCC tumours are richly vascularised (Sjolund et al. 2008; Patard et al. 2009; Qian et al. 2009), accounting for the increase of CD31 gene expression in the tumours compared to normal renal tissue ($P<0.01$) (Figure 5.7 C). The significant up-regulation of MFng ($P<0.05$) and LFng ($P<0.01$) in the 18 CCRCC tumour samples compared to normal renal samples

(Figure 5.7 A and B) suggests that both Fringes may play a role in the CCRCC tumours in which Notch signalling is constitutively active (Sjolund et al. 2008). However, MFng and expression did not correlate with the expression of DLL4 or JAG1 (Figure 5.9 B and C) or CD31 endothelial marker (Figure 5.8 C). Furthermore, the level of MFng expression varies much more within the 18 cases of CCRCC tumours, as indicated by the big mean distribution of MFng gene expression (Figure 5.7) and a subgroup with high expression. DLL4 gene expression was most abundant in relative to MFng, LFng and JAG1 (Figure 5.10). This could be due to DLL4 being a Notch downstream gene which is up-regulated upon Notch activation in CCRCC, as also shown in HUVEC and HIMEC-1 in Chapter 3. It is not surprising that MFng does not correlate with the Notch ligands, as it exerts effects by targeting the receptors at protein level, but the lack of correlation with vasculature is not supported by the immunofluorescence. The factors regulating MFng in tumour vessels are currently unknown, and seem unlikely to be Notch ligands directly as i*n vitro* investigation of HMEC-1 (Figure 5.5) and HUVEC (data now shown, n=1) showed no induction of MFng or other Fringes by either ligand. However, if the effects on tumour vasculature are similar to the retina whereby enhanced endothelial coverage and higher tip cell number were observed in LFng deficient retinas (Benedito et al. 2009), enhancement of the effects of DLL4 will be expected. So a more detailed analysis of vessel size, differentiation and number is planned in these cases.

LFng on the other hand did not appear to be endothelial specific as observed through the relative expression in a panel of tumour and endothelial cell lines (Figure 5.3 B), which may explain the non-correlation with CD31 or DLL4 gene expression in the CCRCC tumours (Figure 5.8 D and Figure 5.9 D). The positive correlation between DLL4 and JAG1 ($P<0.01$) with CD31 ($P<0.01$) gene expression (Figure 5.8 A and B) implies that both the ligands are expressed in the endothelium, as supported by mounting literature (Noguera-Troise et al.

2006; Patel et al. 2006; Ridgway et al. 2006; Li et al. 2007; Segarra et al. 2008; Jubb et al. 2009; Jubb et al. 2010; Sonoshita et al. 2011). However, expression in tumour close to vessels would give a similar finding and currently we are investigating JAG1 staining. The positive correlation between DLL4 and JAG1 further supports our published work that the expression of DLL4 can up-regulate the expression of JAG1 (Harrington et al. 2008).

Hence, immunostaining with a validated Manic Fringe antibody is vital. Ideally, Fringe antibody specific for each homolog should be used to examine the expression pattern of each Fringe, especially Manic Fringe. Fringe expression was visualised to co-localise with CD31 (Figure 5.14) and its protein expression seemed to correspond to MFng relative expression at the transcript level in CCRCC tumours (Table 5.1), in consistent with MFng being the most prevalent Fringe expressed in endothelial cells (Figure 5.3 A and Figure 5.4). This is supported by Benedito and colleagues (2009) who demonstrated that MFng was highly expressed in the eye capillaries of mice, for the first time associating Fringe with physiological angiogenesis. Taken together, the high transcript expression of MFng in the endothelial cells (Figure 5.3 A and Figure 5.4) and its up-regulation in CCRCC compared to normal renal tissue (Figure 5.7) suggest that MFng may have an endothelial specific role, justifying the focus on MFng studies in future work. Therefore, staining should be repeated with a validated specific MFng antibody on more CCRCC tumour and renal tissue samples to compare MFng expression in normal versus tumour sections, which will then be scored to identify the percentage of MFng expression on vessels. Alternatively, *in situ* hybridisation for MFng expression can be employed to enhance the expression signal in tumours, in which it is currently being carried out as a collaborative effort with Genentech. Laser microdissection on tumour vessels followed by QPCR can be performed to examine the expression of Manic Fringe in the tumour endothelium.

Constitutive activation of Notch signalling has been observed in human CCRCC cell lines independently of the VHL/HIF pathway with interestingly higher Notch1 and JAG1 protein expression in CCRCC tumours than normal human renal tissues (Figure 5.7) (Sjolund et al. 2008), whereas the expression of DLL4 is found to be high in endothelial cells in the highly angiogenic CCRCC tumours (Patel et al. 2005). Inhibition of Notch signalling in CCRCC tumour xenograft hampered their growth (Sjolund et al. 2008), indicating that Notch pathway may represent a novel therapeutic strategy in CCRCC. Therefore, it would also be interesting to study the correlation of MFng with DLL4 and JAG1 in each CCRCC tumour pair at the transcript level by QPCR and protein level by immunostaining. Renal Tumour Tissue Microarray (TMA) can be utilised to visualise the expression of MFng by immunostaining or *in situ* hybridisation. The amount of MFng protein present can then be correlated to patient information, such as tumour grade and survival to determine if MFng can be used as a biomarker in highly angiogenic tumours, in this case CCRCC. This opens new avenue to dissect the role of Fringe inhibitors to impair the modulation of Fringe on DLL4- Notch signalling in CCRCC as an alternative to anti-DLL4 therapy.

MFng modulates endothelial Notch signaling by JAG1 and DLL4 in cell co-culture assay (Benedito et al. 2009). Therefore, it would be interesting to study the effect of Manic Fringe on Notch signalling by assessing the target gene expression profile after suppression of MFng in endothelial cells followed by Notch activation by exogenous DLL4 or JAG1 recombinant proteins. The functional role of Fringe in angiogenesis can be assessed by knocking down of MFng expression in endothelial cells followed by survival, migration and hanging drop assays. It is essential for *in vitro* work to translate *in vivo.* Future work includes studying the effects of global MFng knockout in syngeneic model and its effects on Notch signalling by looking at how it affects tumour growth followed by immunostaining to study tumour

vasculature, including vessel density, vessel diameter, pericyte coverage and vessel function. The effects on proliferation and apoptosis as well as on hypoxia and necrosis in tumour tissues will also be studied.

6 Overall Conclusion and Future Perspectives

6.1 Overall conclusion

This thesis has examined the differences between DLL4- and JAG1- on Notch signalling in the regulation of tumour angiogenesis, both *in vitro* and *in vivo*. The effects of DLL4 and JAG1 on Notch signalling in endothelial cells were examined at the transcript and functional level. The changes in the vasculature phenotypes promoted by murine DLL4 and murine JAG1 in U87 xenograft tumours was examined *in vivo*. Chapter 5 assessed Fringe expression in endothelial cells and angiogenic tumours was also assessed based on the hypothesis that Fringe expression may mediate DLL4- and JAG1- Notch signalling in tumour angiogenesis. This chapter summarises the overall findings of the thesis and discusses future perspectives in targeting the DLL4- and JAG1-Notch signalling pathways in tumour angiogenesis.

6.1.1 DLL4- and JAG1- Notch signalling promoted different sprouting phenotypes in *in vitro* and *in vivo.*

Two endothelial cells types, an immortalised human microvascular endothelial cells (HMEC-1), and primary human umbilical vein endothelial cells (HUVEC) were used to compare the effects of DLL4 and JAG1 stimulation on established downstream Notch target genes. In HUVEC, DLL4 was more potent than JAG1 in activating Notch signalling while both recombinant DLL4 and JAG1 proteins displayed equal potency in up-regulating the downstream genes in the latter. In both models, DLL4 up-regulated DLL4 transcript, while JAG1 modestly up-regulated its own expression.

However at the functional level, DLL4 and JAG1 had opposite effects on HMEC-1, most apparent in the hanging drop assay. DLL4 and JAG1 had different roles in sprouting angiogenesis. The role of DLL4 as a negative regulator of angiogenesis was confirmed in the DLL4 knockdown model in which increased sprouting was observed compared to control cells. Conversely, suppressing pro-angiogenic JAG1 in HMEC-1 reduced sprouting compared to control cells whereas treatment with DBZ increased sprouting in siJAG1 spheroids. Over-expressing mDLL4 up-regulated DLL4 expression in HMEC-1 through a feed forward mechanism by activating Notch in the neighbouring cells (Caolo et al. 2010), this then negatively regulates tip cell formation thus reduces sprouting of vessels in mice models (Hellstrom et al. 2007; Lobov et al. 2007; Suchting et al. 2007). In contrast, over-expressing mJAG1 in HMEC-1 allow the cells to take on the more proliferative stalk cell phenotype, contributing to the increase of sprout length and coverage (Phng and Gerhardt 2009). The effects of mDLL4 and mJAG1 on sprouting is recapitulated in the *in vivo* experiment.

The different effects of mDLL4 and mJAG1 on U87 cell proliferation *in vitro* and tumour growth *in vivo* suggested a stroma-dependent mechanism for Notch signalling in U87 xenograft tumours, as revealed by the up-regulation of the human and murine HEY1 gene expression by QPCR. Both mDLL4 and mJAG1 supported U87 xenograft tumour growth through different vasculature phenotypes although both ligands decreased pericyte coverage in a γ-secretase dependent manner. mDLL4 seemed to be more effective in promoting U87 tumour growth compared to mJAG1, again this could be explained by the forward feedback loop of DLL4 expression by mDLL4 thus increasing Notch signalling more than mJAG1 in U87 tumours, supporting the QPCR *in vitro* results in HUVEC. This suggests the importance of DLL4 as the more dominant ligand in Notch signalling compared to JAG1 at the functional level as demonstrated in the *in vitro* work. mDLL4 decreased vessel number, however the

vessels were bigger, similar to the phenotype observed with hDLL4 (Li et al. 2007), whereas mJAG1 increased tumour angiogenesis, both supported the sprouting phenotype in the hanging drop assay *in vitro*. Both ligands increased vessel perfusion and necrosis, thus contributing to enhanced tumour growth by overall promoting nutrient and oxygen uptake by tumour cells. Treatment with DBZ produced non-functional vessels which resulted in tumours starved from nutrients and oxygen, thus increased tumour necrosis and delayed tumour growth in mDLL4 and mJAG1 groups.

Bevacizumab treatment delayed tumour growth for U87 EV, mDLL4 and mJAG1 groups, supporting relevance in clinical setting for glioblastoma cancer patients. However, mDLL4 and mJAG1 mediated resistance to anti-VEGF, which was reversed upon treatment with DBZ. The resistance towards bevacizumab observed in mDLL4 and mJAG1 tumours was independent of pericyte coverage, suggesting interplay with other signalling pathways upon tumour-stroma interaction. The expression of Notch receptors and ligands have been shown to be influenced by the presence of growth factors within the tumour micro-environment, which in turn influences tumour angiogenesis. The inflammatory cytokine, TNFα has been shown to up-regulate JAG1 expression but reduced DLL4, thus promoting tumour angiogenesis (Sainson et al. 2008; Benedito et al. 2009), suggesting that JAG1 and DLL4 responds differently to different inflammatory stimulus, especially in the *in vivo* setting. Furthermore, neutrophils have also been shown to play a role in mediating resistance to anti-VEGF in tumours (Shojaei et al. 2007). As such, macrophage and neutrophil infiltration assessment should be carried out through CD68 and CD11b immunostaining respectively. Interestingly, combination treatment worked better in both mDLL4 and mJAG1 tumour groups as shown by the significant delayed effect on tumour growth by inducing the greatest necrosis compared to single treatment. Both mDLL4 and mJAG1 had very little effect on necrosis as the remaining

pruned vessels in both groups were perfused and functional, however the number of vessels have decreased remarkably thus did not contribute to tumour growth.

DLL4 was abundantly expressed in tumour vessels (Mailhos et al. 2001; Noguera-Troise et al. 2006; Li et al. 2010; Schadler et al. 2010). The massive level of DLL4 expression in the mDLL4 tumour vessels could be a result of positive regulation of Notch signalling by mDLL4 (Caolo et al. 2010). However, less DLL4 expression was detected in U87 mJAG1 vessels, suggesting that mDLL4 is a better inducer of Notch signalling than mJAG1, as supported by the *in vitro* work. Pruning of vessels by bevacizumab in control EV tumours which are positive for DLL4 expression resulted in reduced DLL4-Notch signalling between endothelial cells and tumour cells (Noguera-Troise et al. 2006). DLL4 is induced by hypoxia through HIF-1α (Patel et al. 2005; Diez et al. 2007), thus the high level of DLL4 expression in EV and mJAG1 tumour vessels within the co-treatment group could be the result of increased hypoxia due to formation of non-functional vessels by DBZ which were then pruned by bevacizumab creating a hypoxic tumour microenvironment. However, increase in mJAG1 expression was observed in vessels and tumour cells or stroma in U87 mDLL4 tumours whereas DBZ treatment diminished the phenotype, indicating that DLL4-Notch signalling could induce JAG1 expression

6.1.2 DLL4- versus JAG1-Notch signalling

Taken together from the *in vitro* and *in vivo* work, DLL4 appeared to play a predominant role in tumour vessels compared to JAG1, perhaps the effects are through the amplification of Notch signalling from the DLL4 positive feedback loop. The different levels of expression between DLL4 and JAG1 in the endothelial cells could affect signalling, as the fine tuning

and spatial expression of each ligand expression has been shown to determine the outcomes of Notch signalling (Hofmann and Luisa Iruela-Arispe 2007; Benedito et al. 2009). The spatial expression of DLL4 and JAG1 in vessels controls the specification of endothelial tip and stalk cells as reviewed extensively in (Phng and Gerhardt 2009). While DLL4 is an essential component expressed in the tip cells, JAG1 is readily expressed in the stalk cells (Claxton and Fruttiger 2004; Hellstrom et al. 2007; Gerhardt 2008; Benedito et al. 2009). The communication between tip versus stalk cells during formation of new connections specify the phenotypic outcome of Notch signalling in vessels, in response to environmental cues, for example the VEGF growth factor. While DLL4 is induced by VEGF which acts as a negative regulator of angiogenesis both *in vitro* and *in vivo* (Noguera-Troise et al. 2006; Lobov et al. 2007; Caolo et al. 2010), JAG1 has not been shown to be regulated by VEGF, indicating differential regulation between the two ligands. This is further made complicated by the crosstalk of Notch signalling with other signalling pathways such as the VEGF, FGF, Wnt and Ephrin pathways.

Fringe has been demonstrated to promote DLL-notch signalling (Visan et al. 2006; Stanley and Guidos 2009; Yuan et al. 2011) compared to JAG- notch signalling (Kato et al. 2010; Marklund et al. 2010; Visan et al. 2010). The overlapping expression of Fringe in different cell types and their oscillatory expressions could also add to the complexity of different receptor-ligand combinations, which contribute to the highly dynamic regulation of tumour angiogenesis. Preliminary screening of nine cancer cell lines and four endothelial cell lines, including HUVEC and HMEC-1 revealed high MFng expression in the endothelial cells, implying that MFng may have an endothelial specific role. However, LFng expression was relatively higher in tumour cells lines compared to endothelial cells. Up-regulation of CD31, MFng and LFng in the 18 CCRCC tumour samples compared to normal renal samples

indicates that both Fringes may play a role in the highly vascularised CCRCC tumours in which Notch signalling is constitutively active. Positive correlation between DLL4 and JAG1 with CD31 gene expression implies that both the ligands are expressed in the endothelium. The positive correlation between DLL4 and JAG1 further supports our published work that the expression of DLL4 can up-regulate the expression of JAG1 (Harrington et al. 2008). Fringe expression was visualised to co-localise with CD31 and its protein expression seemed to correspond to MFng relative expression at the transcript level. Although no correlation was observed between the two Fringes and DLL4 or JAG1 in the 18 CCRCC tumours, more work needs to be done to validate MFng antibody and repeated on a larger set of tumour samples, as justified by its highest expression in the endothelial cells compared to LFng and RFng.

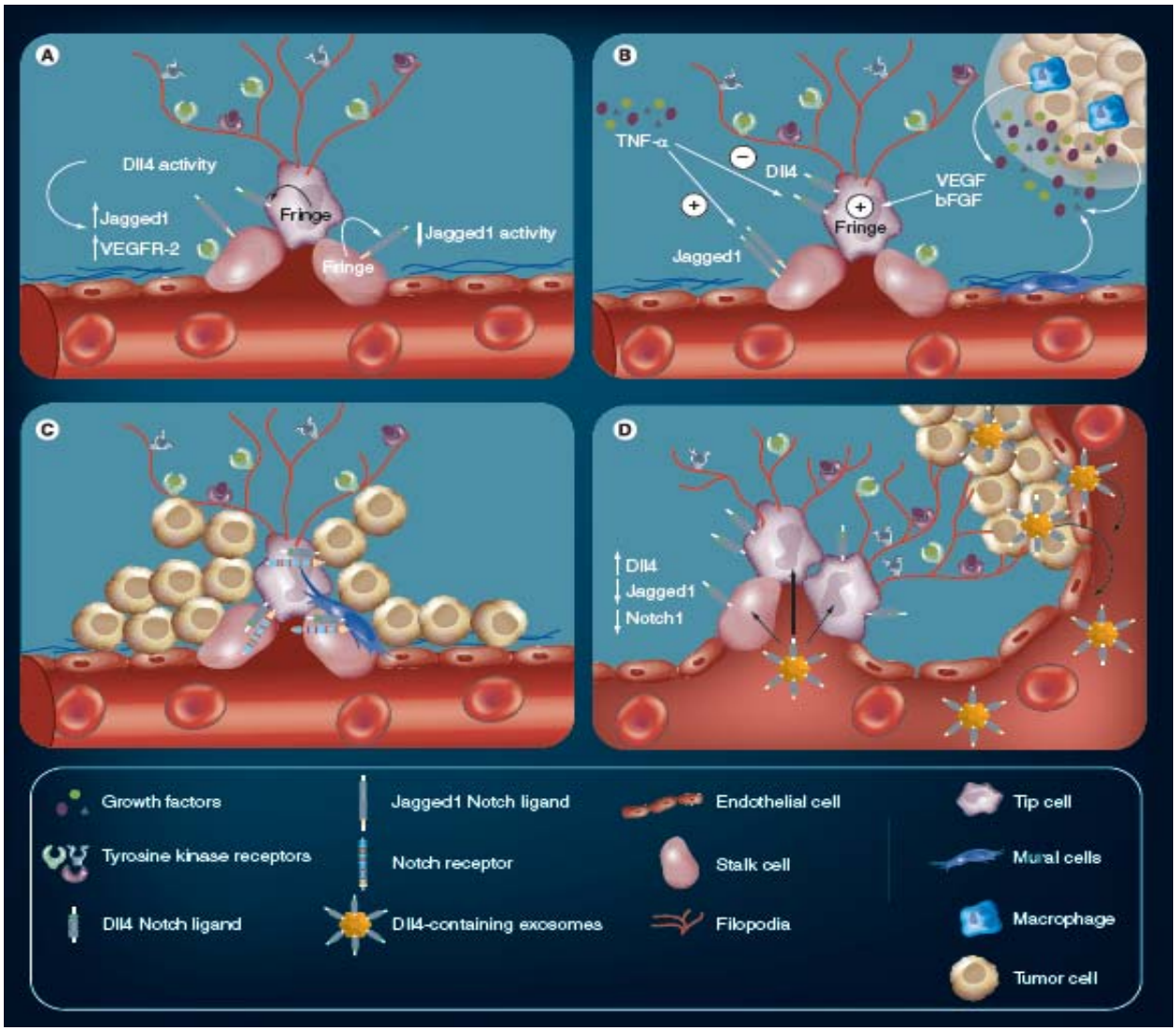
The similar regulation of 10 established DLL4- and JAG1- Notch downstream target genes (preliminary experiment, data not presented), with JAG1 to a lesser extent (Emuss et al. 2009) in HUVEC, which led to a different sprouting phenotype at the functional level *in vitro* and *in vivo* suggests a role exerted through ligand protein interaction with other proteins to initiate Notch signalling. Although juxtacrine signalling mediated by the many interaction combination of Notch ligands and receptors may contribute to the functional diversity of Notch signalling, recently it has been postulated that paracrine signalling may occur through exosomes which are formed in multi-vesicular bodies, a component of the endocytic pathway, and released by cells into the surrounding environment, can have intercellular signalling potential (Simons and Raposo 2009). An additional study focused on establishing a functional relationship between tumour produced exosomes, endothelial signalling and angiogenesis (Hood et al. 2009). Melanoma exosomes were observed to rapidly stimulate the production of endothelial sprouts and influence endothelial tubule morphology (Hood et al. 2009). My colleagues have recently identified a novel mechanism by which endothelial and tumour cells

can incorporate DLL4 into exosomes and modulate Notch signalling in distant cells, without the requirements of a classical Notch signalling being initiated by cell-cell contact (Sheldon et al. 2010). These DLL4-exosomes were transferred to endothelial cells *in vitro* and *in vivo,* resulting in an inhibition of Notch signalling and also reduced Notch1 receptor expression. The DLL4-exosomes increased branching and overall vessel density in an *in vitro* model, demonstrating that DLL4-exosomes are capable of affecting tube formation. Interestingly an increased tip cell phenotype was conveyed when DLL4-exosomes were incorporated. The same phenotype was observed by utilising DLL4-exosomes produced by a glioblastoma cell line over-expressing DLL4. Similarly increased branching was observed, as well as vessel length and lumen within *in vivo* tumour models. Therefore exosomes may restrict stalk cell differentiation, as demonstrated by the down-regulation of stalk cell markers such as JAG1, and thus present a mechanism by which Notch tip cell phenotype is promoted. Future studies will be carried out to compare the effects of JAG1-exosomes by either the tumour cells or endothelium and subsequent promotion of tumour angiogenesis to that of DLL4-exosomes.

Recently, it has been proposed that DSL ligands may also have a distinct role in initiating PDZ-dependent signalling in the DSL expressing cells (Ascano et al. 2003; Six et al. 2004; Popovic et al. 2011), thus representing a novel intrinsic signalling pathway through intracellular protein interaction. The PDZ-binding motifs could be identified at the C-termini of DLL1, DLL4 and JAG1 ligands. It has been shown that DLG-1 (Discs Large 1) is able to interact with the C-terminal PDZ-binding motif of DLL1, whereas no interaction of DLG-1 with JAG1 could be detected. DLG-1 is recruited by DLL1 at cell-cell contacts and play a role in cell adhesion and cell polarity (Six et al. 2004), both steps are essential in angiogenesis. Interestingly, DLG-1 was also identified in the DLL4- containing exosomes (Sheldon et al.

2010), suggesting that DLG-1 may mediate the vasculature differences observed between mDLL4 and mJAG1 tumours.

The mechanisms that affect Notch signalling and their subsequent influence on tumour vasculature is shown in Figure 6.1.



Bridges, Oon and Harris, 2011 (Future Oncology, in press)

Figure 6.1: Illustration demonstrating the mechanisms that effect Notch signalling and their subsequent influence on tumour vasculature.

A) Post-translational modification by Fringe increases (↑) DLL4/Notch signalling which in turn mediates the tip and stalk cell phenotype, as well as reducing (↓) JAG1 activity during physiological angiogenesis. B) Tumour associated growth factors produced by tumour, stromal and inflammatory cells can either up-regulate (indicated by plus sign) or down-regulate (indicated by negative sign) Notch ligand expression in endothelial cells. C) Expression of Notch ligands and receptors in endothelial, tumour and tumour associated vascular cells can induce Notch signalling in neighbouring tumour endothelial cells, which in turn can influence sprouting. D) Paracrine regulation of Notch signalling to the endothelium promoting a tip cell phenotype following incorporation of DLL4 containing exosomes secreted by tumour and/or endothelial cells that act on distant endothelial cells by either diffusion or through the blood stream.

6.2 Future perspectives: Targeting the DLL4- and JAG-1 Notch signalling pathway

The VEGF signalling pathway is a well-characterised pro-angiogenic pathway that plays a critical role in the local growth of many different solid tumours. Not surprisingly then, over the last decade of research numerous inhibitors of angiogenesis mainly targeting the VEGF pathway have emerged and clinically validated as cancer therapy (Ferrara and Kerbel 2005; Jain et al. 2006). However, it has since been observed that patients display resistance (either innate or developed during therapy) to anti-VEGF therapy.

Several studies have attempted to tap into blockade of Notch signalling as therapeutic means for cancer patients by inhibiting tumour growth, both by interfering with Notch signalling within tumour cells and by targeting tumour vasculature compartment that encompasses the endothelial and stromal cells. Notch activation in tumour cells promotes cancer cells to survive and proliferate (Radtke and Raj 2003). γ-secretase inhibitors were one of such concepts to be utilised in the clinic (Shih Ie and Wang 2007; Wei et al. 2010). In one such study inhibition of Notch signalling by γ-secretase inhibitors (N-[N-(3,5-difluorophenacetyl)-L-alanyl]-5-phenylglycine-t-butyl ester) prevented the progression of solid tumours such as medulloblastoma (Hallahan et al. 2004). However the clinical effectiveness of the γ-secretase inhibitor is limited by significant toxic side effects (Li et al. 2010; Yan et al. 2010). Additionally γ-secretase inhibitors were found to display weak selectivity in blocking proteolysis of all four Notch receptors and were found to also affect other signalling pathways (Beel et al. 2009).

Lately, alternative therapeutic antibodies have been developed which target the Notch1 receptor (Wu et al. 2010) or individual ligands, such as DLL4 and have recently entered Phase I clinical trial (Hoey et al. 2009). It is hoped that the use of antibodies targeting Notch signalling will display specific therapeutic efficacy by interfering with tumour Notch signal and tumour angiogenesis to reduce tumour growth, with a lower toxic profile compared to that of γ-secretase inhibitors. In preclinical experiments where DLL4-Notch mediated signalling was blocked (either via systemic administration of DLL4 neutralising antibodies (Noguera-Troise et al. 2006; Ridgway et al. 2006) or by systemic/local administration of modified DLL4 proteins (Noguera-Troise et al. 2006; Scehnet et al. 2007) increased tumour-vessel sprouting with numerous interconnecting branches was observed. Although increased tumour vessel density and sprouting was observed following DLL4 blockade, the vessels formed were non-functional (Noguera-Troise et al. 2006; Ridgway et al. 2006; Sainson and Harris 2007; Scehnet et al. 2007; Thurston et al. 2007; Hoey et al. 2009; Oishi et al. 2010). As a consequence tumours were more hypoxic, as the disorganised tumour vasculature could not efficiently deliver blood to the tumour, which together with the direct effect of the inhibition of DLL4 signalling within tumour cells, tumour growth overall was reduced. Interestingly, a DNA vaccine against Dll4 has been developed to block DLL4 signalling in murine mammary carcinoma model (Haller et al. 2010). The novel therapeutic cancer vaccination has been shown to effectively inhibit tumour growth without triggering toxicity effects as opposed to the other Dll4 signalling blockade strategies, which reported vascular neoplasm, subcutaneous ulceration, heart lesions and liver atrophy (Yan et al. 2010).

Potentially, combination of anti-DLL4-Notch therapy with chemotherapy and other anti-angiogenic therapy will greatly improving survival rates of patients (Wang et al. 2010). For example, targeting Notch1 receptor in preclinical models was found to cause cell growth

inhibition and increased chemo-sensitivity to chemotherapeutic drugs such as doxorubicin and docetaxel in breast cancer cell lines (Zang et al. 2010). Due to cross of Notch signalling pathways with other signalling pathways, targeting the Notch signalling pathway may also have the additional benefit of down-regulating components of other tumour and angiogenic promoting signalling pathways (Efferson et al. 2010). This point is emphasised in research where DLL4 over expressing tumours were found to be resistant to anti-VEGF therapy; blocking DLL4-Notch signalling again sensitised tumours to the effects of the anti-VEGF therapy and tumour growth was reduced (Noguera-Troise et al. 2006; Ridgway et al. 2006). It is likely that blocking DLL4-Notch signalling prevented the up-regulation of the secondary resistance pathways that enable the tumour vasculature to evade anti-VEGF therapy, demonstrating the importance of further anti-angiogenic therapy targeting more than just the VEGF pathway.

From the *in vivo* work (Chapter 4) mJAG1 displayed the same effect as mDLL4 in response to anti-VEGF treatment therefore this opens new avenues to dissect the role of JAG1 in tumour angiogenesis as a targeted therapy. Furthermore, JAG1 expression was demonstrated to be elevated in glioblastoma at the transcript and protein level and has been shown to be important for glioma cell survival and proliferation (Purow et al. 2005). JAG1 expression has also been associated with poor outcome in breast cancer (Dickson et al. 2007). Notably, JAG1 expression was also observed in the vasculature of colon tumours (Sonoshita et al. 2011). If Fringe also represses JAG1-Notch signalling but potentiates DLL4-Notch signalling in tumours, inhibition of JAG1-Notch signalling could possibly enhance anti-VEGF therapy in the tumours. To date there is no known specific Fringe inhibitor to inhibit the addition of GlcNac to O-Fucose, which is an important step to produce a functional trimer or tetramer for the activation of Notch signalling. It would be interesting to dissect the potential role of

Fringe inhibitors to block the modulation of Fringe on DLL4- Notch signalling in highly vascularised tumours which could be an alternative to anti-DLL4 therapy.

Endothelial-mural cell crosstalk may present an attractive potential antiangiogenic target. Mural cells function to provide structural support and stabilise vessels. Endothelial cells lacking pericytes are more susceptible to anti-VEGF therapy (Benjamin et al. 1998), however endothelial cells induce pericyte recruitment to be protected from the effects of anti-VEGF (Benjamin et al. 1998; Bergers and Benjamin 2003). Pericytes are recruited to tumour vessels by PDGFB/ PDGFR beta and Ang-1/Tie2 signalling this inhibition of VEGF signalling in the endothelial cells and PDGFRbeta signalling (Erber et al. 2004). Therefore it may be possible to target tumour pericytes to overcome pericyte mediated VEGF inhibition to enhance tumour vessel destabilization for optimal therapy. A recent study showed that DLL4-Notch signalling contributes to adhesion and differentiation of bone marrow cells into pericytes (Schadler et al. 2010). Silencing DLL4 expression resulted in reduced bone marrow derived pericyte coverage and reduced vessel density which inhibited tumour growth. Conversely, DLL4 over-expressing tumours reduced pericyte coverage on tumour vessels ((Li et al. 2007), unpublished data), possibly through stromal derived factor-1A(SDF-1A)/CXCR4 axis which corresponded to recruitment of PDGFB induced pericyte by SDF-1A chemotaxis gradient (Song et al. 2009). Altogether, these provide a new avenue for DLL4 to be used as a target for treatment of Ewing's sarcoma (Schadler et al. 2010). However, more research is needed to clarify the role of mural cells in tumour angiogenesis to assess the risks and benefits of anti-pericyte therapy.

Further understanding of the mechanism and regulation of DLL4 and JAG1, as well as the other components of Notch signalling influencing tumour angiogenesis will enable the

appropriate Notch component to be targeted as part as a novel anti-angiogenic therapy in the clinic. The future emergence of a specific Notch component inhibitor will likely be an attractive additional therapeutic choice for cancers in combination with other anti-angiogenic therapies or chemotherapies, in particular where the aberrant Notch signalling in the tumour endothelium compartment, or tumour cells themselves is observed.

Part of this chapter was adapted from :

Bridges, E.*, **Oon. C**.*, and Harris, A.. *Notch regulation of tumour angiogenesis.* (Future Oncology, in press) * Joint first authorship

7 Bibliography

Acar, M., H. Jafar-Nejad, et al. (2008). "Rumi is a CAP10 domain glycosyltransferase that modifies Notch and is required for Notch signaling." Cell **132**(2): 247-258.

Ades, E. W., F. J. Candal, et al. (1992). "HMEC-1: establishment of an immortalized human microvascular endothelial cell line." J Invest Dermatol **99**(6): 683-690.

Aguirre-Ghiso, J. A. (2007). "Models, mechanisms and clinical evidence for cancer dormancy." Nat Rev Cancer **7**(11): 834-846.

Aiello, L. P., J. M. Northrup, et al. (1995). "Hypoxic regulation of vascular endothelial growth factor in retinal cells." Arch Ophthalmol **113**(12): 1538-1544.

Alitalo, K., T. Tammela, et al. (2005). "Lymphangiogenesis in development and human disease." Nature **438**(7070): 946-953.

Almog, N. (2010). "Molecular mechanisms underlying tumor dormancy." Cancer Lett **294**(2): 139-146.

Androutsellis-Theotokis, A., R. R. Leker, et al. (2006). "Notch signalling regulates stem cell numbers in vitro and in vivo." Nature **442**(7104): 823-826.

Arboleda-Velasquez, J. F., R. Rampal, et al. (2005). "CADASIL mutations impair Notch3 glycosylation by Fringe." Hum Mol Genet **14**(12): 1631-1639.

Artavanis-Tsakonas, S., M. D. Rand, et al. (1999). "Notch signaling: cell fate control and signal integration in development." Science **284**(5415): 770-776.

Ascano, J. M., L. J. Beverly, et al. (2003). "The C-terminal PDZ-ligand of JAGGED1 is essential for cellular transformation." J Biol Chem **278**(10): 8771-8779.

Augelli-Szafran, C. E., H. X. Wei, et al. "Discovery of notch-sparing gamma-secretase inhibitors." Curr Alzheimer Res **7**(3): 207-209.

Azad, M. B., Y. Chen, et al. (2008). "Hypoxia induces autophagic cell death in apoptosis-competent cells through a mechanism involving BNIP3." Autophagy **4**(2): 195-204.

Baliko, F., T. Bright, et al. (2007). "Inhibition of notch signaling induces neural differentiation in Ewing sarcoma." Am J Pathol **170**(5): 1686-1694.

Beel, A. J., P. Barrett, et al. (2009). "Nonspecificity of binding of gamma-secretase modulators to the amyloid precursor protein." Biochemistry **48**(50): 11837-11839.

Benedito, R., C. Roca, et al. (2009). "The notch ligands Dll4 and Jagged1 have opposing effects on angiogenesis." Cell **137**(6): 1124-1135.

Benedito, R., A. Trindade, et al. (2008). "Loss of Notch signalling induced by Dll4 causes arterial calibre reduction by increasing endothelial cell response to angiogenic stimuli." BMC Dev Biol **8**: 117.

Benjamin, L. E., I. Hemo, et al. (1998). "A plasticity window for blood vessel remodelling is defined by pericyte coverage of the preformed endothelial network and is regulated by PDGF-B and VEGF." Development **125**(9): 1591-1598.

Bergers, G. and L. E. Benjamin (2003). "Tumourigenesis and the angiogenic switch." Nat Rev Cancer **3**(6): 401-410.

Bergers, G. and S. Song (2005). "The role of pericytes in blood-vessel formation and maintenance." Neuro Oncol **7**(4): 452-464.

Bergers, G., S. Song, et al. (2003). "Benefits of targeting both pericytes and endothelial cells in the tumour vasculature with kinase inhibitors." J Clin Invest **111**(9): 1287-1295.

Bingle, L., N. J. Brown, et al. (2002). "The role of tumour-associated macrophages in tumour progression: implications for new anticancer therapies." J Pathol **196**(3): 254-265.

Blancher, C., J. W. Moore, et al. (2000). "Relationship of hypoxia-inducible factor (HIF)-1alpha and HIF-2alpha expression to vascular endothelial growth factor induction and hypoxia survival in human breast cancer cell lines." Cancer Res **60**(24): 7106-7113.

Bland, C. E., P. Kimberly, et al. (2003). "Notch-induced proteolysis and nuclear localization of the Delta ligand." J Biol Chem **278**(16): 13607-13610.

Bocchetta, M., L. Miele, et al. (2003). "Notch-1 induction, a novel activity of SV40 required for growth of SV40-transformed human mesothelial cells." Oncogene **22**(1): 81-89.

Bolos, V., J. Grego-Bessa, et al. (2007). "Notch signaling in development and cancer." Endocr Rev **28**(3): 339-363.

Bondjers, C., M. Kalen, et al. (2003). "Transcription profiling of platelet-derived growth factor-B-deficient mouse embryos identifies RGS5 as a novel marker for pericytes and vascular smooth muscle cells." Am J Pathol **162**(3): 721-729.

Bonnefoy, A., J. Harsfalvi, et al. (2001). "The subendothelium of the HMEC-1 cell line supports thrombus formation in the absence of von Willebrand factor and collagen types I, III and VI." Thromb Haemost **85**(3): 552-559.

Bouis, D., G. A. Hospers, et al. (2001). "Endothelium in vitro: a review of human vascular endothelial cell lines for blood vessel-related research." Angiogenesis **4**(2): 91-102.

Brey, E. M., L. V. McIntire, et al. (2004). "Three-dimensional, quantitative analysis of desmin and smooth muscle alpha actin expression during angiogenesis." Ann Biomed Eng **32**(8): 1100-1107.

Brou, C., F. Logeat, et al. (2000). "A novel proteolytic cleavage involved in Notch signaling: the role of the disintegrin-metalloprotease TACE." Mol Cell **5**(2): 207-216.

Caolo, V., N. M. van den Akker, et al. (2010). "Feed-forward signaling by membrane-bound ligand receptor circuit: the case of NOTCH DELTA-like 4 ligand in endothelial cells." J Biol Chem **285**(52): 40681-40689.

Carlson, T. R., H. Hu, et al. (2008). "Cell-autonomous requirement for beta1 integrin in endothelial cell adhesion, migration and survival during angiogenesis in mice." Development **135**(12): 2193-2202.

Castello, R., A. Estelles, et al. (2002). "Quantitative real-time reverse transcription-PCR assay for urokinase plasminogen activator, plasminogen activator inhibitor type 1, and tissue metalloproteinase inhibitor type 1 gene expressions in primary breast cancer." Clin Chem **48**(8): 1288-1295.

Chantrain, C. F., P. Henriet, et al. (2006). "Mechanisms of pericyte recruitment in tumour angiogenesis: a new role for metalloproteinases." Eur J Cancer **42**(3): 310-318.

Chen, J., N. Imanaka, et al. (2010). "Hypoxia potentiates Notch signaling in breast cancer leading to decreased E-cadherin expression and increased cell migration and invasion." Br J Cancer **102**(2): 351-360.

Chen, J., S. Kesari, et al. (2010). "Inhibition of Notch Signaling Blocks Growth of Glioblastoma Cell Lines and Tumour Neurospheres." Genes Cancer **1**(8): 822-835.

Chen, Y., E. McMillan-Ward, et al. (2007). "Mitochondrial electron-transport-chain inhibitors of complexes I and II induce autophagic cell death mediated by reactive oxygen species." J Cell Sci **120**(Pt 23): 4155-4166.

Chi, J. T., H. Y. Chang, et al. (2003). "Endothelial cell diversity revealed by global expression profiling." Proc Natl Acad Sci U S A **100**(19): 10623-10628.

Chigurupati, S., T. V. Arumugam, et al. (2007). "Involvement of notch signaling in wound healing." PLoS One **2**(11): e1167.

Claxton, S. and M. Fruttiger (2004). "Periodic Delta-like 4 expression in developing retinal arteries." Gene Expr Patterns **5**(1): 123-127.

Coant, N., S. Ben Mkaddem, et al. (2010). "NADPH oxidase 1 modulates WNT and NOTCH1 signaling to control the fate of proliferative progenitor cells in the colon." Mol Cell Biol **30**(11): 2636-2650.

Cohen, B., M. Shimizu, et al. (2010). "Cyclin D1 is a direct target of JAG1-mediated Notch signaling in breast cancer." Breast Cancer Res Treat **123**(1): 113-124.

Corada, M., D. Nyqvist, et al. (2010). "The Wnt/beta-catenin pathway modulates vascular remodeling and specification by upregulating Dll4/Notch signaling." Dev Cell **18**(6): 938-949.

D'Souza, B., A. Miyamoto, et al. (2008). "The many facets of Notch ligands." Oncogene **27**(38): 5148-5167.

Daigle, I. and H. U. Simon (2001). "Critical role for caspases 3 and 8 in neutrophil but not eosinophil apoptosis." Int Arch Allergy Immunol **126**(2): 147-156.

Dang, T. P., A. F. Gazdar, et al. (2000). "Chromosome 19 translocation, overexpression of Notch3, and human lung cancer." J Natl Cancer Inst **92**(16): 1355-1357.

Debbage, P. L., J. Griebel, et al. (1998). "Lectin intravital perfusion studies in tumour-bearing mice: micrometer-resolution, wide-area mapping of microvascular labeling, distinguishing efficiently and inefficiently perfused microregions in the tumour." J Histochem Cytochem **46**(5): 627-639.

Dejana, E., E. Tournier-Lasserve, et al. (2009). "The control of vascular integrity by endothelial cell junctions: molecular basis and pathological implications." Dev Cell **16**(2): 209-221.

Dickson, B. C., A. M. Mulligan, et al. (2007). "High-level JAG1 mRNA and protein predict poor outcome in breast cancer." Mod Pathol **20**(6): 685-693.

Dickson, P. V., J. B. Hamner, et al. (2007). "Bevacizumab-induced transient remodeling of the vasculature in neuroblastoma xenografts results in improved delivery and efficacy of systemically administered chemotherapy." Clin Cancer Res **13**(13): 3942-3950.

Diez, H., A. Fischer, et al. (2007). "Hypoxia-mediated activation of Dll4-Notch-Hey2 signaling in endothelial progenitor cells and adoption of arterial cell fate." Exp Cell Res **313**(1): 1-9.

Djokovic, D., A. Trindade, et al. (2010). "Combination of Dll4/Notch and Ephrin-B2/EphB4 targeted therapy is highly effective in disrupting tumour angiogenesis." BMC Cancer **10**: 641.

Doi, H., T. Iso, et al. (2006). "Jagged1-selective notch signaling induces smooth muscle differentiation via a RBP-Jkappa-dependent pathway." J Biol Chem **281**(39): 28555-28564.

Dotto, G. P. (2008). "Notch tumour suppressor function." Oncogene **27**(38): 5115-5123.

Duarte, A., M. Hirashima, et al. (2004). "Dosage-sensitive requirement for mouse Dll4 in artery development." Genes Dev **18**(20): 2474-2478.

Efferson, C. L., C. T. Winkelmann, et al. (2010). "Downregulation of Notch pathway by a gamma-secretase inhibitor attenuates AKT/mammalian target of rapamycin signaling and glucose uptake in an ERBB2 transgenic breast cancer model." Cancer Res **70**(6): 2476-2484.

Eliasz, S., S. Liang, et al. (2010). "Notch-1 stimulates survival of lung adenocarcinoma cells during hypoxia by activating the IGF-1R pathway." Oncogene **29**(17): 2488-2498.

Emuss, V., D. Lagos, et al. (2009). "KSHV manipulates Notch signaling by DLL4 and JAG1 to alter cell cycle genes in lymphatic endothelia." PLoS Pathog **5**(10): e1000616.

Enge, M., M. Bjarnegard, et al. (2002). "Endothelium-specific platelet-derived growth factor-B ablation mimics diabetic retinopathy." EMBO J **21**(16): 4307-4316.

Erber, R., A. Thurnher, et al. (2004). "Combined inhibition of VEGF and PDGF signaling enforces tumour vessel regression by interfering with pericyte-mediated endothelial cell survival mechanisms." FASEB J **18**(2): 338-340.

Escoubet, B., C. Planes, et al. (1999). "Hypoxia increases glyceraldehyde-3-phosphate dehydrogenase transcription in rat alveolar epithelial cells." Biochem Biophys Res Commun **266**(1): 156-161.

Ferrando, A. A. (2009). "The role of NOTCH1 signaling in T-ALL." Hematology Am Soc Hematol Educ Program: 353-361.

Ferrara, N. and R. S. Kerbel (2005). "Angiogenesis as a therapeutic target." Nature **438**(7070): 967-974.

Fischer, A., C. Leimeister, et al. (2002). "Hey bHLH factors in cardiovascular development." Cold Spring Harb Symp Quant Biol **67**: 63-70.

Fischer, A., N. Schumacher, et al. (2004). "The Notch target genes Hey1 and Hey2 are required for embryonic vascular development." Genes Dev **18**(8): 901-911.

Folkman, J. (1971). "Tumour angiogenesis: therapeutic implications." N Engl J Med **285**(21): 1182-1186.

Foo, S. S., C. J. Turner, et al. (2006). "Ephrin-B2 controls cell motility and adhesion during blood-vessel-wall assembly." Cell **124**(1): 161-173.

Fraisl, P., M. Mazzone, et al. (2009). "Regulation of angiogenesis by oxygen and metabolism." Dev Cell **16**(2): 167-179.

Fruttiger, M. (2002). "Development of the mouse retinal vasculature: angiogenesis versus vasculogenesis." Invest Ophthalmol Vis Sci **43**(2): 522-527.

Fujiwara, H., J. Gu, et al. (2004). "Rac regulates integrin-mediated endothelial cell adhesion and migration on laminin-8." Exp Cell Res **292**(1): 67-77.

Fukushi, J., I. T. Makagiansar, et al. (2004). "NG2 proteoglycan promotes endothelial cell motility and angiogenesis via engagement of galectin-3 and alpha3beta1 integrin." Mol Biol Cell **15**(8): 3580-3590.

Funahashi, Y., S. L. Hernandez, et al. (2008). "A notch1 ectodomain construct inhibits endothelial notch signaling, tumour growth, and angiogenesis." Cancer Res **68**(12): 4727-4735.

Fung, E., S. M. Tang, et al. (2007). "Delta-like 4 induces notch signaling in macrophages: implications for inflammation." Circulation **115**(23): 2948-2956.

Gaetani, P., E. Hulleman, et al. (2010). "Expression of the transcription factor HEY1 in glioblastoma: a preliminary clinical study." Tumouri **96**(1): 97-102.

Gale, N. W., M. G. Dominguez, et al. (2004). "Haploinsufficiency of delta-like 4 ligand results in embryonic lethality due to major defects in arterial and vascular development." Proc Natl Acad Sci U S A **101**(45): 15949-15954.

Garber, K. (2007). "Targeting vessel abnormalization in cancer." J Natl Cancer Inst **99**(13): 991-992, 995.

Georgia, S., R. Soliz, et al. (2006). "p57 and Hes1 coordinate cell cycle exit with self-renewal of pancreatic progenitors." Dev Biol **298**(1): 22-31.

Gerhardt, H. (2008). "VEGF and endothelial guidance in angiogenic sprouting." Organogenesis **4**(4): 241-246.

Gerhardt, H. and C. Betsholtz (2003). "Endothelial-pericyte interactions in angiogenesis." Cell Tissue Res **314**(1): 15-23.

Gong, Y. and F. H. Agani (2005). "Oligomycin inhibits HIF-1alpha expression in hypoxic tumour cells." Am J Physiol Cell Physiol **288**(5): C1023-1029.

Grasl-Kraupp, B., B. Ruttkay-Nedecky, et al. (1995). "In situ detection of fragmented DNA (TUNEL assay) fails to discriminate among apoptosis, necrosis, and autolytic cell death: a cautionary note." Hepatology **21**(5): 1465-1468.

Greenberg, J. I. and D. A. Cheresh (2009). "VEGF as an inhibitor of tumour vessel maturation: implications for cancer therapy." Expert Opin Biol Ther **9**(11): 1347-1356.

Grego-Bessa, J., L. Luna-Zurita, et al. (2007). "Notch signaling is essential for ventricular chamber development." Dev Cell **12**(3): 415-429.

Gu, F., Y. Ma, et al. (2010). "Expression of Stat3 and Notch1 is associated with cisplatin resistance in head and neck squamous cell carcinoma." Oncol Rep **23**(3): 671-676.

Guilmeau, S., M. Flandez, et al. "Heterogeneity of Jagged1 expression in human and mouse intestinal tumours: implications for targeting Notch signaling." Oncogene **29**(7): 992-1002.

Guilmeau, S., M. Flandez, et al. (2010). "Heterogeneity of Jagged1 expression in human and mouse intestinal tumours: implications for targeting Notch signaling." Oncogene **29**(7): 992-1002.

Hagedorn, M., M. Balke, et al. (2004). "VEGF coordinates interaction of pericytes and endothelial cells during vasculogenesis and experimental angiogenesis." Dev Dyn **230**(1): 23-33.

Hahn, K. L., J. Johnson, et al. (2005). "Lunatic fringe null female mice are infertile due to defects in meiotic maturation." Development **132**(4): 817-828.

Hallahan, A. R., J. I. Pritchard, et al. (2004). "The SmoA1 mouse model reveals that notch signaling is critical for the growth and survival of sonic hedgehog-induced medulloblastomas." Cancer Res **64**(21): 7794-7800.

Haller, B. K., A. Brave, et al. (2010). "Therapeutic efficacy of a DNA vaccine targeting the endothelial tip cell antigen delta-like ligand 4 in mammary carcinoma." Oncogene.

Hanahan, D. and J. Folkman (1996). "Patterns and emerging mechanisms of the angiogenic switch during tumourigenesis." Cell **86**(3): 353-364.

Hanlon, L., J. L. Avila, et al. (2010). "Notch1 functions as a tumour suppressor in a model of K-ras-induced pancreatic ductal adenocarcinoma." Cancer Res **70**(11): 4280-4286.

Hansson, E. M., F. Lanner, et al. (2010). "Control of Notch-ligand endocytosis by ligand-receptor interaction." J Cell Sci **123**(Pt 17): 2931-2942.

Harrington, L. S., R. C. Sainson, et al. (2008). "Regulation of multiple angiogenic pathways by Dll4 and Notch in human umbilical vein endothelial cells." Microvasc Res **75**(2): 144-154.

Harrison, H., G. Farnie, et al. (2010). "Regulation of breast cancer stem cell activity by signaling through the Notch4 receptor." Cancer Res **70**(2): 709-718.

Hayashi, H. and T. Kume (2008). "Foxc transcription factors directly regulate Dll4 and Hey2 expression by interacting with the VEGF-Notch signaling pathways in endothelial cells." PLoS One **3**(6): e2401.

Hellstrom, M., L. K. Phng, et al. (2007). "VEGF and Notch signaling: the yin and yang of angiogenic sprouting." Cell Adh Migr **1**(3): 133-136.

Hellstrom, M., L. K. Phng, et al. (2007). "Dll4 signalling through Notch1 regulates formation of tip cells during angiogenesis." Nature **445**(7129): 776-780.

Heroult, M., F. Schaffner, et al. (2006). "Eph receptor and ephrin ligand-mediated interactions during angiogenesis and tumour progression." Exp Cell Res **312**(5): 642-650.

Hicklin, D. J. and L. M. Ellis (2005). "Role of the vascular endothelial growth factor pathway in tumour growth and angiogenesis." J Clin Oncol **23**(5): 1011-1027.

High, F. A., M. M. Lu, et al. (2008). "Endothelial expression of the Notch ligand Jagged1 is required for vascular smooth muscle development." Proc Natl Acad Sci U S A **105**(6): 1955-1959.

Hijioka, H., T. Setoguchi, et al. (2010). "Upregulation of Notch pathway molecules in oral squamous cell carcinoma." Int J Oncol **36**(4): 817-822.

Hiratochi, M., H. Nagase, et al. (2007). "The Delta intracellular domain mediates TGF-beta/Activin signaling through binding to Smads and has an important bi-directional function in the Notch-Delta signaling pathway." Nucleic Acids Res **35**(3): 912-922.

Hodkinson, P. S., P. A. Elliott, et al. (2007). "Mammalian NOTCH-1 activates beta1 integrins via the small GTPase R-Ras." J Biol Chem **282**(39): 28991-29001.

Hoey, T., W. C. Yen, et al. (2009). "DLL4 blockade inhibits tumour growth and reduces tumour-initiating cell frequency." Cell Stem Cell **5**(2): 168-177.

Hofmann, J. J. and M. L. Iruela-Arispe (2007). "Notch signaling in blood vessels: who is talking to whom about what?" Circ Res **100**(11): 1556-1568.

Hofmann, J. J. and M. Luisa Iruela-Arispe (2007). "Notch expression patterns in the retina: An eye on receptor-ligand distribution during angiogenesis." Gene Expr Patterns **7**(4): 461-470.

Holderfield, M. T. and C. C. Hughes (2008). "Crosstalk between vascular endothelial growth factor, notch, and transforming growth factor-beta in vascular morphogenesis." Circ Res **102**(6): 637-652.

Hood, J. L., H. Pan, et al. (2009). "Paracrine induction of endothelium by tumour exosomes." Lab Invest **89**(11): 1317-1328.

Hovinga, K. E., F. Shimizu, et al. (2010). "Inhibition of notch signaling in glioblastoma targets cancer stem cells via an endothelial cell intermediate." Stem Cells **28**(6): 1019-1029.

Hulleman, E., M. Quarto, et al. (2009). "A role for the transcription factor HEY1 in glioblastoma." J Cell Mol Med **13**(1): 136-146.

Hurlbut, G. D., M. W. Kankel, et al. (2007). "Crossing paths with Notch in the hyper-network." Curr Opin Cell Biol **19**(2): 166-175.

Hussein, D., W. Punjaruk, et al. (2011). "Pediatric brain tumour cancer stem cells: cell cycle dynamics, DNA repair, and etoposide extrusion." Neuro Oncol **13**(1): 70-83.

Hutchings, H., N. Ortega, et al. (2003). "Extracellular matrix-bound vascular endothelial growth factor promotes endothelial cell adhesion, migration, and survival through integrin ligation." FASEB J **17**(11): 1520-1522.

Ikeda, E., M. G. Achen, et al. (1995). "Hypoxia-induced transcriptional activation and increased mRNA stability of vascular endothelial growth factor in C6 glioma cells." J Biol Chem **270**(34): 19761-19766.

Ilagan, M. X. and R. Kopan (2007). "SnapShot: notch signaling pathway." Cell **128**(6): 1246.

Iruela-Arispe, M. L. and G. E. Davis (2009). "Cellular and molecular mechanisms of vascular lumen formation." Dev Cell **16**(2): 222-231.

Iso, T., Y. Hamamori, et al. (2003). "Notch signaling in vascular development." Arterioscler Thromb Vasc Biol **23**(4): 543-553.

Iso, T., L. Kedes, et al. (2003). "HES and HERP families: multiple effectors of the Notch signaling pathway." J Cell Physiol **194**(3): 237-255.

Iso, T., T. Maeno, et al. (2006). "Dll4-selective Notch signaling induces ephrinB2 gene expression in endothelial cells." Biochem Biophys Res Commun **341**(3): 708-714.

Jaffe, E. A., R. L. Nachman, et al. (1973). "Culture of human endothelial cells derived from umbilical veins. Identification by morphologic and immunologic criteria." J Clin Invest **52**(11): 2745-2756.

Jain, R. K. (2005). "Antiangiogenic therapy for cancer: current and emerging concepts." Oncology (Williston Park) **19**(4 Suppl 3): 7-16.

Jain, R. K., D. G. Duda, et al. (2006). "Lessons from phase III clinical trials on anti-VEGF therapy for cancer." Nat Clin Pract Oncol **3**(1): 24-40.

Jarriault, S., C. Brou, et al. (1995). "Signalling downstream of activated mammalian Notch." Nature **377**(6547): 355-358.

Jia, J., M. Lin, et al. (2007). "The Notch signaling pathway controls the size of the ocular lens by directly suppressing p57Kip2 expression." Mol Cell Biol **27**(20): 7236-7247.

Jockovich, M. E., M. L. Bajenaru, et al. (2007). "Retinoblastoma tumour vessel maturation impacts efficacy of vessel targeting in the LH(BETA)T(AG) mouse model." Invest Ophthalmol Vis Sci **48**(6): 2476-2482.

Johnston, S. H., C. Rauskolb, et al. (1997). "A family of mammalian Fringe genes implicated in boundary determination and the Notch pathway." Development **124**(11): 2245-2254.

Jubb, A. M., F. M. Buffa, et al. (2009). "Assessment of tumour hypoxia for prediction of response to therapy and cancer prognosis." J Cell Mol Med **14**(1-2): 18-29.

Jubb, A. M., E. J. Soilleux, et al. (2010). "Expression of vascular notch ligand delta-like 4 and inflammatory markers in breast cancer." Am J Pathol **176**(4): 2019-2028.

Jubb, A. M., H. Turley, et al. (2009). "Expression of delta-like ligand 4 (Dll4) and markers of hypoxia in colon cancer." Br J Cancer **101**(10): 1749-1757.

Jundt, F., I. Anagnostopoulos, et al. (2002). "Activated Notch1 signaling promotes tumour cell proliferation and survival in Hodgkin and anaplastic large cell lymphoma." Blood **99**(9): 3398-3403.

Jung, S. G., Y. D. Kwon, et al. (2010). "Prognostic significance of Notch 3 gene expression in ovarian serous carcinoma." Cancer Sci.

Kamath, B. M., N. B. Spinner, et al. (2004). "Vascular anomalies in Alagille syndrome: a significant cause of morbidity and mortality." Circulation **109**(11): 1354-1358.

Kamei, M., W. B. Saunders, et al. (2006). "Endothelial tubes assemble from intracellular vacuoles in vivo." Nature **442**(7101): 453-456.

Kamstrup, M. R., L. M. Gjerdrum, et al. (2010). "Notch 1 as a potential therapeutic target in cutaneous T-cell lymphoma." Blood.

Kanamori, M., T. Kawaguchi, et al. (2007). "Contribution of Notch signaling activation to human glioblastoma multiforme." J Neurosurg **106**(3): 417-427.

Kappas, N. C., G. Zeng, et al. (2008). "The VEGF receptor Flt-1 spatially modulates Flk-1 signaling and blood vessel branching." J Cell Biol **181**(5): 847-858.

Karsan, A. (2008). "Notch and integrin affinity: a sticky situation." Sci Signal **1**(2): pe2.

Kato, T. M., A. Kawaguchi, et al. (2010). "Lunatic fringe potentiates Notch signaling in the developing brain." Mol Cell Neurosci **45**(1): 12-25.

Katoh, M. (2006). "Notch ligand, JAG1, is evolutionarily conserved target of canonical WNT signaling pathway in progenitor cells." Int J Mol Med **17**(4): 681-685.

Kawano, S., T. Morotomi, et al. (2002). "Establishment of dental epithelial cell line (HAT-7) and the cell differentiation dependent on Notch signaling pathway." Connect Tissue Res **43**(2-3): 409-412.

Kiec-Wilk, B., J. Grzybowska-Galuszka, et al. (2010). "The MAPK-dependent regulation of the Jagged/Notch gene expression by VEGF, bFGF or PPAR gamma mediated angiogenesis in HUVEC." J Physiol Pharmacol **61**(2): 217-225.

Kim, S. B., G. W. Chae, et al. (2007). "Activated Notch1 interacts with p53 to inhibit its phosphorylation and transactivation." Cell Death Differ **14**(5): 982-991.

Kleihues, P., D. N. Louis, et al. (2002). "The WHO classification of tumours of the nervous system." J Neuropathol Exp Neurol **61**(3): 215-225; discussion 226-219.

Kopan, R. and M. X. Ilagan (2009). "The canonical Notch signaling pathway: unfolding the activation mechanism." Cell **137**(2): 216-233.

Korff, T. and H. G. Augustin (1998). "Integration of endothelial cells in multicellular spheroids prevents apoptosis and induces differentiation." J Cell Biol **143**(5): 1341-1352.

Korff, T. and H. G. Augustin (1999). "Tensional forces in fibrillar extracellular matrices control directional capillary sprouting." J Cell Sci **112 (Pt 19)**: 3249-3258.

Korff, T., G. Dandekar, et al. (2006). "Endothelial ephrinB2 is controlled by microenvironmental determinants and associates context-dependently with CD31." Arterioscler Thromb Vasc Biol **26**(3): 468-474.

Koukourakis, M. I., A. Giatromanolaki, et al. (2001). "Hypoxia-regulated carbonic anhydrase-9 (CA9) relates to poor vascularization and resistance of squamous cell head and neck cancer to chemoradiotherapy." Clin Cancer Res **7**(11): 3399-3403.

Krebs, L. T., J. R. Shutter, et al. (2004). "Haploinsufficient lethality and formation of arteriovenous malformations in Notch pathway mutants." Genes Dev **18**(20): 2469-2473.

Krebs, L. T., Y. Xue, et al. (2000). "Notch signaling is essential for vascular morphogenesis in mice." Genes Dev **14**(11): 1343-1352.

Kuijper, S., C. J. Turner, et al. (2007). "Regulation of angiogenesis by Eph-ephrin interactions." Trends Cardiovasc Med **17**(5): 145-151.

LaVoie, M. J. and D. J. Selkoe (2003). "The Notch ligands, Jagged and Delta, are sequentially processed by alpha-secretase and presenilin/gamma-secretase and release signaling fragments." J Biol Chem **278**(36): 34427-34437.

Lawson, N. D., N. Scheer, et al. (2001). "Notch signaling is required for arterial-venous differentiation during embryonic vascular development." Development **128**(19): 3675-3683.

Le Borgne, R., A. Bardin, et al. (2005). "The roles of receptor and ligand endocytosis in regulating Notch signaling." Development **132**(8): 1751-1762.

Leek, R. D., R. J. Landers, et al. (1999). "Necrosis correlates with high vascular density and focal macrophage infiltration in invasive carcinoma of the breast." Br J Cancer **79**(5-6): 991-995.

Leek, R. D., K. L. Talks, et al. (2002). "Relation of hypoxia-inducible factor-2 alpha (HIF-2 alpha) expression in tumour-infiltrative macrophages to tumour angiogenesis and the oxidative thymidine phosphorylase pathway in Human breast cancer." Cancer Res **62**(5): 1326-1329.

Lefranc, F., J. Brotchi, et al. (2005). "Possible future issues in the treatment of glioblastomas: special emphasis on cell migration and the resistance of migrating glioblastoma cells to apoptosis." J Clin Oncol **23**(10): 2411-2422.

Leong, K. G., X. Hu, et al. (2002). "Activated Notch4 inhibits angiogenesis: role of beta 1-integrin activation." Mol Cell Biol **22**(8): 2830-2841.

Leong, K. G. and A. Karsan (2006). "Recent insights into the role of Notch signaling in tumourigenesis." Blood **107**(6): 2223-2233.

Leslie, J. D., L. Ariza-McNaughton, et al. (2007). "Endothelial signalling by the Notch ligand Delta-like 4 restricts angiogenesis." Development **134**(5): 839-844.

Lewis, C. E. and J. W. Pollard (2006). "Distinct role of macrophages in different tumour microenvironments." Cancer Res **66**(2): 605-612.

Li, J. L., A. M. Jubb, et al. (2010). "Targeting DLL4 in tumours shows preclinical activity but potentially significant toxicity." Future Oncol **6**(7): 1099-1103.

Li, J. L., R. C. Sainson, et al. (2007). "Delta-like 4 Notch ligand regulates tumour angiogenesis, improves tumour vascular function, and promotes tumour growth in vivo." Cancer Res **67**(23): 11244-11253.

Lidington, E. A., D. L. Moyes, et al. (1999). "A comparison of primary endothelial cells and endothelial cell lines for studies of immune interactions." Transpl Immunol **7**(4): 239-246.

Limbourg, F. P., K. Takeshita, et al. (2005). "Essential role of endothelial Notch1 in angiogenesis." Circulation **111**(14): 1826-1832.

Lin, J. T., M. K. Chen, et al. (2010). "Association of High Levels of Jagged-1 and Notch-1 Expression with Poor Prognosis in Head and Neck Cancer." Ann Surg Oncol.

Lin, S. L., F. C. Chang, et al. (2011). "Targeting endothelium-pericyte cross talk by inhibiting VEGF receptor signaling attenuates kidney microvascular rarefaction and fibrosis." Am J Pathol **178**(2): 911-923.

Lin, W. W. and M. Karin (2007). "A cytokine-mediated link between innate immunity, inflammation, and cancer." J Clin Invest **117**(5): 1175-1183.

Ling, H., J. R. Sylvestre, et al. (2010). "Notch1-induced mammary tumour development is cyclin D1-dependent and correlates with expansion of pre-malignant multipotent duct-limited progenitors." Oncogene.

Liu, H., S. Kennard, et al. (2009). "NOTCH3 expression is induced in mural cells through an autoregulatory loop that requires endothelial-expressed JAGGED1." Circ Res **104**(4): 466-475.

Liu, R., X. Li, et al. (2010). "KSHV-induced notch components render endothelial and mural cell characteristics and cell survival." Blood **115**(4): 887-895.

Liu, W., Y. D. Jung, et al. (2004). "Effects of overexpression of ephrin-B2 on tumour growth in human colorectal cancer." Br J Cancer **90**(8): 1620-1626.

Liu, Z. J., T. Shirakawa, et al. (2003). "Regulation of Notch1 and Dll4 by vascular endothelial growth factor in arterial endothelial cells: implications for modulating arteriogenesis and angiogenesis." Mol Cell Biol **23**(1): 14-25.

Lobov, I. B., R. A. Renard, et al. (2007). "Delta-like ligand 4 (Dll4) is induced by VEGF as a negative regulator of angiogenic sprouting." Proc Natl Acad Sci U S A **104**(9): 3219-3224.

Louvi, A., J. F. Arboleda-Velasquez, et al. (2006). "CADASIL: a critical look at a Notch disease." Dev Neurosci **28**(1-2): 5-12.

Lu, C., T. Bonome, et al. (2007). "Gene alterations identified by expression profiling in tumour-associated endothelial cells from invasive ovarian carcinoma." Cancer Res **67**(4): 1757-1768.

MacKenzie, F., P. Duriez, et al. (2004). "Notch4 inhibits endothelial apoptosis via RBP-Jkappa-dependent and -independent pathways." J Biol Chem **279**(12): 11657-11663.

Mailhos, C., U. Modlich, et al. (2001). "Delta4, an endothelial specific notch ligand expressed at sites of physiological and tumour angiogenesis." Differentiation **69**(2-3): 135-144.

Marklund, U., E. M. Hansson, et al. (2010). "Domain-specific control of neurogenesis achieved through patterned regulation of Notch ligand expression." Development **137**(3): 437-445.

Martinez, J. C., M. M. Muller, et al. (2009). "Nuclear and membrane expression of the angiogenesis regulator delta-like ligand 4 (DLL4) in normal and malignant human tissues." Histopathology **54**(5): 598-606.

Maxwell, P. H. and P. J. Ratcliffe (2002). "Oxygen sensors and angiogenesis." Semin Cell Dev Biol **13**(1): 29-37.

May, W. A., A. Arvand, et al. (1997). "EWS/FLI1-induced manic fringe renders NIH 3T3 cells tumourigenic." Nat Genet **17**(4): 495-497.

Meurette, O., S. Stylianou, et al. (2009). "Notch activation induces Akt signaling via an autocrine loop to prevent apoptosis in breast epithelial cells." Cancer Res **69**(12): 5015-5022.

Moloney, D. J., V. M. Panin, et al. (2000). "Fringe is a glycosyltransferase that modifies Notch." Nature **406**(6794): 369-375.

Morrow, D., A. Scheller, et al. (2005). "Notch-mediated CBF-1/RBP-J{kappa}-dependent regulation of human vascular smooth muscle cell phenotype in vitro." Am J Physiol Cell Physiol **289**(5): C1188-1196.

Moserle, L., A. Amadori, et al. (2009). "The angiogenic switch: implications in the regulation of tumour dormancy." Curr Mol Med **9**(8): 935-941.

Mumm, J. S., E. H. Schroeter, et al. (2000). "A ligand-induced extracellular cleavage regulates gamma-secretase-like proteolytic activation of Notch1." Mol Cell **5**(2): 197-206.

Munro, S. and M. Freeman (2000). "The notch signalling regulator fringe acts in the Golgi apparatus and requires the glycosyltransferase signature motif DXD." Curr Biol **10**(14): 813-820.

Murata, A., K. Okuyama, et al. (2010). "A Notch ligand, Delta-like 1 functions as an adhesion molecule for mast cells." J Immunol **185**(7): 3905-3912.

Murdoch, C., A. Giannoudis, et al. (2004). "Mechanisms regulating the recruitment of macrophages into hypoxic areas of tumours and other ischemic tissues." Blood **104**(8): 2224-2234.

Murphy, P. A., M. T. Lam, et al. (2008). "Endothelial Notch4 signaling induces hallmarks of brain arteriovenous malformations in mice." Proc Natl Acad Sci U S A **105**(31): 10901-10906.

Myers, A. L., R. F. Williams, et al. (2010). "Bevacizumab-induced tumour vessel remodeling in rhabdomyosarcoma xenografts increases the effectiveness of adjuvant ionizing radiation." J Pediatr Surg **45**(6): 1080-1085.

Nam, Y., P. Sliz, et al. (2006). "Structural basis for cooperativity in recruitment of MAML coactivators to Notch transcription complexes." Cell **124**(5): 973-983.

Negus, R. P., G. W. Stamp, et al. (1997). "Quantitative assessment of the leukocyte infiltrate in ovarian cancer and its relationship to the expression of C-C chemokines." Am J Pathol **150**(5): 1723-1734.

Nelson, W. J. and R. Nusse (2004). "Convergence of Wnt, beta-catenin, and cadherin pathways." Science **303**(5663): 1483-1487.

Noguera-Troise, I., C. Daly, et al. (2006). "Blockade of Dll4 inhibits tumour growth by promoting non-productive angiogenesis." Nature **444**(7122): 1032-1037.

Noseda, M., L. Chang, et al. (2004). "Notch activation induces endothelial cell cycle arrest and participates in contact inhibition: role of p21Cip1 repression." Mol Cell Biol **24**(20): 8813-8822.

O'Neill, A. J., S. O'Neill, et al. (2000). "Glutathione depletion-induced neutrophil apoptosis is caspase 3 dependent." Shock **14**(6): 605-609.

Oda, T., A. G. Elkahloun, et al. (1997). "Mutations in the human Jagged1 gene are responsible for Alagille syndrome." Nat Genet **16**(3): 235-242.

Ohno, S., Y. Ohno, et al. (2004). "Correlation of histological localization of tumour-associated macrophages with clinicopathological features in endometrial cancer." Anticancer Res **24**(5C): 3335-3342.

Oishi, H., M. Sunamura, et al. "Blockade of Delta-Like Ligand 4 Signaling Inhibits Both Growth and Angiogenesis of Pancreatic Cancer." Pancreas.

Oishi, H., M. Sunamura, et al. (2010). "Blockade of Delta-Like Ligand 4 Signaling Inhibits Both Growth and Angiogenesis of Pancreatic Cancer." Pancreas.

Olsson, A. K., A. Dimberg, et al. (2006). "VEGF receptor signalling - in control of vascular function." Nat Rev Mol Cell Biol **7**(5): 359-371.

Orimo, A., P. B. Gupta, et al. (2005). "Stromal fibroblasts present in invasive human breast carcinomas promote tumour growth and angiogenesis through elevated SDF-1/CXCL12 secretion." Cell **121**(3): 335-348.

Ozerdem, U., K. A. Grako, et al. (2001). "NG2 proteoglycan is expressed exclusively by mural cells during vascular morphogenesis." Dev Dyn **222**(2): 218-227.

Palomero, T., M. L. Sulis, et al. (2007). "Mutational loss of PTEN induces resistance to NOTCH1 inhibition in T-cell leukemia." Nat Med **13**(10): 1203-1210.

Pang, R. T., C. O. Leung, et al. (2010). "MicroRNA-34a suppresses invasion through downregulation of Notch1 and Jagged1 in cervical carcinoma and choriocarcinoma cells." Carcinogenesis **31**(6): 1037-1044.

Panin, V. M., L. Shao, et al. (2002). "Notch ligands are substrates for protein O-fucosyltransferase-1 and Fringe." J Biol Chem **277**(33): 29945-29952.

Pannequin, J., C. Bonnans, et al. (2009). "The wnt target jagged-1 mediates the activation of notch signaling by progastrin in human colorectal cancer cells." Cancer Res **69**(15): 6065-6073.

Patard, J. J., N. Rioux-Leclercq, et al. (2009). "Absence of VHL gene alteration and high VEGF expression are associated with tumour aggressiveness and poor survival of renal-cell carcinoma." Br J Cancer **101**(8): 1417-1424.

Patel, N. S., M. S. Dobbie, et al. (2006). "Up-regulation of endothelial delta-like 4 expression correlates with vessel maturation in bladder cancer." Clin Cancer Res **12**(16): 4836-4844.

Patel, N. S., J. L. Li, et al. (2005). "Up-regulation of delta-like 4 ligand in human tumour vasculature and the role of basal expression in endothelial cell function." Cancer Res **65**(19): 8690-8697.

Peault, B., M. Rudnicki, et al. (2007). "Stem and progenitor cells in skeletal muscle development, maintenance, and therapy." Mol Ther **15**(5): 867-877.

Pece, S., M. Serresi, et al. (2004). "Loss of negative regulation by Numb over Notch is relevant to human breast carcinogenesis." J Cell Biol **167**(2): 215-221.

Petcherski, A. G. and J. Kimble (2000). "Mastermind is a putative activator for Notch." Curr Biol **10**(13): R471-473.

Phng, L. K. and H. Gerhardt (2009). "Angiogenesis: a team effort coordinated by notch." Dev Cell **16**(2): 196-208.

Phng, L. K., M. Potente, et al. (2009). "Nrarp coordinates endothelial Notch and Wnt signaling to control vessel density in angiogenesis." Dev Cell **16**(1): 70-82.

Popovic, M., J. Bella, et al. (2011). "The interaction of Jagged-1 cytoplasmic tail with afadin PDZ domain is local, folding-independent, and tuned by phosphorylation." J Mol Recognit **24**(2): 245-253.

Prakash, N., E. Hansson, et al. (2002). "Mouse Notch 3 expression in the pre- and postnatal brain: relationship to the stroke and dementia syndrome CADASIL." Exp Cell Res **278**(1): 31-44.

Pratt, E. B., J. S. Wentzell, et al. (2010). "The cell giveth and the cell taketh away: An overview of Notch pathway activation by endocytic trafficking of ligands and receptors." Acta Histochem.

Purow, B. W., R. M. Haque, et al. (2005). "Expression of Notch-1 and its ligands, Delta-like-1 and Jagged-1, is critical for glioma cell survival and proliferation." Cancer Res **65**(6): 2353-2363.

Pusztaszeri, M. P., W. Seelentag, et al. (2006). "Immunohistochemical expression of endothelial markers CD31, CD34, von Willebrand factor, and Fli-1 in normal human tissues." J Histochem Cytochem **54**(4): 385-395.

Qian, C. N., D. Huang, et al. (2009). "Complexity of tumour vasculature in clear cell renal cell carcinoma." Cancer **115**(10 Suppl): 2282-2289.

Qin, L. and M. Zhang (2010). "Maspin regulates endothelial cell adhesion and migration through an integrin signaling pathway." J Biol Chem **285**(42): 32360-32369.

Radtke, F. and K. Raj (2003). "The role of Notch in tumourigenesis: oncogene or tumour suppressor?" Nat Rev Cancer **3**(10): 756-767.

Rafajova, M., M. Zatovicova, et al. (2004). "Induction by hypoxia combined with low glucose or low bicarbonate and high posttranslational stability upon reoxygenation contribute to carbonic anhydrase IX expression in cancer cells." Int J Oncol **24**(4): 995-1004.

Ramachandran, V., T. Arumugam, et al. (2009). "The ADMR receptor mediates the effects of adrenomedullin on pancreatic cancer cells and on cells of the tumour microenvironment." PLoS One **4**(10): e7502.

Ramdass, B., T. T. Maliekal, et al. (2007). "Coexpression of Notch1 and NF-kappaB signaling pathway components in human cervical cancer progression." Gynecol Oncol **104**(2): 352-361.

Rao, S. S., J. O'Neil, et al. (2009). "Inhibition of NOTCH signaling by gamma secretase inhibitor engages the RB pathway and elicits cell cycle exit in T-cell acute lymphoblastic leukemia cells." Cancer Res **69**(7): 3060-3068.

Reedijk, M., S. Odorcic, et al. (2005). "High-level coexpression of JAG1 and NOTCH1 is observed in human breast cancer and is associated with poor overall survival." Cancer Res **65**(18): 8530-8537.

Reedijk, M., S. Odorcic, et al. (2008). "Activation of Notch signaling in human colon adenocarcinoma." Int J Oncol **33**(6): 1223-1229.

Reedijk, M., D. Pinnaduwage, et al. (2008). "JAG1 expression is associated with a basal phenotype and recurrence in lymph node-negative breast cancer." Breast Cancer Res Treat **111**(3): 439-448.

Reynolds, L. P., A. T. Grazul-Bilska, et al. (2000). "Angiogenesis in the corpus luteum." Endocrine **12**(1): 1-9.

Ricci-Vitiani, L., R. Pallini, et al. (2010). "Tumour vascularization via endothelial differentiation of glioblastoma stem-like cells." Nature.

Riccio, O., M. E. van Gijn, et al. (2008). "Loss of intestinal crypt progenitor cells owing to inactivation of both Notch1 and Notch2 is accompanied by derepression of CDK inhibitors p27Kip1 and p57Kip2." EMBO Rep **9**(4): 377-383.

Ridgway, J., G. Zhang, et al. (2006). "Inhibition of Dll4 signalling inhibits tumour growth by deregulating angiogenesis." Nature **444**(7122): 1083-1087.

Rodilla, V., A. Villanueva, et al. (2009). "Jagged1 is the pathological link between Wnt and Notch pathways in colorectal cancer." Proc Natl Acad Sci U S A **106**(15): 6315-6320.

Rosati, E., R. Sabatini, et al. (2009). "Constitutively activated Notch signaling is involved in survival and apoptosis resistance of B-CLL cells." Blood **113**(4): 856-865.

Rose, S. L., M. Kunnimalaiyaan, et al. (2010). "Notch 1 signaling is active in ovarian cancer." Gynecol Oncol **117**(1): 130-133.

Sade, H., S. Krishna, et al. (2004). "The anti-apoptotic effect of Notch-1 requires p56lck-dependent, Akt/PKB-mediated signaling in T cells." J Biol Chem **279**(4): 2937-2944.

Sainson, R. C. and A. L. Harris (2007). "Anti-Dll4 therapy: can we block tumour growth by increasing angiogenesis?" Trends Mol Med **13**(9): 389-395.

Sainson, R. C., D. A. Johnston, et al. (2008). "TNF primes endothelial cells for angiogenic sprouting by inducing a tip cell phenotype." Blood **111**(10): 4997-5007.

Sancho, R., A. Jandke, et al. (2010). "F-box and WD Repeat Domain-Containing 7 Regulates Intestinal Cell Lineage Commitment and Is a Haploinsufficient Suppressor of Intestinal Tumourigenesis." Gastroenterology.

Sarmento, L. M., H. Huang, et al. (2005). "Notch1 modulates timing of G1-S progression by inducing SKP2 transcription and p27 Kip1 degradation." J Exp Med **202**(1): 157-168.

Scehnet, J. S., W. Jiang, et al. (2007). "Inhibition of Dll4-mediated signaling induces proliferation of immature vessels and results in poor tissue perfusion." Blood **109**(11): 4753-4760.

Schadler, K. L., P. A. Zweidler-McKay, et al. (2010). "Delta-like ligand 4 plays a critical role in pericyte/vascular smooth muscle cell formation during vasculogenesis and tumour vessel expansion in Ewing's sarcoma." Clin Cancer Res **16**(3): 848-856.

Schroeter, E. H., J. A. Kisslinger, et al. (1998). "Notch-1 signalling requires ligand-induced proteolytic release of intracellular domain." Nature **393**(6683): 382-386.

Segarra, M., C. K. Williams, et al. (2008). "Dll4 activation of Notch signaling reduces tumour vascularity and inhibits tumour growth." Blood **112**(5): 1904-1911.

Seo, S., H. Fujita, et al. (2006). "The forkhead transcription factors, Foxc1 and Foxc2, are required for arterial specification and lymphatic sprouting during vascular development." Dev Biol **294**(2): 458-470.

Shao, L., D. J. Moloney, et al. (2003). "Fringe modifies O-fucose on mouse Notch1 at epidermal growth factor-like repeats within the ligand-binding site and the Abruptex region." J Biol Chem **278**(10): 7775-7782.

Shawber, C. J., I. Das, et al. (2003). "Notch signaling in primary endothelial cells." Ann N Y Acad Sci **995**: 162-170.

Shawber, C. J., Y. Funahashi, et al. (2007). "Notch alters VEGF responsiveness in human and murine endothelial cells by direct regulation of VEGFR-3 expression." J Clin Invest **117**(11): 3369-3382.

Sheldon, H., E. Heikamp, et al. (2010). "New mechanism for notch signaling to endothelium at a distance by Delta-like 4 incorporation into exosomes." Blood.**116**(13):2385-2394

Shen, J. F., H. B. Rui, et al. (2010). "[Arresting Effect of p16 and dll4 Transfection on Cell Cycle of K562 Cells.]." Zhongguo Shi Yan Xue Ye Xue Za Zhi **18**(3): 588-592.

Sherr, C. J. (2000). "The Pezcoller lecture: cancer cell cycles revisited." Cancer Res **60**(14): 3689-3695.

Shih, A. H. and E. C. Holland (2006). "Notch signaling enhances nestin expression in gliomas." Neoplasia **8**(12): 1072-1082.

Shih Ie, M. and T. L. Wang (2007). "Notch signaling, gamma-secretase inhibitors, and cancer therapy." Cancer Res **67**(5): 1879-1882.

Shimizu, K., S. Chiba, et al. (2001). "Manic fringe and lunatic fringe modify different sites of the Notch2 extracellular region, resulting in different signaling modulation." J Biol Chem **276**(28): 25753-25758.

Shojaei, F., X. Wu, et al. (2007). "Tumour refractoriness to anti-VEGF treatment is mediated by CD11b+Gr1+ myeloid cells." Nat Biotechnol **25**(8): 911-920.

Siekmann, A. F. and N. D. Lawson (2007). "Notch signalling limits angiogenic cell behaviour in developing zebrafish arteries." Nature **445**(7129): 781-784.

Sikandar, S. S., K. T. Pate, et al. (2010). "NOTCH signaling is required for formation and self-renewal of tumour-initiating cells and for repression of secretory cell differentiation in colon cancer." Cancer Res **70**(4): 1469-1478.

Simons, M. and G. Raposo (2009). "Exosomes--vesicular carriers for intercellular communication." Curr Opin Cell Biol **21**(4): 575-581.

Sivridis, E., A. Giatromanolaki, et al. (2002). "Angiogenic co-operation of VEGF and stromal cell TP in endometrial carcinomas." J Pathol **196**(4): 416-422.

Six, E. M., D. Ndiaye, et al. (2004). "The notch ligand Delta1 recruits Dlg1 at cell-cell contacts and regulates cell migration." J Biol Chem **279**(53): 55818-55826.

Sjolund, J., M. Johansson, et al. (2008). "Suppression of renal cell carcinoma growth by inhibition of Notch signaling in vitro and in vivo." J Clin Invest **118**(1): 217-228.

Song, N., Y. Huang, et al. (2009). "Overexpression of platelet-derived growth factor-BB increases tumour pericyte content via stromal-derived factor-1alpha/CXCR4 axis." Cancer Res **69**(15): 6057-6064.

Sonoshita, M., M. Aoki, et al. (2011). "Suppression of colon cancer metastasis by Aes through inhibition of Notch signaling." Cancer Cell **19**(1): 125-137.

Sorensen, I., R. H. Adams, et al. (2009). "DLL1-mediated Notch activation regulates endothelial identity in mouse fetal arteries." Blood **113**(22): 5680-5688.

Sparmann, A. and D. Bar-Sagi (2004). "Ras-induced interleukin-8 expression plays a critical role in tumour growth and angiogenesis." Cancer Cell **6**(5): 447-458.

Stanley, P. (2007). "Regulation of Notch signaling by glycosylation." Curr Opin Struct Biol **17**(5): 530-535.

Stanley, P. and C. J. Guidos (2009). "Regulation of Notch signaling during T- and B-cell development by O-fucose glycans." Immunol Rev **230**(1): 201-215.

Stockhausen, M. T., K. Kristoffersen, et al. (2010). "The functional role of Notch signaling in human gliomas." Neuro Oncol **12**(2): 199-211.

Stylianou, S., R. B. Clarke, et al. (2006). "Aberrant activation of notch signaling in human breast cancer." Cancer Res **66**(3): 1517-1525.

Suchting, S., C. Freitas, et al. (2007). "The Notch ligand Delta-like 4 negatively regulates endothelial tip cell formation and vessel branching." Proc Natl Acad Sci U S A **104**(9): 3225-3230.

Suzuki, M., M. Yamamoto, et al. (2006). "Delta-4 expression on a stromal cell line is augmented by interleukin-6 via STAT3 activation." Exp Hematol **34**(9): 1143-1150.

Tacker, D. H. and A. O. Okorodudu (2004). "Evidence for injurious effect of cocaethylene in human microvascular endothelial cells." Clin Chim Acta **345**(1-2): 69-77.

Takeshita, K., M. Satoh, et al. (2007). "Critical role of endothelial Notch1 signaling in postnatal angiogenesis." Circ Res **100**(1): 70-78.

Tammam, J., C. Ware, et al. (2009). "Down-regulation of the Notch pathway mediated by a gamma-secretase inhibitor induces anti-tumour effects in mouse models of T-cell leukaemia." Br J Pharmacol **158**(5): 1183-1195.

Tammela, T., G. Zarkada, et al. (2008). "Blocking VEGFR-3 suppresses angiogenic sprouting and vascular network formation." Nature **454**(7204): 656-660.

Tatar, O., E. Yoeruek, et al. (2008). "Effect of bevacizumab on inflammation and proliferation in human choroidal neovascularization." Arch Ophthalmol **126**(6): 782-790.

Taylor, K. L., A. M. Henderson, et al. (2002). "Notch activation during endothelial cell network formation in vitro targets the basic HLH transcription factor HESR-1 and downregulates VEGFR-2/KDR expression." Microvasc Res **64**(3): 372-383.

Thurston, G., I. Noguera-Troise, et al. (2007). "The Delta paradox: DLL4 blockade leads to more tumour vessels but less tumour growth." Nat Rev Cancer **7**(5): 327-331.

Trindade, A., S. R. Kumar, et al. (2008). "Overexpression of delta-like 4 induces arterialization and attenuates vessel formation in developing mouse embryos." Blood **112**(5): 1720-1729.

Turner, K. J., J. W. Moore, et al. (2002). "Expression of hypoxia-inducible factors in human renal cancer: relationship to angiogenesis and to the von Hippel-Lindau gene mutation." Cancer Res **62**(10): 2957-2961.

Urs, S., A. Roudabush, et al. (2008). "Soluble forms of the Notch ligands Delta1 and Jagged1 promote in vivo tumourigenicity in NIH3T3 fibroblasts with distinct phenotypes." Am J Pathol **173**(3): 865-878.

Uyttendaele, H., J. Ho, et al. (2001). "Vascular patterning defects associated with expression of activated Notch4 in embryonic endothelium." Proc Natl Acad Sci U S A **98**(10): 5643-5648.

van Es, J. H., M. E. van Gijn, et al. (2005). "Notch/gamma-secretase inhibition turns proliferative cells in intestinal crypts and adenomas into goblet cells." Nature **435**(7044): 959-963.

van Tetering, G., P. van Diest, et al. (2009). "Metalloprotease ADAM10 is required for Notch1 site 2 cleavage." J Biol Chem **284**(45): 31018-31027.

Veeraraghavalu, K., M. Pett, et al. (2004). "Papillomavirus-mediated neoplastic progression is associated with reciprocal changes in JAGGED1 and manic fringe expression linked to notch activation." J Virol **78**(16): 8687-8700.

Veeraraghavalu, K., V. K. Subbaiah, et al. (2005). "Complementation of human papillomavirus type 16 E6 and E7 by Jagged1-specific Notch1-phosphatidylinositol 3-kinase signaling involves pleiotropic oncogenic functions independent of CBF1;Su(H);Lag-1 activation." J Virol **79**(12): 7889-7898.

Villa, N., L. Walker, et al. (2001). "Vascular expression of Notch pathway receptors and ligands is restricted to arterial vessels." Mech Dev **108**(1-2): 161-164.

Visan, I., J. S. Yuan, et al. (2010). "Lunatic fringe enhances competition for delta-like Notch ligands but does not overcome defective pre-TCR signaling during thymocyte beta-selection in vivo." J Immunol **185**(8): 4609-4617.

Visan, I., J. S. Yuan, et al. (2006). "Regulation of intrathymic T-cell development by Lunatic Fringe- Notch1 interactions." Immunol Rev **209**: 76-94.

von Tell, D., A. Armulik, et al. (2006). "Pericytes and vascular stability." Exp Cell Res **312**(5): 623-629.

Wang, M., J. Wang, et al. (2009). "Notch1 expression correlates with tumour differentiation status in ovarian carcinoma." Med Oncol.

Wang, R., K. Chadalavada, et al. (2010). "Glioblastoma stem-like cells give rise to tumour endothelium." Nature.

Wang, T., M. Baron, et al. (2008). "An overview of Notch3 function in vascular smooth muscle cells." Prog Biophys Mol Biol **96**(1-3): 499-509.

Wang, T., C. M. Holt, et al. (2007). "Notch3 activation modulates cell growth behaviour and cross-talk to Wnt/TCF signalling pathway." Cell Signal **19**(12): 2458-2467.

Wang, Y., M. Nakayama, et al. (2010). "Ephrin-B2 controls VEGF-induced angiogenesis and lymphangiogenesis." Nature **465**(7297): 483-486.

Wang, Z., Y. Li, et al. (2010). "Targeting Notch signaling pathway to overcome drug resistance for cancer therapy." Biochim Biophys Acta.

Wang, Z., Y. Li, et al. (2010). "Down-regulation of Notch-1 and Jagged-1 inhibits prostate cancer cell growth, migration and invasion, and induces apoptosis via inactivation of Akt, mTOR, and NF-kappaB signaling pathways." J Cell Biochem **109**(4): 726-736.

Ward, C., D. Kuehn, et al. (2010). "Antibody targeting of cathepsin S inhibits angiogenesis and synergistically enhances anti-VEGF." PLoS One **5**(9).

Wei, P., M. Walls, et al. (2010). "Evaluation of selective gamma-secretase inhibitor PF-03084014 for its antitumour efficacy and gastrointestinal safety to guide optimal clinical trial design." Mol Cancer Ther **9**(6): 1618-1628.

Westhoff, B., I. N. Colaluca, et al. (2009). "Alterations of the Notch pathway in lung cancer." Proc Natl Acad Sci U S A **106**(52): 22293-22298.

Willett, C. G., Y. Boucher, et al. (2004). "Direct evidence that the VEGF-specific antibody bevacizumab has antivascular effects in human rectal cancer." Nat Med **10**(2): 145-147.

Williams, C. K., J. L. Li, et al. (2006). "Up-regulation of the Notch ligand Delta-like 4 inhibits VEGF-induced endothelial cell function." Blood **107**(3): 931-939.

Williams, C. K., M. Segarra, et al. (2008). "Regulation of CXCR4 by the Notch ligand delta-like 4 in endothelial cells." Cancer Res **68**(6): 1889-1895.

Wong, G. T., D. Manfra, et al. (2004). "Chronic treatment with the gamma-secretase inhibitor LY-411,575 inhibits beta-amyloid peptide production and alters

lymphopoiesis and intestinal cell differentiation." J Biol Chem **279**(13): 12876-12882.

Wu, J. and N. Sheibani (2003). "Modulation of VE-cadherin and PECAM-1 mediated cell-cell adhesions by mitogen-activated protein kinases." J Cell Biochem **90**(1): 121-137.

Wu, J. Y., L. Wen, et al. (1996). "The secreted product of Xenopus gene lunatic Fringe, a vertebrate signaling molecule." Science **273**(5273): 355-358.

Wu, K., L. Xu, et al. (2011). "High JAGGED1 expression predicts poor outcome in clear cell renal cell carcinoma." Jpn J Clin Oncol **41**(3): 411-416.

Wu, L., J. C. Aster, et al. (2000). "MAML1, a human homologue of Drosophila mastermind, is a transcriptional co-activator for NOTCH receptors." Nat Genet **26**(4): 484-489.

Wu, L., T. Sun, et al. (2002). "Identification of a family of mastermind-like transcriptional coactivators for mammalian notch receptors." Mol Cell Biol **22**(21): 7688-7700.

Wu, X., Q. Zhou, et al. (2008). "Ageing-exaggerated proliferation of vascular smooth muscle cells is related to attenuation of Jagged1 expression in endothelial cells." Cardiovasc Res **77**(4): 800-808.

Wu, Y., C. Cain-Hom, et al. (2010). "Therapeutic antibody targeting of individual Notch receptors." Nature **464**(7291): 1052-1057.

Wu, Y., L. Chen, et al. (2004). "Overexpression of the C-terminal PG-M/versican domain impairs growth of tumour cells by intervening in the interaction between epidermal growth factor receptor and beta1-integrin." J Cell Sci **117**(Pt 11): 2227-2237.

Wustehube, J., A. Bartol, et al. (2010). "Cerebral cavernous malformation protein CCM1 inhibits sprouting angiogenesis by activating DELTA-NOTCH signaling." Proc Natl Acad Sci U S A **107**(28): 12640-12645.

Wykoff, C. C., N. Beasley, et al. (2001). "Expression of the hypoxia-inducible and tumour-associated carbonic anhydrases in ductal carcinoma in situ of the breast." Am J Pathol **158**(3): 1011-1019.

Wykoff, C. C., N. J. Beasley, et al. (2000). "Hypoxia-inducible expression of tumour-associated carbonic anhydrases." Cancer Res **60**(24): 7075-7083.

Xiao, X., L. Ning, et al. (2009). "Notch1 mediates growth suppression of papillary and follicular thyroid cancer cells by histone deacetylase inhibitors." Mol Cancer Ther **8**(2): 350-356.

Xu, Y., R. A. Swerlick, et al. (1994). "Characterization of expression and modulation of cell adhesion molecules on an immortalized human dermal microvascular endothelial cell line (HMEC-1)." J Invest Dermatol **102**(6): 833-837.

Xue, Y., X. Gao, et al. (1999). "Embryonic lethality and vascular defects in mice lacking the Notch ligand Jagged1." Hum Mol Genet **8**(5): 723-730.

Yamamizu, K., T. Matsunaga, et al. (2010). "Convergence of Notch and beta-catenin signaling induces arterial fate in vascular progenitors." J Cell Biol **189**(2): 325-338.

Yan, M., C. A. Callahan, et al. (2010). "Chronic DLL4 blockade induces vascular neoplasms." Nature **463**(7282): E6-7.

Yao, K., P. Rizzo, et al. (2010). "Notch-1 and Notch-4 Receptors as Prognostic Markers in Breast Cancer." Int J Surg Pathol.

Yuan, J. S., J. B. Tan, et al. (2011). "Lunatic Fringe prolongs Delta/Notch-induced self-renewal of committed alphabeta T-cell progenitors." Blood **117**(4): 1184-1195.

Zang, S., F. Chen, et al. (2010). "RNAi-mediated knockdown of Notch-1 leads to cell growth inhibition and enhanced chemosensitivity in human breast cancer." Oncol Rep **23**(4): 893-899.

Zeng, Q., S. Li, et al. (2005). "Crosstalk between tumour and endothelial cells promotes tumour angiogenesis by MAPK activation of Notch signaling." Cancer Cell **8**(1): 13-23.

Zhang, P., Y. Yang, et al. (2010). "Regulation of NOTCH signaling by reciprocal inhibition of HES1 and Deltex 1 and its role in osteosarcoma invasiveness." Oncogene **29**(20): 2916-2926.

Zhao, N., Y. Guo, et al. (2010). "Akt-mTOR signaling is involved in Notch-1-mediated glioma cell survival and proliferation." Oncol Rep **23**(5): 1443-1447.

Zovein, A. C., A. Luque, et al. (2010). "Beta1 integrin establishes endothelial cell polarity and arteriolar lumen formation via a Par3-dependent mechanism." Dev Cell **18**(1): 39-51.

Appendix: Publications and Presentations

Publications and presentations arising from/related to Thesis

Publications:

1) Sheldon, H., et al., *New mechanism for notch signaling to endothelium at a distance by Delta-like 4 incorporation into exosomes.* Blood, **116** (13):2385-2394.

2) Li, J.L., et al. *DLL4-Notch signalling mediates tumour resistance to anti-VEGF therapy in vivo.* (Manuscript submitted)

3) Bridges, E.*, **Oon. C**.*, and Harris, A.. *Notch regulation of tumour angiogenesis.* (Future Oncology, in press) * Joint first authorship

Conference/Seminar/ Meeting Presentations:

Oral:

1) Seminar presentation, Karolinska Institutet (Sweden)- Year 2011
2) Oxford Weatherall Institute of Molecular Medicine Student Presentation Day- Year 2010

Poster:

1) European Association for Cancer Research (EACR) Conference, Oslo (Norway)- Year 2010
2) Young Life Scientists Angiogenesis Symposium, Chester (UK)- Year 2009
3) Angiogenesis Gordon Research Conference, RI (USA)- Year 2009
4) Notch Meeting, Athens (Greece)- Year 2009
5) Oxford Merton College Biosciences Day- Year 2008, 2009
6) Oxford Medical Sciences DPhil Day- Year 2008, 2009
7) Oxford Weatherall Institute of Molecular Medicine Presentation Day- Year 2008, 2009

Awards:

1) European Association for Cancer Research Meeting Bursary Award (Norway)- Year 2010
2) Angiogenesis Gordon Research Conference Scholarship (Rhode Island, USA)- Year 2009